PhD Thesis

Non-destructive methods for determination of quality attributes of bell peppers

Prepared by

Timea Ignat

This work was carried out under the supervision of

Ze'ev Schmilovitch, DSc

Department of Agricultural Engineering, ARO, Israel

and

József Felföldi, CSc

Corvinus University of Budapest, Faculty of Food Science

Department of Physics-Control

Israel, 2012

PhD School

Name: PhD School of Food Science

Field: Food Science

Head: Péter Fodor, DSc

                      Corvinus University of Budapest

Supervisors: Ze'ev Schmilovitch, DSc

                      Department of Agricultural Engineering

                      ARO, Israel

                      József Felföldi, CSc

                      Department of Physics-Control

                      Faculty of Food Science

                      Corvinus University of Budapest

The applicant met the requirement of the PhD regulations of the Corvinus University of Budapest and the thesis is accepted for the defence process.

………………………….   …………………………...   …………………………...

Signature of Head of School   Signatures of Supervisors

The committee of the PhD School of Food Science, Corvinus University of Budapest approved on the 6th of March 2012 the bellow committee to conduct the public defence:

Committee:

Head of the committee

Erika Békássyné Molnár, DSc

Members

Károly J. Kaffka, CSc

Péter Biacs, DSc

Victor Alchanatis, DSc

Gábor Kollár, CSc

Reviewers

Attila Ombódi, PhD

Tamás Zsom, PhD

Secretary

Klára Pásztorné Huszár, PhD

Acknowledgement

First of all I would like to offer this work to Elohim. Without the help of God this work could not be accomplished.

Thank for my advisors, Dr. Ze'ev Schmilovitch and Dr. József Felföldi for the opportunity to work on this research, for their guidance, help, encouragement and long and fruitful discussions that were so essential for my work. Special thanks for Prof. András Fekete, Dr. Victor Alchanatis and Dr. Amos Mizrach for their continuous support during the long years that this work was accomplished. I would like to thank to Bracha Steiner, Aharon Hoffman and Haim Egozi, those who have assisted in carrying out part of the experiments. To my dear friends in Hungary: Dr.Viktoria Zsom-Muha, Anikó Lambert-Meretei, Andrea Gombai and Bethany Page, and in Israel: Jessica Katz, Susanne Levkovitch, Ronit Rud, Roi Efron, and Avraham Cohen with whom I shared great years of discussions, thoughts, ideas, and lots of laugh. All these wonderful years in Israel have been full of joy and blessings, it is a very precious part in my life and you all have a part in it!

This project was partially supported by the Ministry of Foreign Affairs of Israel; by the Agricultural Engineering, ARO, Israel, and by the research fund of Chief Scientist of the Israeli Agriculture Ministry.

Finally, I would like to thank for my dear parents, brother, sister in law, nephew, niece, and all my believer friends for their continuous prayers, patience, love and encouragement, which helped me to pursue and finish this work.

Timea Ignat

Israel, 2012

ABBREVIATIONS

AA – Ascorbic acid (g/100g)

DAA – Days after anthesis (day)

D_{abs} – Absolute distance of the quality points

DCIP – 2,6-dichlorophenolindophenol

DM – Dry matter (%)

DW – Dry weight

DT – Destructive reference test

Car – Carotenoid content (mg/g)

$CE_{Compression}$ – Coefficient of elasticity (N/mm) of the compression test

$CE_{Rapture}$ – Coefficient of elasticity (N/mm) of the rapture test

$CE_{Relaxation}$ – Coefficient of elasticity (N/mm) of the relaxation test

cv. –Cultivar

cvs. – Cultivars

GLM – Generalized linear model

HPLC – High pressure liquid chromatography

$Int_{Compression}$ – Integral under the load-deformation curve

LV – Latent variable

NCQI – New combined quality index

NDT – Non-destructive test

OP – Osmotic potential (mOsm/kg H_2O)

PC – Principal component

PCR – Principal component regression

PLS – Partial least square

RMSEC – Root mean square error of calibration

RMSECV - Root mean square error of cross validation

RPD – Robust parameter design

SAM_{degree} – Spectral angle map

SVM – Support vector machine

SWIR – Short wave infrared

SWS – Standardized weighted sum

TChl – Total chlorophyll content (mg/g)

TSS – Total soluble solid (Brix %)

VIS-NIR – Visible-near infrared

Table of Contents

1. INTRODUCTION

Export and local market both demands high quality sorted fruits and vegetables, which long preserves its fresh condition on the market. Additionally, there is an increased demand for fruits and vegetables that are beneficial for healthy life style as well as rich in ingredients that positively influence the prevention of any health malfunction.

Since in most of the agricultural products the changes of inner content and outer properties continues after harvesting, therefore it is crucial to determine the optimal harvest time properly. If the time of the harvest is not properly determined than it might negatively influences the quality of the product. It means that some properties either do not reach their optimal level or in the overripe stage the valuable components like vitamin C starts to degrade. Moreover, the shelf life of the fruit is being shortened due to harvest in the overripe or unripe stage. The consequences of being unripe are that the fruit does not get its cultivar specific properties, like colour, taste. The consequence of being overripe is that the produce gets soft faster, gets wrinkled, and tasteless.

The quality of the product is determined by the following attributes: colour, shape, size, and being without fault, damage or signs of sickness moreover, taste, texture, firmness, weight, internal chemical composition. Furthermore the product quality depends on the preferences and requirements of the consumers (Abbott, 1999).

Fresh bell pepper is abundant in valuable nutritional values therefore its popularity increases from year to year mainly as freshly consumed vegetable and as ingredient of processed food in the cuisine. Peppers are one of the main export produce of Israel and of Hungary among many other countries. Several cultivars are grown in Israel mainly in greenhouses or net-houses, in the southern part of the country. In Hungary the growth of bell pepper is not significant, more popular varieties are the 'Yellow Wax', 'Kapija', 'Ho F1', 'HRF', 'Pritamin' and the apple/tomato shaped cultivars. Peppers are mainly grown in greenhouses and open fields. At the present practise the harvest schedule is based on appearance and subjective experience of the growers. Since the maturity of the harvested pepper affects its final quality therefore there is a great importance in the accurate determination of the proper harvest time. Quality of pepper is a complex feature it includes among other characteristic parameters of colour (related to chlorophyll and carotenoid content), firmness, soluble solid, dry matter, and vitamin C content, (Dereje, 2003, Gomez-Ladron and Pardo-Gonzalez, 1996, Zsom-Muha, 2008). Routine measurements of these indices are generally destructive, time and labour consuming.

Harvested peppers need to be sorted and classified based on the requirements of the specific market where the product will be later on sent. Most of the cases, mechanical and manual sorting

lines are based on external appearance, and lacks the ability to examine essential internal quality attributes.

After considering the above facts I found it important to examine the changes during pepper fruit growth in order to develop a non-destructive and objective examination system for the evaluation and prediction of quality attributes of bell peppers during maturation. There is an increasing demand by both growers and packers for rapid, non-destructive evaluation methods for the determination of pepper quality change during growth, maturation and in the process of sorting and classification.

2.   LITERATURE

Bell peppers are taking a dominant place among the vegetables all over the world. Since its dietary value was discovered its place in the daily nutrition is more and more prevailing.

The world chili and pepper production grew from 20.8 million tons in 2000 to 27.5 million tons in 2010 (FAOSTAT, 2012). This fact creates a significant economic drive for more efficient production. The health related attributes of the bell peppers together with the healthy nutrition trend of the last decade creates increasing demand all over the world. More efficient production of the bell peppers will generate significant extra income for growers and packing houses.

2.1. Bell pepper biological attributes

Bell pepper is a cultivar group of the *Capsicum annuum* species, member of the nightshade *Solenaceae* family, which also includes potato, tomato and eggplant. Pepper plant demands warm weather, sunshine and plentiful irrigation.

Bell peppers originated in Mexico, Central America and northern South America. Pepper seeds were later carried to Spain (1493) and throughout the world. Due to the fact that bell peppers are very adaptable plants, being able to be grown in tropical and temperature climates, their cultivation and adoption into varying cuisines spread rapidly throughout many parts of the world. In the *Capsicum annuum* species there are many different varieties from the wild chilli to the sweet consumer types. Among all the cultivars the spice paprika and the sweet fresh consumer varieties gained distinguished importance. Cultivars of the fresh consumer pepper produce cultivated in different colours, size and shape (Fig. 1). The produce of the pepper plant is a puffed berry with hollow inside. The shape of the fruit can be round, flattened round, puffed prism, peaked, and crumpled inside or long thin. The colour of the pepper fruit also can vary greatly: green, yellow, red, orange, purple, white and the pale or transition of the previously mentioned colours. The size of the produce varies from 1 cm to 25 cm. Bell peppers have a delightful, slightly watery crunch. Green and purple peppers have a slightly bitter flavour, while the red, orange and yellow are sweeter and almost fruity (Fig. 2).

Fig. 1 Different cultivars of pepper   **Fig. 2** Bell pepper of different colours

Sweet peppers are plump, bell-shaped vegetables featuring either three or four lobes. They usually range in size from 5 to 13 centimetres in diameter, and 5 to 16 centimetres in length. Inside the thick flesh is an inner cavity with edible bitter seeds and a white spongy core. Bell pepper is an excellent source of vitamin C and natural antioxidants (Salunkhe, 1976). As it is shown in Table 1, 100 g of bell pepper contains 213% of the reference daily intake (RDA) of vitamin C, and 101% of vitamin A. It has high nutritional value, as well as popularity with regard to taste and colour (Frank et al., 2001). The level of ascorbic acid in peppers can vary according to cultivar, stage of maturity, growing conditions (Serrano et al., 2010, Perez-Lopez et al., 2007) and postharvest handling (Sakaldas and Kaynas, 2010, Lee and Kader, 2000). These antioxidants work together to effectively neutralize free radicals, which can travel through the body causing huge amounts of damage to cells (Knekt et al., 2002). Additionally, peppers are remarkable vegetables because of their significant provitamin A concentration, through its concentration of carotenoids such as beta-carotene (Duthie and Crozier, 2000; Pietta 2000). Red pepper is one of the few foods that contain lycopene, a carotenoid whose consumption has been inversely correlated with cancer. Consumption of vitamin C, beta-carotene, and folic acid, all found in bell peppers, is associated with a significantly reduced risk of cancer (Mateljan, 2007). Moreover, it is important to mention the high importance of chlorophyll concentration in pepper, especially in the new cultivar of 'Ever Green' which remains green coloured even in the fully ripe stage. Relevant studies have shown that chlorophyllin a food-grade derivative and structural analogue of chlorophyll strongly inhibits aflatoxin B_1 (AFB$_1$)-DNA damage and hepatocarcinogenesis in the rainbow trout therefore has anti-carcinogenic properties (Breinholt et al., 1995, Simonicha et al., 2008).

Table 1 Nutritional values of red bell pepper

Bell peppers (Capsicum annuum var annuum), red, raw, Nutrition value per 100 g (Source: USDA National Nutrient data base)		
Principle	Nutrient Value	Percentage of RDA
Energy	31 Kcal	1.50%
Carbohydrates	6.03 g	4%
Protein	0.99 g	2%
Total Fat	0.30 g	1%
Cholesterol	0 mg	0%
Dietary Fiber	2.1 g	5.50%
Vitamins:		
Folates	46 mcg	12%
Niacin	0.979 mg	6%
Pyridoxine	0.291 mg	22%
Riboflavin	0.085 mg	6.50%
Thiamin	0.054 mg	4.50%
Vitamin A	3131 IU	101%
Vitamin C	127.7 mg	213%
Vitamin E	1.58 mg	11%
Vitamin K	4.9 mcg	4%
Electrolytes:		
Sodium	4 mg	<1%
Potassium	211 mg	4.50%
Minerals:		
Calcium	7 mg	1%
Copper	0.017 mg	2%
Iron	0.43 mg	5%
Magnesium	12 mg	3%
Manganese	0.112 mg	5%
Phosphorus	26 mg	4%
Selenium	0.1 mcg	<1%
Zinc	0.25 mg	2%
Phyto-nutrients:		
Carotene-ß	1624 mcg	--
Carotene-α	20 mcg	--
Cryptoxanthin-ß	490 mcg	--
Lutein-zeaxanthin	51 mcg	--

As the fruit development advances the pepper fruit changes its size, colour, firmness, texture and internal composition. The cultivar specific colour (red, yellow, orange) develops only at the last stage of the maturation. All the previously mentioned parameters are cultivar specific. For each variety the rate of change of these values are different, therefore the discernment of proper harvest time is a complex issue. Generally the decision of the harvest time is based on the experience of growers.

Bell pepper belongs to the group of non-climacteric agricultural products, which means that the changes occurring after harvest is greatly depend on the state of harvest and post-harvest conditions (Almási et al., 1977).

Today bell pepper is grown in a wide range of climates mainly as an annual crop both in open fields and protected structures. The production of bell and chilli peppers in Israel was 134,700 tons in 2000 and grew to 294,300 tons in 2010, while the exported quantity of bell and chilli peppers in Israel was 20,519 tons in 2000 it grew to be 89,893 tons in the year of 2009. Data

source shows that the harvested area in Israel tripled within the period of 2000-2010. Israel is taking the 17th rank in the worldwide chilli and pepper production (FAOSTAT, 2012). Export markets show increasing demands for high-quality sorted fruits and vegetables, and the revenue from such high-quality products is much higher than the average income.

2.2 Pepper fruit development

Several features describe the development of pepper fruit. In the following lines these features will be detailed.

One of the features of fruit ripening is the change in colour; it is a consequence of chlorophyll disappearance, when the reddish/yellowish colouration due to carotenoids becomes perceptible. The green colour due to chlorophyll and carotenoids such as lutein disappear with the synthesis of chromoplast pigments (Hornero-Mendez and Minguez-Mosquera, 2000). During fruit ripening, chromoplast differentiation, from either chloroplasts or protoplasts, is very often accompanied by carotenogenesis, a de novo carotenoid biosynthesis that increases and even changes the intensity and characteristics of the colour in the ripe fruit (Minguez-Mosquera and Hornero-Mendez, 1994) The mechanism of chlorophyll disappearance is complex and still not fully understood. It has been established that the chlorophyll degradation pathway consists of three main steps involving three different enzymes, namely chlorophyllase, Mg-dechelatase and pheophorbide-a-oxygenase (Vicentiniet al., 1995). During the ripening of pepper fruits, de novo synthesis of carotenoid pigments occurs, and some of these (capsanthin and capsorubin) are exclusive to this genus (Minguez-Mosquera and Hornero-Mendez, 1994). This process is accompanied by a sharp decrease in chlorophylls as a consequence of the degeneration of chloroplast into chromoplast. The role of chlorophyllase during this process seems to be important: its activity is manifested in the ripening process, perhaps being a triggering or modulating factor of the de novo biosynthesis of carotenoid pigments (Hornero-Mendez and Minguez-Mosquera, 2002). The increase in activity has been related to senescence and maturation (Terpstra and Lambers, 1983). Furthermore the chlorophyll and carotenoids contents of pepper can vary in composition and concentration owing to differences in genetics and maturation (Markus et al, 1999; Russo & Howard, 2002).

The longer the fruits are maintained on the plant, the more physiological changes occur causing a switch toward senescence, and altered nutritive components. Change in fruit colour is also associated with loss of cellular integrity and reduced mobilization of macromolecules through the plant (Thimann, 1987). As fruits mature, physiological activity changes, and much of this change is regulated by enzymes. Two enzymes associated with fruit maturity in peppers are β-galactosidase and peroxidase. β-galactosidase in the latter stages of ripening degrades galactose-

containing cell wall polysaccharides causing the release of free galactose, this activity may lead to a loss of cell integrity (Carrington and Pressey, 1996). The amount of nutrients available to plants may influence accumulation of compounds in fruit as they remain attached to the plant. Concentration of β-galactosidase and peroxidase, accumulating prior to harvest, may affect the activity of these compounds after harvest and influence shelf-life and other quality factors. Even if the mode of activity is unclear, there is consensus that β-galactosidase and peroxidase have roles in the changes occurring in developing pepper fruit (Russo and Biles, 2003).

Deepa et al. (2007) found a sharp increase in carotenoid content monitored during three maturity stages and at the red/yellow stage carotenoid content showed the highest concentration in the studied 10 varieties of sweet pepper. Leja et al. (2008) investigated 'Spartacus' sweet pepper (Capsicum annuum) cultivar grown in foil tunnel. They harvested the fruits in three maturity stages: green, turning and red. The contents of total phenols, total carotenoids and evolution of endogenous ethylene were determined. They found during fruit ripening considerable increase in carotenoids. The most distinct synthesis of carotenoids was observed when fruits were converted to the full maturity stage (red colour). Russo and Howard, (2002) studied how growing conditions affect levels of carotenoids in pepper fruits as they mature. Ten pepper cultivars were examined, grown in glasshouse and in open field. Levels of total carotenoids in fruits of most cultivars were not affected by location of production at the green stage. At the turning stage, as well as in the red stage most cultivars had higher levels of total carotenoids if glasshouse grown. However, glasshouse production to improve carotenoid content was not universal, as indicated by higher levels of capsantin found at the red stage in fruits of field-grown pepper (Anaheim type). It is clear that there is no simple conclusion, that can explain the relative amounts and changes in carotenoid levels that occur with changes in colour that occur concurrently with maturation. The various cultivars exhibit variations in the evolution, distribution and chemistry of carotenoids in pepper fruits. Hornero-Mendez and Minguez-Mosquera (2002) suggest that carotenoid formation is a normal process, likely a result of senescence, and independent of chlorophyll catabolism.

Although sweet bell pepper (Capsicum annuum L.) is non-climacteric fruit with regard to postharvest respiratory pattern, mature-harvested pepper will progress to degrade chlorophyll while simultaneously synthesizing a variety of red and yellow carotenoids. Bell pepper is increasingly harvested at full colour due to growing consumer demand for peppers with improved flavour and nutritional aspects (Frank et al., 2001; Fox et al., 2005).

Another feature of fruit ripening is the change in soluble carbohydrates (sucrose, fructose, glucose).

Sucrose, glucose and fructose are the major components of the soluble neutral sugars found in pepper fruit (Nielsen et al., 1991). Nielsen et al. (1991) defined that fruit development can be divided into three phases: (1) an initial phase with high relative growth rate and hexose accumulation, (2) a phase with declining growth rate accumulation of sucrose and starch, and (3) a ripening phase with no further fresh weight increase and with accumulation of hexoses, while sucrose and starch were degraded. According to Nielsen et al. (1991), the carbohydrate metabolism in the growing fruit tissue is important to the partitioning of photosynthetically fixed carbon in the plant. Furthermore, the content of different sugars is critical to the quality of the fruit for consumption. Pepper fruits are harvested both as unripe and ripe, and the sugar content on the fruit tissue depends strongly on the harvest time. According to Nielsen et al. (1991), during maturation of the fruits there was a significant accumulation of hexoses. In the ripe fruits soluble sugars accounted for 4.4% of the fresh weight, which equaled 40% of the dry matter. According to Luning et al. (1994), sweetness in bell pepper appeared to be typical for ripe stages and closely related to glucose, fructose, total sugar, and dry matter content. However, sucrose was not related to changes in sweetness during maturation.

The next feature to be detailed is an effective antioxidant, the ascorbic acid. Despite the importance of AA, its biosynthetic pathway in different plant parts is not completely understood. The natural sugars are considered to be precursors of ascorbic acid, since they produce an increase in this acid when administered through the conductive tissues or the roots (Loewus, 1961). Wheeler and colleagues (1998) proposed the first pathway to gain acceptance. The so-called "Smirnoff-Wheeler" pathway for AA biosynthesis has as its immediate precursor L-galactono-1,4-lactone, and the intermediates involved are phosphorylated sugars and nucleotide-linked sugars. Several studies have confirmed this mechanism (Gatzek et al., 2002). This pathway would appear to be the main one for the biosynthesis of AA, but other pathways cannot be discarded (Barata-Soares et al., 2004).

A change in ascorbate metabolism was monitored by Imahori et al. (1998) during maturation of sweet pepper (Capsicum annuum L.) fruit. They investigated four stages of maturity, based on changes in peel colour from green to yellow; 100% green, 10-20% yellow, 50-60% yellow, 100% yellow. They found that ascorbate content in sweet pepper fruit increased during maturation.

Deepa et al. (2007) monitored with destructive methods (DICP dye titration) 10 cultivars of sweet pepper for the change of ascorbic acid during three maturity stages (defined by changes of colour and weight changes). Based on their study, ascorbic acid content declined progressively with advancing maturity.

Orban et al. (2011) examined the change of vitamin C by destructive Spanyár-method in three cultivars of pepper and in 8 different maturity stages (defined by colour changes). Based on their results the ascorbic acid accumulation increased until 80% of ripeness then decreased.

The textural feature of the pepper is influenced by the firmness of the whole fruit and the firmness of the fruit flesh. Firmness is one of the important factors determining market quality and consumer acceptance of peppers. The outer wall of a pepper covers large locular air spaces and is supported by 3 or 4 carpel walls around the equatorial axis. Placental tissue and seeds are located in the centre of the fruit and contribute little to the support of the wall.

A rapid decrease of flesh firmness during fruit ripening has been observed, and it is primarily due to changes in cell-wall carbohydrate metabolism that result in a decrease of certain structural components of cell wall (Bartley and Knee 1982). Polygalacturonase, pectin methyl esterase, beta-galactosidase and cellulase are the major enzymes related to fruit softening (White, 2002).

Cheng et al. (2008) studied five pepper cultivars with varying degrees in flesh firmness to identify biochemical characteristics related to fruit softening. Firmness of fruit flesh (with epidermis attached) and flesh (without epidermis) was measured at different developmental stages: premature (15–20 days post-anthesis (DPA), stage 1), green mature (commercially ripe, 30–35 DPA, stage 2), colour turning (fruit becoming 30–40 % red, 40–50 DPA, stage 3), and red ripe (fruit totally red, 60–70 DPA, stage 4) with a pressure tester. Firmness with and without the epidermis attached changed similarly in all pepper lines during development. Biochemical characteristics were measured which included insoluble pectin, soluble pectin, and cellulose contents, and the activities of pectin methyl-esterase (PME), polygalacturonase (PG), β-galactosidase, and cellulase. In all varieties, flesh firmness was highest at stage 3, and then decreased during development. Soluble pectin content also increased in all cultivars. Cellulose content normally decreased after stage 3, but these changes varied among varieties. With ripening PG and PME decreased in the most firm varieties, and cellulose and β-galactosidase were the key enzymes involved in the less firm cultivars. The authors concluded that changes of fruit firmness were to some extent correlated to the soluble pectin and cellulose content during development and ripening. However, the key biochemical characteristics causing fruit firmness changes were clearly different among the pepper fruit types.

Tadesse et al. (2002) measured pepper fruit firmness in different growth stages (1-11 weeks after anthesis), using an Effegi penetrometer. Fruit firmness increased with fruit size except that a slight reduction occurred in the final two harvests.

2.3 Definition of quality and maturity

Quality according to Kader (1999) or the degree of excellence or superiority of fresh fruits is a combination of attributes, properties, or characteristics that give each commodity value in terms of human nutrient. The relative importance of each quality component depends upon the commodity and its intended use and varies among producers, handlers, and consumers. To producers a given commodity must have high yield and good appearance, must be easy to harvest, and must withstand long-distance shipping to markets. Appearance quality, firmness, and shelf-life are important from the point of view of wholesale and retail marketers. Consumers judge quality on the basis of appearance, freshness and firmness. Moreover, consumer's satisfaction depends on previous experience of flavour during consumption. Consumers are also concerned about the nutritional quality, which are not only colourful and flavourful components of the diet, but also a good source of energy, vitamins, minerals, dietary fibres and bioactive compounds that enhance human health.

According to Kader (1999) maturity is the stage of development leading to the attainment of physiological or horticultural maturity. Physiological maturity is the stage of development when a fruit will continue ontogeny even if detached. Horticultural maturity is the stage of development when a fruit possesses the prerequisites for utilisation by consumers for a particular purpose. Maturity at harvest is the most important factor that determines storage-life and final fruit quality. Immature fruits are more subject to shrivelling, mechanical damage, and being flavourless. Overripe fruits are likely to become soft and mealy with insipid flavour soon after harvest. Any fruit picked either too early or too late in its season is more susceptible to physiological disorders and has a shorter storage-life than fruit picked at the proper maturity.

2.4. Quality requirements of bell pepper

Consumer interest worldwide in the quality of vegetable products has increased in recent years. Product quality is a complex issue. We can find many different way of describing the maturation and quality change of the pepper (Dereje, 2003; Gomez-Ladron and Pardo-Gonzalez, 1996; Zsom-Muha, 2008; Zsom et al., 2008; Petróczki, 2007; Láng, 1982). Moreover, visual characteristics, properties such as texture, the content of minerals and vitamins, flavour and other organoleptic characteristics must be considered. In addition, new knowledge shows that vegetables are appreciated for their beneficial health effects which underline the importance of nutraceutic properties. Recently, consumer demand for these parameters has greatly increased together with requirements for a higher content of minerals, vitamins, and bioactive substances (Schreiner et al., 2000; Schnitzler and Gruda, 2002).

Table 2 Overviews of quality parameters for pepper produce by different measurement methods

Quality parameter	Measurement method	Reference
colour	subjective (eyesight)	Orban et al. 2011
vitamin C	destructive method (modified Spanyár-method)	
peroxidase enzime	destructive method (DT)	
length, diameter, pericarp tickness, weight	manual	Serrano et al. 2010
colour	colourimeter	
total acidity	DT pH measurement	
total antioxidant activity	DT laboratory measurement	
sugars and organic acids	DT laboratory measurement	
total carotenoids	DT laboratory measurement	
firmness	DT Texture Analyzer, NDT NIR reflectance	Penchaiya, 2009
total soluble solid (TSS)	DT refractometer, NDT NIR reflectance	
diameter, length, weight, and surface area	manual	Diaz-Perez et al., 2007
water loss rate	gravimetrically	
firmness	using a 1–5 scale (1-spongy soft; 2-soft; 3-firm soft; 4-moderately firm; 5-firm)	
total phenolic compounds	DT laboratory measurement	Perez-Lopez, 2007
carotenoids	DT laboratory measurement	
colour	Hunterlab Colorflex spectrophotometer	
ascorbic acid	DT laboratory measurement (HPLC)	
size, weight	manual	Jarrett, 2007
capsaicinoids	DT laboratory measurement (HPLC)	
sucrose, glucose and fructose	DT laboratory measurement (HPLC)	
malic acid, and total acide	DT laboratory measurement (HPLC)	
total soluble solid	DT laboratory measurement	Martínez et al., 2007
titratable acidity	DT laboratory measurement	
fat, ash and protein contents	DT laboratory measurement	
potassium, calcium and sodium	DT laboratory measurement	
zinc, manganese and copper	DT laboratory measurement	
firmness	maximum rupture force, Instron	Raffo et al., 2007
organic acids and ascorbic acid	DT laboratory measurement (HPLC)	
sugars	DT laboratory measurement (HPLC)	
carotenoids	DT laboratory measurement (HPLC)	
phenolic compounds	DT laboratory measurement (HPLC)	
water content	oven-dry	Navarro, 2006
carotenoids	DT laboratory measurement	
antioxidant activity	DT laboratory measurement	
sugars	DT laboratory measurement (HPLC)	
ascorbic acid	DT laboratory measurement (HPLC)	
phenolic acid	DT laboratory measurement	
firmness	impact	Ignat et al., 2003b
ascorbic acid	DT laboratory measurement	Ignat et al., 2003a
firmness	impact	
firmness	impact	Tompos et al., 2003
ascorbic acid	2,6-dichlorophenol-indophenol method	Niklisa et al., 2002
dry matter	oven-dry	
total soluble solids	refractometer	
colour	colourimeter	
carotenoids	DT laboratory measurement (HPLC)	Russo & Howard, 2002
weight, volume	manual	Tadesse et al. 2002
colour	colourimeter	
firmness	Effegi penetrometer	
total soluble solid (TSS)	refractometer	
respiration and ethylene production	gas-liquid chromatograph	
carotenoids	DT laboratory measurement (HPLC)	Hornero-Mendez & Minguez-Mosquera, 2000
ascorbic acid	DT laboratory measurement (HPLC)	Simonne et al. 1997
provitamin A	DT laboratory measurement (HPLC)	
minerals	AOAC methods	
chromatic coordinates	colourimeter	Gomez-Ladron de Guevara & Pardo-Gonzalez, 1996
tint	DT laboratory measurement	
chlorophyll	DT laboratory measurement	
length, diameter, weight	manual	Marcelis & Baan Hofman-Eijer, 1995
dry matter	oven-dry	
weight, length/diameter ratio and the percentage of 2-, 3- or 4-lobed fruit	manual	Greber et al., 1988

In agriculture, quality determination of produce is based on a multitude of features (Dull, 1986): flavour (sweetness, acidity); appearance (colour, size, shape, blemishes, glossiness); and texture (firmness, mouthfeel). Physical and chemical quality attributes as quality parameters of pepper produce were measured by several different parameters as shown in Table 2.

Generally it can be concluded that most of the examined parameters are related to: dimension and weight; to colour, chlorophyll, and carotenoid; to total soluble solid, dry matter or sugars; to organic-, ascorbic-, and phenolic acid; and to firmness. Routine measurements for most of these indices are generally time and labour consuming. However, measurement of the maturity is essential since it affects the final quality of the harvested pepper. Most of the cases the determination of harvest schedule, sorting and classification are done by humans, by mechanical or manual sorting which is based on external indices and criteria, and lacks the ability to examine essential internal quality attribute. Moreover, there is a problem of subjective sorting, the inconsistency of humans in the classification and poor repeatability (Steinmetz et al., 1999b).

A more sufficient non-destructive method is needed to determine the optimum harvest time; to sort and to classify. It will certainly grant more consistent quality in bell pepper market and technical improvement for the growers and packaging houses.

2.5. Methods for quality determination of fruits and vegetables

Determination of agricultural product quality is a continuously developing subject. Especially that the requirements of vendors, customers and the volume of production increased tremendously in the past decades. Therefore it is a continuous task to improve the quality measurement methods in order to achieve higher quality produce from the farmers as well as to develop more efficient sorting and classification lines.

In the following I would like to detail the measurement methods which were used in the present study.

2.5.1. Colour measurements

The external appearance of fruits, particularly their colour, is of prime importance when considering the different attributes which define quality, and destined for fresh consumption. A visual impression which does not coincide with the established standard easily leads to refusal.

Colour is a human perception by definition. The standards for colour spaces representing the visible spectrum were established in 1931 by C.I.E. ("Commission Internationale de l'Eclairage", which in English is the "International Commission on Illumination"). It was intended to provide a standard approximately uniform colour scale. The three curves, $\bar{x}$, $\bar{y}$, and $\bar{z}$, when combined

with the input stimulus and integrated, generate three signals that relate closely to perceived colour. These signals, called tristimulus values, and denoted as X, Y, and Z, form the basis of most popular and useful colour.

There are two forms of colour measurement devices: those that measure spectral reflectance (spectrophotometers) and those that measure only tristimulus values (colorimeters). The main difference is that spectrophotometers measure physical properties (spectral reflectance, spectral transmittance, and spectral absorptance) from which tristimulus values are calculated. Colorimeters typically pass the light through specially designed filters allowing tristimulus values to be calculated directly from detector output levels.

There are many CIE colour spaces, which serve different purposes. They are all "device independent", unlike RGB or CMYK colour spaces which are related to a specific device. These RGB and CMYK spaces usually do not cover the entire visible colour spectrum. The CIE also specify lighting conditions.
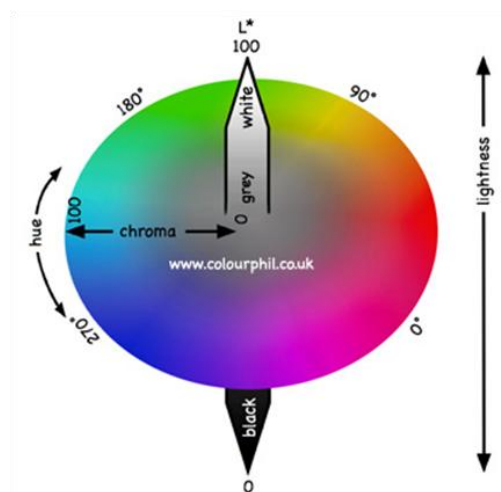
Fig. 3 LCH colour space (http://www.colourphil.co.uk/lab_lch_colour_space.html)

The CIE LCH colour space (applied in the present study) or colour model essentially is in the form of a sphere (Fig. 3). There are three axes; $L*$, $C*$ and $H°$. The $L*$ axis represents *Lightness*. This is vertical; from 0, which has no lightness (i.e. absolute black), at the bottom; through 50 in the middle, to 100 which is maximum lightness (i.e. absolute white) at the top. The $C*$ axis represents *Chroma* or "saturation". This ranges from 0 at the centre of the circle, which is completely unsaturated (i.e. a neutral grey, black or white) to 100 or more at the edge of the circle for very high Chroma (saturation) or "colour purity". Around the edge of the coloured circle can be seen every possible saturated colour, or *Hue*. This circular axis is known as $H°$ for *Hue*. The units are in the form of degrees (or angles), ranging from 0° (red) through 90° (yellow), 180° (green), 270° (blue) and back to 0°. LCH is device-independent.

Colour has long been used in the assessment of fruit quality. In fruits, a decrease in chlorophyll content is correlated with increasing maturity; this is traditionally used as the criterion for visual assessment of fruit maturity (Crisosto et al., 2007). Some fruits have one colour homogeneously distributed on the skin surface, and the averaged surface colour is a good quality indicator for these fruits. In the early years of application of computer vision to fruit inspection, fruit colour assessment relied on grey-scale images captured by monochrome cameras, for instance, for classification of oranges in colour classes. This approach is only applicable when the product is mono-coloured, and defect detection is not required. Other fruits, like some cultivars of peaches, and apples, have a secondary colour that is frequently used as an indicator of maturity, which often is not reliable. Produce colour sorting in modern packinghouses is performed using RGB colour video-cameras. Each pixel in a colour image consists of three intensity values, since any colour can be reproduced by the combination of three primary colour components: blue, green, and red. Each of these components: R, G and B, covers a large part of the visible spectrum. The techniques require previous and also continuous training to adapt the system to the great colour variability present in products like fruits (Blasco et al., 2007; Lleo et al., 2009). Image colour accuracy and spatial resolution have been greatly improved in three-chip (CCD, CMOS) cameras (Pitre et al., 2010). Three-chip colour cameras use dichroic prisms to direct the light in each of the three wavebands.

Gomez-Ladron de Guevara and Pardo-Gonzalez, (1996) studied the evolution of colour in 13 paprika pepper varieties by means of Minolta CR-200 colorimeter (CIELAB colour coordinates). The authors found that among the CIELAB colour attributes, saturation (S*) is the most appropriate for distinguishing the different fruit ripening phases.

Tadesse et al. (2002) studied the effect of harvesting sweet pepper at different stages of growth and development on physicochemical attributes. Colour change (LCH values) of the fruit skin was measured at three points on the surface by Minolta Chromameter (CR-100). Hue angle declined with time while chroma values increased with fruit maturity. They found that colour change and TSS were reasonable indicators of maturity of sweet pepper fruit complemented with fruit firmness.

The evolution of fruit weight, colour, nutritive (sugars and organic acids) and bioactive compounds (total phenolics, carotenoids, and ascorbic acid) was evaluated along the growth cycle with applied mix of nitrophenolates in the irrigation system by Serrano et al. (2010). Colour measurements were conducted by Minolta colorimeter CR200 (L*, a*, b*). They found that colour (a*) and carotenoid evolution was similar for both control and treated fruits along the growing process. The colour a* parameter varied very little from fruit set to day 36 and increased

23

sharply from days 39 to 57, due to colour changes from green to red, which occurred in the last phase of fruit growth, when the fruit was near its maximum weight.

In general, online fruit colour grading by means of computer vision is considered solved and is widely used now by the industry. However, colour sorting is not suitable for measuring or assessing internal quality, which may require multi- and hyperspectral imaging.

2.5.2. Visible and NIR spectral measurements

Chemical bonds absorb light energy at specific wavelengths; therefore some compositional information can be determined from spectra measured by spectrophotometers or spectrometers. Within the visible wavelength range, the major absorbers are the pigments: chlorophylls, carotenoids, anthocyanins and other coloured compounds. Water, carbohydrates, fats and proteins have absorption bands in the NIR region.

The reflectance properties of a product in the visible region (approximately 400–750 nm) are perceived by humans as colour, which provide pigment information about commodities. Skin colour has been considered indicative of maturity for some horticultural products such as banana, mango, and tomato (Edan et al., 1997). Colour, in the human perception directly relates to product appearance (Abbott, 1999), and the relationship of pigments, and therefore the VIS reflectance fingerprint, with deterioration and evolution of fruits during ripening has been established. Many constituents of fruit quality, including those that contribute to taste and aroma as well as antioxidant potential are synthesized in chloroplasts or chromoplasts, and in the genes (Barry, 2009). In the food industry, quality factors are often linked to product pigments or colour features. VIS imaging sensors are thus effective techniques for quality detection of fruits, especially for maturity and ripeness.

Ortiz et al. (2001) related VIS-NIR spectral information to soluble solids, acidity and firmness of peach fruits. Zude et al. (2006) examined soluble solid content in apples by VIS-NIR. Wang et al. (2011) estimated vitamin C content in chilies using quantitative analysis technique based on VIS-NIR diffuse reflectance spectroscopy. Significant correlations were found between the chlorophyll content of apple fruit and spectral transmittance recordings, using the red-edge values as well as various indices used in remote sensing and partial least square regression in the spectral range from 600 to 750 nm by Zude (2003). Merzlyak et al. (2003) studied the diffuse light reflectance of apple fruit in the spectrum range from 400 to 800 nm. They used five apple cultivars, all picked in mature condition and obtained significant correlation between different reflectance indices and fruit chlorophyll content. Xudong et al. (2009) non-destructively

measured quality indices (soluble solids contents, titratable acidity, vitamin C content, and colour) of intact Nanfeng mandarins by using the VIS-NIR spectral range.

NIR radiation covers the range of the electromagnetic spectrum between 780 and 2500 nm (Sheppard et al., 1987). In NIR spectroscopy, the product is irradiated with NIR radiation, and the spectrum of the reflected or transmitted radiation is measured. The spectral characteristics of the incident ray are modified while it passes through the product due to wavelength dependent absorption and scattering processes. This change depends on both the chemical composition and the physical properties of the product (Nicolai et al., 2007). The short-wave infrared region is that part of the electromagnetic spectrum lying between 750 and 1900 nm, associated with vibration and combination overtones of the fundamental O–H, C–H and N–H bonds, which are the primary structural components of organic molecules (Williams and Norris, 2002).

Chemometric statistical techniques such as partial least squares regression (PLS), multi-linear regression (MLR) and principal component analysis (PCA) are then applied to correlate the NIR spectrum to quality attributes such as the sugar content, acidity, firmness or storage period of the product (Schmilovitch et al., 2000).

NIR measurements have been successfully used to non-destructively quantify and characterize fruits and vegetables ingredients, and these techniques have been used successfully for rapid analysis of multiple components, such as oil, protein (Schmilovitch et al., 2001; Shenk et al., 1992), dry matter (Schmilovitch et al., 2000), firmness (Penchaiya et al., 2009, Schmilovitch et al., 2000) and total soluble solids (Penchaiya et al., 2009; Schmilovitch et al., 2000; Zude et al., 2006) in a wide variety of agricultural produce. Blanco et al. (1993) used NIR diffuse reflectance spectroscopy to determine ascorbic acid in pharmaceutical products. Microstructure of the fruit and vegetable tissue affects the propagation of NIR, therefore NIR spectroscopy has successfully applied in measuring microstructure related attributes such as internal damage (Clark et al., 2003), stiffness (Lammertyn et al., 1998).

More widespread use of these technologies depends on several factors. The most important technical factor is the prediction model's robustness. The accuracy of the NIR calibration models should be sufficient in predicting unknown samples which did not participate in the calibration model. Calibration models should be based on large datasets, including samples from different origins, climate conditions, and seasons. The issues of temperature sensitivity of NIR measurements should be considered (Roger et al., 2003) and transfer of a calibration model to a different spectrophotometer (Greensill et al., 2001).

2.5.3. Hyperspectral imaging

Multi- or hyperspectral cameras permit image acquisition at many wavelengths. Multispectral imaging means to acquire images fewer than ten wavelengths. If the number of wavelength is more than ten, then we talked about hyperspectral imaging. The acquired images can be visualized in a hyper cube with the X and Y dimensions being the length and width of the image and the Z dimension being spectral wavelengths. The dataset also could be envisioned as single wavelength pictures of the object, with as many pictures as the number of wavelengths used. Such imaging can provide information about the spatial distribution of constituents (pigments, sugars, moisture, etc.) near the product's surface (Ruiz-Altisent et al., 2010).

Imaging and spectroscopy are integrated in hyperspectral imaging, therefore it simultaneously acquires both spectral and spatial information from the product, thus making it especially suitable and much more powerful for inspecting horticultural and food products (Kim et al., 2001; Gowen et al., 2007). Hyperspectral imaging is implemented in line scanning mode or in filter-based imaging mode (Lu and Chen, 1999). In line (push-broom) scanning mode, the imaging system line scans the moving product item, from which three-dimensional hyperspectral images, also called hypercubes, are created. Line scanning mode is most commonly used because it is relatively easy to implement, and preferable when online applications are needed. In filter-based imaging mode, spectral images are acquired from the stationary product item for a sequence of wavebands using either liquid crystal tunable filter (LCTF) or acousto-optic tunable filter (AOTF). Filter-based hyperspectral imaging systems require more complicated calibration and are not suitable for online applications (Ruiz-Altisent et al., 2010).

Hyperspectral imaging technology was used for measuring fruit maturity, firmness and soluble solids content (ElMasry et al., 2007; Lu and Peng, 2007; Noh et al., 2007), and for detecting bruises and bitter pits on apple and mushroom (Nicolai et al., 2006; Gowen et al., 2008) deterioration in mushroom (Taghizadeh et al., 2010) and chilling injury and internal defect of cucumber (Cheng et al., 2004; Ariana and Lu, 2010). Hyperspectral imaging is feasible for implementation into fast, online sorting and grading of horticultural products (Ariana and Lu, 2010).

2.5.4. Mechanical methods for firmness measurement

Mechanical properties of the fruit relate to texture. Harker et al. (1997) examined the cellular basis of fruit texture and the human physiology involved in its perception. Mechanical tests of texture include the familiar puncture, compression and shear tests, as well as creep, impact, sonic

and ultrasonic methods (Brown and Sarig, 1994; Chen, 1996; Abbott et al., 1997; Felföldi and Ignát 1999; Tompos et al., 2003; Ignat et al., 2003; Ignat et al., 2010).

2.5.4.1. Ultrasonic vibration

Ultrasound technology has been known for many years, its main application areas being medical diagnostics, and industrial processes and inspections. At high frequencies and low power it can be used as an analytical and diagnostic tool, and at a very high power it can assist processing. Ultrasonic vibrations are above the audible frequency range: >20 kHz. Ultrasound is generated by a transducer contains a ceramic crystal which is excited by a short electrical pulse that has a typical form of several sine cycles. Through the piezoelectric effect, this electrical energy is converted to a mechanical wave that is propagated as a short sonic pulse at the fundamental frequency of the transducer. This energy is transferred into the material or body under analysis and propagated through it (Krautkramer and Krautkramer, 1990). The ultrasound signal emerging from the test specimen is sensed by a piezoelectric element that acts as a receiver, converting any ultrasound impinging on it, back to electrical energy. When the system operates in 'pulse-echo' mode, the same piezoelectric element acts as a transmitter and a receiver alternately; when a 'through-transmission' mode is used, a second piezoelectric element acts as a receiver.

Ultrasonic energy will propagate through a material until the sound wave encounters an impedance change, which means that there are some changes in the material density or/and the velocity of the sound wave (Kuttruff, 1991). The energy attenuation of the ultrasound beam and the speed of wave propagation depend on the nature of the material and its structure (Kuttruff, 1991). The most physical or chemical changes in the material, cause changes in the attenuation and velocity of the propagated beam.

The potential for ultrasound in the food industry has been recognized since the 1970s (Povey and Wilkinson, 1980), and developments regarding the technique have progressed rapidly over the years (Povey, 1998). However, development of the ultrasound technique as a means of evaluating food quality has not progressed as fast in the fresh fruit sector as in the food industry. Lack of appropriate equipment, sufficiently powerful to penetrate but, at the same time, sufficiently gentle to avoid damage to the sensitive tissues of fruit and vegetables, has been an important deterrent (Porteous et al., 1981; Mizrach et al., 1989). However, some advances in equipment design, and availability of new instruments and sensors, mainly designed for industrial use with new composite materials, has facilitated progress and has stimulated more studies and developments of ultrasonic methods and techniques for the fresh fruit and vegetables market (Mizrach et al., 1989). Recently, ultrasonic techniques have been investigated for the

sensory analysis of various quality parameters in agricultural produce. Various devices and measuring techniques, based on ultrasonic waves, have been developed for non-destructively monitoring some physiochemical, biochemical, and mechanical changes that occur in fruit tissues during the various stages of their pre- and postharvest existence. These stages include growth and maturation (Self et al., 1994; Chivers et al., 1995; Mizrach et al., 1999a, b; Gaete-Garreton et al., 2005, Ignat et al., 2010), storage under various conditions (Flitsanov et al., 2000; Mizrach et al., 2000; Verlinden et al., 2004) and shelf-life (Mizrach and Flitsanov, 1999; Mizrach, 2000; Johnston et al., 2002). Many studies, describe difficulties and limitations in applying the ultrasound technique for quality evaluation in the pre- and postharvest processes. This suggests that the technology is not yet ripe for commercial use and that there is a lot yet to be done in order to bring it into a widely used sorting tool (Mizrach, 2008).

2.5.4.2. Mechanical tests

Under mechanical loading, fruits and vegetables exhibit viscoelastic behaviour which depends on both the amount of force applied and the rate of loading. However, for practical purposes, they are often assumed to be elastic and loading rate is largely ignored. Measurement of elastic properties requires consideration of only force and deformation, whereas viscoelastic measurement involves functions of force, deformation and time. Nonetheless, because even the firmest fruits and vegetables do have a viscous component to their force-deformation behaviour, loading rate (test speed) should be held constant in instrumental tests and should be reported. The viscous component has minimal contribution to perceived texture in most firm fruits and vegetables (e.g. apple or carrot), but is quite significant in soft fruits, notably tomato, cherry, pepper and citrus. That is why a creep or relaxation measurement is often more suitable for the latter products than is a puncture test (Abbott, 1999).

Most non-destructive mechanical methods measure elastic properties: modulus of elasticity at very small deformations. Modulus of elasticity measures the capacity of the material to take elastic deformation and is the stress–strain ratio, commonly measured by the slope of the force and deformation curve prior to rupture for a tissue specimen with constant cross-sectional area (Abbott, 1999).

Puncture or compression tests made at relatively low speeds, typical of such instruments as the Magness–Taylor fruit firmness tester and electronic universal testing instruments, are considered quasi static. Typical stress-strain curve is shown in Fig. 4.
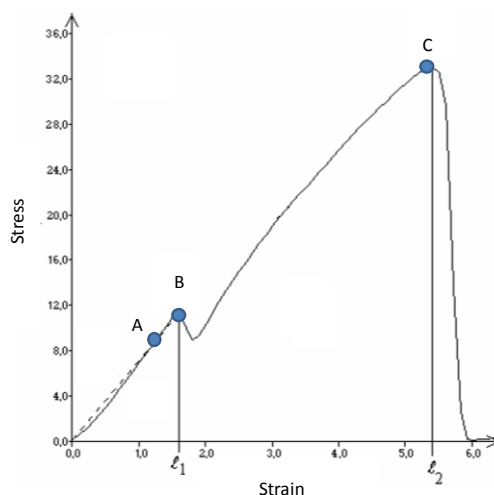
Fig. 4 Typical stress-strain curve

The portion of the initial slope up to inflection represents non-destructive elastic deformation (A). Beyond that portion, cells start to rupture and there may be a bioyield point (B) where a noticeable change in slope occurs before the rupture point (C) at which significant tissue failure occurs. Beyond rupture, the force may again increase, level off, or decrease as deformation increases.

Puncture force-deformation curves appear similar to compression curves. Firmness of horticultural products can be measured by compression or puncture with various probes at different force or deformation levels, depending on the purpose of the measurement and how the quality attributes are defined. Horticulturists tend to define firmness as the maximum force attained. On the other hand, the slope of the force-deformation curve, reflecting apparent elastic modulus, is often used by materials engineers as an index of firmness. Bourne (1982) found that the best relationships to sensory firmness, hardness and crispness are obtained with forces at or beyond deformations that cause tissue damage.

Penetrometer testers such as the Magness-Taylor are widely used for fruits and vegetables. The Magness-Taylor tester was developed primarily as an objective measurement of picking maturity (Magness and Taylor, 1925). Penetrometer measurements are moderately well correlated with human perception of firmness and with storage life, and consequently this technique has received acceptance for a number of horticultural commodities, such as apple, cucumber, kiwifruit, pear and peach. Compression and penetration techniques due to their low speeds and often destructive nature, are not very adaptable for on-line sorting of horticultural products.

Mechanical techniques have been developed to non-destructively measure some quality parameters of fruit and vegetables, mainly for firmness estimation, providing an alternative to the destructive Magness–Taylor penetrometry (Garcia-Ramos et al., 2005; Nicolai et al., 2006).

Major mechanical techniques include the measurement of variables extracted from quasi static force-deformation curves (Fekete and Felfoldi, 2000), the analysis of impact forces (Felfoldi and Ignat, 1999), and the measurement of acoustic responses to vibrations (Felfoldi, 1996) and impacts.

Measuring the variables of force-deformation curves by applying a small deformation force to the fruit with a metallic plunger in such a way that it causes no damage, the non-destructive force-deformation curve can be recorded. The curve is produced by applying a small load for a fixed period of time (Macnish et al., 1997) or by calculating the force necessary to reach a pre-set deformation (Fekete and Felfoldi, 2000). This non-destructive technique has led to the development of a number of force-deformation devices. One of them is the durometer which has been widely used for tomatoes, cherries (Clayton et al., 1998) and other soft fruits. Macnish et al. (1997) describe two non-destructive devices for measuring firmness: the Analogue Firmness Meter and the Digital Firmness Meter. These devices have been used with tomatoes and mangos. The fruit is placed in a v-shaped structure, and then a 40 mm diameter disc is applied to it. A non-spectroscopic method of measuring mechanical deformation with a laser has been developed by Hung et al. (1999), known as the "laser air-puff", this device measures the deformation of fruits subjected to a short but strong current of air (69 kPa in 100 ms). Lu and Tipper (2009) develop a portable bioyield detection device to measure apple fruit firmness, which measure force at the bioyield point as an indication of fruit firmness.

Firmness testers have a wide range of application, some of them can be integrated to sorting lines.

2.6. Prediction of bell pepper quality

For the determine of pepper quality - which had been described in chapter 2.1.4 - as efficiently and accurately as possible, appropriate sensors should be selected and algorithms must be developed. In recent years the prediction of quality parameters for pepper by different chemometric procedures started to take place. Especially as the awareness of this vegetable's importance greatly increased and its quality prediction became more urgent to pursue. Table 3 give an overview of the recently conducted works on the prediction of quality parameters of peppers from different cultivars. Most of the work was focused on internal components, especially on capsaicionids. Penchaiya et al. (2009) found prediction models for soluble solids and firmness using SWIR spectral measurements and PLS regression. Tadesse et al. (2002) used generalized linear model (GLM) to build prediction model which it needs destructive measurements of the fruit. Ignat et al. (2010) used non-destructive (ultrasonic, colorimeter and relaxation) methods to predict DW and TSS content of three cultivars of bell pepper. Ignat et al.

(2011b) established prediction models for the estimation of total chlorophyll and carotenoid content using VIS-NIR and SWIR spectral measurement, and by linear and non-linear chemometric procedures.

There is a need to develop methods and algorithms for the evaluation and prediction of global quality changes in pepper which relates to maturation and senescence, during growth, development, storage and shelf life. Moreover, there is a need to establish complex prediction models using several cultivars and different growing conditions and technologies.

Table 3 Overviews of prediction of quality parameters for pepper produce by different measurement and regression methods

Predicted componenet	DT Method	NDT Method	Regression Method	Reference
chlorophyll, carotenoid	Conventional method	VIS-NIR, SWIR	PLSR	Ignat et al., 2011b
ascorbic acid	2, 6-dichloro-indophenol titration method	VIS-NIR, SWIR	PLSR	Ignat et al., 2011a
vitamin C	2, 6-dichloro-indophenol titration method	VIS-NIR	PLSR	Wang et al., 2011
DW, TSS	Conventional method, Refractometer	Ulrtasonic, Relaxation, Colour	PCR	Ignat et al., 2010
organic acids, fatty acids, amino acids; minor compounds such as trigonelline, C4-substituted pyridine, choline, and cinnamic derivatives	Conventional method	HRMAS-NMR	PLSR-DA	Ritota et al., 2010
firmness	Texture Analyzer	SWIR	PLSR	Penchaiya et al., 2009
soluble solid (SSC)	Refractometer	SWIR	PLSR	
capsaicinoids	Conventional method	NIR	PCR, PLSR	Park et al., 2008
capsaicinoids	HPLC	UV−VIS	PLSR	Davis et al., 2007
carotenoids	Comparison to carotenoid standards	FT-Raman	-	Schulz et al., 2005
lutein, beta-carotene, capsanthin	Measurements of relative change	NIR-FT-Ramman	-	Baranski et al., 2005
weight, volume	manual colourimeter			Tadesse et al. 2002
colour				
firmness	Effegi penetrometer refractometer	-	PCA, GLM	
total soluble solid (TSS)				
respiration and ethylene production	gas-liquid chromatograph			
capsaicinoids	HPLC	NIR		Tsou et al., 1997

2.7. Prediction of quality by fusion

Sensor fusion is analogous to the cognitive process used by humans to integrate data continually from their senses to make interferences about the external world. Sensor (or data) fusion refers to the acquisition, processing, and combination of information generated by multiple knowledge sources and sensors (Hall, 1992). The objective is to provide optimal use of the available

information for detection, estimation, and decision-making. The original motivation for sensor fusion in the early Eighties was rooted in military radar applications. Later on the implementation of sensor fusion systems became common in a wide variety of applications, due to advances in sensor technology, signal processing algorithms, high performance computing and communication (Varshney, 1997). The advantages of sensor fusion are that it offers redundancy, complementary, real-time performance and cost-effective information (Luo et al., 2002).

There are three major ways in which multiple sensors interact (Brooks and Iyengar, 1998; Faceli et al., 2004): complementary when they do not depend on each other directly, but are combined to give a more complete image of the phenomena being studied; competitive sensors provide independent measurement of the same information, regarding a physical phenomenon; cooperative sensors, combine data from independent sensors to derive information that would be unavailable from the individual sensors.

Fusion of redundant information can reduce overall uncertainty and thus increase the accuracy with which the features are perceived by the systems (Durrant-Whyte, 1988; Janssen and Niehsen, 2004). In addition, complementary information from multiple sensors allows features in the environment to be perceived that would otherwise be impossible to acquire if we only used the information supplied from each individual sensor operating separately (Janssen and Niehsen, 2004; Luo et al., 2002).

The methodology for fusion suggested by Steinmetz et al. (1999b) shown in Fig. 5. They suggest a process containing eight steps to establish fusion. The process starts with the examination of the different properties of the produce. The next step is to choose the appropriate destructive (reference) and non-destructive tests for the measurement of the produce properties, followed by the selection of the best fitting chemometric procedure. The suggested process contains the evaluation of the system and possibilities for its improvement.

Table 4 present an overview of the some of the research works which were conducted in the recent years in the field of agriculture, focusing on the quality prediction of fruits and vegetables. As it is presented in the overview there are no standard rules in making fusion. In the realization of fusion a wide range of sensors are used online or in the training set with wide spectrum of statistical regression, classification and learning machines in order to predict the quality of the product. But in each cited cases it was concluded that by fusion the error of regression or error of classification was significantly reduced. This fact encourages the continuation of this research field to be used in wider product range and as a possible tool in the complex quality prediction.
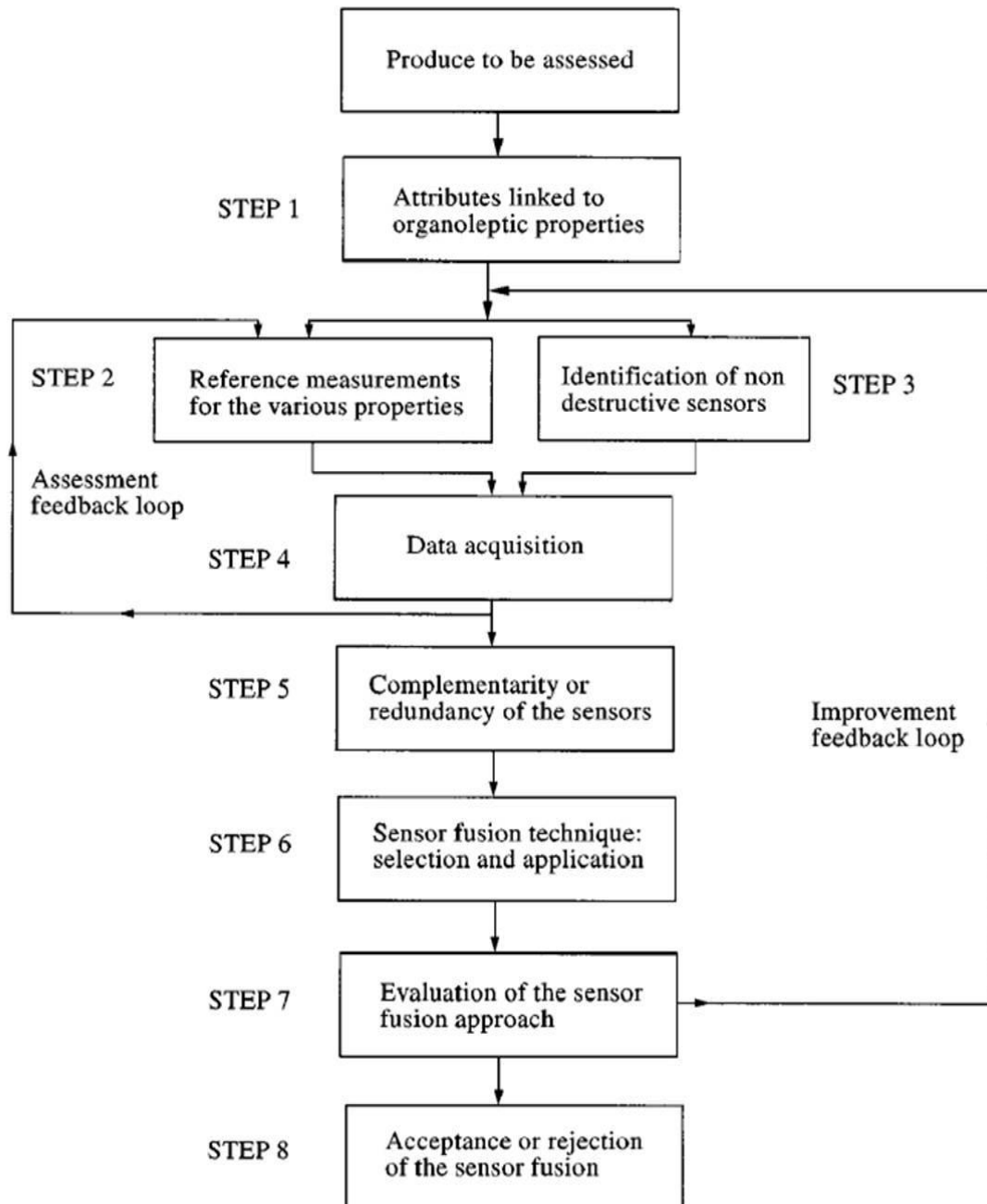
Fig. 5 Description of the methodology (Steinmetz et al., 1997)

Table 4 Overviews of prediction of quality parameters by fusion

Agricultural product	Predicted componenet	DT Method	NDT Method	Statistical Method	Reference
pepper	shrinkage		Weight	ANN	Mohebbi et al., 2011
	firmness	Texture Analyzer			
	colour		Image acqusition		
pepper	DW	Conventional method,	Ulrtasonic, relaxation,	PCR	Ignat et al., 2010
	TSS	Refractometer	colour		
tomato	colour		colorimeter	Bayesian classifier	Baltazar et al., 2008
	firmness		impact and acoustic test		
apple			electronic nose (Enose),	PCA, PNN	Li et al., 2007
	bruise		surface acoustic wave		
			sensor (zNose^{TM})		
apple			Acoustic impulse	PLS, discriminant partial	Zude et al., 2006
	firmness		resonance frequency	least squares (D-PLS)	
			sensor		
	soluble solids content (SSC)		VIS/NIR		
apple	colour, shape, weight, size, defects	Manual measurements	Colorimeter	Fuzzy logic	Kavdir and Guyer, 2003
eggplant	colour, length, girth, bruises		image processing	ANN	Saito et al., 2003
peach	Firmness	Penetrometer (Magness–Taylor)	MMS1-NIR, electronic nose	PLS, PLS/DA	Natale et al., 2002
	SSC	refractometer			
	Acidity, chlorophyll, carotinoids, anthocyans	Laboratory measurement			
peach				k-means clustering, stepwise discriminant analysis	Ortiz et al., 2001
	soluble solid (SS)	Refractometer	VIS-NIR		
	titratable acidity	Titration			
	firmness	Magness-Taylor penetration, Confined compression test, Shear rupture test	Non-destructive impact response		
apple	sugar	Refractometer	Vision system, NIR	multilayer neural network (MNN)	Steinmetz et al., 1999a
orange	size, weight		Vision system	PCA, MLR, FDA, NN	Steinmetz et al., 1997
	firmness		Impact firmness sensor		
	total soluble solids (TSS)	Refractometer	NIR		
	acidity	Titration			
	colour		Colorimeter		
peach			sound-based sensor, micro-deformation based sensor, impact based sensor	Bayesian classifiers associated with heuristic methods for identity fusion	Steinmetz et al., 1996
	firmness, stiffness	Magness-Taylor, Instron-type machine			
cantaloupes	colour, size, shape		NDT sensors	NN	Ozer et al., 1995
	firmness				
	weight				

3. OBJECTIVES

The objectives of the present work are:

I.   To explore the relationship between several non-destructive testing methods and the state of maturity, inner composition, textural, and physiological parameters (DT parameters).

II. To develop a rapid reliable non-destructive cost effective system to measure quality index of bell pepper.

The above objectives were realized in the following steps:

A. Examination of internal and external quality changes during growth and maturation for the selected, three different final colour (green, yellow, red) bell pepper cultivars.

B. Evaluation of textural and internal content prediction ability of several NDT methods such as:
   a.   Colour measurement
   b.   Relaxation test
   c.   Ultrasonic test
   d.   Spectral measurements in the range of visible-near infrared
   e.   Spectral measurements in the range of short wave infrared
   f.   Hyperspectral imaging.

C. Evaluation of the synergetic effect of the combination of the above NDT methods by fusion.

D. Evaluation of the synergetic effect of the fused DT quality parameters and NDT methods by fusion.

4.   MATERIALS AND METHODS

The experiment of the present study based on a preliminary experiment which was carried out during March-May 2009 on fruits taken from 2 greenhouses: 'Vergasa' (red) and 'Ever Green' (green) cultivars. The preliminary experiment consisted from two parts: the examination of changes during fruit development and the storability of the harvested fruit. Based on the results and experiences of the preliminary experiments (Appendix 9.2.1) the presents studies' experiment was chosen and established.

4.1. Plant material

The experiments were carried out from December 2009 through February 2010, and involved fruits of three cultivars of different colours, taken from three greenhouses from the same area of En Tamar region, Israel. The particular cv.-s were 'Ever Green' (green final colour variety), 'No. 117' (yellow final colour variety), and 'Celica' (red final colour variety). Each cultivar was grown in a separate greenhouse; plants were grown on the soil with drip irrigation. Plants were irrigated 3 times a day, with 5 m^3 solution contains 10 l fertilizer (7 % Nitrogen, 3% Phosphorus, and 7% Potassium). Pepper plants were grown in the 'Spanish' system, which means that the plants were supported vertically by ropes (Fig. 6).

Fig. 6 'Spanish' system, vertically supported growing technology

The peppers chosen for the study were marked during their flowering stage (Fig. 7a). Fruits (Fig. 7b) were picked nine times at weekly intervals, during the 9-week growing period, from the 34th day after flowering (DAA) until full ripening (88th day). Each picked batch of each variety

contained 20 fruits; altogether 180 fruits of each cultivar were collected. Table 5 presents all the collected pepper samples according to DAA. Shortly after picking, fruit had been cooled and kept in an air-conditioned laboratory at 23°C. First, each batch of 60 fruits (20 pieces of 'Ever Green', 20 pieces of 'No.117' and 20 pieces of 'Celica') were numbered, weighed and measured their length and diameter at the shoulder of the fruit, then each pepper sample was subjected to NDT measurements than immediately followed by sampling from the same location for further destructive determinations. All the examinations were carried out on one particular surface of the pepper fruit as it is depicted in the below figure (Fig. 7c).

| **Fig. 7a** Marking of the fruits in the flowering stage | **Fig. 7c** Marked pepper fruit in the unripe stage ('Celica' cv. is depicted) | **Fig. 7c** Chosen surface of DT and NDT measurements |
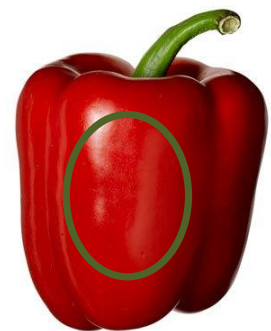
4.2. Experimental setup for non-destructive testing

4.2.1. Colorimeter

Shortly after picking, each fruit's colour was measured by colorimeter. Minolta Data Processor DP-301 of Chroma Meter CR-300 series was used for colorimetric measurements. Colour indices were taken at half length and two sides of each pepper fruit. The first measured side is the dedicated side, where all the measurements were conducted (Fig. 4c), and the second side is the opposite side of the dedicated surface. The two measurements were averaged. The following colour indices were recorded: Lightness (L), Chroma (C) and Hue (h).

Table 5 Presentation of the collected pepper fruits according to the DAA

DAA	Ever Green	No.117	Celica
34th	Picture is missing	Picture is missing	Picture is missing
40th			
47th			
54th			
60th			
67th			
74th			
81st			
88th			

4.2.2. Spectral measurement

The experimental arrangement for testing pepper fruits included a USB2000 (Ocean Optics, Dunedin, FL, USA) minispectrometer (Figs 8a and 8b), with spectral range 340–1014 nm; grating, 600 lines blazed at 750 nm; optical spectral resolution, 1.2 nm at FWHM (Full Width at Half Maximum); spectral sampling interval, 0.5 nm, 2048 data points with bidirectional

reflection probe (BIF600-UV-VIS). The instrument uses one fibre to collect radiation reflected toward the spectrometer, and a bundle of six fibres to carry light from the LS-1 Tungsten Halogen Light Source (Ocean Optics, Dunedin, FL, USA). The incident beam, carried via the bidirectional reflection probe fell perpendicularly onto the fruit sample, and the reflected light was collected by the collecting fibre and guided to the slit of the spectrometer. The setup included a cone (25-mm-diameter base, 15 mm in height, with a slope of 450), which shielded the optical assembly and the measured surface of the fruit from ambient radiation. Because of noise in the ranges of 340–477 nm and 950–1014 nm in the spectral data of the USB2000 spectrometer, the spectral range had to be reduced to 477–950 nm.
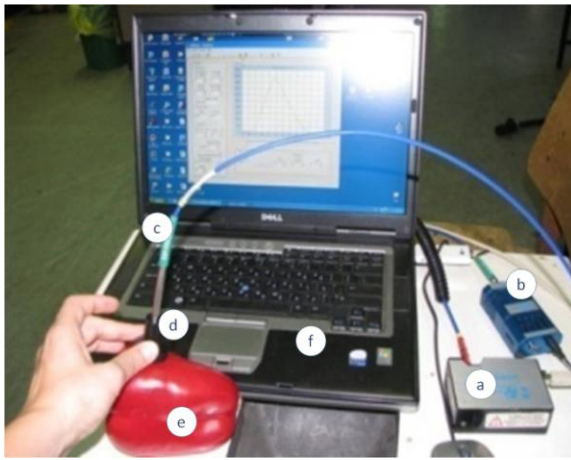
Fig. 8a Experimental setup for VIS-NIR spectral measurements; a: USB2000 spectrometer, b: Illumination source, c: Bidirectional reflectance probe, d: ∅ 25 mm cone, e: Pepper sample, f: PC for data acquisition.
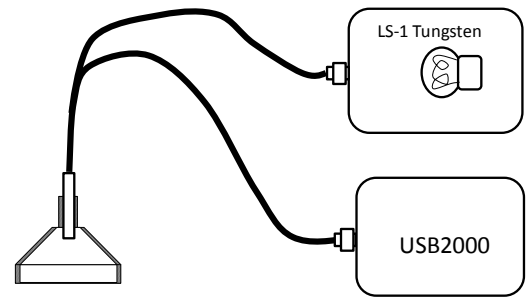
Fig. 8b Schematic of the optical setup for VIS-NIR spectral measurements
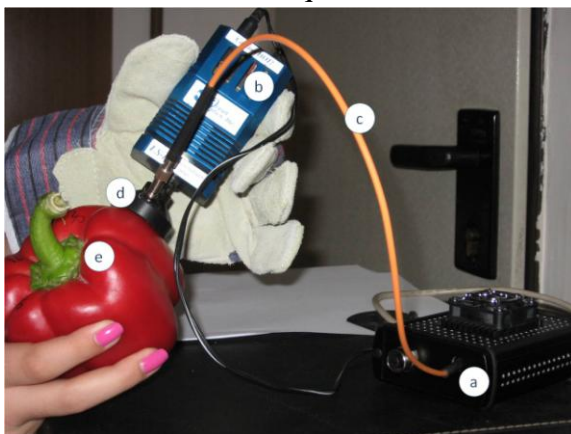
Fig. 9a Experimental setup for SWIR spectral measurements; a: Liga spectrometer, b: Illumination source, c: Fibre-optic, d: ∅ 30 mm cone, e: Pepper sample.
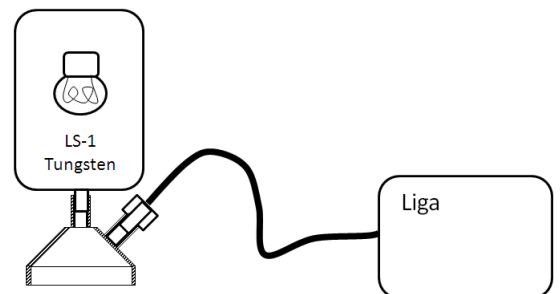
Fig. 9b Schematic of the optical setup for SWIR spectral measurements

Spectral measurements also were obtained with a Liga SWIR spectrophotometer (STEAG Micro Parts, Dortmund, Germany) with a single directional fibre-optic connected to a cone attachment (Figs 9a and 9b). The light source of this instrument is an LS-1 Tungsten Halogen Light Source (Ocean Optics, Dunedin, FL, USA). The detector assembly included a cone that fitted tightly against the pepper surface to prevent scattered radiation reaching the detectors. The surface area observed through the cone was 30 mm in diameter. The incident beam from the light source was projected perpendicularly onto the fruit sample and radiation reflected at an angle of 45° was collected by the G-8160 detector. Altogether 128 data points were acquired in each scan, covering an 850-1888 nm range interval with optical spectral resolution of 8.1 nm. Both configurations were calibrated with a Spectralon, WS-1-SL standard white ceramic background disc (Ocean Optics, Dunedin, FL, USA).

The spectral measurement systems were arranged in reflectance mode for receiving the signals from the peel and flesh of the fruit. The sampled pepper was positioned so that the VIS-NIR and SWIR detector assembly sampled a region at one marked site on the circumference of the largest cross-section perpendicular to the stem–blossom axis. Each fruit was scanned 10 times in the sampled region by moving slightly the cone on the surface; the readings were automatically averaged to yield one spectrum signal.

4.2.3. Hyperspectral system

Scheme of the hyperspectral imaging system is presented on Fig 10a. The spectral component is selected using an acousto-optic tuneable filter (AOTF) which acts as an electronically tuned band-pass filter. The image sampled by the AOTF filter is captured by a black and white CCD cooled camera (COOL-1300Q/QC, VDS, DE) with a pixel resolution of 1280x1024, and 640x512 with 2x2 binning technology. Binning technology enables 4 adjacent pixels to be combined in one pixel, resulting in increased light for each pixel. The lens angle was 12° horizontally and 9° vertically. The control of the AOTF was done by a Direct Digital Synthesizer (DDS) which sends a radio frequency wave to the AOTF through an amplifier, and thereby changes the filter characteristics.

The measurements were conducted in the wavelength range of 550-850 nm, in step of 5 nm. Custom software was written to control the hyperspectral camera. For the processing of the hyperspectral images and for the building of the hyperspectral cubes a Matlab code was written. The code includes:

- flat filed correction of the images,
- calculation of the absolute reflectance using the empirical line,

- exclusion of the saturated pixels,
- sampling of the hyperspectral cube (Fig 11),
- and calculation of the averaged spectra (Fig 12-13), SAM and PQS indices.
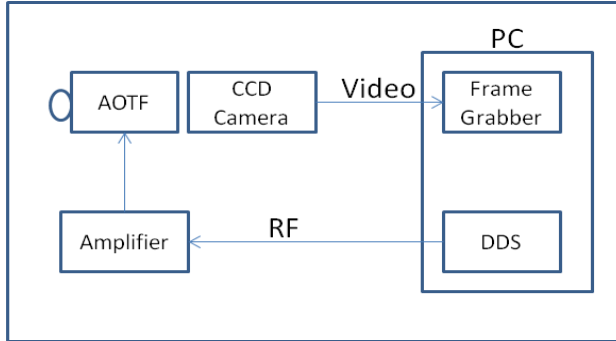
Fig. 10a Hyperspectral imaging system architecture
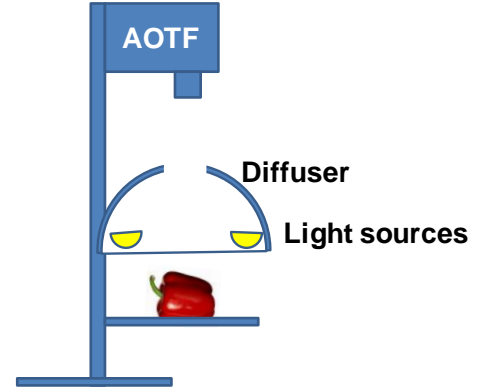
Fig. 10b Scheme of the hyperspectral measurement setup

Hyperspectral images were acquired of each pepper samples. The scheme of the setup is presented on Fig. 10b. Three spectral processing methods were implemented in this work: for the selected pixels (Fig 11) of the hypercube, the averaged reflectance spectra, the spectral angle mapper: SAM (exact method detailed in chapter: 4.4.3.) and the polar quality system: PQS value (exact method detailed in chapter: 4.4.4.) were calculated. The present work contains only the result of the 1st location of the hyperspectral sampling. Pretreatment of the averaged reflectance spectra was conducted by first derivative of reflectance (D_1R), the $\log(1/R)$, and its first- ($D_1(\log(1/R))$), and second derivative ($D_2(\log(1/R))$). The resulted data were used to examine the hyperspectral imaging as quality measurement method. Chemometric procedures were performed with Matlab software (exact methods detailed in chapter: 4.4.).
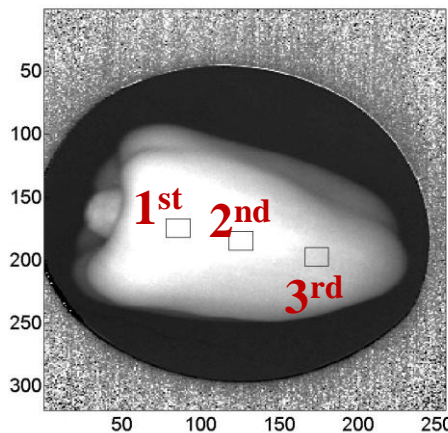
Fig. 11 Example for the spectral sampling of the hyperspectral cube (Pepper sample is taken from the 47th DAA 'Ever Green' cultivar).
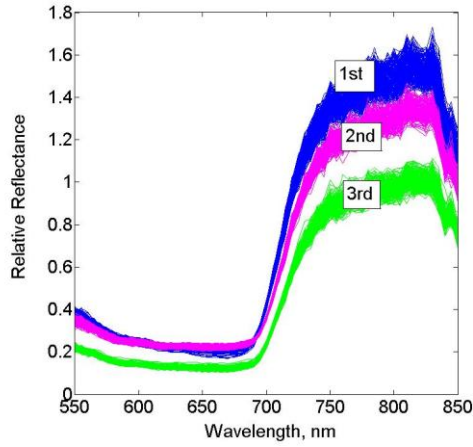
Fig. 12 Relative reflectance spectrums of the sampled areas of the pepper sample. The spectrums are showing the sampled areas of Fig 11.
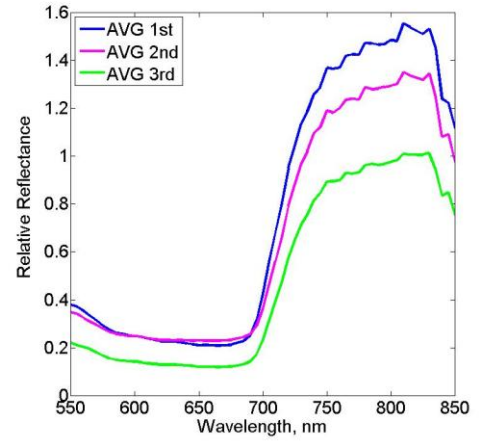
Fig. 13 Averaged relative reflectance spectrums of the sampled areas of the pepper sample. The graph shows the averaged spectrums of Fig 12.

4.2.4. Ultrasonic test

A high-power, low-frequency ultrasonic pulse generator-receiver (Krautkramer Model USL33) and a pair of 50-kHz ultrasonic transducers (Fig. 14) were used to generate the signal; coupled to a microcomputer system for data acquisition and analysis. Exponential-type Plexiglas beam-focusing elements were used to reduce the 55-mm beam diameter of each transducer to the desired area of contact with the fruit. The transducers were mounted with an angle of about 120˚ between their axes, enabling an ultrasonic signal to be transmitted and received over a short distance between their tips across the peel of the fruit (Mizrach, 1999). The ultrasonic measurement was conducted once, on a relatively flat area which was previously chosen on the pepper fruit. The pulse amplitude of the transmitted ultrasonic signal was measured at eight points with 0.25 mm spacing (0.5, 0.75, 1, 1.25, 1.5, 1.75, 2 and 2.25 mm) between the two probes, along the length of the fruit. The attenuation of the ultrasonic signal − based on the eight measurement points − was calculated according to the below equation (Krautkramer and Krautkramer, 1990) [1].

$$A = A_0 e^{-\alpha \times l} \qquad [1]$$

where, l is the distance between the input and collection probes, A and A_0, respectively, are the ultrasonic signal amplitudes at the beginning and the end of a distance l along the propagation path of the ultrasonic wave, and α is the apparent attenuation coefficient of the signal.
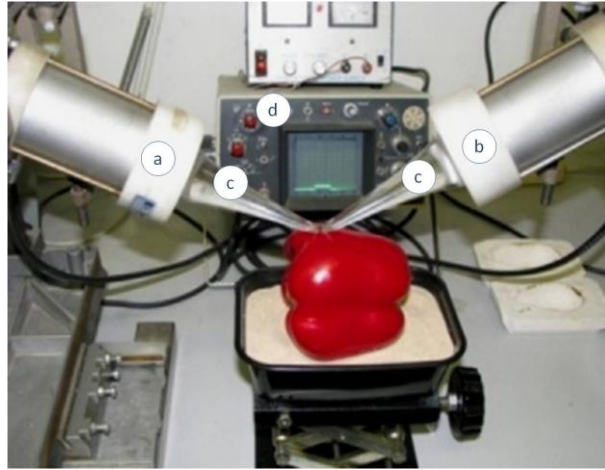
Fig. 14 Experimental setup for ultra sonic measurements; a: transducer, b: receiver, c: exponential-type Plexiglas beam-focusing elements, d: microcomputer system.

4.2.5. Stress relaxation of intact fruit

Relaxation test was chosen to follow non-destructively the changes in firmness of the pepper samples during growth and development. Relaxation test showed strong correlation with the generally adapted pressure gage method measuring firmness of whole bell pepper fruit (Meir et al., 1995) in the preliminary executed experiments 2009 spring season (Appendix 9.2.1).

General purpose relaxation test was carried out with Lloyd LR SK Instrument (Lloyd Instruments Ltd., UK). The material testing machine is a twin column bench mounted instrument. The machine is controlled by NEXYGEN 4.1 material test and data analysis software. The features of the instrument are: high accuracy interchangeable XLC load cells, crosshead travel 975 mm, speed range 0.01– 1016 mm/min, data sampling rate 8 kHz and full PC integration with NEXYGEN 4.1 material test and data analysis software.

The general purpose relaxation test was carried out on intact fruit laid on its side on a flat plate and was compressed by a moving plate at a standard (selectable) speed (200 mm/min) until a load limit (20 N) was achieved (Fig. 15a). The hold time was 10 seconds. The results were analyzed by Nexygen 4.1 - Material Test and Data Analysis Software. At the end of the test the rate of relaxation [N/s] and the remaining deformation [mm] was recorded. A typical diagram for relaxation test is presented in Fig 15b. Additionally, a coefficient of elasticity ($CE_{Relaxation}$, N/mm) was calculated from the phase of loading of the pepper sample with 20N.

The relaxation test was considered as a NDT test based on preliminary experiments (Appendix 9.2.1). In the preliminary experiments the peppers sample were tested by relaxation test and stored for 2 weeks on 7 ºC, followed by shelf life storage at 20 °C for 3 days. After the storage and shelf life the pepper samples were examined and no physiological degradation was found on them.
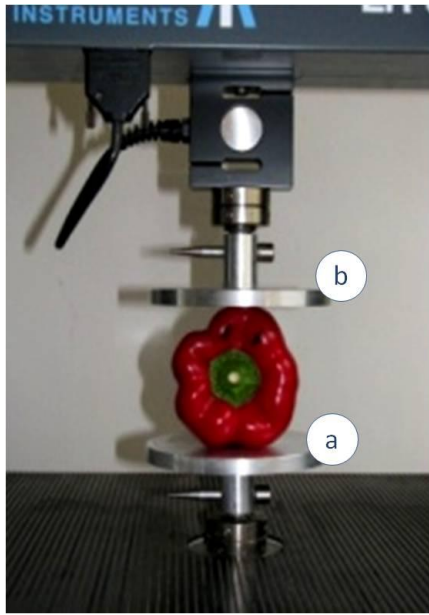
Fig. 15a Experimental setup for relaxation test; a: flat plate, b: moving plate.
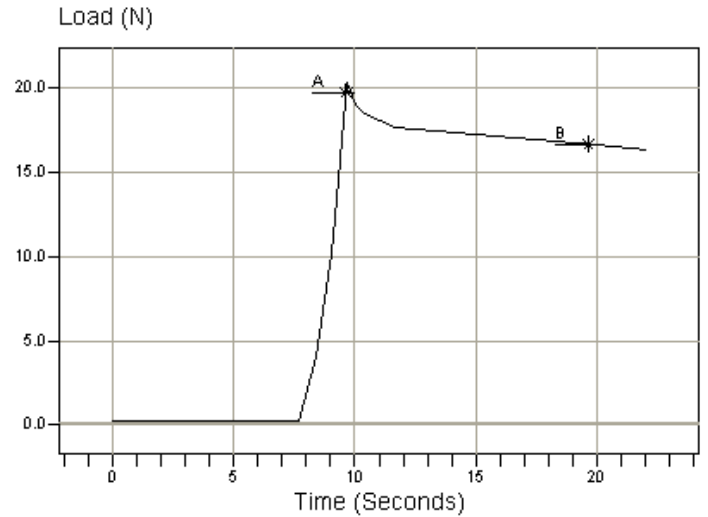
Fig. 15b Typical diagram for relaxation test

4.3. Experimental setup for reference measurements

4.3.1. Rupture test

Compress to Rupture Test was carried out with Lloyd LR SK Instrument (Lloyd Instruments Ltd., UK), described in detail in the 4.2.5 paragraph. Strip (3 cm by 3 cm) was cut from the designated side. The strip was placed, laying on its peel on the lower plate and weighted with the upper plate (1250 g) on the top, to avoid the deflection of the strip during the test (Fig 16a and 16b). The pepper strip was measured from the fruit flesh side because the aim of the measurement was to follow the changes in the pepper flash. The strength of the peel or its change was not the concern of the present study. Both plates had a centred 16 mm diameter hole. The speed of the 8 mm diameter penetration probe was 100 mm/min. The tip of the penetration probe was slightly curved. As force was applied, the load and deformation were recorded simultaneously and stored by Nexygen 4.1 software. Each strip of pepper was characterized by the coefficient of elasticity ($CE_{Rupture}$, N/mm), calculated from the specific section of the test (Fig. 16c) before the proportionality limit (Bourne, 1982).

Fig. 16a Experimental setup for rapture test
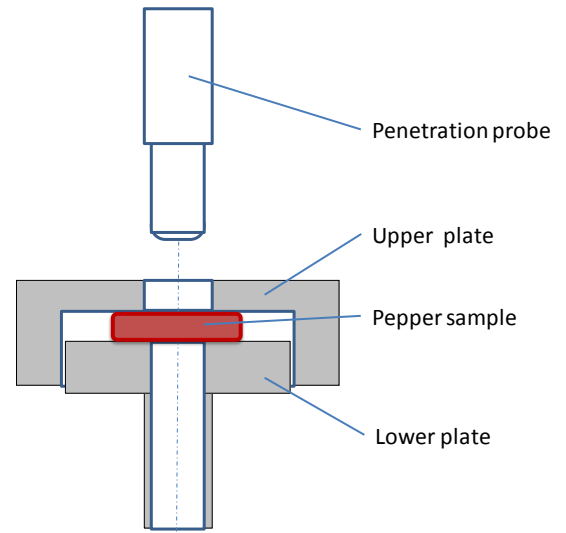
Fig. 16b Schematic diagram of the setup for rapture test
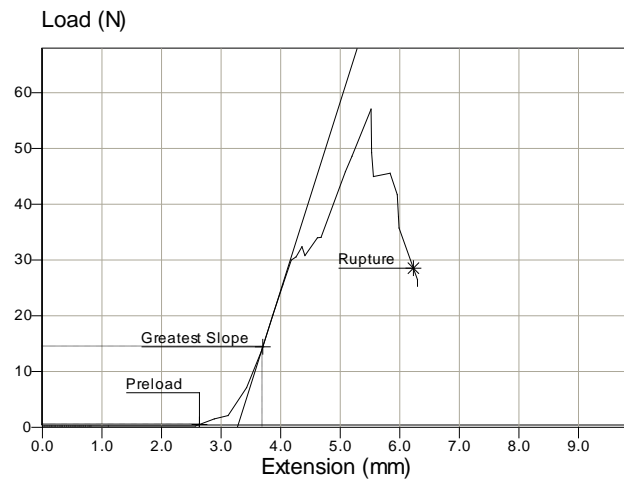
Fig. 16c Typical diagram for rapture test

4.3.2. Compression test

Compress to Limit Test was carried out by Lloyd LR SK Instrument (Lloyd Instruments Ltd., UK), described in detail in the 4.2.5 paragraph. Test disk of 15 mm diameter was cut from the dedicated side of the pepper. The disk was placed on the centre of the lower plate (Fig. 17a) in a way that its peel was laying on the lower plate. The speed of the upper plate was 100 mm/min. The upper plate was compressing the sample until a certain point when the distance between the probe and the lower plate was 1 mm. As force was applied, the load and deformation were recorded simultaneously and stored by Nexygen 4.1 software. Each fruit was characterized by two calculated parameters: the coefficient of elasticity ($CE_{Compression}$, N/mm), calculated from a specific section of the load-deformation curve (Fig. 17b) before the proportionality limit (Bourne, 1982); and the integral of the area under the load-deformation curve ($Int_{Compression}$). In the later parameter the integral was calculated from the start of deformation until the proportionality limit.
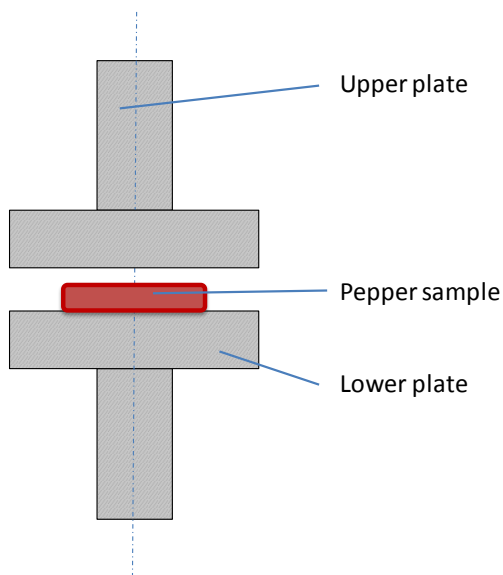
Fig. 17a Schematic diagram of the setup for compression test
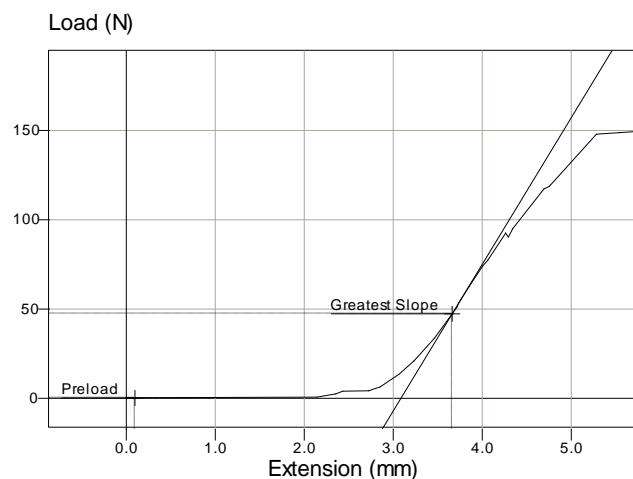
Fig. 17b Typical diagram for rapture test

4.3.3. Dry matter % (DM) determination

Approximately 10 g sample was taken from the location at which NDT measurements had been performed. Each sample was weighed (w_b) and dried at 60˚C in a forced-air oven for 72 h, than it was weighted again (w_a) and percentage of DM was calculated [2]. DM is expressed in %.

DM = (w_a/w_b)*100   [2]

4.3.4. Total soluble solid (TSS) determination

Sample was taken from the location at which NDT measurements had been performed; small cuts were made on the inner side of it, in order to ease the juice of the pepper sample to be squeezed. TSS measurements were taken by a digital refractometer (Atago, PR-1). The TSS was expressed in Brix %.

4.3.5. Ascorbic acid measurement

Determination of ascorbic acid (AA) content was carried out based on the AOAC official method (AOAC 2000). A sample of approximately 4 g was taken from the pericarp location at which spectral measurements had been performed earlier; it was frozen and kept at -18˚C in a 50-ml closed tube. For examination of the vitamin C content, frozen tissue was macerated in 25 ml of 3% metaphosphoric-acetic-acid (HPO_3-CH_3COOH) extracting solution by an Ultra-Turrax homogenizer (TP 18-10, Janke & Kunkel KG), and the extracted solution was vacuum filtered through a Whatman fiberglass filter disk. Residues remaining in the homogenizer and on the filter disk were washed with extracting solution, and the final volume of filtrate was measured in

a graduated cylinder. Twenty milliliters of solution were transferred to an Erlenmeyer flask and 20 ml of metaphosphoric-sulfuric-acetic-acid (HPO_3-CH_3COOH-H_2SO_4) was added to maintain proper acidity (pH about 1.2) and to prevent autoxidation of ascorbic acid. Titration from a 50 ml burette was carried out with 25% 2,6-dichlorophenolindophenol (DCIP) standard solution until a light but distinct rose-pink colour persisted for more than 5 s. The blue dye DCIP is reduced to a colourless form on addition of ascorbic acid, as shown in Fig. 18, but it imparts a pink colour to the acidic solution. From each sample two titrations were performed; if they differed by more than 0.1 ml in reagent consumption, a third titration was conducted and the outlier was discarded. The ascorbic acid content was calculated according to the pre-prepared calibration with a standard ascorbic acid calibration solution set, and expressed as milligrams of ascorbic acid per 100 g of fresh sample.

Standardization of indophenols dye reagent was made each time when new stock solution has been prepared. For calibration 50 ml 1 mg/ml concentration standard ascorbic acid solution was prepared and titration series (0.1, 0.3, 0.5, 0.7, 1.0, 1.3, 1.5, 1.7, 2.0, 2.3, 2.5 mg/ml) were carried out. Fig. 18b shows a typical calibration result.
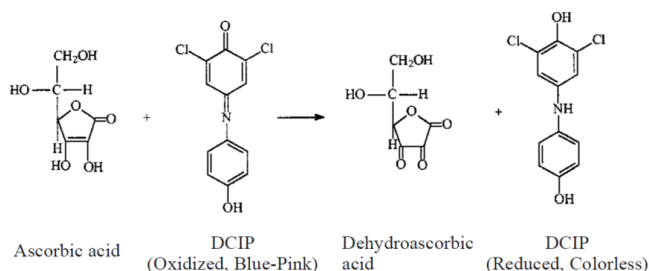
Fig. 18a The reduction of 2,6-dichlorophenolindophenol with ascorbic acid
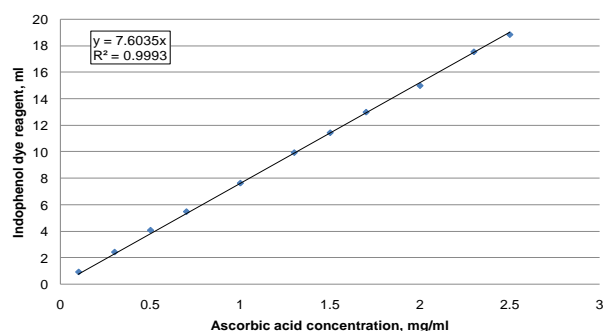
Fig. 18b Standardization of indophenols dye reagent with 1 mg/ml ascorbic acid standard solution

4.3.6. Chlorophyll and carotenoid measurement

Determination of total chlorophyll and carotenoid content were carried out by extraction in absolute ethanol and spectral determination of absorbance in the wavelength of 470, 648.6 and 664.2 nm. Approximately 0.7 g sample was taken from the pericarp at the location at which spectral measurement had been performed earlier; it was put to 80% of ethanol, it was frozen and kept on -18˚C in 15 ml closable tubes. At the time of examination of the chlorophyll and carotenoid content, frozen tissue was macerated in mortar with absolute ethanol until only white tissue remained from the pepper sample. The macerated tissue and liquid was vacuum filtered through Whatman fibreglass filter disk. Remnants on filter disk were washed with absolute ethanol and filtered. The final volume of filtration was measured in graduated tubes. The spectral

measurement was conducted by Genesys Spectrophotometer (Thermo Fisher Scientific Inc., Waltham, MA, USA) in a quartz cuvette. All the process from extraction to spectral measurement was carried out in dim light to avoid degradation of the chlorophyll and carotenoid in the sample. Calculation of total chlorophyll and carotenoid content were carried out based on the below equations (Lichtenthaler, 1987) [3-6]:

$$C_a=13.36\ A_{664.2} - 5.19\ A_{648.6} \qquad [3]$$
$$C_b=27.43\ A_{648.6} - 8.12\ A_{664.2} \qquad [4]$$
$$C_{a+b}=5.24\ A_{664.2} + 22.24\ A_{648.6} \qquad [5]$$
$$C_c=(1000\ A_{470}- 2.13\ C_a - 97.64\ C_b)/209 \qquad [6]$$

where A is the absorbance of the sample, measured by Genesys Spectrophotometer. Calibration of the method was conducted by pure chlorophyll a and b component in the ratio of 3 to 1 (Lichtenthaler, 1987). The total chlorophyll and carotenoid concentration was expressed in mg per g of fresh weight.

4.3.7. Determination of osmotic potential

A section of approximately 40 mm^2, was cut from the pepper from the dedicated side of the fruit. The fruit was pre-washed with tap water and dried.

The tissue was frozen in 1.5 ml micro-test-tubes at -5°C. The frozen tissue was crushed inside the tubes with a glass rod, the bottom of the tubes was pin-pricked and the tubes, set inside another 1.5 ml tube, centrifuged for 4 min in a refrigerated centrifuge (Sigma Laboratory Centrifuges, Germany) at 5°C at 10,000 rpm. 100 μl of the fluids collected in the lower micro-test-tube and were used for measurement of osmotic potential (OP) using a cryoscopic micro-osmometer (μOsmette, Precision Systems, Natick, MA, USA) by measuring the freezing point of 100 μl of sap. Results are presented in mOsm kg H_2O^{-1}.

4.4. Analysis

4.4.1. Spectral analysis by linear regression model

The spectrometers' data were analyzed by chemometric procedure of Partial least-squares (PLS) regression. PLS regression is a technique used with data that contain correlated predictor variables. This technique constructs new predictor variables, known as components, as linear combinations of the original predictor variables. PLS constructs these components while considering the observed response values, leading to a parsimonious model with reliable predictive power. PLS therefore combines information about the variances of both the predictors and the responses, while also considering the correlations among them.

PLSR software was used for model development (PLS, Eigenvector Research, Wenatchee, WA, USA), run under MATLAB software version R2011a (MathWorks, Natick, MA, USA). Comparisons were made among the PLS regression models built by the reflectance spectra (R), and the pre-processed spectra's such as the first derivative of R (D_1R), the log(1/R), it's first (D_1log(1/R)), and second derivative (D_2log(1/R)).

Regression models were formulated which related the reflectance spectra to ascorbic acid, in each tested fruit. The error associated with the results of the regression model is defined by the root mean square error of calibration (RMSEC) [7]:

$$RMSEC = \sqrt{\frac{\sum_{i=1}^{n}(\hat{y}_i - y_i)^2}{n}} \qquad [7]$$

where $\hat{y}_i$ is the predicted value of the ascorbic acid of sample i, y_i is the value of ascorbic acid of sample i, as measured destructively and n is the number of calibration samples. RMSEC is a measure of how well the model fits the data. Root mean square error of cross validation (RMSECV) is a measure of a model's ability to predict new samples. The RMSECV is defined as in eq. [7], except that $\hat{y}_i$ are predictions for samples not included in the model calibration. RMSEC and RMSECV are expressed in the unit of the related laboratory measurement. Cross validation was performed by using 67% of the data (random selected) for calibrating the regression model and the rest 33% of the data for validating it. This procedure was performed seven times.

4.4.2. Spectral analysis by non-linear regression model

Based on Bayesian theorem (Lee, 2004, Gelman et al., 2004, Fearn et al., 2010) Kernel algorithm was developed. The algorithm was written and run under Matlab software. The samples were randomly separated to two equal sets: calibration and validation sets. The samples in the calibration set were grouped by K-means clustering based on squared Euclidean distances. The number of groups in each set of data was optimized by the algorithm, as well as the smoothing parameter for the kernel density estimate was automatically chosen by the algorithm and differs in each data set. In the calibration procedure the algorithm estimates the distribution of each distinct group of samples. The Kernel algorithm used the latent variables of the spectral data - produced by PLSR - as independent the variables. By using latent variables, the number of dimension of the kernel density estimate could be reduced. Multidimensional (number of dimensions depend on the number of latent variables) kernel density estimate was the basis for the predictions. Each group in the calibration set had a multidimensional kernel density estimate. For each sample, the probabilities of belonging to any of the groups were obtained in the

prediction procedure. Predicted concentration was determined for each sample by the highest probability estimate. The whole process was repeated with exchanged calibration and validation sets, in order to calculate the prediction for all the samples.

Support Vector Machine (SVM) supervised learning algorithms was used as well for model development (PLS, Eigenvector Research, Wenatchee, WA, USA), run under MATLAB software version R2011a (MathWorks, Natick, MA, USA). Supervised learning (machine learning) takes a known set of input data and known responses to the data, and seeks to build a predictor model that generates reasonable predictions for the response to new data.

4.4.3. Spectral Angle Mapper (SAM)

Spectral Angle Mapper is a method that calculates the angle between two vectors. When the spectral response curve is regarded as a vector, (each vector consists of all the wavelengths), SAM can express the angle between a known pixel and an unknown pixel (Park et al., 2007). This calculation is less sensitive to changes in the reflectance from an object caused by changes in light source intensity and incidence angle. The decision if two materials (an unknown sample and a known material from a dataset) are the same is directly related to the angle: the closer the angle to zero, the materials are more similar. The angle calculation is shown in eq. [8].

$$\theta = \cos^{-1}\left[\frac{\sum_{\lambda=1}^{N} R_\lambda \mu_{\lambda k}}{\sqrt{\sum_{\lambda=1}^{N} R_\lambda^2 \sum_{\lambda=1}^{N} \mu_{\lambda k}^2}}\right] = \frac{\vec{R}^T \vec{\mu}_k}{\|R\|\|\mu_k\|} \qquad [8]$$

where N: the number of wavelengths, R_λ: the obtained sample in a specific wavelength, k: the number of groups that exist (different kinds of materials) and $\mu_{\lambda k}$: average of a previously obtained data on a specific wavelength. The advantages of the method are that it uses all of the information and it's immune to changes in intensity due to incited angle or source change. The disadvantage of the method is its sensitivity to noise.

In the present work the SAM was calculated from the VIS-NIR, SWIR and hyperspectral imaging measurements and expressed in degrees (SAM_{degree}).

4.4.4. Polar qualification system (PQS)

A quality point of the spectrum was calculated based on the theory of PQS developed by Kaffka and Gyarmati (1991), with modification of the way of differentiating among the central mass points of the samples. I wrote a code for the computations which were carried out under Matlab software.

As a first step (Fig. 19) reflectance spectrum was normalized (3 different way: MSC (multiplicative scatter correction with offset, the mean is the reference spectrum), Normalize (normalize rows of matrix) and SNV (standard normal deviate), therefore it resulted 3 normalized spectrums) and was put into polar co-ordinate system. The next step was the transformation of polar co-ordinate data to two-dimensional Cartesian (x, y) coordinates.
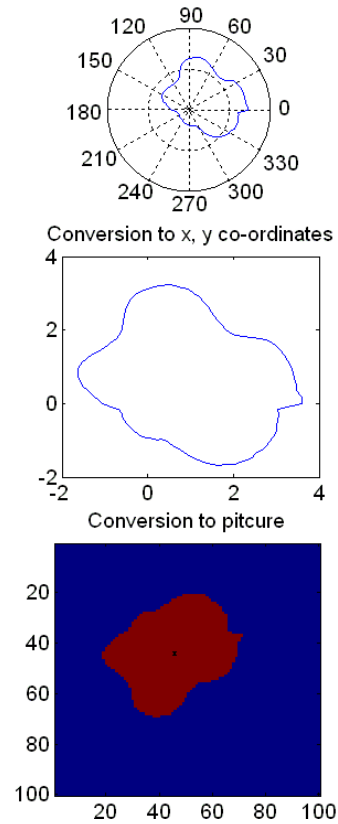
Fig. 19 Steps of spectral quality point calculation

In the final step, the central mass of the object was determined. It resulted the x, y co-ordinate of the quality point of the spectrum as its central mass point. x, y co-ordinates of the central mass of the spectrum was calculated for each sample and for each spectrometer and hyperspectral data. For the x, y set of co-ordinates the median co-ordinate was calculated and relative to this point the distance was calculated for each spectral quality point (D_{abs}). Moreover, the 1st and 2nd principal components (PC) were calculated from the x, y dataset which carries the information of the variance in the location of the co-ordinates. The quality points were calculated from the reflectance (R) and the log(1/R) spectral data.

4.4.5. Multiple-comparison tests

Multiple comparison test returns a pairwise comparison results with comparison intervals around them. It conducts the comparison of the means of several groups; to test the hypothesis that they

are all the same (H_0), against the general alternative that they are not all the same (H_1). The outputs are: the compared means, the estimated difference in means, and the confidence interval for the difference. Multiple comparisons procedures are used to control for the family-wise error rate, to ensure that the probability of incorrectly rejecting the null hypothesis for any of the pairwise comparisons in the family does not exceed alpha (0.05). Multiple comparison tests were conducted by Matlab R2011a.

4.4.6. Cross Correlation

Correlation test was conducted by Matlab R2011a software to examine the relationship among the measured variables. Matrix (R) of correlation coefficients was calculated from the matrix of observations and variables. The calculated matrix is related to the covariance matrix by eq. [9]. For testing the hypothesis of no correlation among variables: p-values were calculated. Each p-value is the probability of getting a correlation as large as the observed value by random chance, when the true correlation is zero. If p is less than 0.05, then the correlation R(i,j) is significant. The correlation test was carried out with $\alpha = 0.05$.

$$R_{(i,j)} = \frac{C_{(i,j)}}{\sqrt{C_{(i,i)}C_{(j,j)}}} \qquad [9]$$

Correlation coefficient measures the degree to which two things vary together or oppositely. First, the maximum positive correlation is 1.00. Since the correlation is the average product of the standard scores for the cases on two variables, and since the standard deviation of standardized data is 1.00, then if the two standardized variables covary positively and perfectly, the average of their products across the cases will equal 1.00. On the other hand, if two things vary oppositely and perfectly, then the correlation will equal -1.00. Therefore correlation coefficient measures whether two things covary perfectly or near perfectly and whether positively or negatively. If the coefficient is, say, .80 or .90, then the corresponding variables closely vary together in the same direction; if -.80 or -.90, they vary together in opposite directions.

4.4.7. Robustness

Residual predictive deviation (RPD) index was determined, to evaluate the goodness of the models; it is calculated as the ratio of performance to deviation [10]:

RPD=STD/RMSECV   [10]

where STD is the standard deviation of the measured parameter and RMSECV is the root mean square error of cross validation. Based on the recommendation of Fearn (2002); if RPD is below

2, then the model is not sufficient enough, while if it is around 10, then the model has a great potential in measurement. If the RPD value is between 2-10 than the interpretation of the results is depend on the measured parameter and on the purpose of the measurement. Williams (2001) gives more restrict borders in defining the goodness of models: 0-2.3 'very poor', 2.4-3 'poor', 3.1-4.9 'fair', 5-6.4 'good', 6.5-8 'very good', and above 8.1 is 'excellent'.

Since RPD does not include other statistical parameters of the regression model like latent variables or calibration error, therefore a more complex index would be desired for the evaluation of the goodness or robustness of regression models.

4.4.8. Standardized weighted sum index

Standardized weighted sum index (SWS) was developed as a generalized index to compare between models' performance. As a first step criterion weighting (Malczewski, 1999) was used to generate weights for each statistical parameter of the regression model. Weights were determined based on pairwise comparison method developed by Saaty (1980). This method involves pairwise comparisons of the evaluation criteria, to create a ratio matrix. These pairwise comparisons are used as an input and the procedure yields the relative weight of each criterion as output. Specifically, the weights are determined by normalizing the eigenvector associated with the maximum eigenvalue of the (reciprocal) ratio matrix. The weight expresses the importance of each criterion relative to others. Thus, the larger the weight, the more important is the criterion in the overall utility.

In the present work pairwise comparisons to determine the weights were done by three specialists (experts in chemometric procedures: Dr. Zeev Schmilovitch, Dr. Victor Alchanatis and Dr. David Bonfil), and their assigned weights were averaged (Table 6). An example for the detailed calculation of the weights can be seen in Appendix 9.2.2.

Table 6 Resultant weights of the pairwise comparisons for the statistical parameters

Statistical parameter	Weight
LV	0.09
r^2	0.18
RMSEC	0.07
RMSECV	0.39
RMSECV/RMSEC	0.17
RPD	0.10
Sum of the weights	1

In the second step, each statistical parameter of the regression model was standardized according to its range, and the standardized values were then multiplied by the corresponding weights, then the weighted values were summarized for each model eq. [11]. The quality of the model is evaluated by the sum of the weighted values: the higher the sum, the better the model. The outcomes are displayed in the tables of the results under SWS. SWS enable the overall comparison of different regression models and as well as gives direction in the selection of the most robust model. For better evaluation, the ratio between RMSECV and RMSEC was introduced, to provide information about the relationship between calibration and cross-validation. SWS is comprised by two parts; the first part is contribution of statistical parameters aimed to have as low values as possible (LV, RMSEC, RMSECV, RMSECV/RMSEC), while in the second part statistical parameters aimed to have as high values as possible (r^2, RPD).

$$SWS = \sum_{i=1}^{4} \left(1 - \frac{a_i - min_i}{max_i - min_i}\right) * w_i + \sum_{j=1}^{2} \left(\frac{b_j - min_j}{max_j - min_j}\right) * w_j \qquad [11]$$

where *SWS* is the standardized weighted sum; *i* is the index of statistical parameter *a*: LV, RMSEC, RMSECV, RMSECV/RMSEC; *j* is the index of statistical parameter *b*: r^2, RPD; *min* is the minimum of the range of the particular statistical parameter; *max* is the maximum of the range of the particular statistical parameter; *w* is the weight of the particular statistical parameter. For each PLS regression model the SWS index was computed. Therefore the quality of the model is evaluated by the SWS values: the higher the SWS, the better the model is.

4.4.9. Fusion

Sensor fusion is analogous to the cognitive process used by humans to integrate data continually from their senses to make interferences about the external world. Sensor or data fusion refers to the acquisition, processing, and combination of information generated by multiple knowledge sources and sensors (Hall, 1992). The objective is to provide optimal or near-optimal use of the available information for detection, estimation, and decision-making.

In the present work the methodology suggested by Steinmetz (1999b) was applied (Fig 5):

   a. identifying the properties of the produce that are important for its organoleptics properties: internal content, colour, texture
   b. identifying the reference methods (qualitative or quantitative) that are currently used for assessing the quality of the produce: TSS, DM, AA, OP, total chlorophyll, carotenoid, texture (Coefficient of elasticity of the compression and the rupture tests)

c. identifying the non-destructive methods that can be used for measuring the selected properties of the produce: relaxation test, ultrasound, VIS-NIR, SWIR and hyperspectral measurements

d. acquiring data on the produce with the selected non-destructive sensors and reference methods: measurements during growing and maturation

e. assessing the level of redundancy or complementarity in the non-destructive sensors: PLS models

f. selecting and applying the proper multisensor fusion method: PLS, PCR, Kernel, SVM

g. evaluating the sensor fusion system developed by comparing its performance to the reference methods: SWS

h. acceptance, rejection or improvement of the proposed sensor fusion method.

Model evaluation was conducted for comparison of a single-sensor system to a multisensor system. In this step SWS index was applied to evaluate the performance of the single and multisensor systems. Performance is defined as the ability of the fusion model to provide a better prediction of the properties of the produce than that made by a single sensor.

In this work fusion was realized in three levels:

1. Fusion of the NDT parameters
2. Combination of the cultivars
3. Fusion of the DT parameters

5. RESULTS AND DISCUSSION

5.1. Defining the maturity stages

In defining the three maturity stages the changes of weight (Fig. 20) and total soluble solid (Fig. 21) were considered (Nilsen et al., 1991). On that basis the *premature stage* lasted until the pepper fruit's weight and TSS significantly did not increase, the *green stage* encompassed the period during which both TSS and weight are changing, and the *mature stage* began when the weight and the TSS significantly do not increase anymore. Relating the results to these three basic growth stages - premature (<54th DAA), green (60th – 67th DAA) and mature (>74th DAA) - it enabled us to highlight the characteristic trends.
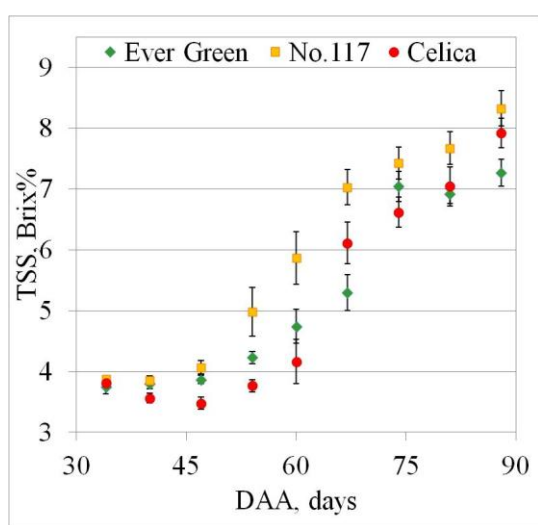
Fig. 20 Change of TSS with error bars of 95% confidence interval for 'Ever Green', 'No.117', and 'Celica' bell pepper cultivars
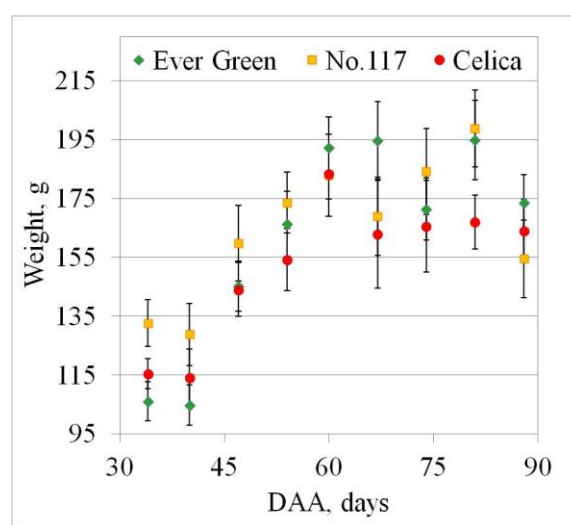
Fig. 21 Change of weight with error bars of 95% confidence interval for 'Ever Green', 'No.117', and 'Celica' bell pepper cultivars

5.2. Results of the physiological attribute changes in pepper fruits during growth and maturation

5.2.1. Changes of TSS during growth and maturation

Total Soluble solid levels in pepper depend on several factors, including cultivar, season, and maturity stage. Changes of the measured TSS in the three bell pepper cultivars are shown in Fig. 22 with the mean value and 95% confidence interval. The level of TSS was varied for all three cultivars and during growing season from 3.2 to 9.3 Brix %. For all three cultivars the TSS started a sharp increase at the 54 days after anthesis (DAA). Prominent increase in TSS occurred in case of 'No.117' cv. as well as this cv. reached the highest average TSS content (8.3 Brix%)

to the 88th DAA. The 'Ever Green' and 'Celica' cultivars alternately accumulated in soluble solids, by the 88th DAA their average TSS content were 7.3 and 7.9 Brix%, respectively. The TSS increased during the whole ripening process, in agreement with previous studies (Tadesse et al, 2001, Penchaiya et al., 2009). The changes of TSS for all three cultivars were sigmoid like.
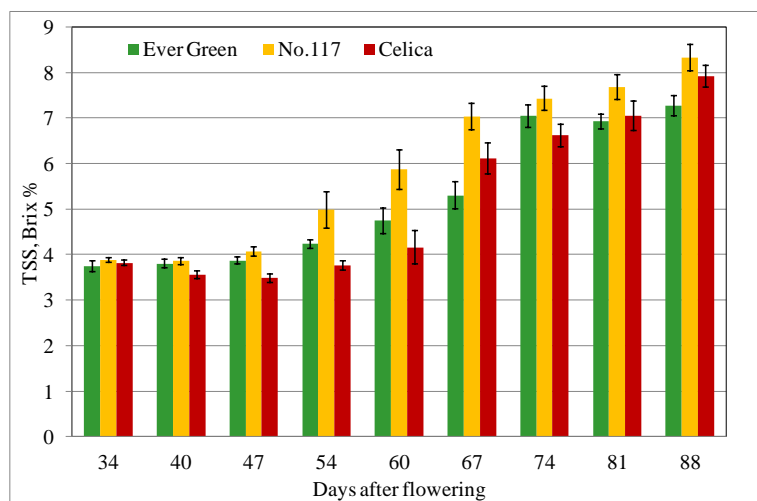
Fig. 22 Change of TSS with error bars of 95% confidence interval during ripening of three cultivars of bell peppers

Multiple comparison tests were performed to analyze the differences in TSS between the three cultivars during the defined three maturity stages (chapter 5.1). Table 7 presents results of multiple comparison tests for 'Ever Green' 'No.117' and 'Celica' cultivars with the mean values and standard error of the measured TSS. Significant difference was found for TSS among the cvs. in the premature stage.

Matutity stage	Cultivar	TSS, Brix %
Premature	Ever Green	3.9 ± 0.049 a
	No.117	4.2 ± 0.049 b
	Celica	3.7 ± 0.049 c
Green	Ever Green	5.0 ± 0.16 a
	No.117	6.5 ± 0.16 b
	Celica	5.1 ± 0.16 a
Mature	Ever Green	7.1 ± 0.09 a
	No.117	7.81 ± 0.09 b
	Celica	7.2 ± 0.09 a

Table 7 Result of the multiple comparison tests for TSS with the mean values and standard error. Means with the same letter do not differ significantly (95%).
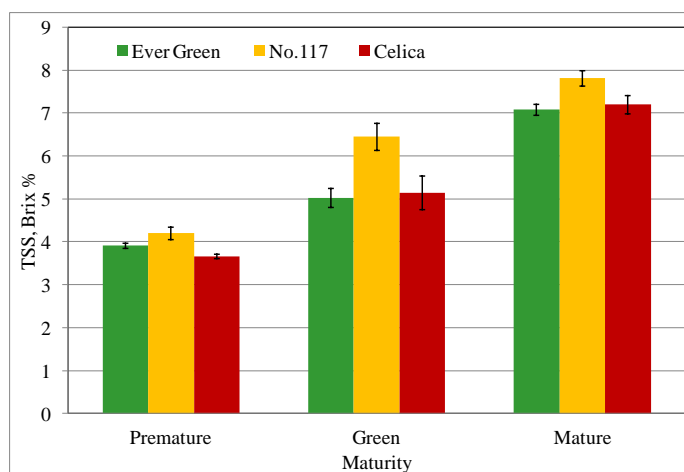
Fig. 23 Change of TSS with error bars of 95% confidence interval during premature, green and mature stages of 'Ever Green', 'No.117', and 'Celica' bell pepper cultivars

Consistently in the green and mature stages the 'No.117' cv. deferred significantly from the other cvs. In that manner, Fig. 23 demonstrates the changes of average TSS during the three maturity stages, with error bar of 95% confidence intervals for 'Ever Green', 'No.117' and 'Celica' cultivars. Throughout the three maturity stages the 'No.117' cv. distinctively increased in TSS content.

5.2.2. Changes of DM during growth and maturation

The level of dry matter just as the TSS depends on several factors, including cultivar, season, and maturity stage. Changes of the DM in the three bell pepper cultivars are shown in Fig. 24 with the mean value and 95% confidence interval. The level of DM was varied for all three cultivars and during growing season from 4.3 to 10.7 %. The DM gradually increased through the whole period of growth especially after the 47th DAA. Prominent increase occurred in case of 'No.117' and 'Ever Green' cvs. during the period of 47-60th DAA, while the 'Celica' cv. sharply increased in DM from the 60th to the 67th DAA. The highest average DM content (9.7 %) was reached by 'No.117' cv., at the 88th DAA, followed by 'Celica' and 'Ever Green' with 9.5 % and 9.1 %, respectively. Similarly to TSS, DM also took a sigmoid trend in the course of DAA. The level of DM and its increase in the pepper cultivars studied in this paper is in agreement with the ranges described in the literature (Marcelis and Baan Hofman-Eijer, 1995, Roura et.al., 2001).
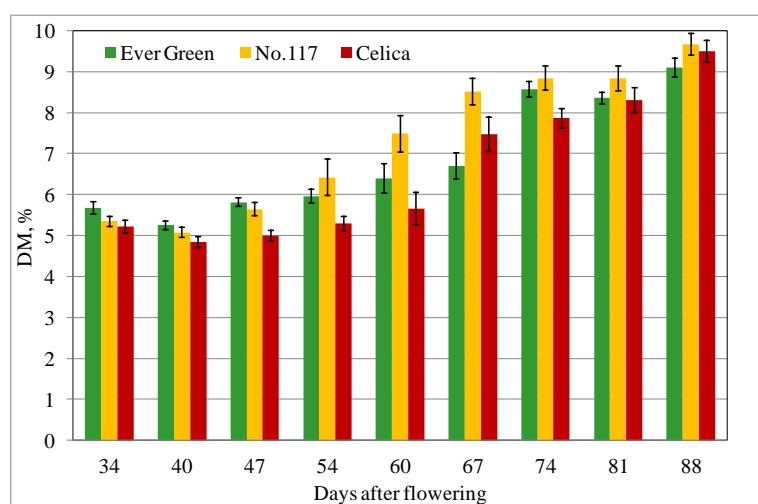
Fig. 24 Change of DM with error bars of 95% confidence interval
during ripening of three cultivars of bell peppers

Determination of the maturity stages described in chapter 5.1 allows emphasizing the trends of DM change. Multiple comparison tests were performed to analyze the differences in DM between the three cultivars during growth. Table 8 presents results of multiple comparison tests for 'Ever Green' 'No.117' and 'Celica' cultivars with the mean values and standard error of the

measured DM. 'Celica' was found to be significantly different from the other two cvs. in the premature stage, while consistently in the green and mature stages the 'No.117' cv. deferred significantly from the other two cvs. In that manner, Fig. 25 demonstrates the changes of average TSS during the three maturity stages, with error bar of 95% confidence intervals for 'Ever Green', 'No.117' and 'Celica' cultivars. 'No.117' cv. distinctively increased in DM from the premature stage to the green stage while for the 'Ever Green' and 'Celica' cvs. this change occurred from the green stage to the mature stage.

Matutity stage	Cultivar	DM, %
Premature	Ever Green	5.7 ± 0.06 a
	No.117	5.6 ± 0.06 a
	Celica	5.1 ± 0.06 b
Green	Ever Green	6.6 ± 0.17 a
	No.117	8.0 ± 0.17 b
	Celica	6.6 ± 0.17 a
Mature	Ever Green	8.7 ± 0.1 a
	No.117	9.1 ± 0.1 b
	Celica	8.6 ± 0.1 a

Table 8 Result of the multiple comparison tests for DM with the mean values and standard error. Means with the same letter do not differ significantly (95%).
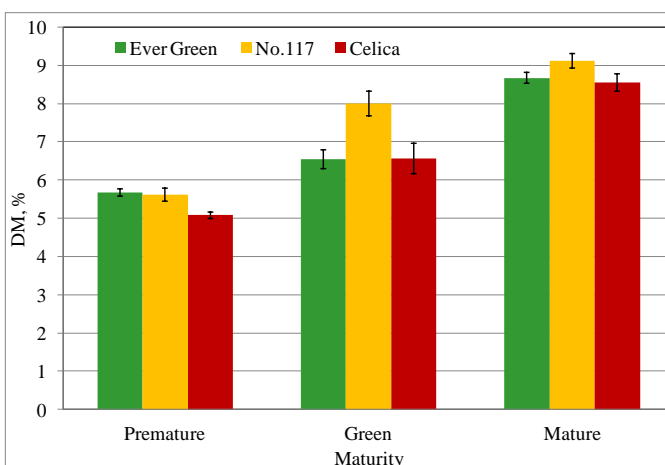
Fig. 25 Change of DM with error bars of 95% confidence interval during premature, green and mature stages of 'Ever Green', 'No.117', and 'Celica' bell pepper cultivars

5.2.3. Changes of osmotic potential during growth and maturation

The sigmoid trend of OP change during fruit development is very similar to the changes of TSS. Fig. 26 shows the changes of the measured OP in the three bell pepper cultivars with the mean value and error bars of 95% confidence interval. The level of OP was varied for all three cultivars and during growing season from 170 to 677 osmol/kg. For 'No.117' cv. the OP started a sharp increase at the 54th trough 67th DAA; while for 'Ever Green' it was moderate increase until the 67th DAA and then prominently accelerated the OP. In case of 'Celica' cv. the OP almost did not change until the 60th DAA, than it greatly increased at the 67th DAA and kept its moderate growth until the 88th DAA. The highest average OP (554 osmol/kg) was reached by the 'No.117' cv. followed by 'Celica' and 'Ever Green' cvs., with 545 and 515 osmol/kg OP, respectively.

Determination of the maturity stages described in chapter 5.1 allows emphasizing the trends of OP change. Multiple comparison tests were performed to analyze the differences in TSS between

the three cultivars during growing and maturation. Table 9 presents results of multiple comparison tests for 'Ever Green', No. 117 and 'Celica' cvs, with the mean values and standard error of the measured OP. In the premature stage the average OP for 'Celica' cv found to be significantly lower compare to the other two the cvs. Consistently in the green and mature stages the 'No.117' cv. the average OP was significantly higher than the average OP in the other two cvs. In that manner, Fig. 27 demonstrates the changes of average OP during the three maturity stages, with error bar of 95% confidence intervals for 'Ever Green', No. 117 and 'Celica' cultivars. Throughout the green and mature stages the 'No.117' cv. distinctively increased in OP.
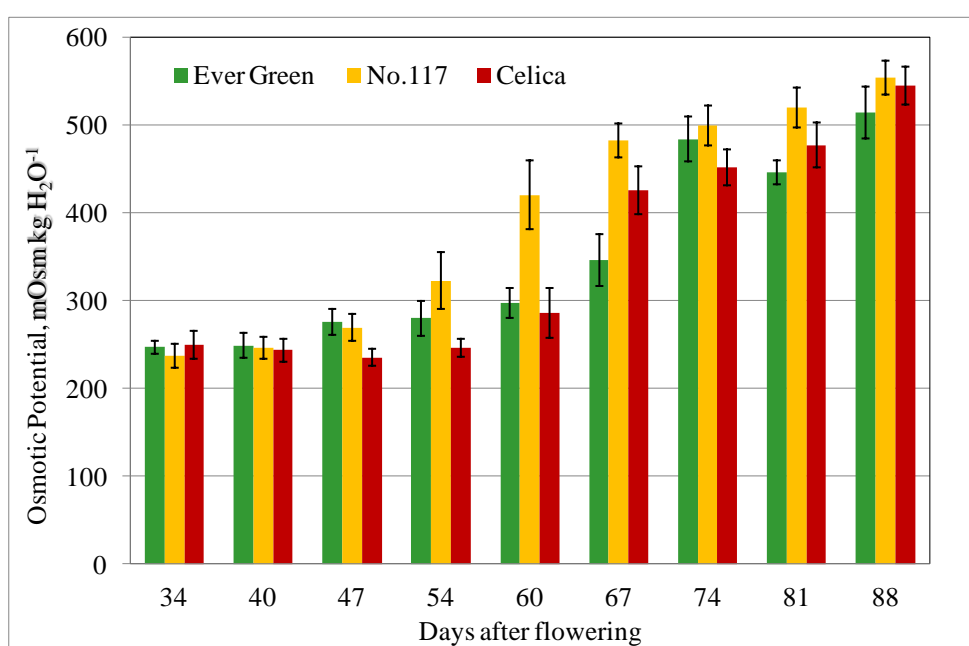
Fig. 26 Change of OP with error bars of 95% confidence interval during ripening of three cultivars of bell peppers

Matutity stage	Cultivar	OP, osmol/kg
Premature	Ever Green	263 ± 4.7 a
	No.117	269 ± 4.7 a
	Celica	244 ± 4.7 b
Green	Ever Green	322 ± 12.4 a
	No.117	451 ± 12.4 b
	Celica	356 ± 12.4 a
Mature	Ever Green	482 ± 7.7 a
	No.117	524 ± 7.7 b
	Celica	491 ± 7.7 a

Table 9 Result of the multiple comparison tests for OP with the mean values and standard error. Means with the same letter do not differ significantly (95%).
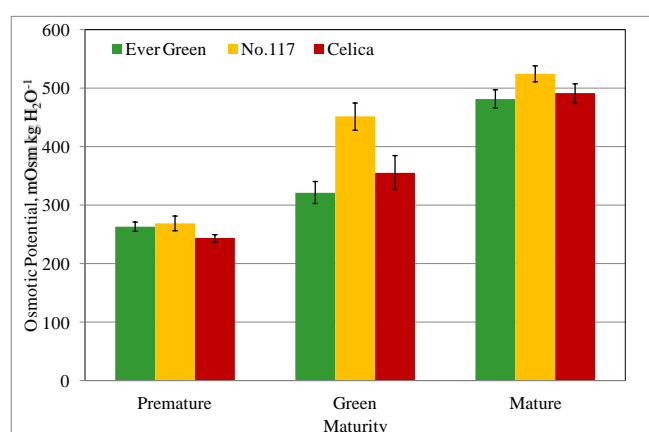
Fig. 27 Change of OP with error bars of 95% confidence interval during premature, green and mature stages of 'Ever Green', 'No.117', and 'Celica' bell pepper cultivars

5.2.4. Changes of vitamin C during growth and maturation

The vitamin C levels in vegetables depend on several factors, including cultivar, season, and maturity stage. Changes of the measured ascorbic acid concentration in the three bell pepper cultivars are shown in Fig. 28 with the mean value and 95% confidence interval. The level of vitamin C was varied from 1.3 to 169.5 mg/100g fresh weight (FW). Differences were detected among the examined cultivars. The measurements with DCIP titration showed increasing vitamin C concentration during the ripening process, in agreement with previous studies that reported an increase in ascorbic acid concentration during pepper maturation (Marin et al, 2004, Osuna-Garcia et al., 1998, Howard et al., 2000) and decrease at a certain point in the ripe stage (Orban et al., 2011). The vitamin C content reaches its maximum around the 67-74th DAA for all three cultivars.
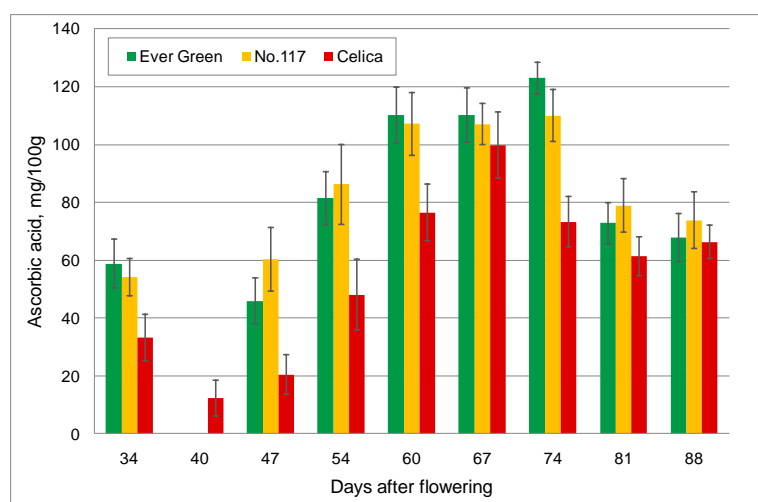
Fig. 28 Change of ascorbic acid contents with error bars of 95% confidence interval during ripening of three cultivars of bell peppers

Determination of the maturity stages described in chapter 5.1 allows emphasizing the trends of vitamin C change. Multiple comparison tests were performed to analyze the differences in vitamin C content between the three cultivars during growing and maturation. Table 10 presents results of multiple comparison tests for 'Ever Green' No. 117 and 'Celica' cultivars with the mean values and 95% confidence interval of the measured ascorbic acid concentration. Significant difference was found in vitamin C concentration during the growing stages only for the 'Celica' variety. In that manner, the results in Fig. 29 shows that the 'Ever Green' and No. 117 cultivars are do not differ significantly in vitamin C content, while the 'Celica' variety is lower all through the growing period relatively to the other varieties by 118%, 25% and 31% in the premature, green and mature stages, respectively. Furthermore, one would expect that red

and yellow cultivars would have yielded higher concentration of vitamin C, but the result demonstrates that external appearance might not be sufficient enough to estimate the content of ascorbic acid.

Maturity stage	Cultivar	Ascorbic acid, mg/100g
Premature	Ever Green	62.08 ± 10.81 a
	No.117	66.95 ± 10.11 a
	Celica	28.53 ± 10.11 b
Green	Ever Green	110.27 ± 12.25 a
	No.117	107.15 ± 12.25 a
	Celica	88.19 ± 12.25 b
Mature	Ever Green	87.9 ± 10.61 a
	No.117	87.89 ± 10.67 a
	Celica	67.01 ± 10.68 b

Table 10 Result of the multiple comparison tests for ascorbic acid concentration with the mean values and 95% confidence interval. Means with the same letter do not differ significantly (95%).
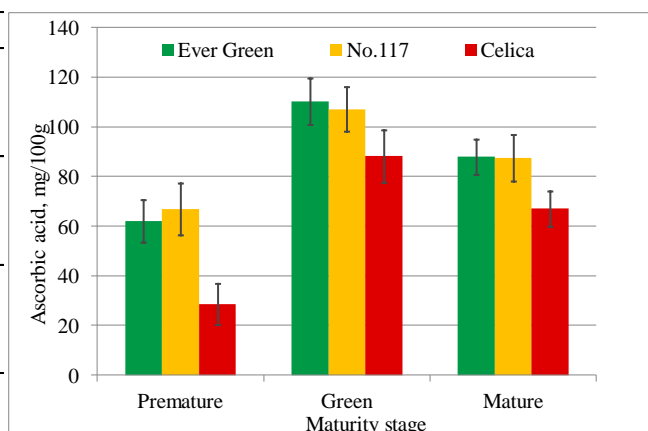
Fig. 29 Change of ascorbic acid contents with error bars of 95% confidence interval during premature, green and mature stages of 'Ever Green', 'No.117', and 'Celica' bell pepper cultivars

5.2.5. Changes of total chlorophyll and carotenoid content during growth and maturation

The chlorophyll and carotenoid levels in vegetables depend on several factors, including cultivar, season, but mostly the stage of maturity even in the stay green variety. Changes of the measured total chlorophyll and carotenoid content in the three bell pepper cultivars are shown in Fig. 31-32 with the mean value and 95% confidence interval. The level of total chlorophyll content was varied from 0.0004 to 0.1163 mg/g fresh weight (FW) while the carotenoid concentration felt between 0.0024 and 0.27 mg/g FW. Differences were detected among the examined cultivars. The total chlorophyll content drastically decreased during the ripening process in the 'Celica' and in the 'No.117' cultivars as the fruits changed colour from green to their cultivar characteristic colour, while for the 'Ever Green' variety the total chlorophyll content only slightly decreased. The colour development started first in the 'No.117' yellow cultivar as it can be observed in the 60th DAA (Fig. 31). Interestingly the gradual decrement of the total chlorophyll content stared already on the 54th DAA foretelling the coming colour change (Fig. 32) while no visible colour change can be observed on the pepper fruits. Meanwhile the carotenoid content did not changed notably. The measured carotenoid concentration only started to increase after the chlorophyll concentration notably decreased.
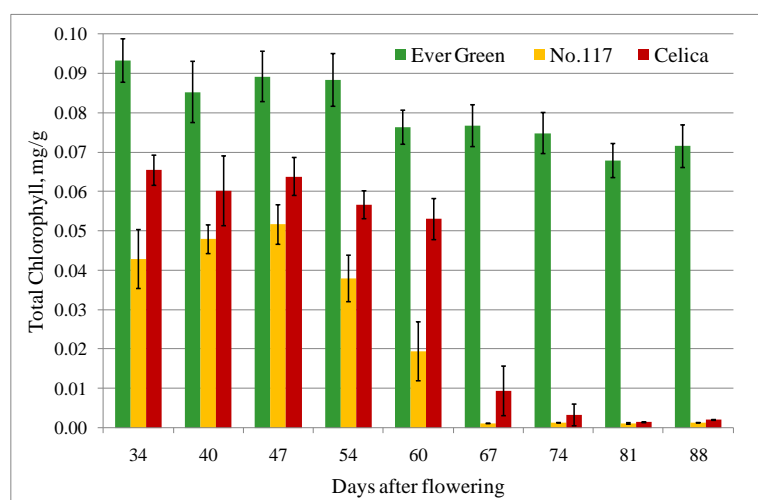
Fig. 30 Change of total chlorophyll contents with error bars of 95% confidence interval during ripening of three cultivars of bell peppers
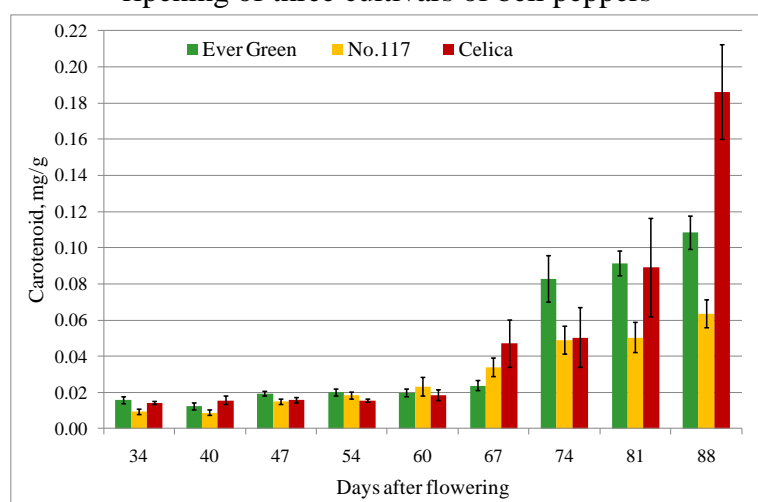
Fig. 31 Change of carotenoid contents with error bars of 95% confidence interval during ripening of three cultivars of bell peppers
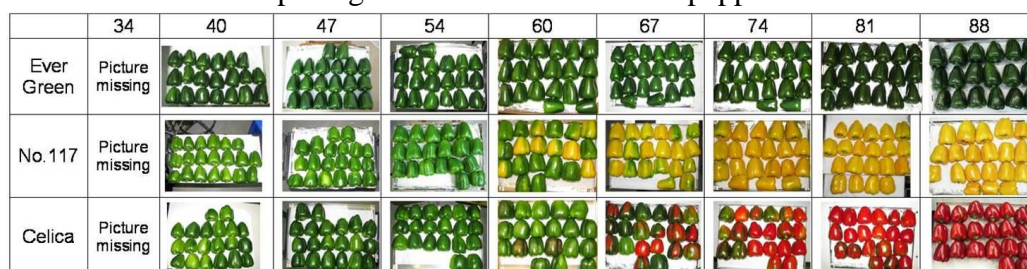
Fig. 32 Colour development of the three bell pepper varieties during the ripening process Fig. 25 Change of carotenoid contents with error bars of 95% confidence interval during ripening of three cultivars of bell peppers

The total chlorophyll change in the 'Celica' variety is much more radical than in the yellow ('No.117') bell peppers, but in both cases sigmoid trend of change could be observed. From the 60th to the 67th DAA the average chlorophyll concentration dropped 6 times while the carotenoid concentration increment was 3 times. As for the 'Ever Green' cultivar the colour remains green in the whole process of ripening. While the colour is consistent the total chlorophyll

concentration significantly dropped after the 54th DAA and remained on the level between 0.07-0.08 mg/g. Furthermore the carotenoid content significantly starts to increase only after the 67th DAA. At the full ripening stage as it was expected, the total chlorophyll content of the red ('Celica') and yellow ('No.117') peppers basically vanishes and in the green variety ('Ever Green') it remains on high level. Considering the final carotenoid levels in the fully ripened fruits the 'Celica' reached the highest level (average 0.185 mg/g), half of that amount accumulated in the 'Ever Green' variety and surprisingly in the fruits of the 'No.117' yellow cultivar stored up the lease amount of carotenoids, its concentration was only the third of the red bell peppers. The 'Ever Green' variety turned out particularly valuable as it contains high concentration of chlorophyll along with considerable amount of carotenoids. The condition that the fruits remain green coloured even though the presence of carotenoids comes from the attribute (feature, property) that the carotenoids are masked by the chlorophylls.

Table 11 Result of the multiple comparison tests for total chlorophyll content with the mean values and standard error. Means with the same letter do not differ significantly (95%).

Matutity stage	Cultivar	Total Chlorophyll, mg/g fresh weight
Premature	Ever Green	0.089 ± 0.002 a
	No.117	0.0487 ± 0.002 b
	Celica	0.0665 ± 0.002 c
Green	Ever Green	0.0765 ± 0.003 a
	No.117	0.0111 ± 0.003 b
	Celica	0.0337 ± 0.003 c
Mature	Ever Green	0.0714 ± 0.001 a
	No.117	0.0013 ± 0.001 b
	Celica	0.0024 ± 0.001 b
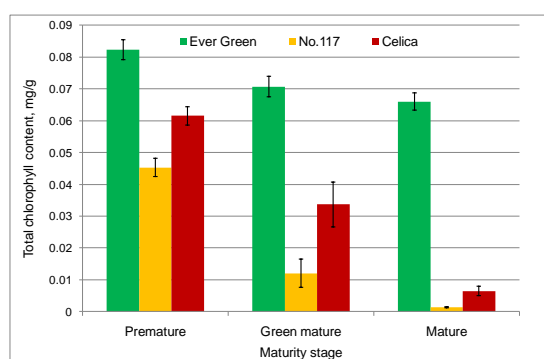
Table 12 Result of the multiple comparison tests for carotenoid content with the mean values and standard error. Means with the same letter do not differ significantly (95%).

Matutity stage	Cultivar	Carotenoid, mg/g fresh weight
Premature	Ever Green	0.017 ± 5.3e-4 a
	No.117	0.013 ± 5.3e-4 b
	Celica	0.015 ± 5.3e-4 a
Green	Ever Green	0.022 ± 2.6e-3 a
	No.117	0.028 ± 2.6e-3 ab
	Celica	0.032 ± 2.6e-3 bc
Mature	Ever Green	0.094 ± 6.3e-3 a
	No.117	0.054 ± 6.3e-3 b
	Celica	0.11 ± 6.3e-3 a

Fig. 33 Change of total chlorophyll contents with error bars of 95% confidence interval during premature, green and mature stages of 'Ever Green', 'No.117', and 'Celica' bell pepper cultivars
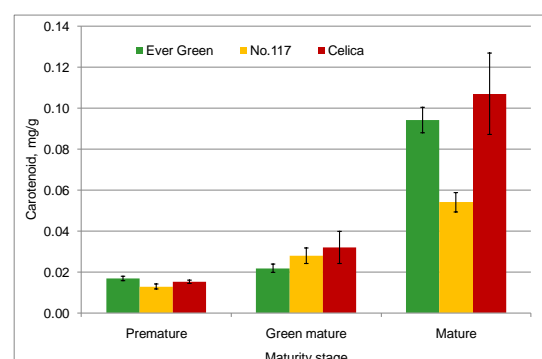
Fig. 34 Change of carotenoid contents with error bars of 95% confidence interval during premature, green and mature stages of 'Ever Green', 'No.117', and 'Celica' bell pepper cultivars

Determination of the maturity stages described in chapter 5.1 allows emphasizing the trends of chlorophyll and carotenoid change. Multiple comparison tests were performed to analyse the differences in total chlorophyll content between the three cultivars during growing and maturation. Table 11 and 12 present (Fig. 33-34) the results of multiple comparison tests for 'Ever Green' 'No. 117' and 'Celica' cultivars with the mean values and standard error of the measured total chlorophyll and carotenoid content. Significant difference was found in total chlorophyll concentration during the premature and green mature stages for all three bell pepper varieties; while the difference of chlorophyll content in the mature stage for the 'No.117' and 'Celica' varieties are insignificant. Considering the carotenoid concentration the 'Celica' and 'Ever Green' cultivars are significantly different from the 'No.117' variety in the premature and mature stages while in the green mature stage the 'Celica' differ significantly from the 'Ever Green' and the 'No.117' notably not vary from the other cultivars. Consequently it can be concluded that the external appearance might not be sufficient enough to estimate the internal chlorophyll and carotenoid composition of different cultivars of bell pepper fruits.

5.3. Spectral Analysis

Figure 35 and 36 show the averaged reflectance spectra's of the 34th (1st pick) and 88th (9th pick) DAA harvested pepper fruits from the VIS-NIR and hyperspectral measurements, respectively. At the 34th DAA the reflectance spectra's of the three pepper cultivars look alike, they are dominated by the characteristic spectral signatures of chlorophylls. While at the 88th DAA the three pepper cultivars are different from one another as their pigment composition changes and their typical colour develops to its variety specific colour.

In the case of SWIR range (Fig. 37) the different cultivars in the observed maturity stages does not result remarkable change in the spectral signature. Water bands at 970 nm, 1200 nm and 1400 nm represent a clear reflectance signature in all the spectra's. Moreover, sugar probably influences the peak at 1700 nm. The first derivatives of both spectral ranges distinguish the signature bands as described above.

Comparisons were made among the models of regression analysis of the reflectance spectra (R), its first derivative (D_1R), the log(1/R) and its first (D_1log(1/R)) and second derivative (D_2log(1/R)). Figures 38-40 show an example (averaged reflectance spectra's of the 1st harvest 'Celica' cv.) for the spectral pre-treatments in the VIS-NIR, hyperspectral and SWIR spectral range, respectively.
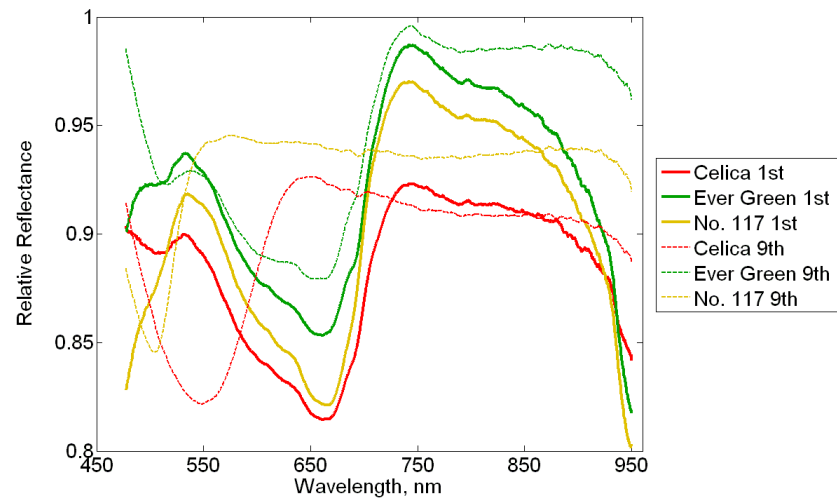
Fig. 35 Averaged VIS-NIR reflectance spectra of the 1ˢᵗ and 9ᵗʰ harvest 'Celica', 'Ever Green' and 'No.117' cultivars respectively.
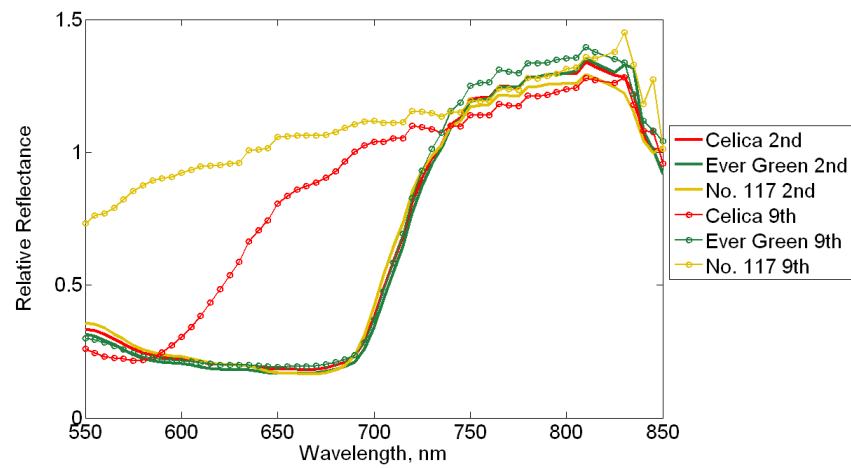
Fig. 36 Averaged hyper cube reflectance spectra of the 1ˢᵗ and 9ᵗʰ harvest 'Celica', 'Ever Green' and 'No.117' cultivars respectively.
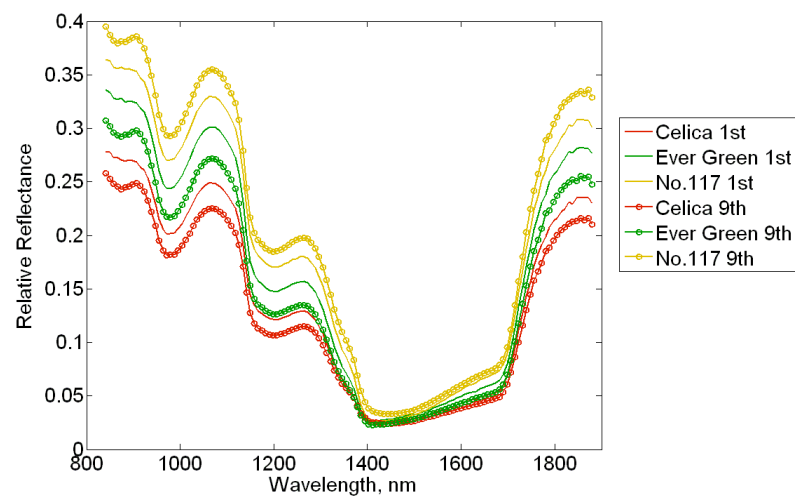
Fig. 37 Averaged SWIR reflectance spectra of the 1ˢᵗ and 9ᵗʰ harvest 'Celica', 'Ever Green' and 'No.117' cultivars respectively
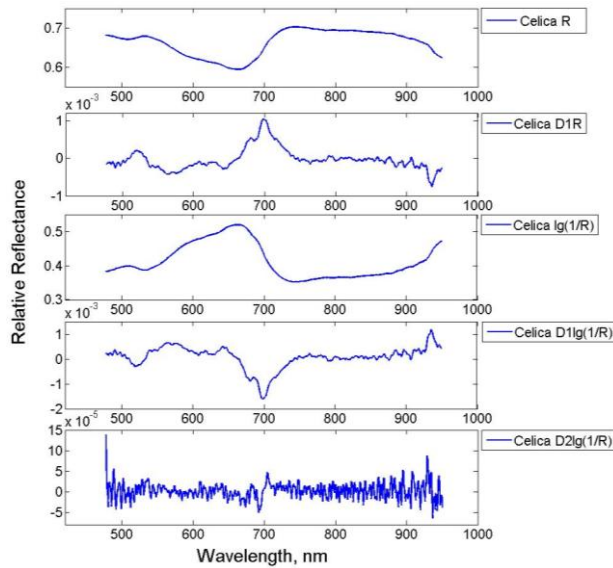
Fig. 38 Averaged VIS-NIR pre-processed reflectance spectra of the 1st harvest of 'Celica' cultivar.
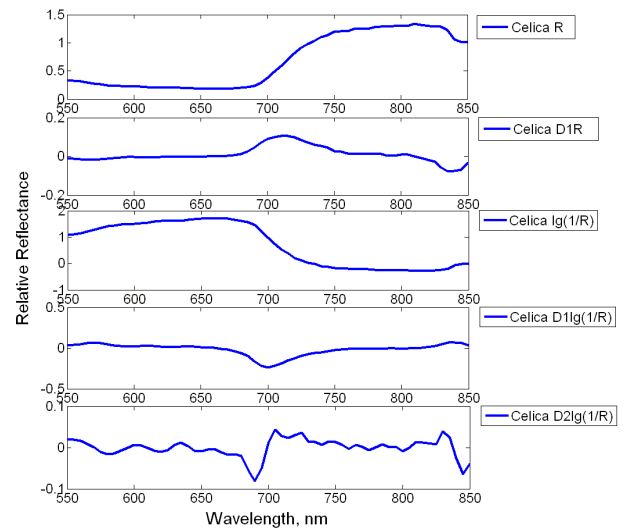
Fig. 39 Averaged hyper cube pre-processed reflectance spectra of the 1st harvest of 'Celica' cultivar.
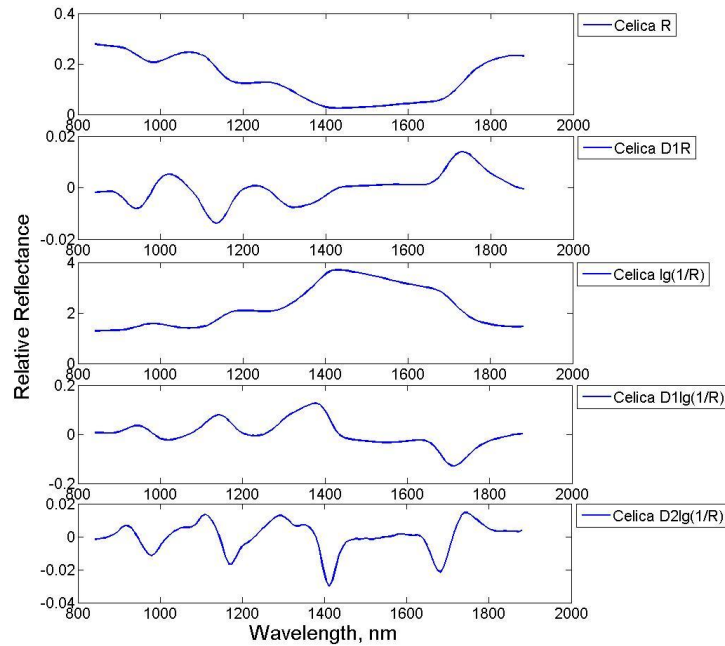
Fig. 40 Averaged SWIR pre-processed reflectance spectra of the 1st harvest of 'Celica' cultivar.

5.4. Cross correlation analysis among the destructively measured reference parameters

For examination of the relationship among the destructively tested reference parameters, matrices of correlation coefficients were calculated for each pepper variety. The compared variables are: DAA, TSS, DM, AA (ascorbic acid), TChl (total chlorophyll), Car (carotenoid), OP (osmotic potential), $CE_{Compression}$, $Int_{Copmression}$, $CE_{Rupture}$, and Weight of the pepper sample.

Results of the correlation test are shown in Table 13 for 'Ever Green', 'No.117' and 'Celica' cvs., respectively.

Table 13 Covariance matrix among reference parameters for 'Ever Green', 'No.117' and 'Celica' cvs., respectively with 95% significance level.

Ever Green	DAA	TSS	DM	AA	TChl	Car	OP	$CE_{Compression}$	$Int_{Compression}$	$CE_{Rupture}$	Weight
DAA	1										
TSS	0.90	1									
DM	0.86	0.97	1								
AA	0.28	0.32	0.27	1							
TChl	-0.55	-0.45	-0.40	-0.11	1						
Car	0.81	0.89	0.91	0.08	-0.32	1					
OP	0.84	0.91	0.92	0.20	-0.42	0.88	1				
$CE_{Compression}$	-0.56	-0.55	-0.49	-0.31	0.40	-0.46	-0.50	1			
$Int_{Compression}$	0.00	-0.02	-0.03	-0.11	0.15	0.00	0.00	0.00	1		
$CE_{Rupture}$	-0.47	-0.55	-0.52	-0.29	0.28	-0.46	-0.47	0.44	0.21	1	
Weight	0.58	0.41	0.32	0.48	-0.41	0.21	0.30	-0.47	0.02	-0.27	1
No.117	DAA	TSS	DM	AA	TChl	Car	OP	$CE_{Compression}$	$Int_{Compression}$	$CE_{Rupture}$	Weight
DAA	1										
TSS	0.90	1									
DM	0.88	0.98	1								
AA	0.57	0.61	0.59	1							
TChl	-0.82	-0.88	-0.86	-0.70	1						
Car	0.80	0.84	0.82	0.43	-0.68	1					
OP	0.87	0.94	0.93	0.59	-0.85	0.75	1				
$CE_{Compression}$	-0.39	-0.36	-0.34	-0.38	0.43	-0.31	-0.33	1			
$Int_{Compression}$	-0.13	-0.16	-0.16	-0.17	0.11	-0.12	-0.16	-0.04	1		
$CE_{Rupture}$	-0.51	-0.57	-0.56	-0.45	0.63	-0.47	-0.55	0.43	0.12	1	
Weight	0.32	0.15	0.14	0.28	-0.24	0.04	0.19	-0.33	0.21	-0.21	1
Celica	DAA	TSS	DM	AA	TChl	Car	OP	$CE_{Compression}$	$Int_{Compression}$	$CE_{Rupture}$	Weight
DAA	1										
TSS	0.89	1									
DM	0.88	0.98	1								
AA	0.56	0.58	0.59	1							
TChl	-0.86	-0.89	-0.86	-0.52	1						
Car	0.69	0.78	0.80	0.33	-0.60	1					
OP	0.87	0.95	0.93	0.55	-0.88	0.76	1				
$CE_{Compression}$	-0.43	-0.39	-0.37	-0.29	0.40	-0.20	-0.36	1			
$Int_{Compression}$	0.07	0.02	0.01	-0.05	-0.02	0.00	0.00	-0.07	1		
$CE_{Rupture}$	-0.67	-0.67	-0.66	-0.63	0.66	-0.45	-0.67	0.33	0.09	1	
Weight	0.51	0.31	0.31	0.50	-0.34	0.14	0.29	-0.23	0.10	-0.41	1

Absolut value of the Correlation Coefficient

| 1-0.8 |
| 0.8-0.6 |
| 0.6-0.4 |
| 0.4-0.2 |
| 0.2-0 |

For all three cultivars strong and good correlation was found among DAA, TSS, DM, OP, carotenoid, and total chlorophyll content. Moderate and good correlation was found among the coefficient of elasticity of the rupture test and the other reference parameters. The coefficient of elasticity of the compression test gave moderate correlation with the DAA and total chlorophyll for all three pepper varieties, and only in case of the 'Ever Green' cv. it correlated moderately with the other reference parameters. In case of the other two cultivars it resulted poor correlation. The change of the samples weight during the growth has moderate to poor correlation to the other reference parameters. The index calculated from the area under the compression curve did not show any correlation with the other reference parameters. Consequently, since it does not

show any trend in the advancement with DAA, this parameter will be disregarded in the further analysis.

5.5. Correlation and regression analysis

5.5.1. Correlation and regression analysis for ascorbic acid and NDT methods

5.1.1.1. Correlation analysis for rate of relaxation, colour measurement, and ultrasonic test

Table 14 shows the results of cross correlation analysis for ascorbic acid with the calculated indices of relaxation test (Rate of relaxation, Remaining deformation, Coefficient of elasticity from relaxation test), with the parameters of colour measurements (L, C, h) and ultrasonic attenuation. The resulted coefficients of correlation (r) present poor correlation between the AA and the correlated parameters. Exception is the calculated coefficient of elasticity from the relaxation test which indicates 25 % common variance.

Table 14 Covariance matrix between ascorbic acid and non-destructive measurements for 'Ever Green', 'No.117', and 'Celica' cultivars, respectively, with, 95% significance level.

Ascorbic Acid	Rate of Relaxation	Remaining Deformation	Coefficient of elasticity Relaxation	Colour Measurement			Ultrasonic Attenuation
				L	C	h	
Ever Green	0.06	0.19	0.49	0.15	0.19	0.19	0.31
No.117	0.34	0.26	0.20	0.39	0.41	0.45	0.35
Celica	0.15	0.04	0.43	0.34	0.11	0.45	0.41

5.1.1.2. PLS Regression for VIS-NIR and SWIR spectral analysis and hyperspectral imaging

The coefficients of variance for ascorbic acid were 53.7%, 35.6% and 60.8% for 'Ever Green', 'No.117' and 'Celica' cultivars, respectively. The average squared intercorrelations found to be poor between ascorbic acid-total soluble solid (0.27), ascorbic acid-dry matter (average: 0.26) and ascorbic acid-total chlorophyll content (average: 0.25). Relatively high coefficient of variance and low squared intercorrelation indicate that prediction by the VIS-NIR, SWIR and hyperspectral imaging method is applicable.

It is generally required of a robust PLS regression model to have as few factors as possible and the lowest possible error values of calibration and validation (Bjorsvik and Martens, 1992).

For all three cultivars, Table 15 presents the results from PLS regression for VIS-NIR, hyperspectral imaging and SWIR, respectively. The following statistical parameters are shown for each model: no. of latent variables, LV; coefficient of determination, r^2; root-mean-square error of calibration, RMSEC; root-mean-square error of cross-validation, RMSECV; robust

parameter design, RPD; ratio of RMSECV and RMSEC, and standardized weighted sum index, SWS.

Comparison of the PLS models among the two wavelength ranges (VIS-NIR, SWIR) and hyperspectral imaging shows that the VIS-NIR models were obtained with fewer LVs (average, 6), higher r^2 (average, 0.71), lower RMSEC (average, 9.77 mg per 100 g), lower RMSECV (average, 16.48 mg per 100 g), higher RPD (average, 2.11) and higher SWS (average, 0.6). Whereas the hyperspectral models resulted the lower ratio of RMSECV and RMSEC (average, 1.14).

Table 15 Performance measures of PLS regression models for ascorbic acid, using data from the VIS-NIR, Hyperspectral, and SWIR spectral region. Models for the three pepper varieties are presented: 'Ever Green', 'No, 117' and 'Celica'.

PLS	Ascorbic acid, mg/100g	Statistical parameter	LV	r^2	RMSEC	RMSECV	RPD	RMSECV/ RMSEC	SWS
		R	9	0.79	8.7	15.2	2.1	1.8	0.72
	Ever Green	log(1/R)	8	0.75	11.1	15.9	2.0	1.4	0.66
		D1R	2	0.76	13.0	16.3	2.0	1.3	0.66
		D1log(1/R)	4	0.73	8.2	16.3	2.0	2.0	0.60
		D2log(1/R)	3	0.73	9.9	16.5	1.9	1.7	0.60
	No.117	R	11	0.67	6.3	16.9	2.3	2.7	0.45
		log(1/R)	10	0.64	8.8	17.8	2.2	2.0	0.39
VIS-NIR		D1R	4	0.62	9.5	17.3	2.2	1.8	0.52
		D1log(1/R)	6	0.64	10.5	18.1	2.1	1.7	0.41
		D2log(1/R)	4	0.57	8.1	18.2	2.1	2.3	0.35
	Celica	R	10	0.77	8.7	15.3	2.2	1.8	0.72
		log(1/R)	**8**	**0.78**	**11.1**	**15.1**	**2.2**	**1.4**	**0.79**
		D1R	5	0.76	7.6	15.6	2.2	2.0	0.71
		D1log(1/R)	3	0.74	12.1	16.4	2.1	1.4	0.66
		D2log(1/R)	2	0.74	12.9	16.1	2.1	1.2	0.72
	Ever Green	R	8	0.73	15.2	17.0	1.9	1.1	0.52
		log(1/R)	8	0.73	15.1	17.1	1.9	1.1	0.51
		D1R	4	0.72	15.0	16.7	1.9	1.1	0.59
		D1log(1/R)	7	0.75	13.1	16.7	1.9	1.3	0.57
		D2log(1/R)	2	0.68	15.7	17.6	1.8	1.1	0.48
	No.117	R	7	0.58	15.9	17.4	2.2	1.1	0.50
Hyperspectral imaging		log(1/R)	7	0.55	15.4	17.3	2.2	1.1	0.50
		D1R	3	0.51	17.0	17.8	2.2	1.0	0.46
		D1log(1/R)	5	0.54	15.8	18.1	2.1	1.1	0.41
		D2log(1/R)	5	0.56	15.5	18.5	2.1	1.2	0.37
	Celica	R	10	0.70	14.3	16.9	2.0	1.2	0.52
		log(1/R)	10	0.73	13.9	16.1	2.1	1.2	0.63
		D1R	8	0.72	14.4	16.0	2.1	1.1	0.66
		D1log(1/R)	6	0.69	15.5	17.3	2.0	1.1	0.51
		D2log(1/R)	8	0.70	14.6	17.6	1.9	1.2	0.45
	Ever Green	R	8	0.75	12.6	15.7	2.0	1.2	0.69
		log(1/R)	9	0.77	11.7	16.0	2.0	1.4	0.64
		D1R	9	0.70	13.2	17.5	1.8	1.3	0.44
		D1log(1/R)	9	0.77	11.5	16.3	2.0	1.4	0.60
		D2log(1/R)	10	0.77	10.9	16.4	1.9	1.5	0.58
	No.117	R	10	0.70	11.2	16.1	2.4	1.4	0.67
SWIR		log(1/R)	9	0.70	12.0	16.2	2.4	1.4	0.66
		D1R	10	0.68	12.3	16.8	2.3	1.4	0.57
		D1log(1/R)	7	0.63	14.7	18.6	2.1	1.3	0.36
		D2log(1/R)	10	0.62	12.3	18.7	2.1	1.5	0.30
	Celica	R	8	0.71	14.2	17.1	2.0	1.2	0.51
		log(1/R)	7	0.65	15.8	18.7	1.8	1.2	0.30
		D1R	12	0.70	14.4	18.9	1.8	1.3	0.26
		D1log(1/R)	8	0.65	15.7	18.4	1.8	1.2	0.33
		D2log(1/R)	11	0.70	11.9	18.9	1.8	1.6	0.24

In the VIS-NIR range, for 'Ever Green' the reflectance (R), for 'No.117' the 1st derivative of reflectance (D_1R), whereas for cv. 'Celica' the $D_2log(1/R)$ gave the highest SWS and therefore the best model. The relevant SWS indices were 0.72, 0.52, and 0.79 for 'Ever Green', 'No. 117' and 'Celica', respectively.

By the hyperspectral imaging for 'Ever Green' and 'Celica' cultivars the 1st derivative of reflectance (D_1R), while for 'No.117' cv. the reflectance (R) and log(1/R), resulted the highest SWS and therefore the best model. The relevant SWS indices were 0.59, 0.66, and 0.50 for 'Ever Green', 'Celica' and, 'No. 117' respectively.

In the SWIR spectral range the best results were obtained with the models based on reflectance spectra (R) for all three cultivars, with SWS 0.66, 0.67 and 0.51 for 'Ever Green', 'Celica' and, 'No. 117' respectively.

The overall comparison of models from the two spectral ranges and hyperspectral imaging resulted VIS-NIR spectral measurements to yield stronger correlation to predict vitamin C content in 'Ever Green' and 'Celica' bell pepper cultivars while SWIR spectral measurement was found best for 'No. 117' variety. As a matter of fact, efficient models were achieved in the VIS-NIR range for 'Ever Green' cv., which retains its green colour even in the fully ripe stage. It means that the ascorbic acid change during the growth and maturation is not indirectly correlated with the spectral information but direct correlation is presumed.
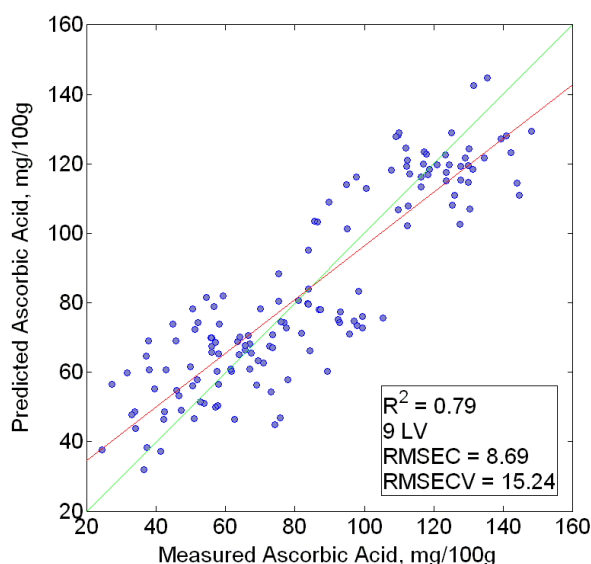
Fig. 41 Scatter plot of ascorbic acid content for 'Ever Green' variety, as predicted by PLS regression model and as measured in the laboratory. The PLS model was built with the reflectance (R) of the spectral data in the VIS-NIR range.
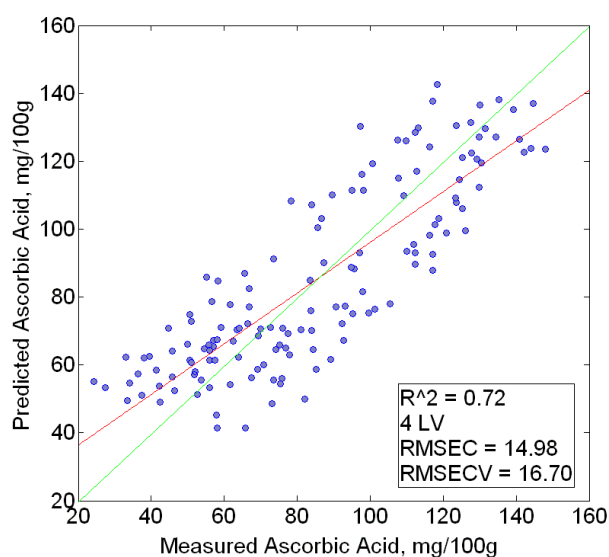
Fig. 42 Scatter plot of ascorbic acid content for 'Ever Green' variety, as predicted by PLS regression model and as measured in the laboratory. The PLS model was built with the 1st derivative (D_1R) of the spectral data from the hyperspectral imaging.

PLSR prediction and measured values for cv. 'Ever Green' are shown in Figs. 41-43, as examples for VIS-NIR, hyperspectral imaging and SWIR, respectively. In all the three figures, the ordinate and abscissa axes represent the measured and the fitted values. For the VIS-NIR (Fig. 41) a model with nine LVs obtained $r^2 = 0.79$ and RMSECV = 15.2, for the hyperspectral imaging (Fig. 42) a model with four LVs obtained $r^2 = 0.72$ and RMSECV = 16.7, whereas for SWIR (Fig. 43) eight LVs were needed to achieve $r^2 = 0.75$ and RMSECV = 15.7.

Fig. 43 Scatter plot of ascorbic acid content for 'Ever Green' variety, as predicted by PLS regression model and as measured in the laboratory. The PLS model was built with the reflectance (R) of the spectral data in the SWIR range.

The Variable Importance in Projection (VIP) scores indicate the significance of specific wavelengths in the model, and Fig. 44 presents the VIP scores for the reflectance model in the VIS-NIR spectral range for cv. 'Ever Green'. Three wavelength ranges are the most significant in the model: 477–530, 670–695, and 870–950 nm. The ranges 477-530 and 670-695 nm are related to the chlorophyll a and b and carotenoid contents; the range 870-950 nm relates to internal chemical composition (C-H stretch) and texture. Based on the VIP scores the significant wavelengths in the visible range were about half as important as those above 870 nm. Thus, the relative significance of the wavelength range above 870 nm suggests that the textural and chemical composition have greater influence on the relationship between ascorbic acid content and spectral response of bell pepper fruits than the colour information in the spectra.

Figure 45 presents the VIP scores of the reflectance model in the SWIR spectral range for cv. 'Ever Green'. Two main wavelength ranges were found that significantly influenced the regression model: the range of 840–910 nm was found to be meaningfully related to texture and chemical composition, as in the VIS-NIR model; the range of 1350–1800 nm is associated with

the vibration modes of the first overtones of C-H and O-H bond stretching. These chemical bonds are found in the molecules of ascorbic acid, water.

Fig. 44 VIP Scores for reflectance (R) spectra (VIS-NIR) of 'Ever Green' cultivar
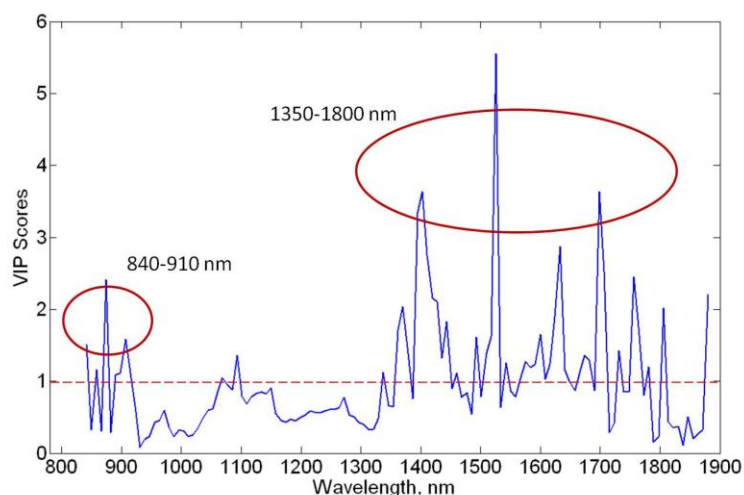
Fig. 45 VIP Scores for reflectance (R) spectra (SWIR) of 'Ever Green' cultivar

5.5.2. Correlation and regression analysis for total chlorophyll content and NDT methods

5.5.2.1. Correlation analysis for rate of relaxation, colour measurement, and ultrasonic test

The results of cross correlation analysis for total chlorophyll with the calculated indices of relaxation test (Rate of relaxation, Remaining deformation, coefficient of elasticity from relaxation test), with the parameters of colour measurements (L, C, h) and ultrasonic attenuation shown in table 16.

The highest coefficient of correlation (r) was found for 'No. 117' with the parameters L, C, h from the colour measurements, as well as for 'Celica' cv. with C and h, whereas h indicated only 25 % of common variance in case of 'Ever Green' cv. Ultrasonic attenuation showed 20-25 % of

common variance in case of 'No. 117' and 'Celica' cultivars, but very poorly correlated with the chlorophyll content in case of the 'Ever Green' cv. Likewise correlation showed in case of coefficient of elasticity from the relaxation test and chlorophyll content for all three cultivars. Moderate correlation of coefficient was found between the rate of relaxation, remaining deformation and chlorophyll content in case of 'No. 117' and 'Celica' cultivars.

Table 16 Covariance matrix between total chlorophyll and non-destructive measurements for 'Ever Green', 'No.117', and 'Celica' cultivars, respectively, with 95% significance level.

Total Chlorophyll	Rate of Relaxation	Remaining Deformation	Coefficient of elasticity Relaxation	Colour Measurement			Ultrasonic Attenuation
				L	C	h	
Ever Green	0.19	0.18	0.15	0.06	0.15	0.55	0.25
No.117	0.65	0.51	0.01	0.90	0.90	0.91	0.43
Celica	0.46	0.33	0.20	0.06	0.70	0.89	0.45

5.5.2.2. PLS Regression for VIS-NIR and SWIR spectral analysis and hyperspectral imaging

The coefficients of variance for total chlorophyll content were 19.1%, 101.6% and 85.2% for 'Ever Green', 'No.117' and 'Celica' cultivars, respectively. The average squared intercorrelations found to be poor between total chlorophyll-total soluble solid (0.55), total chlorophyll-dry matter (average: 0.50) and total chlorophyll-carotenoid content (average: 0.28). Relatively high coefficient of variance and relatively low squared intercorrelation indicate that prediction by the VIS-NIR, SWIR and hyperspectral imaging method is applicable.

Table 17 presents for all three cultivars, the results from PLS regression for VIS-NIR, hyperspectral imaging and SWIR, respectively. The following statistical parameters are shown for each model: no. of latent variables, LV; coefficient of determination, r^2; root-mean-square error of calibration, RMSEC; root-mean-square error of cross-validation, RMSECV; robust parameter design, RPD; ratio of RMSECV and RMSEC, and standardized weighted sum index, SWS.

Comparison of the PLS models among the two wavelength ranges (VIS-NIR, SWIR) and hyperspectral imaging shows that the VIS-NIR and hyperspectral models were obtained with fewer LVs (average, 6), whereas SWIR models achieved higher r^2 (average, 0.85), lower RMSECV (average, 0.0068 mg/g), higher RPD (average, 3.42) and higher SWS (average, 0.62). Whereas hyperspectral models resulted lower RMSECV/RMSEC (average, 1.11), with average SWS: 0.62.

In the VIS-NIR range, for 'Ever Green' the reflectance (R), for 'No.117' the 1st derivative of reflectance (D_1R), whereas for cv. 'Celica' the log(1/R) and 1st derivative of reflectance (D_1R)

gave the highest SWS and therefore the best model. The relevant SWS indices were 0.51, 0.65, and 0.59 for 'Ever Green', 'No. 117' and 'Celica', respectively.

Table 17 Performance measures of PLS regression models for total chlorophyll content, using data from the VIS-NIR, Hyperspectral, and SWIR spectral region. Models for the three pepper varieties are presented: 'Ever Green', 'No, 117' and 'Celica'.

PLS	Total Chlorophyll, mg/g	Statistical parameter	LV	r^2	RMSEC	RMSECV	RPD	RMSECV/ RMSEC	*SWS*
VIS-NIR	Ever Green	R	6	0.60	0.007	0.008	1.7	1.2	*0.51*
		log(1/R)	7	0.62	0.007	0.009	1.6	1.3	*0.49*
		D_1R	5	0.61	0.003	0.008	1.7	2.7	*0.37*
		D_1log(1/R)	5	0.62	0.004	0.009	1.6	2.5	*0.38*
		D_2log(1/R)	2	0.32	0.008	0.010	1.5	1.2	*0.46*
	No.117	R	9	0.95	0.003	0.005	4.2	1.9	*0.61*
		log(1/R)	7	0.91	0.005	0.007	3.4	1.3	*0.63*
		D_1R	5	0.95	0.003	0.005	4.2	2.0	*0.65*
		D_1log(1/R)	5	0.94	0.003	0.006	4.1	2.1	*0.63*
		D_2log(1/R)	3	0.90	0.005	0.007	3.2	1.5	*0.64*
	Celica	R	9	0.92	0.005	0.008	3.4	1.5	*0.56*
		log(1/R)	9	0.93	0.005	0.008	3.7	1.5	*0.59*
		D_1R	5	0.93	0.004	0.008	3.6	1.9	*0.59*
		D_1log(1/R)	5	0.92	0.004	0.008	3.3	2.0	*0.56*
		D_2log(1/R)	3	0.87	0.006	0.010	2.8	1.5	*0.58*
Hyperspectral imaging	Ever Green	R	8	0.40	0.009	0.010	1.4	1.1	*0.41*
		log(1/R)	9	0.43	0.009	0.010	1.4	1.1	*0.40*
		D_1R	5	0.44	0.009	0.010	1.4	1.1	*0.46*
		D_1log(1/R)	6	0.44	0.009	0.010	1.4	1.1	*0.44*
		D_2log(1/R)	5	0.48	0.008	0.010	1.4	1.3	*0.45*
	No.117	R	5	0.95	0.005	0.005	4.3	1.1	*0.74*
		log(1/R)	5	0.95	0.005	0.005	4.5	1.1	*0.74*
		D_1R	5	0.95	0.005	0.005	4.4	1.1	*0.74*
		D_1log(1/R)	5	0.95	0.005	0.005	4.4	1.1	*0.74*
		D_2log(1/R)	**3**	**0.95**	**0.005**	**0.005**	**4.4**	**1.1**	***0.76***
	Celica	R	5	0.93	0.008	0.008	3.5	1.1	*0.66*
		log(1/R)	5	0.95	0.007	0.007	4.0	1.1	*0.70*
		D_1R	7	0.96	0.006	0.007	4.3	1.1	*0.69*
		D_1log(1/R)	5	0.95	0.006	0.007	4.0	1.1	*0.69*
		D_2log(1/R)	7	0.95	0.006	0.007	3.9	1.2	*0.66*
SWIR	Ever Green	R	8	0.66	0.006	0.008	1.8	1.3	*0.50*
		log(1/R)	10	0.71	0.005	0.008	1.9	1.5	*0.48*
		D_1R	10	0.61	0.007	0.008	1.7	1.2	*0.47*
		D_1log(1/R)	8	0.63	0.007	0.008	1.8	1.2	*0.51*
		D_2log(1/R)	9	0.71	0.006	0.007	1.9	1.3	*0.51*
	No.117	R	8	0.96	0.004	0.005	5.0	1.3	*0.72*
		log(1/R)	6	0.96	0.004	0.005	4.9	1.1	*0.75*
		D_1R	6	0.96	0.004	0.005	4.7	1.1	*0.74*
		D_1log(1/R)	6	0.96	0.004	0.005	4.9	1.1	*0.75*
		D_2log(1/R)	7	0.96	0.004	0.005	5.0	1.2	*0.73*
	Celica	R	8	0.92	0.007	0.008	3.5	1.2	*0.61*
		log(1/R)	8	0.91	0.007	0.008	3.4	1.2	*0.60*
		D_1R	8	0.93	0.006	0.007	3.8	1.2	*0.64*
		D_1log(1/R)	7	0.92	0.007	0.008	3.6	1.1	*0.64*
		D_2log(1/R)	6	0.92	0.007	0.008	3.5	1.2	*0.64*

In case of the hyperspectral imaging for 'Ever Green' the 1st derivative of reflectance (D_1R), for 'No.117' cv. the $D_2log(1/R)$ and for 'Celica' the $log(1/R)$ resulted with the highest SWS and therefore the best model. The relevant SWS indices were 0.46, 0.76, and 0.70 for 'Ever Green', 'Celica' and, 'No. 117' respectively.

The best models were achieved in the SWIR spectral range for 'Ever Green' and 'Celica' by the $D_1log(1/R)$ and $D_2log(1/R)$, whereas for 'No. 117' the $log(1/R)$ resulted with the models, with SWS 0.51, 0.75 and 0.64, respectively.

The overall comparison of models from the two spectral ranges and hyperspectral imaging resulted hyperspectral imaging and SWIR spectral measurements to yield stronger correlation to predict total chlorophyll content for all three bell pepper cultivars.

PLSR prediction and measured values for cv. 'No. 117' are shown in Figs. 46-48, as examples for VIS-NIR, hyperspectral imaging and SWIR, respectively. In both figures, the ordinate and abscissa axes represent the measured and the fitted values. For the VIS-NIR (Fig. 46) a model with five LVs obtained r^2=0.95 and RMSECV=0.0055, for the hyperspectral imaging (Fig. 47) a model with three LVs was sufficient to achieve r^2=0.95 and RMSECV=0.0052, whereas for SWIR (Fig. 48) six LVs were needed to achieve r^2=0.96 and RMSECV =0.0047.

Fig. 46 Scatter plot of total chlorophyll content for 'No. 117' variety, as predicted by PLS regression model and as measured in the laboratory. The PLS model was built with the 1st derivative of reflectance (R) in the VIS-NIR range.

Fig. 47 Scatter plot of total chlorophyll content for 'No. 117' variety, as predicted by PLS regression model and as measured in the laboratory. The PLS model was built with the $D_2log(1/R)$ of the spectral data from the hyperspectral imaging.

Fig. 48 Scatter plot of total chlorophyll content for 'No. 117' variety, as predicted by PLS regression model and as measured in the laboratory. The PLS model was built with the log(1/R) of the spectral data in the SWIR range.
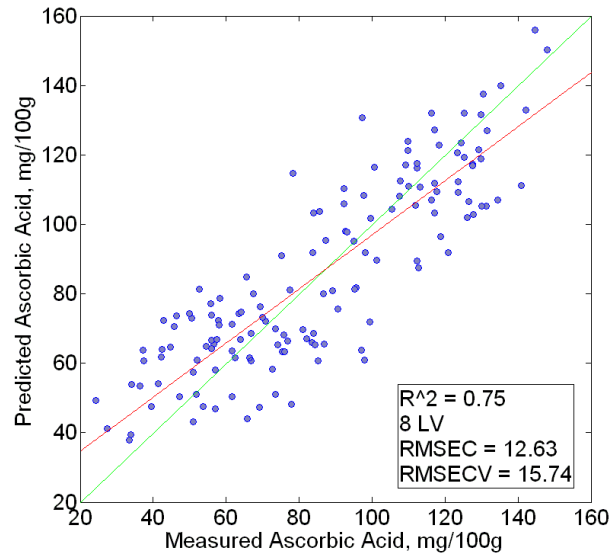
The Variable Importance in Projection (VIP) scores indicate the significance of specific wavelengths in the model, and Fig. 49 presents the VIP scores for the reflectance model in the VIS-NIR spectral range for cv. 'No. 117'. One wide wavelength range was found to be significant in the model 570-690 related to the chlorophyll a and b and carotenoid contents.

Figure 50 presents the VIP scores of the reflectance model in the SWIR spectral range for cv. 'No. 117'. One very significant wavelength range was found that significantly influenced the regression model: the range of 1350–1430 nm. It is associated with the vibration modes of the first overtones of C-H and O-H bond stretching.

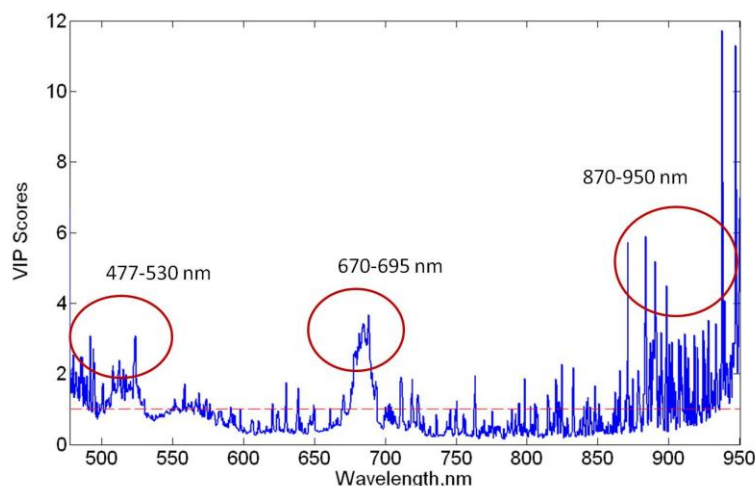**Fig. 49** VIP Scores for reflectance (R) spectra (VIS-NIR) of 'No.117' cultivar

Fig. 50 VIP Scores for reflectance (R) spectra (SWIR) of 'No.117' cultivar

5.5.3. Correlation and regression analysis for carotenoid content and NDT methods

5.5.3.1. Correlation analysis for rate of relaxation, colour measurement, and ultrasonic test

The results of cross correlation analysis for carotenoid content with the calculated indices of relaxation test (Rate of relaxation, Remaining deformation, coefficient of elasticity from relaxation test), with the parameters of colour measurements (L, C, h) and ultrasonic attenuation shown in table 18.

The highest coefficient of correlation (r) was found for all three cultivars with the colour parameter of h, moderate to poor correlation was found with the L and C. Poor correlation was found with the ultrasonic attenuation in case of all three cultivars. Whereas the rate of relaxation had moderate correlation with the carotenoid content in case of 'Ever Green' and 'No. 117' cultivars. Coefficient of elasticity from the relaxation test and carotenoid content did not show close relationship for none of the cultivars.

Table 18 Covariance matrix between carotenoid and non-destructive measurements for 'Ever Green', 'No.117', and 'Celica' cultivars, respectively, with 95% significance level.

Carotenoid	Rate of Relaxation	Remaining Deformation	Coefficient of elasticity Relaxation	Colour Measurement			Ultrasonic Attenuation
				L	C	h	
Ever Green	0.70	0.64	0.15	0.46	0.53	0.82	0.31
No.117	0.66	0.38	0.09	0.74	0.76	0.85	0.47
Celica	0.49	0.38	0.10	0.38	0.60	0.76	0.36

5.5.3.2. PLS Regression for VIS-NIR and SWIR spectral analysis and hyperspectral imaging

The coefficients of variance for carotenoid content were 88.8%, 73.8% and 125.8% for 'Ever Green', 'No.117' and 'Celica' cultivars, respectively. The average squared intercorrelations found to be poor between carotenoid-total soluble solid (0.70), carotenoid-dry matter (average: 0.71) and carotenoid-total chlorophyll (average: 0.28). Although the high coefficient of variance but because of the fair squared intercorrelation indicate that prediction by the VIS-NIR, SWIR and hyperspectral imaging method is applicable with the consideration of possible intercorrelation with TSS and DM.

Table 19 presents for all three cultivars, the results from PLS regression for VIS-NIR, hyperspectral imaging and SWIR, respectively. The following statistical parameters are shown for each model: no. of latent variables, LV; coefficient of determination, r^2; root-mean-square error of calibration, RMSEC; root-mean-square error of cross-validation, RMSECV; robust parameter design, RPD; ratio of RMSECV and RMSEC, and standardized weighted sum index, SWS.

Table 19 Performance measures of PLS regression models for carotenoid content, using data from the VIS-NIR, Hyperspectral, and SWIR spectral region. Models for the three pepper varieties are presented: 'Ever Green', 'No, 117' and 'Celica'.

PLS	Carotenoid, mg/g	Statistical parameter	LV	r^2	RMSEC	RMSECV	RPD	RMSECV/ RMSEC	SWS
VIS-NIR	Ever Green	R	8	0.92	0.007	0.010	3.9	1.4	0.55
		log(1/R)	8	0.91	0.007	0.011	3.5	1.6	0.48
		D_1R	3	0.92	0.007	0.010	3.9	1.4	0.60
		D_1log(1/R)	3	0.90	0.008	0.011	3.5	1.4	0.58
		D_2log(1/R)	3	0.88	0.009	0.012	3.3	1.3	0.56
	No.117	R	7	0.91	0.005	0.006	3.7	1.2	0.64
		log(1/R)	7	0.89	0.006	0.007	3.1	1.2	0.62
		D_1R	4	0.89	0.004	0.006	3.7	1.5	0.61
		D_1log(1/R)	5	0.89	0.004	0.007	3.4	1.6	0.55
		D_2log(1/R)	3	0.81	0.007	0.009	2.4	1.4	0.53
	Celica	R	8	0.95	0.007	0.010	6.6	1.3	0.64
		log(1/R)	7	0.93	0.010	0.012	5.3	1.2	0.61
		D_1R	5	0.92	0.007	0.012	5.2	1.8	0.49
		D_1log(1/R)	4	0.92	0.009	0.014	4.5	1.6	0.52
		D_2log(1/R)	3	0.86	0.012	0.017	3.7	1.4	0.47
Hyperspectral imaging	Ever Green	R	9	0.87	0.012	0.014	2.8	1.2	0.47
		log(1/R)	9	0.89	0.012	0.013	3.0	1.1	0.52
		D_1R	8	0.86	0.011	0.014	2.8	1.3	0.46
		D_1log(1/R)	7	0.87	0.012	0.013	3.0	1.1	0.53
		D_2log(1/R)	8	0.78	0.012	0.016	2.4	1.3	0.37
	No.117	R	8	0.91	0.005	0.006	4.0	1.1	0.66
		log(1/R)	8	0.92	0.005	0.006	4.0	1.1	0.66
		D_1R	8	0.90	0.005	0.006	3.9	1.1	0.65
		D_1log(1/R)	8	0.91	0.005	0.006	4.0	1.2	0.65
		D_2log(1/R)	5	0.86	0.006	0.007	3.3	1.2	0.63
	Celica	R	6	0.95	0.009	0.011	5.7	1.2	0.66
		log(1/R)	**10**	**0.97**	**0.007**	**0.008**	**7.5**	**1.2**	**0.68**
		D_1R	7	0.96	0.008	0.010	6.2	1.2	0.66
		D_1log(1/R)	9	0.96	0.008	0.010	6.5	1.2	0.65
		D_2log(1/R)	8	0.95	0.009	0.012	5.4	1.3	0.59
SWIR	Ever Green	R	8	0.87	0.010	0.012	3.3	1.2	0.51
		log(1/R)	8	0.89	0.010	0.012	3.3	1.3	0.51
		D_1R	9	0.89	0.010	0.013	3.0	1.3	0.48
		D_1log(1/R)	7	0.85	0.012	0.014	2.8	1.2	0.49
		D_2log(1/R)	5	0.88	0.010	0.012	3.3	1.3	0.55
	No.117	R	7	0.84	0.007	0.007	3.0	1.1	0.59
		log(1/R)	7	0.87	0.005	0.006	3.6	1.2	0.62
		D_1R	5	0.82	0.007	0.008	2.7	1.1	0.59
		D_1log(1/R)	6	0.88	0.005	0.006	3.7	1.2	0.65
		D_2log(1/R)	5	0.83	0.006	0.007	3.1	1.3	0.58
	Celica	R	8	0.90	0.013	0.016	3.9	1.2	0.48
		log(1/R)	8	0.89	0.013	0.016	3.9	1.2	0.48
		D_1R	8	0.90	0.014	0.017	3.7	1.2	0.47
		D_1log(1/R)	7	0.88	0.013	0.015	4.2	1.2	0.52
		D_2log(1/R)	6	0.85	0.013	0.018	3.5	1.4	0.41

Comparison of the PLS models among the two wavelength ranges (VIS-NIR, SWIR) and hyperspectral imaging shows that the VIS-NIR models were obtained with fewer LVs (average, 5), whereas hyperspectral imaging models achieved higher r^2 (average, 0.91), lower RMSECV (average, 0.01 mg/g), higher RPD (average, 4.31), lower RMSECV/RMSEC (average, 1.19) and higher SWS (average, 0.59).

In the VIS-NIR range, for 'Ever Green' the 1st derivative of reflectance (D_1R), for 'No.117' and 'Celica' the reflectance (R) gave the highest SWS and therefore the best model. The relevant SWS indices were 0.60, 0.64, and 0.64 for 'Ever Green', 'No. 117' and 'Celica', respectively.

In case of the hyperspectral imaging for 'Ever Green' the $D_1\log(1/R)$, for 'No.117' and 'Celica' cultivars the $\log(1/R)$ resulted with the highest SWS and therefore the best model. The relevant SWS indices were 0.53, 0.66, and 0.68 for 'Ever Green', 'Celica' and, 'No. 117' respectively.

The best models were achieved in the SWIR spectral range for 'Ever Green' by the $D_2\log(1/R)$ spectral treatment, whereas for 'No. 117' and 'Celica' cultivars by the $D_1\log(1/R)$ resulted the best models, with SWS 0.51, 0.75 and 0.64, respectively.

The overall comparison of models from the two spectral ranges and hyperspectral imaging resulted hyperspectral imaging to yield efficient models to predict carotenoid content for 'No. 117' and 'Celica' bell pepper cultivars; whereas for 'Ever Green' variety the VIS-NIR spectral measurements yielded the best carotenoid predictions.

PLSR prediction and measured values for cv. 'Celica' are shown in Figs. 51-53, as examples for VIS-NIR, hyperspectral imaging and SWIR, respectively. In both figures, the ordinate and abscissa axes represent the measured and the fitted values. For the VIS-NIR (Fig. 51) a model with eight LVs obtained r^2=0.95 and RMSECV=0.0096, for the hyperspectral imaging (Fig. 52) a model with ten LVs obtained r^2=0.97 and RMSECV=0.0084, whereas for SWIR (Fig. 53) seven LVs were needed to achieve r^2=0.88 and RMSECV =0.015.

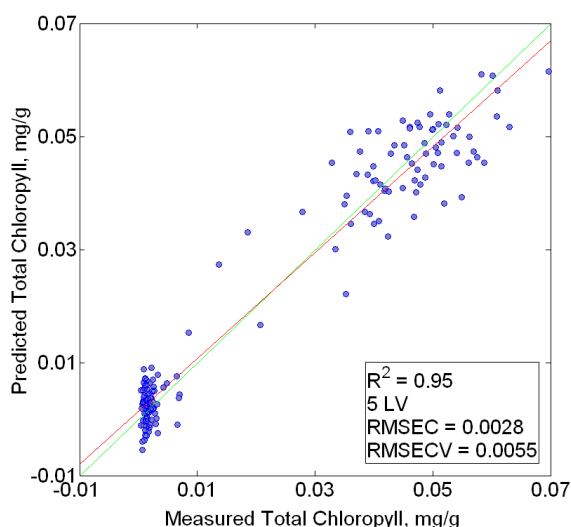**Fig. 51** Scatter plot of carotenoid content for 'Celica' variety, as predicted by PLS regression model and as measured in the laboratory. The PLS model was built with the reflectance (R) spectral data in the VIS-NIR range.
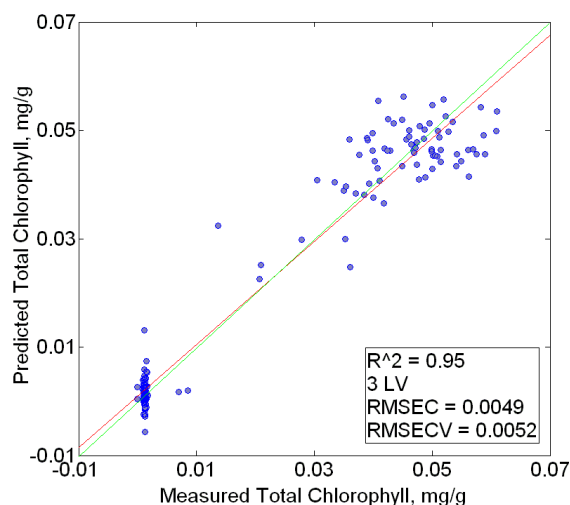
Fig. 52 Scatter plot of carotenoid content for 'Celica' variety, as predicted by PLS regression model and as measured in the laboratory. The PLS model was built with the $\log(1/R)$ of the spectral data from the hyperspectral imaging.
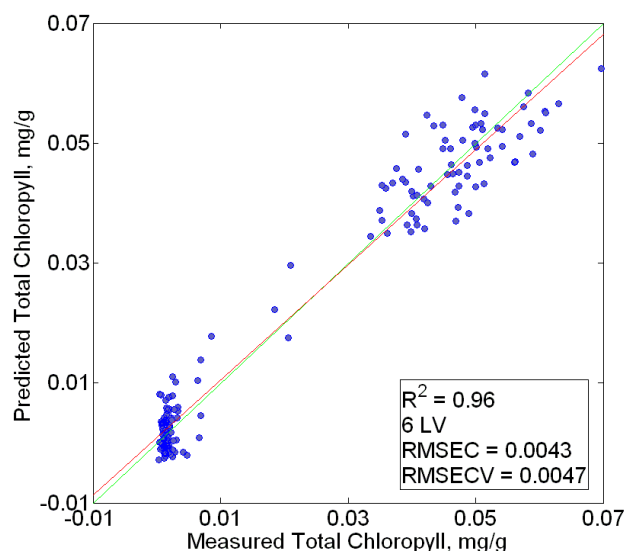
Fig. 53 Scatter plot of carotenoid content for 'Celica' variety, as predicted by PLS regression model and as measured in the laboratory. The PLS model was built with the $D_1\log(1/R)$ of the spectral data in the SWIR range.

The Variable Importance in Projection (VIP) scores indicate the significance of specific wavelengths in the model, and Fig. 54 presents the VIP scores for the reflectance model in the VIS-NIR spectral range for cv. 'Celica'. Two wavelength ranges were found to be significant in the model: 477-490 and 520-690 related to the chlorophyll a and b and carotenoid contents.

Figure 55 presents the VIP scores of the reflectance model in the SWIR spectral range for cv. 'Celica'. Similarly to the model for total chlorophyll prediction, one very significant wavelength range was found that significantly influenced the regression model: the range of 1320–1430 nm. It is associated with the vibration modes of the first overtones of C-H and O-H bond stretching.
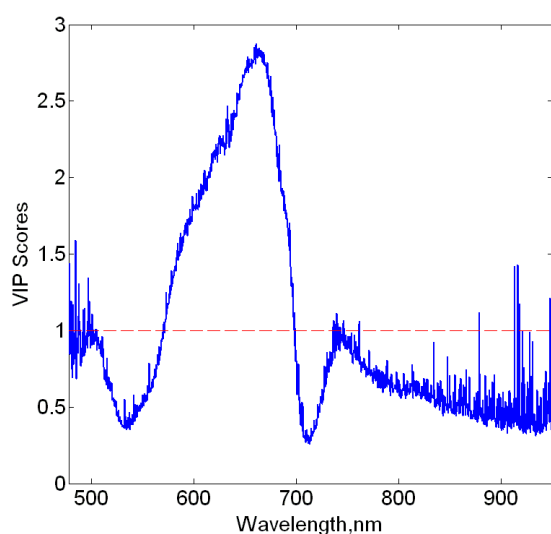

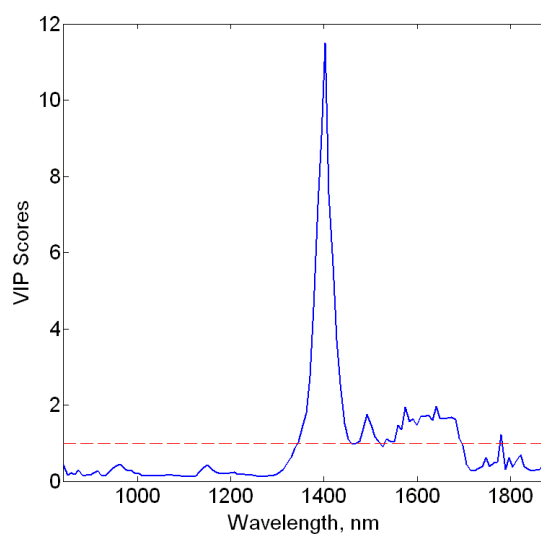**Fig. 54** VIP Scores for reflectance (R) spectra (VIS-NIR) of 'Celica' cultivar
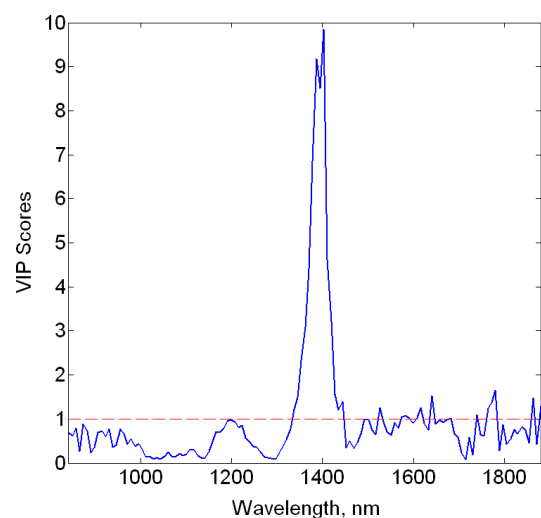
Fig. 55 VIP Scores for reflectance (R) spectra (SWIR) of 'Celica' cultivar

5.5.4. Correlation and regression analysis for total soluble solid (TSS) and NDT methods

5.5.4.1. Correlation analysis for rate of relaxation, colour measurement, and ultrasonic test

The results of cross correlation analysis for TSS with the calculated indices of relaxation test (Rate of relaxation, Remaining deformation, Coefficient of elasticity from relaxation test), with the parameters of colour measurements (L, C, h) and ultrasonic attenuation shown in table 20. The highest coefficient of correlation (r) was found for all three cultivars for TSS with the colour parameter of h, good correlation was found with the L and C in case of 'No. 117' cv. Poor correlation was found with the ultrasonic attenuation and remaining deformation in case of all three cultivars, whereas the rate of relaxation had moderate correlation with the TSS in case of all three cultivars. Coefficient of elasticity from the relaxation test and carotenoid content did not show close relationship for none of the cultivars.

Table 20 Covariance matrix between TSS and non-destructive measurements for 'Ever Green', 'No.117', and 'Celica' cultivars, respectively, with 95% significance level.

TSS	Rate of Relaxation	Remaining Deformation	Coefficient of elasticity Relaxation	Colour Measurement			Ultrasonic Attenuation
				L	C	h	
Ever Green	0.66	0.54	0.04	0.44	0.47	0.81	0.37
No.117	0.67	0.47	0.12	0.87	0.89	0.92	0.48
Celica	0.53	0.36	0.17	0.21	0.67	0.94	0.45

5.1.1.3. PLS Regression for VIS-NIR and SWIR spectral analysis and hyperspectral imaging

The coefficients of variance for carotenoid content were 28.2%, 30.2% and 33.5% for 'Ever Green', 'No.117' and 'Celica' cultivars, respectively. The average squared intercorrelations found to be poor between TSS-ascorbic acid (0.25), TSS-DM (average: 0.95) and TSS-total chlorophyll content (average: 0.55). Although the relatively high coefficient of variance with poor squared intercorrelation between TSS and ascorbic acid and total chlorophyll, but good squared intercorrelation with the dry matter indicate that prediction by the VIS-NIR, SWIR and hyperspectral imaging method is applicable with the consideration of possible intercorrelation with DM.

Table 21 presents for all three cultivars, the results from PLS regression for VIS-NIR, hyperspectral imaging and SWIR, respectively. The following statistical parameters are shown for each model: no. of latent variables, LV; coefficient of determination, r^2; root-mean-square error of calibration, RMSEC; root-mean-square error of cross-validation, RMSECV; robust

parameter design, RPD; ratio of RMSECV and RMSEC, and standardized weighted sum index, SWS.

Table 21 Performance measures of PLS regression models for TSS, using data from the VIS-NIR, Hyperspectral, and SWIR spectral region. Models for the three pepper varieties are presented: 'Ever Green', 'No, 117' and 'Celica'.

PLS	TSS, Brix %	Statistical parameter	LV	r^2	RMSEC	RMSECV	RPD	RMSECV/ RMSEC	SWS
VIS-NIR	Ever Green	R	8	0.94	0.25	0.36	4.1	1.4	0.77
		log(1/R)	9	0.92	0.25	0.42	3.5	1.7	0.57
		D_1R	3	0.93	0.28	0.38	3.9	1.4	0.79
		D_1log(1/R)	3	0.93	0.29	0.38	3.9	1.3	0.80
		D_2log(1/R)	3	0.93	0.28	0.39	3.8	1.4	0.76
	No.117	R	6	0.91	0.47	0.55	3.2	1.2	0.50
		log(1/R)	5	0.88	0.56	0.62	2.9	1.1	0.37
		D_1R	4	0.92	0.31	0.51	3.5	1.6	0.49
		D_1log(1/R)	4	0.91	0.34	0.54	3.3	1.6	0.44
		D_2log(1/R)	3	0.90	0.42	0.59	3.0	1.4	0.40
	Celica	R	8	0.95	0.29	0.38	4.6	1.3	0.80
		log(1/R)	8	0.95	0.30	0.39	4.4	1.3	0.78
		D_1R	4	0.95	0.26	0.40	4.3	1.5	0.74
		D_1log(1/R)	4	0.95	0.25	0.39	4.4	1.6	0.75
		D_2log(1/R)	3	0.93	0.34	0.50	3.5	1.5	0.56
Hyperspectral imaging	Ever Green	R	12	0.85	0.45	0.58	2.5	1.3	0.30
		log(1/R)	13	0.87	0.43	0.56	2.6	1.3	0.35
		D_1R	8	0.82	0.52	0.62	2.4	1.2	0.27
		D_1log(1/R)	8	0.83	0.50	0.61	2.4	1.2	0.28
		D_2log(1/R)	9	0.83	0.44	0.62	2.4	1.4	0.23
	No.117	R	4	0.92	0.49	0.53	3.4	1.1	0.57
		log(1/R)	6	0.93	0.43	0.47	3.8	1.1	0.68
		D_1R	6	0.92	0.45	0.51	3.5	1.1	0.58
		D_1log(1/R)	4	0.92	0.47	0.51	3.5	1.1	0.60
		D_2log(1/R)	5	0.92	0.43	0.50	3.5	1.2	0.60
	Celica	**R**	**6**	**0.95**	**0.34**	**0.37**	**4.7**	**1.1**	**0.89**
		log(1/R)	5	0.95	0.37	0.39	4.4	1.1	0.85
		D_1R	4	0.95	0.35	0.39	4.5	1.1	0.87
		D_1log(1/R)	5	0.95	0.33	0.38	4.6	1.1	0.86
		D_2log(1/R)	6	0.94	0.35	0.43	4.0	1.2	0.73
SWIR	Ever Green	R	9	0.90	0.34	0.45	3.3	1.3	0.59
		log(1/R)	9	0.91	0.33	0.44	3.3	1.3	0.61
		D_1R	9	0.89	0.39	0.49	3.0	1.3	0.52
		D_1log(1/R)	8	0.89	0.39	0.51	2.9	1.3	0.48
		D_2log(1/R)	5	0.91	0.35	0.46	3.2	1.3	0.61
	No.117	R	6	0.91	0.52	0.57	3.1	1.1	0.47
		log(1/R)	6	0.92	0.46	0.52	3.4	1.1	0.56
		D_1R	6	0.90	0.50	0.59	3.0	1.2	0.41
		D_1log(1/R)	5	0.92	0.46	0.53	3.4	1.2	0.55
		D_2log(1/R)	4	0.92	0.46	0.53	3.4	1.2	0.56
	Celica	R	7	0.92	0.39	0.48	3.6	1.2	0.61
		log(1/R)	7	0.94	0.38	0.44	3.9	1.2	0.71
		D_1R	6	0.92	0.43	0.50	3.5	1.2	0.59
		D_1log(1/R)	5	0.93	0.43	0.48	3.6	1.1	0.65
		D_2log(1/R)	4	0.92	0.41	0.50	3.5	1.2	0.60

Comparison of the PLS models among the two wavelength ranges (VIS-NIR, SWIR) and hyperspectral imaging shows that the VIS-NIR models were obtained with fewer LVs (average, 5), higher r^2 (average, 0.93), lower RMSECV (average, 0.45 Brix%), higher RPD (average,

3.75), whereas hyperspectral imaging models achieved lower RMSECV/RMSEC (average, 1.17).

In the VIS-NIR range, for 'Ever Green' the $D_1\log(1/R)$, for 'No.117' and 'Celica' the reflectance (R) gave the highest SWS and therefore the best model. The relevant SWS indices were 0.80, 0.50, and 0.80 for 'Ever Green', 'No. 117' and 'Celica', respectively.

In case of the hyperspectral imaging for 'Ever Green' and 'No.117' the $\log(1/R)$, while for 'Celica' the reflectance (R) resulted with the highest SWS and therefore the best model. The relevant SWS indices were 0.35, 0.68, and 0.89 for 'Ever Green', 'Celica' and, 'No. 117' respectively.

The best models were achieved in the SWIR spectral range for all three cultivars by the $\log(1/R)$, with SWS 0.61, 0.56 and 0.71, respectively.

The overall comparison of models from the two spectral ranges and hyperspectral imaging resulted hyperspectral imaging to yield efficient models to predict TSS for 'No. 117' and 'Celica' bell pepper cultivars; whereas for 'Ever Green' variety the VIS-NIR spectral measurements yielded the best carotenoid predictions. Worth to mention, that even though in case of the 'Ever Green' variety there is no significant colour change still in the VIS-NIR spectral range very reliable strong prediction models were achieved, with average SWS: 0.74.

PLSR prediction and measured values for cv. 'Celica' are shown in Figs. 56-58, as examples for VIS-NIR, hyperspectral imaging and SWIR, respectively.
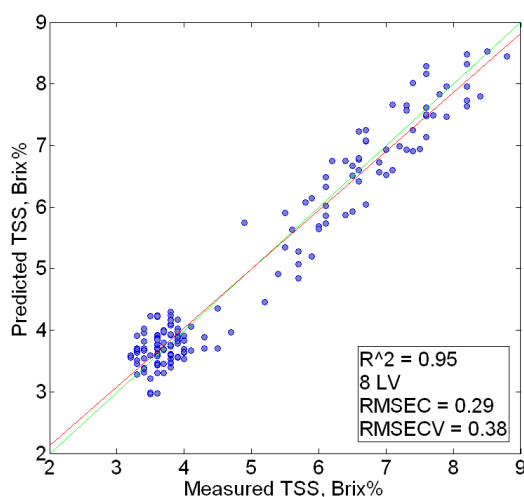
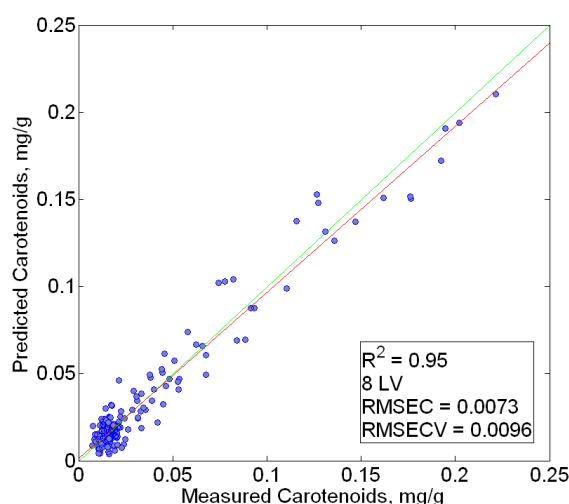**Fig. 56** Scatter plot of TSS for 'Celica' variety, as predicted by PLS regression model and as measured in the laboratory. The PLS model was built with the reflectance (R) of the spectral data in the VIS-NIR range.
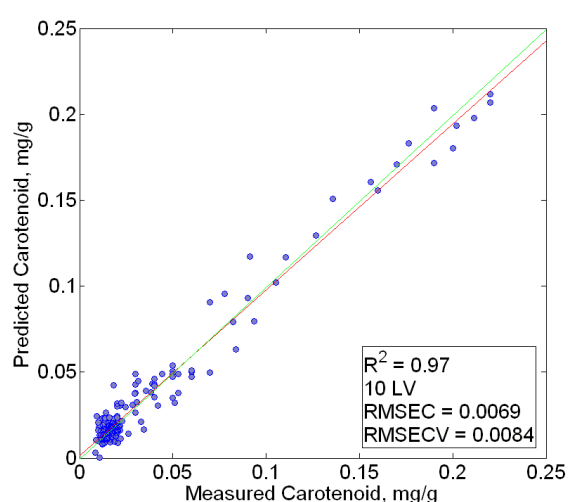
Fig. 57 Scatter plot of TSS for 'Celica' variety, as predicted by PLS regression model and as measured in the laboratory. The PLS model was built with the reflectance (R) of the spectral data from the hyperspectral imaging.
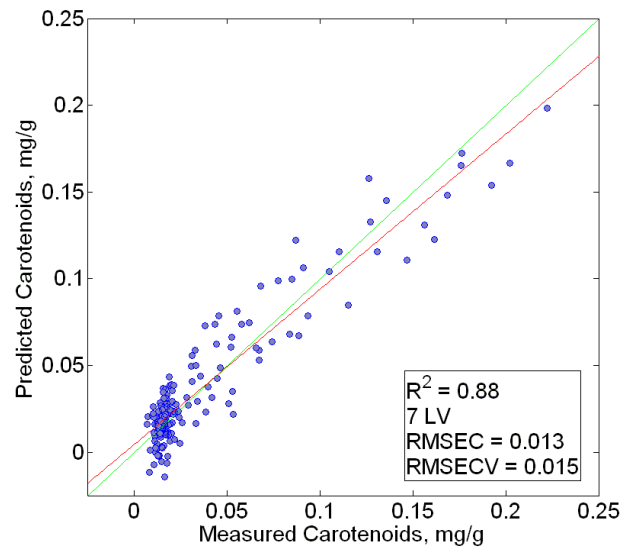
Fig. 58 Scatter plot of TSS for 'Celica' variety, as predicted by PLS regression model and as measured in the laboratory. The PLS model was built with the log(1/R) of the spectral data in the SWIR range.

In all figures, the ordinate and abscissa axes represent the measured and the fitted values. For the VIS-NIR (Fig. 56) a model with eight LVs obtained r^2=0.95 and RMSECV=0.38, for the hyperspectral imaging (Fig. 57) a model with six LVs obtained r^2=0.95 and RMSECV=0.37, whereas for SWIR (Fig. 58) seven LVs were needed to achieve r^2=0.92 and RMSECV =0.48.
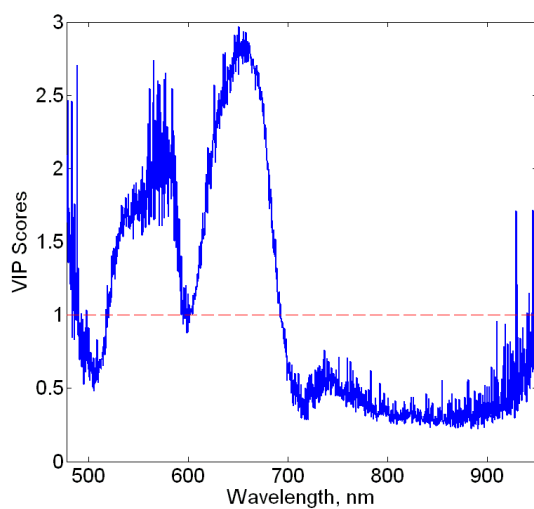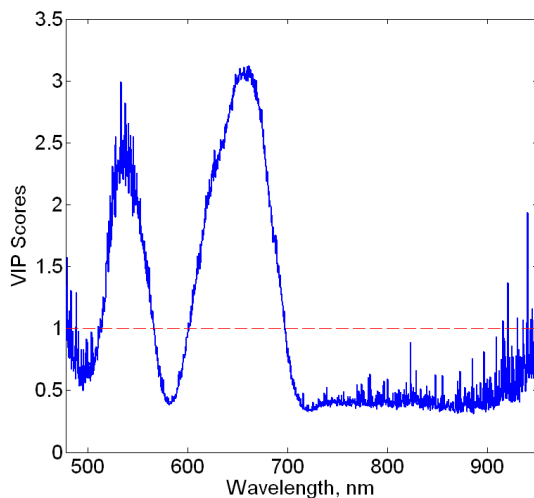

Fig. 59 VIP Scores for reflectance (R) spectra (VIS-NIR) of 'Celica' cultivar
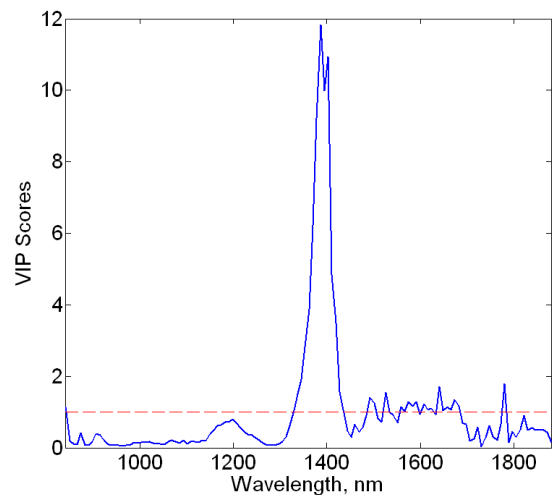
Fig. 60 VIP Scores for reflectance (R) spectra (SWIR) of 'Celica' cultivar

The Variable Importance in Projection (VIP) scores indicate the significance of specific wavelengths in the model, and Fig. 59 presents the VIP scores for the reflectance model in the VIS-NIR spectral range for cv. 'Celica'. Two wavelength ranges were found to be significant in the model: 510-560 and 600-695 related to the chlorophyll a and b and carotenoid contents. In case of the 'Ever Green' cultivar three significant ranges were found to contribute to the

prediction model: 477-540, 670-710 and 850-950 nm the VIP scores (not presented). The 850-950 nm range is associated with the vibration modes of the first overtones of C-H and O-H bond stretching and can be the reason achieving good models for TSS prediction.

Figure 60 presents the VIP scores of the reflectance model in the SWIR spectral range for cv. 'Celica'. Similarly to the model for total chlorophyll prediction, one very significant wavelength range was found that significantly influenced the regression model: the range of 1320–1430 nm. It is associated with the vibration modes of the first overtones of C-H and O-H bond stretching. These bonds commonly found in carbohydrates.

5.5.5. Correlation and regression analysis for dry matter (DM) and NDT methods

5.5.5.1. Correlation analysis for rate of relaxation, colour measurement, and ultrasonic test

Table 22 shows the results of cross correlation analysis for DM with the calculated indices of relaxation test (Rate of relaxation, Remaining deformation, Coefficient of elasticity from relaxation test), with the parameters of colour measurements (L, C, h) and ultrasonic attenuation. The highest coefficient of correlation (r) was found for all three cultivars for DM with the colour parameter of h, good correlation was found with the L and C in case of 'No. 117' cv. Poor correlation was found for DM with the ultrasonic attenuation and remaining deformation in case of all three cultivars, whereas the rate of relaxation had moderate correlation with the DM in case of all three cultivars. Coefficient of elasticity from the relaxation test and carotenoid content did not show close relationship for none of the cultivars.

Table 22 Covariance matrix between DM and non-destructive measurements for 'Ever Green', 'No.117', and 'Celica' cultivars, respectively, with, 95% significance level.

DM	Rate of Relaxation	Remaining Deformation	Coefficient of elasticity Relaxation	Colour Measurement			Ultrasonic Attenuation
				L	C	h	
Ever Green	0.67	0.53	0.01	0.44	0.50	0.77	0.38
No.117	0.66	0.46	0.14	0.85	0.87	0.89	0.49
Celica	0.52	0.37	0.18	0.25	0.66	0.92	0.46

5.5.5.2. PLS Regression for VIS-NIR and SWIR spectral analysis and hyperspectral imaging

The coefficients of variance for DM were 20.9%, 24.2% and 26.4% for 'Ever Green', 'No.117' and 'Celica' cultivars, respectively. The average squared intercorrelations found to be good between DM-TSS (0.95), DM-ascorbic acid (average: 0.23) and DM-total chlorophyll content (average: 0.40). Although the relatively high coefficient of variance with poor squared intercorrelation between DM and ascorbic acid and total chlorophyll, but good squared

intercorrelation with the TSS indicate that prediction by the VIS-NIR, SWIR and hyperspectral imaging method is applicable with the consideration of possible intercorrelation with TSS.

For all three cultivars, Table 23 presents the results from PLS regression for VIS-NIR, hyperspectral imaging and SWIR, respectively. The following statistical parameters are shown for each model: no. of latent variables, LV; coefficient of determination, r^2; root-mean-square error of calibration, RMSEC; root-mean-square error of cross-validation, RMSECV; robust parameter design, RPD; ratio of RMSECV and RMSEC, and standardized weighted sum index, SWS.

Comparison of the PLS models among the two wavelength ranges (VIS-NIR, SWIR) and hyperspectral imaging shows that the VIS-NIR models were obtained with fewer LVs (average, 5), higher r^2 (average, 0.91), lower RMSECV (average, 0.50 %), higher RPD (average, 3.37) and higher SWS (average, 0.61). Whereas the hyperspectral models resulted the lower ratio of RMSECV and RMSEC (average, 1.18). As a further result of the comparison shows that overall the averaged results of the three methods are slightly differ from one another.

In the VIS-NIR range, for all three cultivars the reflectance (R) gave the highest SWS and therefore the best model. The relevant SWS indices were 0.79, 0.53, and 0.76 for 'Ever Green', 'No. 117' and 'Celica', respectively.

By the hyperspectral imaging for 'Ever Green' the 1st derivative of reflectance (D$_1$R), for 'No.117' cv. the log(1/R), while for 'Celica' the reflectance (R) resulted the highest SWS and therefore the best model. The relevant SWS indices were 0.37, 0.65, and 0.79 for 'Ever Green', 'Celica' and, 'No. 117' respectively.

In the SWIR spectral range the best results were obtained with the models based on log(1/R) spectra for all three cultivars, with SWS 0.64, 0.66 and 0.63 for 'Ever Green', 'Celica' and, 'No. 117' respectively.

The overall comparison of models from the two spectral ranges and hyperspectral imaging resulted VIS-NIR spectral measurements to yield stronger correlation to predict DM content in 'Ever Green' bell pepper cultivar, while hyperspectral imaging was found best for 'No. 117' and 'Celica' variety. Worth to pay attention on the efficient models, achieved by the VIS-NIR spectral measurements in case of the 'Ever Green' cultivar, which retains its green colour even in the fully ripe stage; it means that the DM change during the growth and maturation is not indirectly correlated with the spectral information but direct correlation is presumed.

PLSR prediction and measured values for cv. 'Celica' are shown in Figs. 61-63, as examples for VIS-NIR, hyperspectral imaging and SWIR, respectively. In both figures, the ordinate and abscissa axes represent the measured and the fitted values. For the VIS-NIR (Fig. 61) a model

with eight LVs obtained r^2=0.94 and RMSECV=0.43, for the hyperspectral imaging (Fig. 62) a model with six LVs obtained r^2=0.94 and RMSECV=0.43, whereas for SWIR (Fig. 63) seven LVs were needed to achieve r^2=0.92 and RMSECV=0.50.

Table 23 Performance measures of PLS regression models for DM, using data from the VIS-NIR, Hyperspectral, and SWIR spectral region. Models for the three pepper varieties are presented: 'Ever Green', 'No, 117' and 'Celica'.

PLS	DM, %	Statistical parameter	LV	r^2	RMSEC	RMSECV	RPD	RMSECV/ RMSEC	SWS
VIS-NIR	Ever Green	R	8	0.93	0.26	0.37	3.8	1.4	0.79
		log(1/R)	8	0.90	0.30	0.44	3.3	1.5	0.64
		D_1R	3	0.92	0.31	0.42	3.4	1.4	0.75
		$D_1log(1/R)$	3	0.91	0.32	0.43	3.3	1.3	0.73
		$D_2log(1/R)$	3	0.92	0.31	0.43	3.3	1.4	0.73
	No.117	R	3	0.90	0.56	0.58	3.0	1.0	0.53
		log(1/R)	3	0.86	0.64	0.66	2.7	1.0	0.38
		D_1R	4	0.90	0.34	0.56	3.2	1.6	0.48
		$D_1log(1/R)$	4	0.88	0.34	0.60	3.0	1.7	0.38
		$D_2log(1/R)$	3	0.91	0.40	0.56	3.1	1.4	0.52
	Celica	R	8	0.94	0.33	0.43	4.1	1.3	0.76
		log(1/R)	9	0.94	0.30	0.43	4.0	1.5	0.70
		D_1R	4	0.92	0.28	0.50	3.5	1.8	0.55
		$D_1log(1/R)$	3	0.92	0.39	0.51	3.4	1.3	0.64
		$D_2log(1/R)$	3	0.91	0.35	0.52	3.4	1.5	0.59
Hyperspectral imaging	Ever Green	R	12	0.84	0.46	0.58	2.5	1.3	0.37
		log(1/R)	12	0.84	0.45	0.57	2.5	1.3	0.37
		D_1R	9	0.84	0.47	0.59	2.4	1.3	0.37
		$D_1log(1/R)$	9	0.83	0.48	0.60	2.4	1.3	0.34
		$D_2log(1/R)$	12	0.82	0.42	0.63	2.3	1.5	0.23
	No.117	R	6	0.91	0.50	0.55	3.2	1.1	0.57
		log(1/R)	6	0.92	0.46	0.51	3.5	1.1	0.65
		D_1R	8	0.91	0.47	0.55	3.2	1.2	0.54
		$D_1log(1/R)$	4	0.90	0.52	0.57	3.1	1.1	0.55
		$D_2log(1/R)$	2	0.89	0.58	0.60	3.0	1.0	0.51
	Celica	**R**	**6**	**0.94**	**0.39**	**0.43**	**4.0**	**1.1**	**0.79**
		log(1/R)	6	0.93	0.39	0.44	4.0	1.1	0.77
		D_1R	3	0.93	0.44	0.47	3.7	1.1	0.74
		$D_1log(1/R)$	6	0.93	0.40	0.45	3.9	1.1	0.75
		$D_2log(1/R)$	6	0.92	0.44	0.52	3.3	1.2	0.60
SWIR	Ever Green	R	8	0.87	0.39	0.52	2.8	1.3	0.51
		log(1/R)	9	0.91	0.34	0.45	3.2	1.3	0.64
		D_1R	9	0.89	0.40	0.49	2.9	1.2	0.58
		$D_1log(1/R)$	7	0.89	0.40	0.49	2.9	1.2	0.59
		$D_2log(1/R)$	4	0.89	0.42	0.48	3.0	1.2	0.64
	No.117	R	6	0.90	0.51	0.58	3.0	1.1	0.49
		log(1/R)	8	0.93	0.39	0.48	3.7	1.2	0.66
		D_1R	9	0.92	0.39	0.50	3.5	1.3	0.60
		$D_1log(1/R)$	7	0.91	0.45	0.54	3.3	1.2	0.56
		$D_2log(1/R)$	5	0.90	0.43	0.56	3.2	1.3	0.52
	Celica	R	7	0.90	0.45	0.55	3.2	1.2	0.54
		log(1/R)	7	0.92	0.42	0.50	3.5	1.2	0.63
		D_1R	5	0.91	0.49	0.55	3.1	1.1	0.56
		$D_1log(1/R)$	5	0.92	0.45	0.52	3.4	1.2	0.62
		$D_2log(1/R)$	5	0.91	0.41	0.54	3.2	1.3	0.56
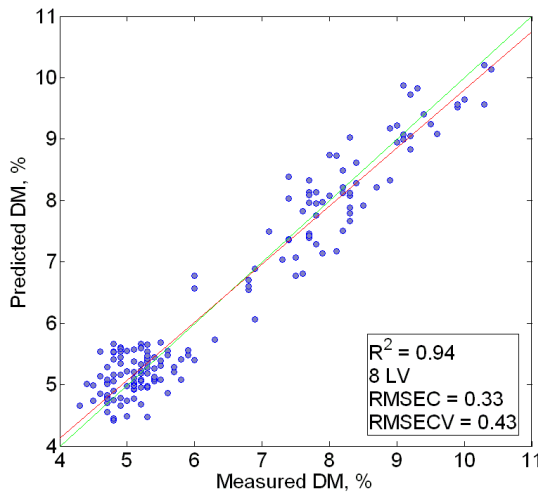
Fig. 61 Scatter plot of DM for 'Celica' variety, as predicted by PLS regression model and as measured in the laboratory. The PLS model was built with the reflectance (R) of the spectral data in the VIS-NIR range.
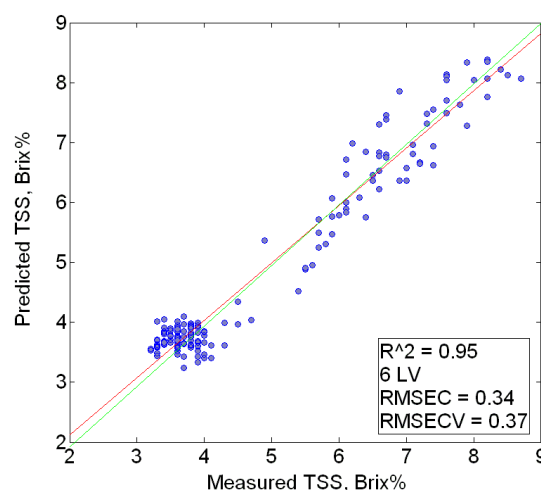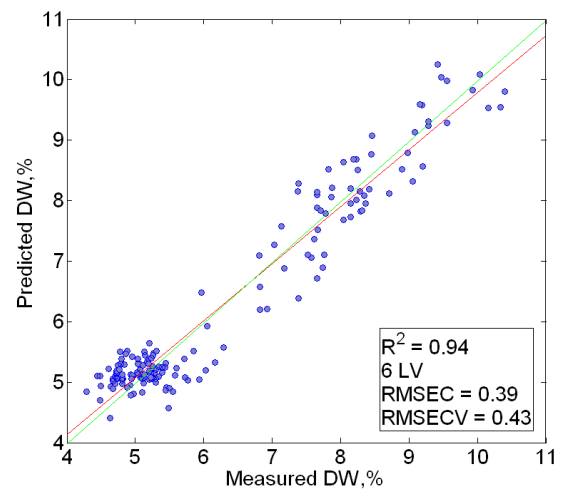

Fig. 62 Scatter plot of DM for 'Celica' variety, as predicted by PLS regression model and as measured in the laboratory. The PLS model was built with the reflectance (R) of the spectral data from the hyperspectral imaging.
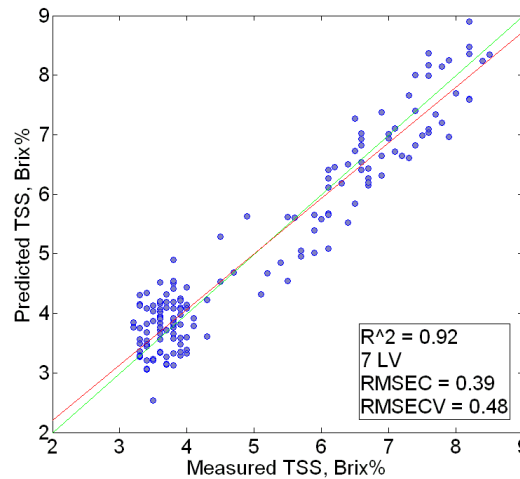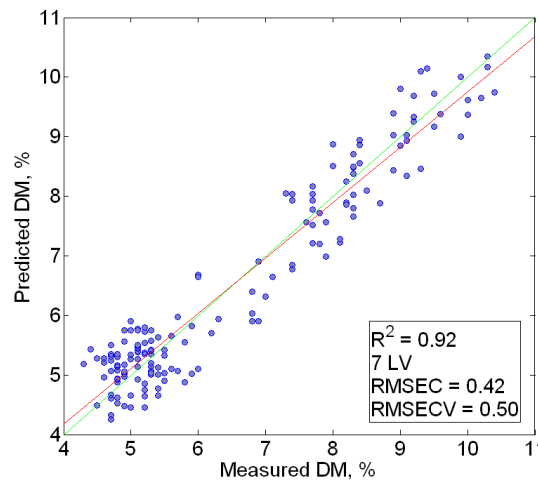

Fig. 63 Scatter plot of DM content for 'Celica' variety, as predicted by PLS regression model and as measured in the laboratory. The PLS model was built with the log(1/R) of the spectral data in the SWIR range.

The Variable Importance in Projection (VIP) scores indicate the significance of specific wavelengths in the model, and Fig. 64 presents the VIP scores for the reflectance model in the VIS-NIR spectral range for cv. 'Celica'. Two wavelength ranges were found to be the most significant in the model: 510–560, 600–700 nm. These ranges are related to the chlorophyll a and b and carotenoid contents.

Figure 65 presents the VIP scores of the reflectance model in the SWIR spectral range for cv. 'Celica'. One very significant wavelength range was found that significantly influenced the

regression model: 1320–1420 nm; it is associated with the vibration modes of the first overtones of C-H and O-H bond stretching.
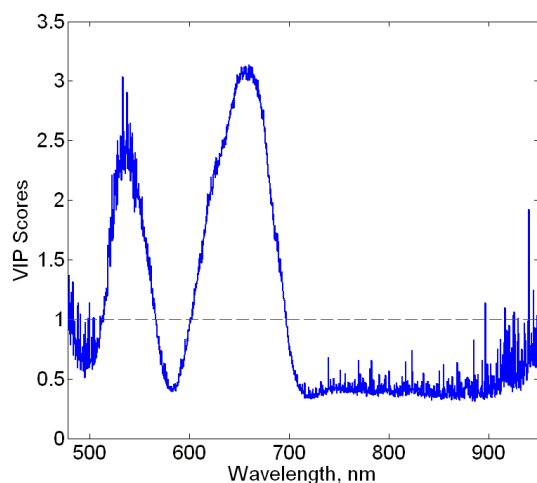
Fig. 64 VIP Scores for reflectance (R) spectra (VIS-NIR) of 'Celica' cultivar
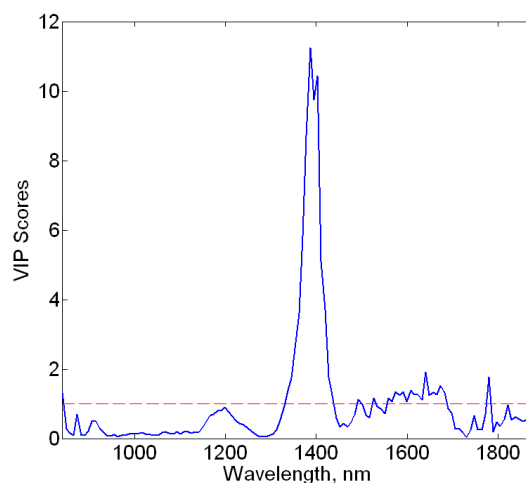
Fig. 65 VIP Scores for reflectance (R) spectra (SWIR) of 'Celica' cultivar

5.5.6. Correlation and regression analysis for osmotic potential (OP) and NDT methods

5.5.6.1. Correlation analysis for rate of relaxation, colour measurement, and ultrasonic test

Table 24 shows the results of cross correlation analysis for OP with the calculated indices of relaxation test (Rate of relaxation, Remaining deformation, Coefficient of elasticity from relaxation test), with the parameters of colour measurements (L, C, h) and ultrasonic attenuation. The highest coefficient of correlation (r) was found for all three cultivars for DM with the colour parameter of h, good correlation was found with the L and C in case of 'No. 117' cv. Poor correlation was found for DM with the ultrasonic attenuation and remaining deformation in case of all three cultivars, whereas the rate of relaxation had slight correlation with the DM in case of all three cultivars. Coefficient of elasticity from the relaxation test and carotenoid content did not show close relationship for none of the cultivars.

Table 24 Covariance matrix between OP and non-destructive measurements for 'Ever Green', 'No.117', and 'Celica' cultivars, respectively, with, 95% significance level.

OP	Rate of Relaxation	Remaining Deformation	Coefficient of elasticity Relaxation	Colour Measurement			Ultrasonic Attenuation
				L	C	h	
Ever Green	0.64	0.52	0.02	0.44	0.45	0.78	0.33
No.117	0.61	0.44	0.13	0.85	0.87	0.88	0.43
Celica	0.50	0.35	0.16	0.18	0.66	0.91	0.44

5.5.6.2. PLS Regression for VIS-NIR and SWIR spectral analysis and hyperspectral imaging

The coefficients of variance for OP were 31.4%, 33.1% and 35.4% for 'Ever Green', 'No.117' and 'Celica' cultivars, respectively. The average squared intercorrelations found to be fair between OP-TSS (0.87), OP-DM (average: 0.86) and poor between OP-total chlorophyll content (average: 0.51). Although the relatively high coefficient of variance, but fair squared intercorrelation with the TSS and DM indicate that prediction by the VIS-NIR, SWIR and hyperspectral imaging method is applicable with the consideration of possible intercorrelation with TSS and DM.

For all three cultivars, Table 25 presents the results from PLS regression for VIS-NIR, hyperspectral imaging and SWIR, respectively. The following statistical parameters are shown for each model: no. of latent variables, LV; coefficient of determination, r^2; root-mean-square error of calibration, RMSEC; root-mean-square error of cross-validation, RMSECV; robust parameter design, RPD; ratio of RMSECV and RMSEC, and standardized weighted sum index, SWS.

Comparison of the PLS models among the two wavelength ranges (VIS-NIR, SWIR) and hyperspectral imaging shows that the VIS-NIR models were obtained with fewer LVs (average, 4), higher r^2 (average, 0.88), lower RMSECV (average, 41.6 %), higher RPD (average, 2.95) and higher SWS (average, 0.58). Whereas the hyperspectral models resulted the lower ratio of RMSECV and RMSEC (average, 1.10). As a further result of the comparison shows that overall the averaged results of the three methods are slightly differ from one another.

In the VIS-NIR range, for 'Ever Green' and 'Celica' cultivars the 1st derivative of reflectance (D_1R), whereas for 'No.117' cultivar the reflectance (R) gave the highest SWS, and therefore the best model. The relevant SWS indices were 0.68, 0.58, and 0.77 for 'Ever Green', 'No. 117' and 'Celica', respectively.

By the hyperspectral imaging for 'Ever Green' the $D_1log(1/R)$, for and 'No.117' the $log(1/R)$, while for 'Celica' cultivar the 1st derivative of reflectance (D_1R) resulted the highest SWS and therefore the best model. The relevant SWS indices were 0.39, 0.61, and 0.92 for 'Ever Green', 'No. 117' and 'Celica', respectively.

In the SWIR spectral range the best results were obtained with the models based on $D_2log(1/R)$ spectra for 'Ever Green' and 'No. 117' cultivars, while for 'Celica' the 1st derivative of reflectance (D_1R), with SWS 0.54, 0.54 and 0.65 for 'Ever Green', 'No. 117' and 'Celica', respectively.

The overall comparison of models from the two spectral ranges and hyperspectral imaging resulted VIS-NIR spectral measurements to yield stronger correlation to predict OP in 'Ever

Green' bell pepper cultivar, while hyperspectral imaging was found best for 'No. 117' and 'Celica' variety. Worth to pay attention on the efficient models, achieved by the VIS-NIR spectral measurements in case of the 'Ever Green' cultivar, which retains its green colour even in the fully ripe stage; it means that the OP change during the growth and maturation is not depend or related to the colour change of the pepper.

Table 25 Performance measures of PLS regression models for OP, using data from the VIS-NIR, Hyperspectral, and SWIR spectral region. Models for the three pepper varieties are presented: 'Ever Green', 'No, 117' and 'Celica'.

PLS	OP, osmol/kg	Statistical parameter	LV	r^2	RMSEC	RMSECV	RPD	RMSECV/ RMSEC	SWS
VIS-NIR	Ever Green	R	8	0.87	27.6	37.8	2.9	1.4	0.59
		log(1/R)	8	0.85	29.4	41.3	2.6	1.4	0.48
		D_1R	3	0.87	27.0	36.7	3.0	1.4	0.68
		D_1log(1/R)	3	0.86	29.4	38.3	2.9	1.3	0.65
		D_2log(1/R)	3	0.85	27.7	38.7	2.8	1.4	0.60
	No.117	R	3	0.88	44.2	45.8	2.9	1.0	0.58
		log(1/R)	4	0.85	49.2	50.7	2.6	1.0	0.44
		D_1R	3	0.86	36.5	48.1	2.7	1.3	0.44
		D_1log(1/R)	3	0.86	38.5	50.6	2.6	1.3	0.38
		D_2log(1/R)	2	0.87	38.4	48.2	2.7	1.3	0.47
	Celica	R	7	0.90	33.1	38.5	3.2	1.2	0.68
		log(1/R)	8	0.91	27.6	36.2	3.4	1.3	0.69
		D_1R	3	0.92	25.5	34.8	3.6	1.4	0.77
		D_1log(1/R)	3	0.90	27.6	37.0	3.4	1.3	0.71
		D_2log(1/R)	3	0.89	28.3	41.7	3.0	1.5	0.55
Hyperspectral imaging	Ever Green	R	8	0.76	44.4	52.2	2.1	1.2	0.25
		log(1/R)	8	0.76	47.9	52.6	2.1	1.1	0.26
		D_1R	6	0.80	40.7	48.7	2.2	1.2	0.37
		D_1log(1/R)	6	0.80	42.7	48.5	2.3	1.1	0.39
		D_2log(1/R)	6	0.74	42.5	54.3	2.0	1.3	0.19
	No.117	R	4	0.87	42.9	46.4	2.8	1.1	0.54
		log(1/R)	5	0.89	39.9	43.2	3.0	1.1	0.61
		D_1R	2	0.86	48.0	49.2	2.7	1.0	0.50
		D_1log(1/R)	2	0.88	44.7	45.7	2.9	1.0	0.60
		D_2log(1/R)	2	0.85	47.9	50.0	2.6	1.0	0.47
	Celica	R	5	0.92	30.9	32.9	3.8	1.1	0.90
		log(1/R)	5	0.92	31.2	34.1	3.6	1.1	0.85
		D_1R	**3**	**0.92**	**31.5**	**32.9**	**3.8**	**1.0**	**0.92**
		D_1log(1/R)	3	0.91	33.7	36.5	3.4	1.1	0.81
		D_2log(1/R)	3	0.89	36.3	39.8	3.1	1.1	0.71
SWIR	Ever Green	R	9	0.84	31.6	42.8	2.6	1.4	0.45
		log(1/R)	9	0.85	31.2	40.9	2.7	1.3	0.51
		D_1R	10	0.80	36.7	48.8	2.2	1.3	0.28
		D_1log(1/R)	9	0.82	34.9	44.7	2.4	1.3	0.42
		D_2log(1/R)	5	0.84	32.2	41.8	2.6	1.3	0.54
	No.117	R	7	0.84	43.3	52.6	2.5	1.2	0.31
		log(1/R)	7	0.88	40.4	46.3	2.8	1.1	0.49
		D_1R	7	0.87	37.9	47.5	2.7	1.3	0.43
		D_1log(1/R)	6	0.88	38.3	45.5	2.9	1.2	0.52
		D_2log(1/R)	4	0.88	37.8	45.4	2.9	1.2	0.54
	Celica	R	7	0.88	34.8	42.4	2.9	1.2	0.56
		log(1/R)	7	0.90	33.4	40.4	3.1	1.2	0.62
		D_1R	6	0.89	35.1	40.2	3.1	1.1	0.65
		D_1log(1/R)	5	0.89	36.4	42.0	3.0	1.2	0.62
		D_2log(1/R)	4	0.89	35.2	41.8	3.0	1.2	0.62

PLSR prediction and measured values for cv. 'Celica' are shown in Figs. 66-68, as examples for VIS-NIR, hyperspectral imaging and SWIR, respectively. In both figures, the ordinate and abscissa axes represent the measured and the fitted values. For the VIS-NIR (Fig. 66) a model with three LVs obtained r^2=0.92 and RMSECV=34.77, for the hyperspectral imaging (Fig. 67) a model with three LVs obtained r^2=0.92 and RMSECV=32.92, whereas for SWIR (Fig. 68) six LVs were needed to achieve r^2=0.89 and RMSECV=40.23.
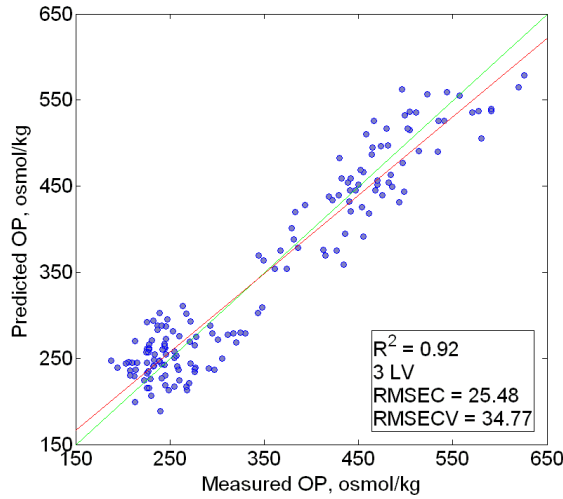
Fig. 66 Scatter plot of OP for 'Celica' variety, as predicted by PLS regression model and as measured in the laboratory. The PLS model was built with the 1st derivative (D_1R) of the spectral data in the VIS-NIR range.
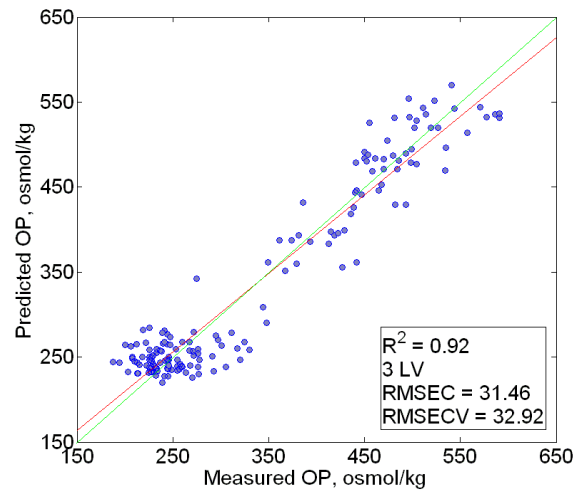
Fig. 67 Scatter plot of OP for 'Celica' variety, as predicted by PLS regression model and as measured in the laboratory. The PLS model was built with the 1st derivative (D_1R) of the spectral data from the hyperspectral imaging.
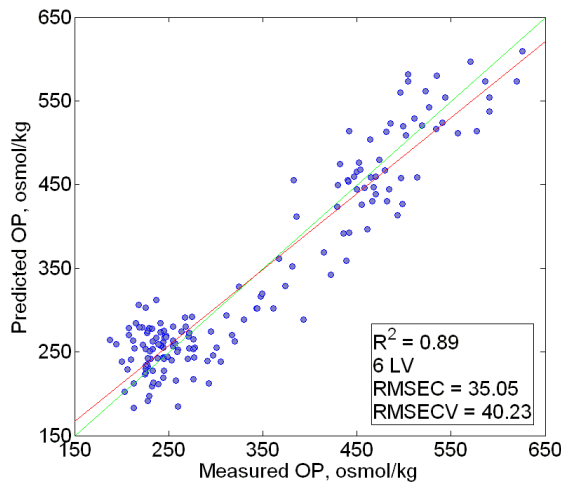
Fig. 68 Scatter plot of OP content for 'Celica' variety, as predicted by PLS regression model and as measured in the laboratory. The PLS model was built with the 1st derivative (D_1R) of the spectral data in the SWIR range.

The Variable Importance in Projection (VIP) scores indicate the significance of specific wavelengths in the model, and Fig. 69 presents the VIP scores for the reflectance model in the VIS-NIR spectral range for cv. 'Celica'. Two wavelength ranges were found to be the most significant in the model: 510–560, 600–700 nm. These ranges are related to the chlorophyll a and b and carotenoid contents.

Figure 70 presents the VIP scores of the reflectance model in the SWIR spectral range for cv. 'Celica'. One very significant wavelength range was found that significantly influenced the regression model: 1320–1420 nm; it is associated with the vibration modes of the first overtones of C-H and O-H bond stretching.
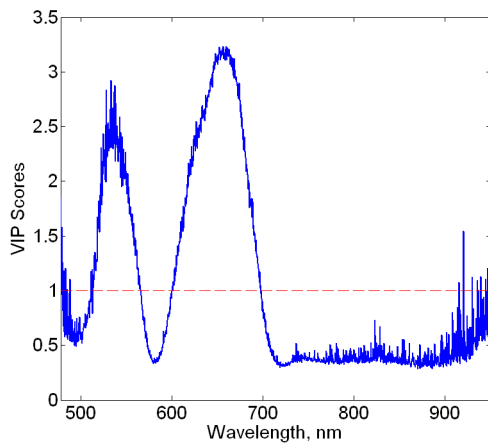
Fig. 69 VIP Scores for reflectance (R) spectra (VIS-NIR) of 'Celica' cultivar
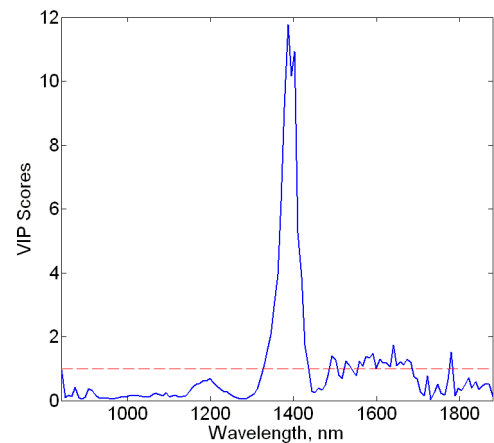
Fig. 70 VIP Scores for reflectance (R) spectra (SWIR) of 'Celica' cultivar

5.5.7. Correlation and regression analysis for coefficient of elasticity from compression test and NDT methods

5.5.7.1. Correlation analysis for rate of relaxation, colour measurement, and ultrasonic test

Table 26 shows the results of cross correlation analysis for coefficient of elasticity of compression test ($CE_{Compression}$) with the calculated indices of relaxation test (Rate of relaxation, Remaining deformation, coefficient of elasticity relaxation test), with the parameters of colour measurements (L, C, h) and ultrasonic attenuation. $CE_{Compression}$ did not show considerable correlation with any of the correlated parameters.

Table 26 Covariance matrix between $CE_{Compression}$ and non-destructive measurements for 'Ever Green', 'No.117', and 'Celica' cultivars, respectively, with, 95% significance level.

Coefficient of elasticity Compression	Rate of Relaxation	Remaining Deformation	Coefficient of elasticity Relaxation	Colour Measurement			Ultrasonic Attenuation
				L	C	h	
Ever Green	0.26	0.19	0.21	0.29	0.25	0.52	0.34
No.117	0.25	0.15	0.21	0.43	0.42	0.45	0.36
Celica	0.10	0.06	0.21	0.02	0.29	0.41	0.39

5.5.7.2. PLS Regression for VIS-NIR and SWIR spectral analysis and hyperspectral imaging

The coefficients of variance for $CE_{Compression}$ were 37.2%, 36.7% and 32.0% for 'Ever Green', 'No.117' and 'Celica' cultivars, respectively. The average squared intercorrelations found to be fair between $CE_{Compression}$ -TSS (0.19), $CE_{Compression}$ -DM (average: 0.16) and poor between $CE_{Compression}$ -total chlorophyll content (average: 0.17). Based on the coefficient of variance and the low squared intercorrelation among the variables indicate that prediction by the VIS-NIR, SWIR and hyperspectral imaging method is applicable.

For all three cultivars, Table 27 presents the results from PLS regression for VIS-NIR, hyperspectral imaging and SWIR, respectively. The following statistical parameters are shown for each model: no. of latent variables, LV; coefficient of determination, r^2; root-mean-square error of calibration, RMSEC; root-mean-square error of cross-validation, RMSECV; robust parameter design, RPD; ratio of RMSECV and RMSEC, and standardized weighted sum index, SWS.

Comparison of the PLS models among the two wavelength ranges (VIS-NIR, SWIR) and hyperspectral imaging shows that the hyperspectral models were obtained with fewer LVs (average, 3) and lower ratio of RMSECV and RMSEC (average, 1.07). Whereas VIS-NIR models resulted lower RMSECV (average, 8.66 %), higher RPD (average, 1.55) and higher SWS (average, 0.58). higher r^2 (average, 0.88). As a further result of the comparison shows that overall the averaged results of the three methods are slightly differ from one another.

In the VIS-NIR range for 'Ever Green' cultivar the $D_2log(1/R)$, for 'No.117' cultivar the 1st derivative of reflectance (D_1R), whereas for 'Celica' the $D_1log(1/R)$ gave the highest SWS, and therefore the best model. The relevant SWS indices were 0.50, 0.81, and 0.70 for 'Ever Green', 'No. 117' and 'Celica', respectively.

By the hyperspectral imaging for 'Ever Green' the 1st derivative of reflectance (D_1R), for and 'No.117' the $log(1/R)$, while for 'Celica' cultivar the $D_2log(1/R)$ resulted the highest SWS and therefore the best model. The relevant SWS indices were 0.37, 0.72, and 0.67 for 'Ever Green', 'No. 117' and 'Celica', respectively.

In the SWIR spectral range the best results were obtained with the models based on reflectance (R) spectra for 'Ever Green' cultivar, while for 'No. 117' and 'Celica' cultivars the $D_2log(1/R)$, with SWS 0.50, 0.71 and 0.67 for 'Ever Green', 'No. 117' and 'Celica', respectively.

The overall comparison of models from the two spectral ranges and hyperspectral imaging resulted SWIR spectral measurements to yield stronger correlation to predict $CE_{Compression}$ in

'Ever Green' bell pepper cultivar, while VIS-NIR yield the best models for 'No. 117' and hyperspectral imaging was found best for 'Celica' variety.

Table 27 Performance measures of PLS regression models for $CE_{Compression}$, using data from the VIS-NIR, Hyperspectral, and SWIR spectral region. Models for the three pepper varieties are presented: 'Ever Green', 'No, 117' and 'Celica'.

PLS	Coefficient of elasticity Compression, N/mm	Statistical parameter	LV	r^2	RMSEC	RMSECV	RPD	RMSECV/ RMSEC	SWS
VIS-NIR	Ever Green	R	6	0.54	9.3	11.3	1.6	1.2	0.42
		log(1/R)	6	0.44	9.5	12.4	1.5	1.3	0.26
		D_1R	2	0.45	9.1	11.4	1.6	1.3	0.43
		$D_1log(1/R)$	2	0.42	9.5	11.7	1.6	1.2	0.40
		$D_2log(1/R)$	2	0.55	8.8	10.9	1.7	1.2	0.50
	No.117	R	5	0.37	7.0	7.4	1.5	1.1	0.68
		log(1/R)	7	0.46	5.3	7.2	1.6	1.3	0.60
		D_1R	**2**	**0.49**	**5.8**	**6.7**	**1.7**	**1.1**	**0.81**
		$D_1log(1/R)$	2	0.46	5.9	6.9	1.6	1.2	0.76
		$D_2log(1/R)$	2	0.51	5.1	6.5	1.7	1.3	0.79
	Celica	R	5	0.26	7.1	7.7	1.4	1.1	0.60
		log(1/R)	6	0.32	6.9	7.7	1.4	1.1	0.58
		D_1R	2	0.37	6.1	7.2	1.5	1.2	0.69
		$D_1log(1/R)$	2	0.41	6.1	7.1	1.5	1.2	0.70
		$D_2log(1/R)$	2	0.40	5.5	7.8	1.4	1.4	0.53
Hyperspectral imaging	Ever Green	R	5	0.43	11.6	12.6	1.5	1.1	0.33
		log(1/R)	5	0.46	11.6	12.5	1.5	1.1	0.35
		D_1R	4	0.47	10.9	12.3	1.5	1.1	0.37
		$D_1log(1/R)$	5	0.43	11.2	12.9	1.4	1.2	0.27
		$D_2log(1/R)$	2	0.34	11.9	13.2	1.4	1.1	0.28
	No.117	R	4	0.38	7.1	7.5	1.5	1.1	0.69
		log(1/R)	2	0.37	7.4	7.6	1.5	1.0	0.72
		D_1R	3	0.34	7.1	7.7	1.5	1.1	0.67
		$D_1log(1/R)$	3	0.38	7.0	7.6	1.5	1.1	0.68
		$D_2log(1/R)$	3	0.33	7.1	8.0	1.4	1.1	0.61
	Celica	R	4	0.26	7.0	7.4	1.4	1.1	0.65
		log(1/R)	4	0.24	7.2	7.6	1.4	1.1	0.63
		D_1R	2	0.24	7.4	7.7	1.4	1.0	0.65
		$D_1log(1/R)$	2	0.24	7.6	7.9	1.3	1.0	0.62
		$D_2log(1/R)$	2	0.27	7.2	7.5	1.4	1.0	0.67
SWIR	Ever Green	R	6	0.56	9.8	10.9	1.7	1.1	0.50
		log(1/R)	6	0.57	9.8	11.0	1.7	1.1	0.50
		D_1R	3	0.52	10.6	11.5	1.6	1.1	0.49
		$D_1log(1/R)$	4	0.47	10.9	12.3	1.5	1.1	0.36
		$D_2log(1/R)$	3	0.55	9.9	11.3	1.6	1.1	0.49
	No.117	R	7	0.44	6.0	7.5	1.5	1.2	0.60
		log(1/R)	9	0.51	5.2	6.8	1.7	1.3	0.64
		D_1R	3	0.36	6.9	7.4	1.5	1.1	0.70
		$D_1log(1/R)$	7	0.43	6.1	7.4	1.5	1.2	0.61
		$D_2log(1/R)$	2	0.42	6.5	7.4	1.5	1.1	0.71
	Celica	R	6	0.34	6.7	7.5	1.4	1.1	0.60
		log(1/R)	7	0.39	6.2	7.3	1.5	1.2	0.62
		D_1R	5	0.34	6.6	7.6	1.4	1.1	0.61
		$D_1log(1/R)$	5	0.35	6.7	7.4	1.4	1.1	0.63
		$D_2log(1/R)$	2	0.36	6.7	7.5	1.4	1.1	0.67

PLSR prediction and measured values for cv. 'No. 117' are shown in Figs. 71-73, as examples for VIS-NIR, hyperspectral imaging and SWIR, respectively. In both figures, the ordinate and abscissa axes represent the measured and the fitted values. For the VIS-NIR (Fig. 71) a model with two LVs obtained $r^2=0.49$ and RMSECV=6.66, for the hyperspectral imaging (Fig. 72) a model with two LVs obtained $r^2=0.37$ and RMSECV=7.55, whereas for SWIR (Fig. 73) two LVs were needed to achieve $r^2=0.42$ and RMSECV=7.35.
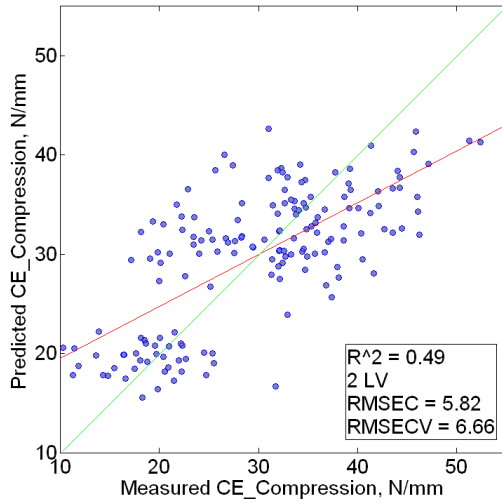
Fig. 71 Scatter plot of CE$_{Compression}$ for 'No.117' variety, as predicted by PLS regression model and as measured in the laboratory. The PLS model was built with the 1st derivative (D$_1$R) of the spectral data in the VIS-NIR range.
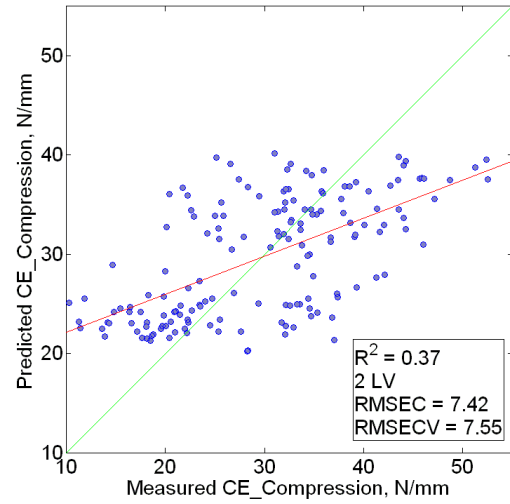
Fig. 72 Scatter plot of CE$_{Compression}$ for 'No.117' variety, as predicted by PLS regression model and as measured in the laboratory. The PLS model was built with the log(1/R) of the spectral data from the hyperspectral imaging.
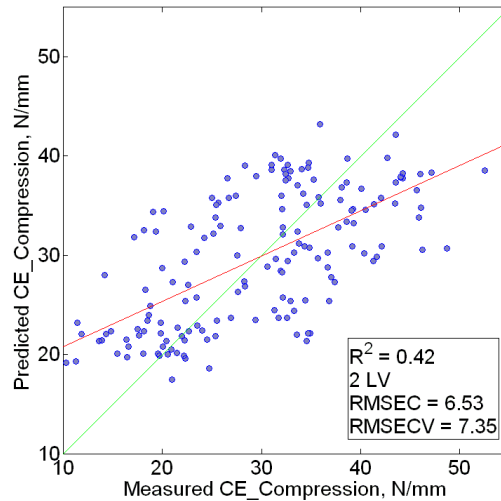
Fig. 73 Scatter plot of CE$_{Compression}$ content for 'No.117' variety, as predicted by PLS regression model and as measured in the laboratory. The PLS model was built with the D$_2$log(1/R)of the spectral data in the SWIR range.

The Variable Importance in Projection (VIP) scores indicate the significance of specific wavelengths in the model, and Fig. 74 presents the VIP scores for the reflectance model in the VIS-NIR spectral range for cv. 'No.117'. The following wavelength ranges were found to be the most significant in the model: 477–690, 830–950 nm. The range of 477-690 nm is related to the chlorophyll a and b and carotenoid contents, while the range of 830–950 nm is related to chemical and textural composition.

Figure 75 presents the VIP scores of the reflectance model in the SWIR spectral range for cv. 'No.117'. The below wavelength ranges were found to significantly influencing the regression model: 850-900, 1350–1450 and 1550-1888 nm; it is associated with the vibration modes of the first overtones of C-H and O-H bond stretching.

Fig. 74 VIP Scores for reflectance (R) spectra (VIS-NIR) of 'No.117' cultivar

Fig. 75 VIP Scores for reflectance (R) spectra (SWIR) of 'No.117' cultivar

5.5.8. Correlation and regression analysis for coefficient of elasticity from rupture test and NDT methods

5.5.8.1. Correlation analysis for rate of relaxation, colour measurement, and ultrasonic test

Table 28 shows the results of cross correlation analysis for coefficient of elasticity of rupture test ($CE_{Rupture}$) with the calculated indices of relaxation test (Rate of relaxation, Remaining deformation, coefficient of elasticity from relaxation test), with the parameters of colour measurements (L, C, h) and ultrasonic attenuation. $CE_{Rupture}$ did not show considerable correlation with any of the correlated parameters, except slight correlation was found for 'No.117' cultivars with the L, C, h parameters of the colour measurements.

Table 28 Covariance matrix between $CE_{Rupture}$ and non-destructive measurements for 'Ever Green', 'No.117', and 'Celica' cultivars, respectively, with, 95% significance level.

Coefficient of elasticity Rupture	Rate of Relaxation	Remaining Deformation	Coefficient of elasticity Relaxation	Colour Measurement			Ultrasonic Attenuation
				L	C	h	
Ever Green	0.33	0.20	0.08	0.11	0.20	0.48	0.23
No.117	0.42	0.42	0.09	0.58	0.57	0.60	0.41
Celica	0.31	0.23	0.26	0.16	0.38	0.62	0.41

5.5.8.2. PLS Regression for VIS-NIR and SWIR spectral analysis and hyperspectral imaging

The coefficients of variance for $CE_{Rupture}$ were 27.3%, 21.9% and 27.8% for 'Ever Green', 'No.117' and 'Celica' cultivars, respectively. The average squared intercorrelations found to be fair between $CE_{Rupture}$ -TSS (0.36), $CE_{Rupture}$ -DM (average: 0.34) and poor between $CE_{Rupture}$ - total chlorophyll content (average: 0.27). Based on the coefficient of variance and the low squared intercorrelation among the variables indicate that prediction by the VIS-NIR, SWIR and hyperspectral imaging method is applicable.

For all three cultivars, table 29 presents the results from PLS regression for VIS-NIR, hyperspectral imaging and SWIR, respectively. The following statistical parameters are shown for each model: no. of latent variables, LV; coefficient of determination, r^2; root-mean-square error of calibration, RMSEC; root-mean-square error of cross-validation, RMSECV; robust parameter design, RPD; ratio of RMSECV and RMSEC, and standardized weighted sum index, SWS.

Comparison of the PLS models among the two wavelength ranges (VIS-NIR, SWIR) and hyperspectral imaging shows that the VIS-NIR models were obtained with fewer LVs (average, 4), whereas SWIR models resulted with higher r^2 (average, 0.51), lower RMSECV (average, 3.28), higher RPD (average, 1.61), lower ratio of RMSECV and RMSEC (average, 1.12), and higher SWS (average, 0.62). As a further result of the comparison shows that overall the averaged results of the three methods are slightly differ from one another.

In the VIS-NIR range for 'Ever Green' cultivar the $D_1\log(1/R)$, for 'No.117' cultivar the reflectance (R), whereas for 'Celica' the $D_2\log(1/R)$ gave the highest SWS, and therefore the best model. The relevant SWS indices were 0.57, 0.73, and 0.73 for 'Ever Green', 'No. 117' and 'Celica', respectively.

By the hyperspectral imaging for 'Ever Green' the reflectance (R), for and 'No.117' the $D_2\log(1/R)$, while for 'Celica' cultivar the $D_1\log(1/R)$ resulted the highest SWS and therefore the best model. The relevant SWS indices were 0.33, 0.79, and 0.76 for 'Ever Green', 'No. 117' and 'Celica', respectively.

In the SWIR spectral range the best results were obtained with the models based on $D_2\log(1/R)$ spectra for 'Ever Green' cultivar, while for 'No. 117' and 'Celica' cultivars the $D_2\log(1/R)$, with SWS 0.46, 0.81 and 0.67 for 'Ever Green', 'No. 117' and 'Celica', respectively.

Table 29 Performance measures of PLS regression models for $CE_{Rupture}$, using data from the VIS-NIR, Hyperspectral, and SWIR spectral region. Models for the three pepper varieties are presented: 'Ever Green', 'No, 117' and 'Celica'.

PLS	Coefficient of elasticity Rupture, N/mm	Statistical parameter	LV	r^2	RMSEC	RMSECV	RPD	RMSECV/ RMSEC	*SWS*
VIS-NIR	Ever Green	R	6	0.45	3.2	3.9	1.5	1.2	*0.45*
		log(1/R)	7	0.45	2.8	3.9	1.5	1.4	*0.43*
		D_1R	2	0.46	3.0	3.8	1.5	1.3	*0.52*
		$D_1\log(1/R)$	3	0.52	2.4	3.6	1.6	1.5	*0.57*
		$D_2\log(1/R)$	2	0.46	2.9	3.9	1.5	1.3	*0.49*
	No.117	R	4	0.40	2.5	2.6	1.6	1.0	*0.73*
		log(1/R)	4	0.38	2.5	2.7	1.5	1.0	*0.72*
		D_1R	5	0.44	1.0	2.8	1.5	2.8	*0.56*
		$D_1\log(1/R)$	2	0.34	2.6	3.0	1.4	1.2	*0.62*
		$D_2\log(1/R)$	2	0.39	2.1	2.7	1.5	1.3	*0.71*
	Celica	R	8	0.66	2.4	3.3	1.8	1.4	*0.64*
		log(1/R)	7	0.62	2.7	3.4	1.7	1.3	*0.60*
		D_1R	2	0.64	2.7	3.2	1.8	1.2	*0.71*
		$D_1\log(1/R)$	2	0.64	2.7	3.3	1.8	1.2	*0.70*
		$D_2\log(1/R)$	2	0.68	2.5	3.2	1.8	1.3	*0.73*
Hyperspectral imaging	Ever Green	R	6	0.27	3.9	4.2	1.4	1.1	*0.33*
		log(1/R)	6	0.28	4.0	4.4	1.3	1.1	*0.29*
		D_1R	4	0.24	4.0	4.4	1.3	1.1	*0.29*
		$D_1\log(1/R)$	4	0.25	4.0	4.6	1.3	1.1	*0.26*
		$D_2\log(1/R)$	3	0.28	3.6	4.5	1.3	1.2	*0.29*
	No.117	R	8	0.45	2.2	2.6	1.6	1.2	*0.72*
		log(1/R)	6	0.46	2.3	2.5	1.6	1.1	*0.76*
		D_1R	2	0.44	2.5	2.6	1.6	1.0	*0.77*
		$D_1\log(1/R)$	2	0.45	2.5	2.6	1.6	1.0	*0.78*
		$D_2\log(1/R)$	2	0.45	2.5	2.6	1.6	1.0	*0.79*
	Celica	R	12	0.72	2.4	3.0	1.9	1.3	*0.69*
		log(1/R)	9	0.68	2.7	3.1	1.9	1.1	*0.70*
		D_1R	3	0.58	3.4	3.6	1.6	1.0	*0.60*
		$D_1\log(1/R)$	4	0.70	2.8	3.1	1.9	1.1	*0.76*
		$D_2\log(1/R)$	9	0.68	2.4	3.3	1.8	1.4	*0.64*
SWIR	Ever Green	R	5	0.40	3.7	4.0	1.5	1.1	*0.43*
		log(1/R)	5	0.41	3.6	3.9	1.5	1.1	*0.44*
		D_1R	6	0.45	3.4	4.0	1.5	1.2	*0.43*
		$D_1\log(1/R)$	5	0.41	3.5	4.0	1.5	1.1	*0.43*
		$D_2\log(1/R)$	2	0.41	3.5	4.0	1.5	1.1	*0.46*
	No.117	R	6	0.49	2.3	2.5	1.6	1.1	*0.77*
		log(1/R)	6	0.48	2.3	2.5	1.7	1.1	*0.78*
		D_1R	4	0.47	2.3	2.6	1.6	1.1	*0.77*
		$D_1\log(1/R)$	4	0.46	2.3	2.6	1.6	1.1	*0.77*
		$D_2\log(1/R)$	**2**	**0.50**	**2.3**	**2.5**	**1.6**	**1.1**	***0.81***
	Celica	R	7	0.66	2.8	3.2	1.8	1.2	*0.67*
		log(1/R)	7	0.63	2.8	3.4	1.7	1.2	*0.62*
		D_1R	4	0.62	3.0	3.4	1.7	1.1	*0.66*
		$D_1\log(1/R)$	5	0.62	3.0	3.4	1.7	1.1	*0.63*
		$D_2\log(1/R)$	3	0.65	3.0	3.3	1.7	1.1	*0.67*

The overall comparison of models from the two spectral ranges and hyperspectral imaging resulted VIS-NIR spectral measurements to yield stronger correlation to predict $CE_{Rupture}$ in 'Ever Green' bell pepper cultivar, while SWIR yield the best models for 'No. 117' and hyperspectral imaging was found best for 'Celica' variety.

PLSR prediction and measured values for cv. 'No. 117' are shown in Figs. 76-78, as examples for VIS-NIR, hyperspectral imaging and SWIR, respectively. In both figures, the ordinate and abscissa axes represent the measured and the fitted values. For the VIS-NIR (Fig. 76) a model with four LVs obtained r^2=0.40 and RMSECV=2.65, for the hyperspectral imaging (Fig. 77) a model with two LVs obtained r^2=0.45 and RMSECV=2.56, whereas for SWIR (Fig. 78) two LVs were needed to achieve r^2=0.50 and RMSECV=2.50.
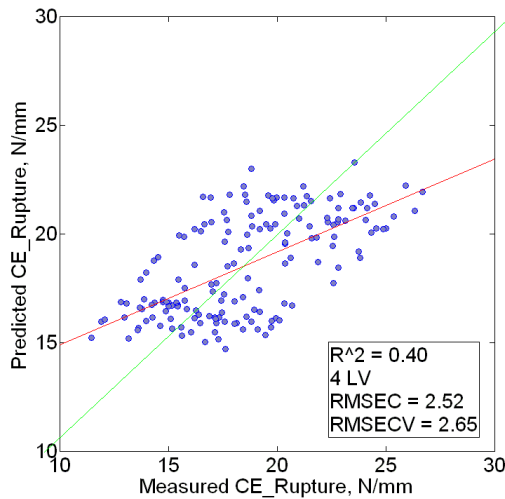
Fig. 76 Scatter plot of $CE_{Rupture}$ for 'No.117' variety, as predicted by PLS regression model and as measured in the laboratory. The PLS model was built with the reflectance (R) of the spectral data in the VIS-NIR range.
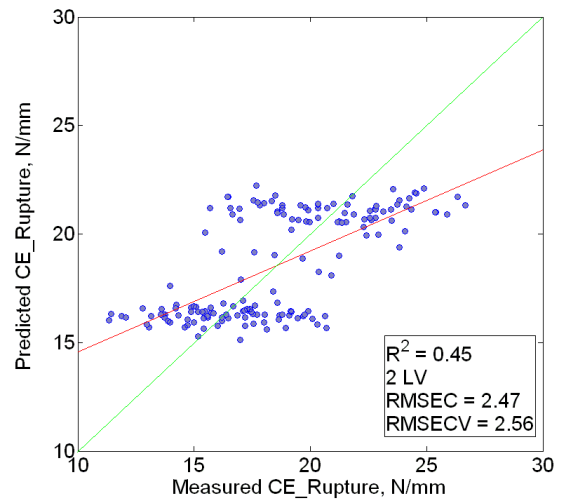
Fig. 77 Scatter plot of $CE_{Rupture}$ for 'No.117' variety, as predicted by PLS regression model and as measured in the laboratory. The PLS model was built with the $D_2log(1/R)$ of the spectral data from the hyperspectral imaging.

The Variable Importance in Projection (VIP) scores indicate the significance of specific wavelengths in the model, and Fig. 79 presents the VIP scores for the reflectance model in the VIS-NIR spectral range for cv. 'No.117'. One wide wavelength range was found to be significant in the model: 560–695 nm. It is related to the chlorophyll a and b and carotenoid contents.

Figure 80 presents the VIP scores of the reflectance model in the SWIR spectral range for cv. 'No.117'. The below wavelength range was found to significantly influencing the regression model: 1350–1500 and 1550-1790 nm; it is associated with the vibration modes of the first overtones of C-H and O-H bond stretching.
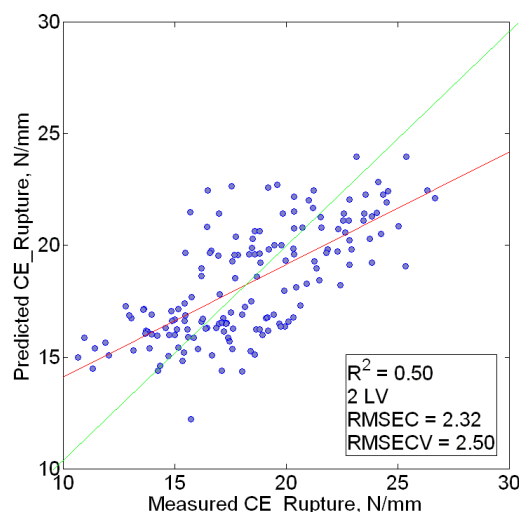
Fig. 78 Scatter plot of CE$_{Rupture}$ content for 'No.117' variety, as predicted by PLS regression model and as measured in the laboratory. The PLS model was built with the D$_2$log(1/R)of the spectral data in the SWIR range.
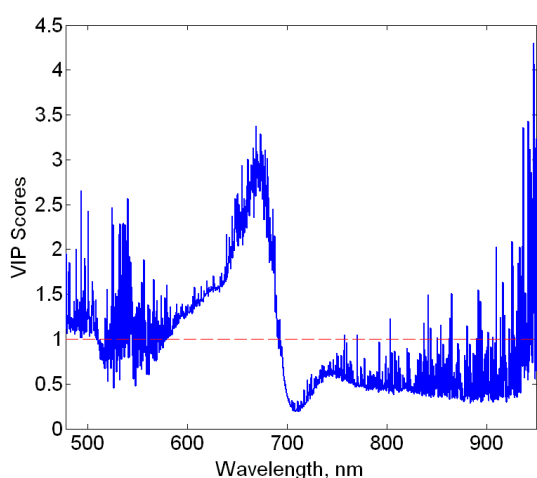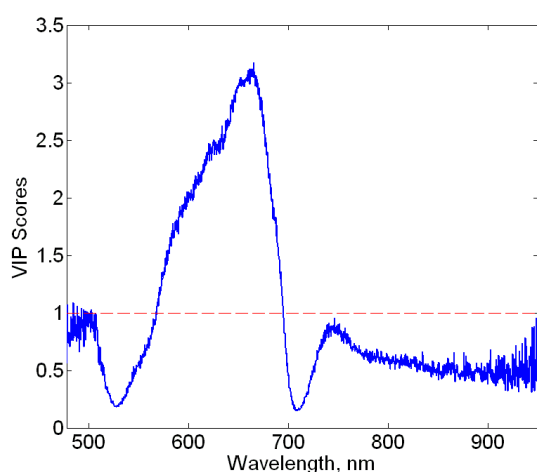

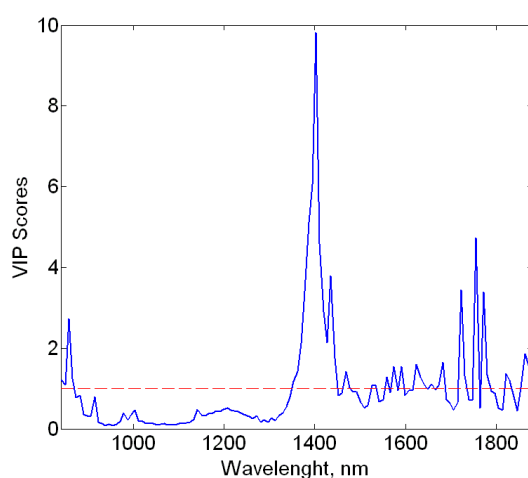**Fig. 79** VIP Scores for reflectance (R) spectra (VIS-NIR) of 'No.117' cultivar
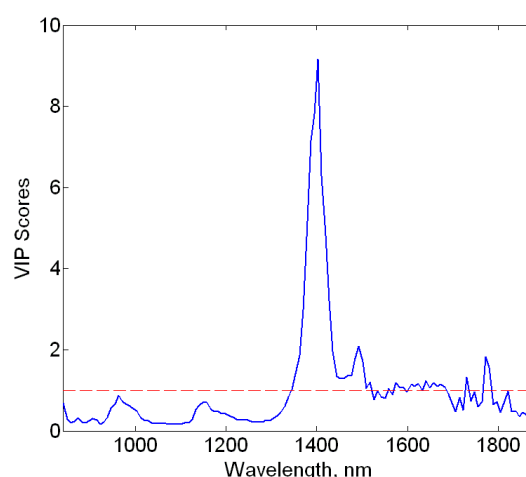
Fig. 80 VIP Scores for reflectance (R) spectra (SWIR) of 'No.117' cultivar

5.5.9. Correlation and regression analysis for days after anthesis (DAA) and NDT methods

5.5.9.1. Correlation analysis for rate of relaxation, colour measurement, and ultrasonic test

The results of cross correlation analysis for DAA with the calculated indices of relaxation test (Rate of relaxation, Remaining deformation, coefficient of elasticity from relaxation test), with the parameters of colour measurements (L, C, h) and ultrasonic attenuation shown in table 30.

The highest coefficient of correlation (r) was found for all three cultivars for DAA with the colour parameter of h, good correlation was found with the L and C in case of 'No. 117' cv. Poor

correlation was found with the ultrasonic attenuation, remaining deformation and coefficient of elasticity of relaxation test in case of all three cultivars, whereas the rate of relaxation showed slight correlation with the DAA in case of 'Ever Green' and 'No.117' cultivars.

Table 30 Covariance matrix between DAA and non-destructive measurements for 'Ever Green', 'No.117', and 'Celica' cultivars, respectively, with 95% significance level.

DAA	Rate of Relaxation	Remaining Deformation	Coefficient of elasticity Relaxation	Colour Measurement			Ultrasonic Attenuation
				L	C	h	
Ever Green	0.56	0.38	0.26	0.40	0.37	0.86	0.48
No.117	0.64	0.37	0.24	0.85	0.87	0.91	0.47
Celica	0.40	0.20	0.38	0.18	0.65	0.89	0.55

5.5.9.2. PLS Regression for VIS-NIR and SWIR spectral analysis and hyperspectral imaging

The coefficient of variance for DAA was 28.9%. The average squared intercorrelations found to be poor between DAA-TSS (average: 0.80), DAA-DM (average: 0.76) and DAA-total chlorophyll content (average: 0.55). The good squared intercorrelation between DAA and TSS, DM and total chlorophyll content indicate that prediction by the VIS-NIR, SWIR and hyperspectral imaging method is applicable with the consideration of possible intercorrelation.

Table 31 presents for all three cultivars, the results from PLS regression for VIS-NIR, hyperspectral imaging and SWIR, respectively. The following statistical parameters are shown for each model: no. of latent variables, LV; coefficient of determination, r^2; root-mean-square error of calibration, RMSEC; root-mean-square error of cross-validation, RMSECV; robust parameter design, RPD; ratio of RMSECV and RMSEC, and standardized weighted sum index, SWS.

Comparison of the PLS models among the two wavelength ranges (VIS-NIR, SWIR) and hyperspectral imaging shows that the VIS-NIR models were obtained with fewer LVs (average, 6), higher r^2 (average, 0.97), lower RMSECV (average, 3.25), higher RPD (average, 5.48) and higher SWS (average, 0.77), whereas hyperspectral imaging models achieved lower RMSECV/RMSEC (average, 1.25).

In the VIS-NIR range, for all three varieties the $D_2log(1/R)$ gave the highest SWS and therefore the best model. The relevant SWS indices were 0.91, 0.82, and 0.84 for 'Ever Green', 'No. 117' and 'Celica', respectively.

In case of the hyperspectral imaging for 'Ever Green' the reflectance (R), for 'No.117' the $log(1/R)$, while for 'Celica' the $D_1log(1/R)$ resulted with the highest SWS and therefore the best model. The relevant SWS indices were 0.38, 0.75, and 0.64 for 'Ever Green', 'No. 117' and, 'Celica' respectively.

The best models were achieved in the SWIR spectral range for 'Ever Green' and 'No. 117' cultivars by the log(1/R), whereas for 'Celica' the D_2log(1/R), with SWS 0.66, 0.72 and 0.75, respectively.

Table 31 Performance measures of PLS regression models for DAA, using data from the VIS-NIR, Hyperspectral, and SWIR spectral region. Models for the three pepper varieties are presented: 'Ever Green', 'No, 117' and 'Celica'.

PLS	DAA, days	Statistical parameter	LV	r^2	RMSEC	RMSECV	RPD	RMSECV/ RMSEC	*SWS*
VIS-NIR	*Ever Green*	R	9	0.98	1.6	2.8	6.4	1.8	*0.80*
		log(1/R)	9	0.96	1.5	3.4	5.1	2.3	*0.64*
		D_1R	3	0.98	1.9	2.7	6.4	1.4	*0.90*
		D_1log(1/R)	4	0.98	1.5	2.7	6.4	1.8	*0.85*
		D_2log(1/R)	**3**	**0.99**	**1.5**	**2.5**	**6.9**	**1.7**	***0.91***
	No.117	R	9	0.97	2.0	3.3	5.3	1.6	*0.74*
		log(1/R)	9	0.96	2.1	3.8	4.6	1.8	*0.65*
		D_1R	4	0.97	1.9	3.1	5.6	1.6	*0.82*
		D_1log(1/R)	4	0.96	2.0	3.9	4.5	1.9	*0.68*
		D_2log(1/R)	3	0.98	1.6	3.0	5.9	1.9	*0.82*
	Celica	R	7	0.96	2.7	3.6	4.9	1.3	*0.76*
		log(1/R)	9	0.95	2.4	3.9	4.5	1.6	*0.67*
		D_1R	4	0.97	1.9	3.4	5.2	1.8	*0.76*
		D_1log(1/R)	4	0.96	2.1	3.6	4.9	1.7	*0.75*
		D_2log(1/R)	3	0.98	1.9	3.1	5.7	1.6	*0.84*
Hyperspectral imaging	*Ever Green*	R	12	0.87	5.1	6.4	2.8	1.2	*0.38*
		log(1/R)	12	0.86	5.3	6.8	2.6	1.3	*0.32*
		D_1R	8	0.85	5.7	6.9	2.5	1.2	*0.35*
		D_1log(1/R)	9	0.85	5.7	7.0	2.5	1.2	*0.33*
		D_2log(1/R)	11	0.82	4.9	7.8	2.2	1.6	*0.19*
	No.117	R	9	0.95	3.4	4.1	4.3	1.2	*0.69*
		log(1/R)	7	0.95	3.5	3.8	4.6	1.1	*0.75*
		D_1R	8	0.94	3.7	4.5	3.9	1.2	*0.64*
		D_1log(1/R)	7	0.94	3.6	4.3	4.1	1.2	*0.69*
		D_2log(1/R)	6	0.94	3.4	4.4	4.0	1.3	*0.67*
	Celica	R	11	0.92	4.0	5.0	3.5	1.3	*0.55*
		log(1/R)	10	0.92	4.0	4.9	3.6	1.2	*0.57*
		D_1R	6	0.92	4.5	5.1	3.4	1.1	*0.60*
		D_1log(1/R)	6	0.93	4.1	4.8	3.7	1.2	*0.64*
		D_2log(1/R)	7	0.91	4.0	5.4	3.2	1.4	*0.54*
SWIR	*Ever Green*	R	10	0.93	3.0	4.7	3.8	1.5	*0.58*
		log(1/R)	10	0.95	2.9	4.1	4.3	1.4	*0.66*
		D_1R	12	0.94	3.3	4.7	3.8	1.4	*0.57*
		D_1log(1/R)	12	0.93	3.3	4.9	3.6	1.5	*0.53*
		D_2log(1/R)	6	0.94	3.3	4.5	3.9	1.4	*0.66*
	No.117	R	8	0.95	3.3	4.0	4.4	1.2	*0.71*
		log(1/R)	8	0.95	3.3	4.0	4.4	1.2	*0.72*
		D_1R	10	0.95	2.9	3.9	4.5	1.4	*0.69*
		D_1log(1/R)	8	0.96	3.1	3.9	4.5	1.3	*0.72*
		D_2log(1/R)	6	0.94	3.3	4.4	4.0	1.3	*0.67*
	Celica	R	8	0.94	3.3	4.3	4.1	1.3	*0.67*
		log(1/R)	8	0.94	3.4	4.3	4.1	1.2	*0.67*
		D_1R	7	0.94	3.7	4.4	4.0	1.2	*0.67*
		D_1log(1/R)	5	0.94	3.8	4.2	4.1	1.1	*0.72*
		D_2log(1/R)	5	0.95	2.9	3.8	4.6	1.3	*0.75*

The overall comparison of models from the two spectral ranges and hyperspectral imaging resulted VIS-NIR to yield the most efficient models to predict DAA for all three bell pepper cultivars. Worth to mention, that even though in case of the 'Ever Green' variety there is no significant colour change still in the VIS-NIR spectral range very reliable prediction models were achieved for DAA.

PLSR prediction and measured values for cv. 'Ever Green' are shown in Figs. 81-83, as examples for VIS-NIR, hyperspectral imaging and SWIR, respectively. In both figures, the ordinate and abscissa axes represent the measured and the fitted values. For the VIS-NIR (Fig. 81) a model with three LVs obtained r^2=0.986 and RMSECV=2.5, for the hyperspectral imaging (Fig. 82) a model with twelve LVs obtained r^2=0.87 and RMSECV=6.36, whereas for SWIR (Fig. 83) ten LVs were needed to achieve r^2=0.95 and RMSECV =4.09.
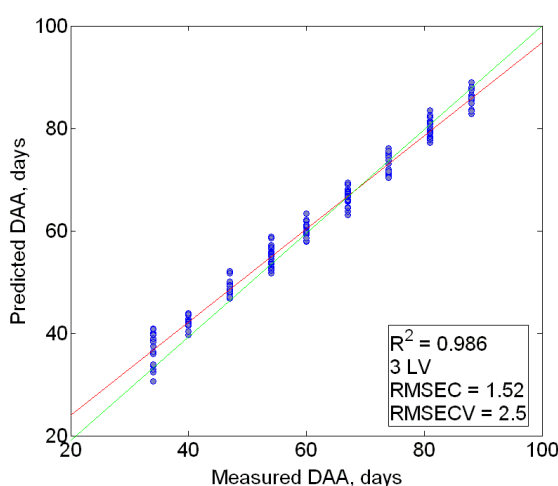
Fig. 81 Scatter plot of DAA for 'Ever Green' variety, as predicted by PLS regression model and as measured in the laboratory. The PLS model was built with the $D_2log(1/R)$ of the spectral data in the VIS-NIR range.
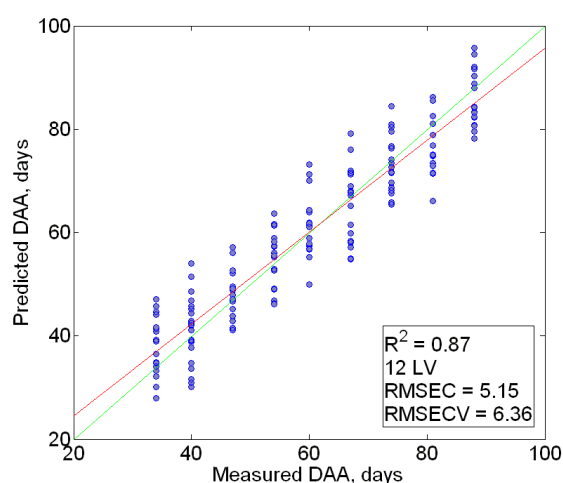
Fig. 82 Scatter plot of DAA for 'Ever Green' variety, as predicted by PLS regression model and as measured in the laboratory. The PLS model was built with the reflectance (R) of the spectral data from the hyperspectral imaging.

The Variable Importance in Projection (VIP) scores indicate the significance of specific wavelengths in the model, and Fig. 84 presents the VIP scores for the reflectance model in the VIS-NIR spectral range for cv. 'Ever Green'. The following wavelength ranges were found to be significant in the model: 477-550, 680-690 and 880-950 nm. The ranges of 477-550, 680-690 nm are related to chlorophyll a, b and carotenoid contents. The range of 880-950 nm is associated with the vibration modes of the first overtones of C-H and O-H bond. These bonds can be found for example in carbohydrates, ascorbic acid.
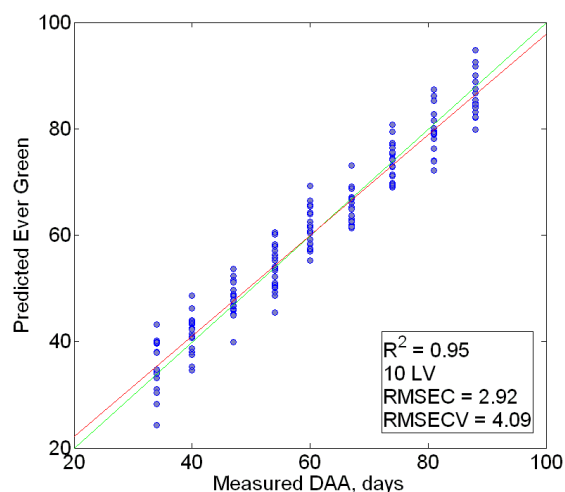
Fig. 83 Scatter plot of DAA for 'Ever Green' variety, as predicted by PLS regression model and as measured in the laboratory. The PLS model was built with the log(1/R) of the spectral data in the SWIR range.

Figure 85 presents the VIP scores of the reflectance model in the SWIR spectral range for cv. ' Ever Green '. The below wavelength ranges were found to significantly influencing the regression model: 850-920, 1380–1800 nm. It is associated with the vibration modes of the first overtones of C-H and O-H bond stretching. These bonds commonly found in carbohydrates. Significance of the wavelength ranges above 850 nm indicates, that the regression models influenced by indirect correlation; as it was presumed in chapter 5.5.10.1.
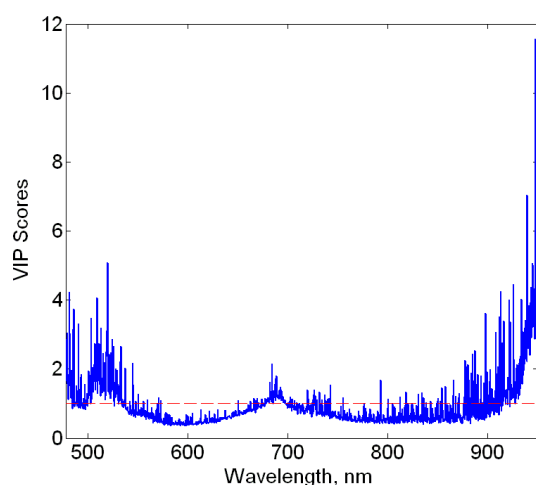
Fig. 84 VIP Scores for reflectance (R) spectra (VIS-NIR) of 'Ever Green' cultivar
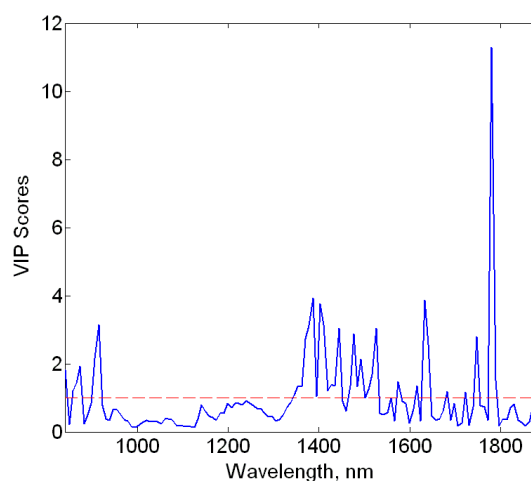
Fig. 85 VIP Scores for reflectance (R) spectra (SWIR) of 'Ever Green' cultivar

106

5.6. FUSION

5.6.1. 1st level fusion: Fusion of NDT parameters

In the first level of fusion the NDT parameters were fused in order to analyze the effect of combination of data to predict the DT quality attributes of bell peppers. As a first step of the fusion different feature extractions were applied on the data from the different measurement methods. For the VIS-NIR, SWIR and hyperspectral spectral data the SAM_{degree} of the spectra, D_{abs}, PC1 and PC2 of the quality point based on the PQS system and the LV-s from the best PLSR models were calculated. The scheme of the fusion is presented on figure 86. The list of the fused variables is found in Appendix 2.

Fig. 86 Scheme for fusion of NDT methods
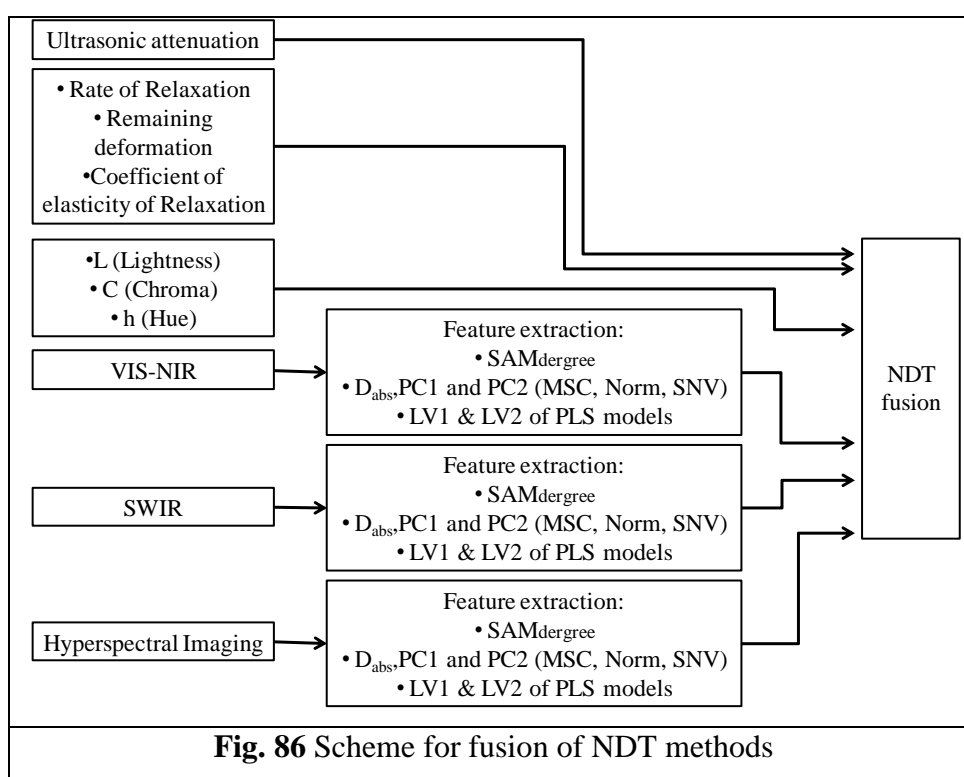
Model evaluation is relevant for the comparison of the single-sensor system to a multisensory system. The comparison is based on the performance of the model's ability to predict the properties of the produce. The evaluation of model performance of the two systems was carried out with application of SWS index.

Table 32-33 shows the detailed results for the comparison PLS regression models for singe-sensor and multisensor systems. Single-sensor system means the use of VIS-NIR or Hyperspectral imaging or SWIR spectral measurements. Multisensor system means the NDT data fusion. Have to be mentioned that in the evaluation the SWS index was calculated to one particular variety along with one particular DT parameter in order to be able to compare the

performance of the regression models. As the results present in each case the fused data gave better models with higher SWS indices. Moreover, the fused models are predicting the DT parameters with similar or lower number of latent variables (LV), they have generally higher correlation of determination as well as lower RMSECV. Altogether the fusion of the NDT parameters found to be sufficient and beneficial for the prediction of DT quality parameters in the examined three bell pepper cultivars.

Table 32 Performance measures of PLS regression models for TSS, DM, AA and OP, using data from the VIS-NIR, Hyperspectral, SWIR spectral range and fused NDT methods. Models for the three pepper varieties are presented: 'Ever Green', 'No, 117' and 'Celica'.

DT	Cultivar	NDT	LV	r^2	RMSEC	RMSECV	RPD	RMSECV/ RMSEC	SWS	% of difference in RMSECV
TSS, Birix %	Ever Green	VIS-NIR	3	0.93	0.29	0.38	3.9	1.3	0.71	21%
		Hyperspectral imaging	13	0.87	0.43	0.56	2.6	1.3	0.17	46%
		SWIR	9	0.91	0.33	0.44	3.3	1.3	0.40	32%
		Fusion of NDT	**5**	**0.96**	**0.22**	**0.30**	**4.9**	**1.3**	**0.81**	
	No.117	VIS-NIR	6	0.91	0.47	0.55	3.2	1.2	0.22	31%
		Hyperspectral imaging	6	0.93	0.43	0.47	3.8	1.1	0.57	19%
		SWIR	6	0.92	0.46	0.52	3.4	1.1	0.36	27%
		Fusion of NDT	**7**	**0.96**	**0.28**	**0.38**	**4.7**	**1.4**	**0.74**	
	Celica	VIS-NIR	8	0.95	0.29	0.38	4.6	1.3	0.35	16%
		Hyperspectral imaging	6	0.95	0.34	0.37	4.7	1.1	0.57	14%
		SWIR	7	0.94	0.38	0.44	3.9	1.2	0.14	27%
		Fusion of NDT	**3**	**0.97**	**0.27**	**0.32**	**5.5**	**1.2**	**0.93**	
DM, %	Ever Green	VIS-NIR	8	0.93	0.26	0.37	3.8	1.4	0.64	11%
		Hyperspectral imaging	9	0.84	0.47	0.59	2.4	1.3	0.08	44%
		SWIR	4	0.89	0.42	0.48	3.0	1.2	0.56	31%
		Fusion of NDT	**4**	**0.95**	**0.26**	**0.33**	**4.3**	**1.3**	**0.92**	
	No.117	VIS-NIR	3	0.9	0.56	0.58	3.0	1.0	0.26	21%
		Hyperspectral imaging	6	0.92	0.46	0.51	3.5	1.1	0.57	10%
		SWIR	8	0.93	0.39	0.48	3.7	1.2	0.69	4%
		Fusion of NDT	**6**	**0.94**	**0.31**	**0.46**	**3.9**	**1.5**	**0.78**	
	Celica	VIS-NIR	8	0.94	0.33	0.43	4.1	1.3	0.64	5%
		Hyperspectral imaging	6	0.94	0.39	0.43	4.0	1.1	0.78	5%
		SWIR	7	0.92	0.42	0.50	3.5	1.2	0.10	18%
		Fusion of NDT	**2**	**0.94**	**0.37**	**0.41**	**4.2**	**1.1**	**0.97**	
AA, g/100g	Ever Green	VIS-NIR	9	0.79	8.7	15.2	2.1	1.8	0.43	9%
		Hyperspectral imaging	4	0.72	15.0	16.7	1.9	1.1	0.26	17%
		SWIR	8	0.75	12.6	15.7	2.0	1.2	0.39	12%
		Fusion of NDT	**5**	**0.83**	**10.0**	**13.9**	**2.3**	**1.4**	**0.90**	
	No.117	VIS-NIR	4	0.62	9.5	17.3	2.2	1.8	0.21	27%
		Hyperspectral imaging	7	0.55	15.4	17.3	2.2	1.1	0.22	27%
		SWIR	10	0.70	11.2	16.1	2.4	1.4	0.37	22%
		Fusion of NDT	**6**	**0.81**	**9.3**	**12.6**	**3.1**	**1.4**	**0.91**	
	Celica	VIS-NIR	8	0.78	11.1	15.1	2.2	1.4	0.40	14%
		Hyperspectral imaging	8	0.72	14.4	16.0	2.1	1.1	0.32	19%
		SWIR	8	0.71	14.2	17.1	2.0	1.2	0.11	24%
		Fusion of NDT	**4**	**0.83**	**10.7**	**13.0**	**2.6**	**1.2**	**0.93**	
OP, osmol/kg	Ever Green	VIS-NIR	3	0.87	27.0	36.7	3.0	1.4	0.64	11%
		Hyperspectral imaging	6	0.80	42.7	48.5	2.3	1.1	0.17	33%
		SWIR	5	0.84	32.2	41.8	2.6	1.3	0.40	22%
		Fusion of NDT	**3**	**0.90**	**27.2**	**32.5**	**3.4**	**1.2**	**0.94**	
	No.117	VIS-NIR	3	0.88	44.2	45.8	2.9	1.0	0.28	0%
		Hyperspectral imaging	5	0.89	39.9	43.2	3.0	1.1	0.80	-6%
		SWIR	4	0.88	37.8	45.4	2.9	1.2	0.21	-1%
		Fusion of NDT	**2**	**0.88**	**39.9**	**45.8**	**2.8**	**1.1**	**0.22**	
	Celica	VIS-NIR	3	0.92	25.5	34.8	3.6	1.4	0.59	10%
		Hyperspectral imaging	3	0.92	31.5	32.9	3.8	1.0	0.82	5%
		SWIR	6	0.89	35.1	40.2	3.1	1.1	0.13	22%
		Fusion of NDT	**3**	**0.93**	**26.8**	**31.4**	**4.0**	**1.2**	**0.91**	

Table 33 Performance measures of PLS regression models for total chlorophyll, carotenoid, Coefficient of elasticity of Compression and Coefficient of elasticity of Rupture, using data from the VIS-NIR, Hyperspectral, SWIR spectral range and fused NDT methods. Models for the three pepper varieties are presented: 'Ever Green', 'No, 117' and 'Celica'.

DT	Cultivar	NDT	LV	r^2	RMSEC	RMSECV	RPD	RMSECV/ RMSEC	SWS	% of difference in RMSECV
Total Chlorophyll, mg/g	Ever Green	VIS-NIR	6	0.6	0.007	0.008	1.7	1.2	0.53	19%
		Hyperspectral imaging	5	0.44	0.009	0.010	1.4	1.1	0.24	35%
		SWIR	9	0.71	0.006	0.007	1.9	1.3	0.61	7%
		Fusion of NDT	**4**	**0.77**	**0.005**	**0.007**	**2.1**	**1.3**	**0.83**	
	No.117	VIS-NIR	5	0.95	0.003	0.005	4.2	2.0	0.10	30%
		Hyperspectral imaging	3	0.95	0.005	0.005	4.4	1.1	0.27	30%
		SWIR	6	0.96	0.004	0.005	4.9	1.1	0.31	30%
		Fusion of NDT	**7**	**0.98**	**0.003**	**0.004**	**6.6**	**1.4**	**0.85**	
	Celica	VIS-NIR	9	0.93	0.005	0.008	3.7	1.5	0.12	25%
		Hyperspectral imaging	5	0.95	0.007	0.007	4.0	1.1	0.63	14%
		SWIR	6	0.92	0.007	0.008	3.5	1.2	0.21	25%
		Fusion of NDT	**5**	**0.96**	**0.005**	**0.006**	**4.7**	**1.3**	**0.92**	
Carotenoid, mg/g	Ever Green	VIS-NIR	3	0.92	0.007	0.010	3.9	1.4	0.50	24%
		Hyperspectral imaging	7	0.87	0.012	0.013	3.0	1.1	0.17	42%
		SWIR	5	0.88	0.010	0.012	3.3	1.3	0.23	37%
		Fusion of NDT	**5**	**0.96**	**0.006**	**0.008**	**5.2**	**1.3**	**0.84**	
	No.117	VIS-NIR	7	0.91	0.005	0.006	3.7	1.2	0.11	33%
		Hyperspectral imaging	8	0.92	0.005	0.006	4.0	1.1	0.29	33%
		SWIR	6	0.88	0.005	0.006	3.7	1.2	0.06	33%
		Fusion of NDT	**5**	**0.95**	**0.003**	**0.004**	**5.6**	**1.2**	**0.83**	
	Celica	VIS-NIR	8	0.95	0.007	0.010	6.6	1.3	0.65	29%
		Hyperspectral imaging	10	0.97	0.007	0.008	7.5	1.2	0.77	15%
		SWIR	7	0.88	0.013	0.015	4.2	1.2	0.26	52%
		Fusion of NDT	**8**	**0.98**	**0.005**	**0.007**	**8.8**	**1.5**	**0.80**	
Coefficient of elasticity Compression, N/mm	Ever Green	VIS-NIR	2	0.55	8.80	10.90	1.7	1.2	0.58	6%
		Hyperspectral imaging	4	0.47	10.90	12.30	1.5	1.1	0.22	16%
		SWIR	6	0.56	9.80	10.90	1.7	1.1	0.64	6%
		Fusion of NDT	**3**	**0.63**	**8.40**	**10.30**	**1.8**	**1.2**	**0.81**	
	No.117	VIS-NIR	2	0.49	5.82	6.70	1.7	1.1	0.70	4%
		Hyperspectral imaging	2	0.37	7.40	7.60	1.5	1.0	0.26	16%
		SWIR	2	0.42	6.50	7.40	1.5	1.1	0.30	13%
		Fusion of NDT	**3**	**0.55**	**5.53**	**6.40**	**1.8**	**1.2**	**0.74**	
	Celica	VIS-NIR	2	0.41	6.10	7.10	1.5	1.2	0.69	2%
		Hyperspectral imaging	2	0.27	7.20	7.50	1.4	1.0	0.26	7%
		SWIR	2	0.36	6.70	7.50	1.4	1.1	0.30	7%
		Fusion of NDT	**3**	**0.43**	**5.92**	**6.97**	**1.5**	**1.2**	**0.76**	
Coefficient of elasticity Rupture, N/mm	Ever Green	VIS-NIR	3	0.52	2.40	3.60	1.6	1.5	0.79	0%
		Hyperspectral imaging	6	0.27	3.90	4.20	1.4	1.1	0.17	14%
		SWIR	2	0.41	3.50	4.00	1.5	1.1	0.55	10%
		Fusion of NDT	**4**	**0.54**	**2.70**	**3.60**	**1.6**	**1.3**	**0.86**	
	No.117	VIS-NIR	4	0.40	2.50	2.60	1.6	1.0	0.17	8%
		Hyperspectral imaging	2	0.45	2.50	2.60	1.6	1.0	0.32	8%
		SWIR	2	0.50	2.30	2.50	1.6	1.1	0.53	4%
		Fusion of NDT	**4**	**0.54**	**2.00**	**2.40**	**1.7**	**1.2**	**0.74**	
	Celica	VIS-NIR	2	0.68	2.50	3.20	1.8	1.3	0.26	16%
		Hyperspectral imaging	4	0.70	2.80	3.10	1.9	1.1	0.46	13%
		SWIR	3	0.65	3.00	3.30	1.7	1.1	0.23	18%
		Fusion of NDT	**5**	**0.77**	**2.10**	**2.70**	**2.2**	**1.3**	**0.74**	

PLS, PCR, Kernel and SVM regression analysis were used to build the models. Table 34-35 shows the result for each cultivar and for each DT parameter. The following statistical parameters are shown for each model: no. of latent variables, LV; coefficient of determination, r^2; root-mean-square error of calibration, RMSEC; root-mean-square error of cross-validation, RMSECV; robust parameter design, RPD; ratio of RMSECV and RMSEC, and standardized weighted sum index, SWS.

Comparing the single sensor and multi sensor models for all three pepper cultivars the fused NDT data (multi sensor models) gave higher SWS indices in predicting each one of the DT

parameters, compare to the single sensor models. It means that with the fusion of the relaxation, ultrasonic, colour, spectral and hyperspectral data altogether is more capable to predict inner composition and textural state of different variety of bell pepper cultivars; regardless of the fact that the pepper variety is changing its colour during the growth of maturation or not.

Overall comparison of the different regression methods, based on the SWS index showed that PLS and SVM regressions were most suitable to predict DT parameters from the fused NDT parameters.

Table 34 Performance measures of PLS, PCR, Kernel and SVM regression models for TSS, DM, AA and OP, using data from the fused NDT methods. Models for the three pepper varieties are presented: 'Ever Green', 'No, 117' and 'Celica'.

DT	Cultivar	Regression analysis	LV	r^2	RMSEC	RMSECV	RPD	RMSECV/ RMSEC	SWS
TSS, Brix %	Ever Green	PLS	5	0.96	0.22	0.30	4.9	1.3	0.84
		PCR	7	0.94	0.35	0.37	3.9	1.1	0.73
		Kernel	5	0.93	0.29	0.40	3.7	1.4	0.64
		SVM	5	0.96	0.23	0.29	5.0	1.3	0.86
	No.117	PLS	7	0.96	0.28	0.38	4.6	1.4	0.70
		PCR	8	0.93	0.44	0.48	3.7	1.1	0.57
		Kernel	7	0.94	0.40	0.47	3.8	1.2	0.57
		SVM	7	0.96	0.22	0.36	4.9	1.6	0.67
	Celica	PLS	3	0.97	0.27	0.32	5.5	1.2	0.90
		PCR	6	0.97	0.29	0.32	5.5	1.1	0.89
		Kernel	3	0.93	0.41	0.50	3.5	1.2	0.56
		SVM	**3**	**0.97**	**0.26**	**0.31**	**5.6**	**1.2**	**0.91**
DM, %	Ever Green	**PLS**	**4**	**0.95**	**0.26**	**0.33**	**4.3**	**1.3**	**0.89**
		PCR	7	0.93	0.35	0.39	3.7	1.1	0.77
		Kernel	4	0.91	0.43	0.44	3.2	1.0	0.70
		SVM	4	0.94	0.25	0.35	4.1	1.4	0.83
	No.117	PLS	6	0.94	0.31	0.46	3.9	1.5	0.66
		PCR	10	0.92	0.47	0.51	3.5	1.1	0.58
		Kernel	6	0.92	0.37	0.51	3.5	1.4	0.58
		SVM	6	0.94	0.28	0.43	4.1	1.5	0.69
	Celica	PLS	2	0.94	0.37	0.41	4.2	1.1	0.83
		PCR	6	0.94	0.39	0.43	4.1	1.1	0.77
		Kernel	3	0.90	0.42	0.54	3.2	1.3	0.53
		SVM	2	0.95	0.31	0.40	4.4	1.3	0.83
Ascorbic acid, mg/100g	Ever Green	PLS	5	0.83	10.0	13.9	2.3	1.4	0.73
		PCR	9	0.70	15.8	17.2	1.9	1.1	0.41
		Kernel	9	0.82	9.2	18.2	1.7	2.0	0.36
		SVM	5	0.79	9.7	15.0	2.1	1.5	0.85
	No.117	PLS	6	0.81	9.3	12.6	3.1	1.4	0.85
		PCR	11	0.63	15.0	16.7	2.3	1.1	0.42
		Kernel	6	0.78	14.7	19.0	2.0	1.3	0.37
		SVM	6	0.76	9.2	13.6	2.8	1.5	0.82
	Celica	PLS	4	0.83	10.7	13.0	2.6	1.2	0.82
		PCR	10	0.79	13.2	14.4	2.4	1.1	0.65
		Kernel	10	0.72	11.7	17.9	1.9	1.5	0.35
		SVM	**4**	**0.85**	**10.1**	**11.9**	**2.8**	**1.2**	**0.92**
OP, osmol/kg	Ever Green	PLS	3	0.90	27.2	32.5	3.4	1.2	0.81
		PCR	8	0.90	31.4	33.7	3.2	1.1	0.75
		Kernel	3	0.84	35.6	38.3	2.9	1.1	0.65
		SVM	3	0.89	27.2	33.6	3.3	1.2	0.76
	No.117	PLS	2	0.88	39.9	45.8	2.8	1.1	0.53
		PCR	7	0.88	43.1	44.7	2.9	1.0	0.53
		Kernel	3	0.86	46.6	47.3	2.8	1.0	0.51
		SVM	2	0.90	36.8	40.4	3.2	1.1	0.69
	Celica	**PLS**	**3**	**0.93**	**26.8**	**31.4**	**4.0**	**1.2**	**0.88**
		PCR	10	0.94	28.4	30.1	4.1	1.1	0.87
		Kernel	3	0.87	37.4	38.2	3.3	1.0	0.71
		SVM	3	0.93	25.2	31.7	3.9	1.3	0.85

Table 35 Performance measures of PLS, PCR, Kernel and SVM regression models for total chlorophyll, carotenoid, Coefficient of elasticity of Compression and Coefficient of elasticity of Rupture, using data from the fused NDT methods. Models for the three pepper varieties are presented: 'Ever Green', 'No, 117' and 'Celica'.

| DT	Cultivar	Regression analysis	LV	r^2	RMSEC	RMSECV	RPD	RMSECV/ RMSEC	*SWS*
Total Chlorophyll, mg/g	Ever Green	PLS	4	0.77	0.0052	0.0065	2.1	1.3	*0.60*
		PCR	11	0.69	0.0065	0.0072	1.9	1.1	*0.51*
		Kernel	4	0.36	0.0104	0.0119	1.2	1.1	*0.40*
		SVM	4	0.76	0.0051	0.0065	2.1	1.3	*0.60*
	No.117	PLS	7	0.98	0.0025	0.0035	6.6	1.4	*0.74*
		PCR	10	0.97	0.0038	0.0043	5.4	1.1	*0.70*
		Kernel	7	0.95	0.0048	0.0050	4.6	1.0	*0.71*
		SVM	**7**	**0.98**	**0.0022**	**0.0033**	**7.0**	**1.5**	***0.74***
	Celica	PLS	5	0.96	0.0045	0.0060	4.7	1.3	*0.69*
		PCR	9	0.94	0.0065	0.0071	3.9	1.1	*0.63*
		Kernel	6	0.91	0.0084	0.0087	3.2	1.0	*0.62*
		SVM	6	0.94	0.0040	0.0066	4.2	1.7	*0.63*
Carotenoids, mg/g	Ever Green	PLS	5	0.96	0.0058	0.0076	5.2	1.3	*0.73*
		PCR	7	0.93	0.0086	0.0093	4.2	1.1	*0.66*
		Kernel	5	0.94	0.0089	0.0093	4.2	1.0	*0.69*
		SVM	5	0.97	0.0043	0.0063	6.2	1.5	*0.78*
	No.117	**PLS**	**5**	**0.95**	**0.0032**	**0.0040**	**5.6**	**1.2**	***0.87***
		PCR	11	0.93	0.0046	0.0053	4.2	1.2	*0.73*
		Kernel	5	0.85	0.0042	0.0080	2.8	1.9	*0.48*
		SVM	5	0.95	0.0030	0.0040	5.5	1.3	*0.85*
	Celica	PLS	8	0.98	0.0047	0.0071	8.8	1.5	*0.75*
		PCR	9	0.96	0.0085	0.0102	6.2	1.2	*0.65*
		Kernel	6	0.95	0.0118	0.0129	4.9	1.1	*0.57*
		SVM	6	0.98	0.0052	0.0076	8.2	1.5	*0.77*
Coefficient of elasticity Rupture, N/mm	Ever Green	PLS	4	0.54	2.7	3.6	1.6	1.3	*0.56*
		PCR	4	0.45	3.6	3.7	1.6	1.0	*0.52*
		Kernel	4	0.50	4.2	4.5	1.3	1.1	*0.34*
		SVM	4	0.50	2.8	3.7	1.6	1.3	*0.52*
	No.117	PLS	4	0.54	2.0	2.4	1.7	1.2	*0.81*
		PCR	3	0.44	2.6	2.7	1.6	1.0	*0.73*
		Kernel	4	0.43	3.1	3.1	1.3	1.0	*0.61*
		SVM	4	0.44	2.1	2.6	1.6	1.3	*0.72*
	Celica	**PLS**	**5**	**0.77**	**2.1**	**2.7**	**2.2**	**1.3**	***0.88***
		PCR	11	0.69	2.8	3.1	1.9	1.1	*0.69*
		Kernel	5	0.72	2.8	3.0	1.9	1.1	*0.77*
		SVM	5	0.75	2.1	2.8	2.1	1.3	*0.84*
Coefficient of elasticity Compression, N/mm	Ever Green	PLS	3	0.63	8.4	10.3	1.8	1.2	*0.64*
		PCR	4	0.58	10.2	10.6	1.8	1.0	*0.64*
		Kernel	4	0.51	12.0	13.0	1.4	1.1	*0.39*
		SVM	3	0.60	8.6	10.6	1.8	1.2	*0.60*
	No.117	**PLS**	**3**	**0.55**	**5.5**	**6.4**	**1.8**	**1.2**	***0.88***
		PCR	11	0.44	6.6	7.1	1.6	1.1	*0.71*
		Kernel	3	0.32	8.2	10.1	1.1	1.2	*0.42*
		SVM	3	0.54	5.8	6.7	1.7	1.2	*0.85*
	Celica	PLS	3	0.43	5.9	7.0	1.5	1.2	*0.75*
		PCR	4	0.27	7.3	7.6	1.4	1.0	*0.66*
		Kernel	4	0.29	9.7	9.8	1.1	1.0	*0.49*
		SVM	2	0.46	6.3	6.9	1.5	1.1	*0.81*

Cross validated prediction and measured values for cv. 'Celica' are shown in Figs. 87-90, as examples for PLS, PCR, Kernel and SVM, respectively. In the figures, the ordinate and abscissa axes represent the measured and the fitted values. For PLS (Fig. 87) a model with three LVs

obtained r^2=0.97 and RMSECV=0.32, for PCR (Fig. 88) a model with six PCs obtained r^2=0.97 and RMSECV=0.32, for Kernel (Fig. 89) a model with three LVs obtained r^2=0.93 and RMSECV=0.50, whereas for SVM (Fig. 90) three LVs were needed to achieve r^2=0.97 and RMSECV =0.31.
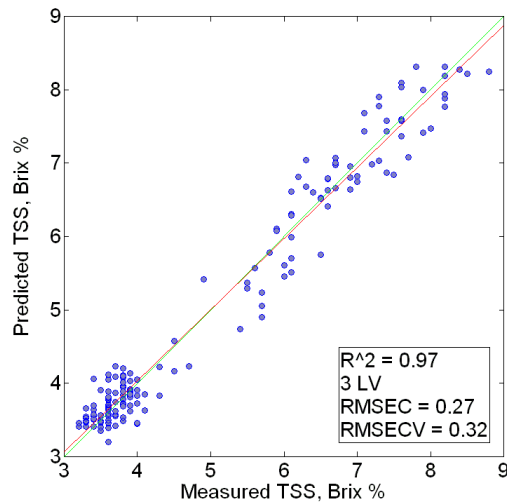
87 Scatter plot of TSS for 'Celica' variety, as predicted by PLS regression model and as measured in the laboratory. The PLS model was built with the fused NDT data.
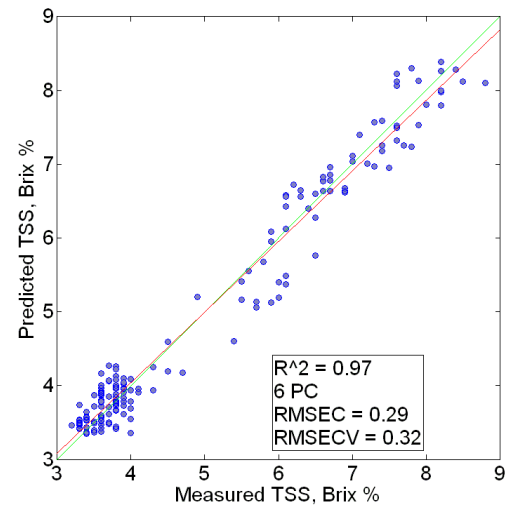
88 Scatter plot of TSS for 'Celica' variety, as predicted by PCR regression model and as measured in the laboratory. The PLS model was built with the fused NDT data.
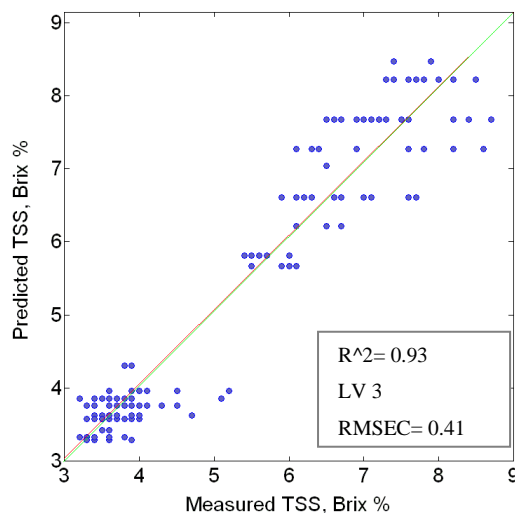
89 Scatter plot of TSS for 'Celica' variety, as predicted by Kernel regression model and as measured in the laboratory. The PLS model was built with the fused NDT data.
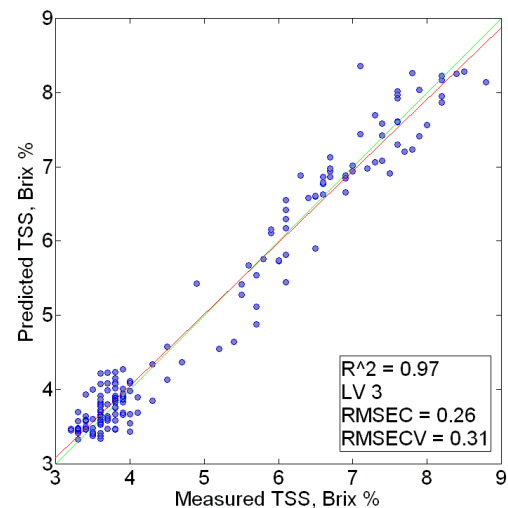
90 Scatter plot of TSS for 'Celica' variety, as predicted by SVM regression model and as measured in the laboratory. The PLS model was built with the fused NDT data.

5.6.2. 2nd level fusion: fused NDT parameters related with combined cultivar dataset

Up to this point we examined each pepper cultivar separately. In the second level of fusion we would like to check the possibility of combining the cultivars regardless of the fact that they are differentiate in their final colour and build general models for predicting each DT parameters. Table 36 presents the result of the PLS, PCR, Kernel and SVM regression analyses'.

Table 36 Performance measures of PLS, PCR, Kernel and SVM regression models for DT parameters, using data from the fused NDT methods. Models of the combination of the three pepper varieties are presented.

| DT	Cultivar	Regression analysis	LV	r^2	RMSEC	RMSECV	RPD	RMSECV/ RMSEC	*SWS*
TSS, Brix%	Ever Green & No.117& Celica	PLS	5	0.93	0.40	0.45	3.8	1.11	*0.67*
		PCR	4	0.87	0.62	0.64	2.7	1.02	*0.36*
		Kernel	5	0.93	0.42	0.47	3.6	1.13	*0.58*
		SVM	**5**	**0.93**	**0.37**	**0.43**	**4.0**	**1.16**	***0.67***
DM, %	Ever Green & No.117& Celica	PLS	5	0.93	0.42	0.46	3.6	1.11	*0.71*
		PCR	4	0.84	0.65	0.67	2.5	1.02	*0.33*
		Kernel	**5**	**0.92**	**0.48**	**0.49**	**3.4**	**1.01**	***0.74***
		SVM	5	0.92	0.39	0.46	3.7	1.16	*0.67*
AA, mg/100g	Ever Green & No.117& Celica	PLS	8	0.77	14.2	16.4	2.4	1.16	*0.73*
		PCR	11	0.51	22.0	22.6	1.7	1.03	*0.19*
		Kernel	8	0.73	20.3	20.7	1.9	1.02	*0.51*
		SVM	**8**	**0.77**	**14.1**	**16.1**	**2.4**	**1.14**	***0.77***
OP, osmol/kg	Ever Green & No.117& Celica	PLS	5	0.89	37.0	40.6	3.0	1.10	*0.62*
		PCR	5	0.83	48.4	49.3	2.5	1.02	*0.22*
		Kernel	5	0.89	42.0	42.0	2.9	1.00	*0.64*
		SVM	**5**	**0.90**	**33.8**	**38.8**	**3.2**	**1.15**	***0.67***
Total Chlorophyll, mg/g	Ever Green & No.117& Celica	PLS	9	0.94	0.006	0.007	4.3	1.16	*0.59*
		PCR	15	0.86	0.011	0.011	2.8	1.05	*0.43*
		Kernel	**9**	**0.91**	**0.009**	**0.009**	**3.4**	**1.05**	***0.64***
		SVM	9	0.95	0.006	0.007	4.5	1.17	*0.60*
Carotenoid, mg/g	Ever Green & No.117& Celica	PLS	9	0.92	0.008	0.010	4.4	1.20	*0.64*
		PCR	10	0.76	0.016	0.016	2.8	1.03	*0.39*
		Kernel	**9**	**0.92**	**0.008**	**0.010**	**4.5**	**1.21**	***0.65***
		SVM	9	0.94	0.007	0.009	5.0	1.32	*0.63*
Coefficient of elasticity Compression, N/mm	Ever Green & No.117& Celica	PLS	5	0.62	7.62	8.43	1.9	1.11	*0.64*
		PCR	16	0.49	8.71	9.20	1.8	1.06	*0.33*
		Kernel	5	0.63	9.50	9.72	1.7	1.02	*0.33*
		SVM	**5**	**0.65**	**7.20**	**8.11**	**2.0**	**1.13**	***0.72***
Coefficient of elasticity Rupture, N/mm	Ever Green & No.117& Celica	**PLS**	**5**	**0.61**	**2.74**	**3.02**	**1.8**	**1.10**	***0.73***
		PCR	16	0.51	3.09	3.24	1.7	1.05	*0.38*
		Kernel	5	0.60	3.29	3.39	1.6	1.03	*0.33*
		SVM	5	0.62	2.66	3.01	1.8	1.13	*0.70*

Overall view of the results shows that the PCR regression needed significantly more PC-s to build the models. Moreover, this method generally has higher RMSECV. Therefore it is not suggested for analysis of combined varieties and fused NDT dataset for bell pepper evaluation.

Most of the cases the Kernel and SVM regressions resulted with the most efficient models. In case of TSS, AA, OP, and Coefficient of elasticity of Compression the SVM gave the highest SWS scores, 0.67, 0.77, 0.67, and 0.72 respectively. Whereas for DM, total chlorophyll, and

carotenoid the Kernel method resulted with the highest SWS: 0.74, 0.64, and 0.65, respectively. PLS gave the highest score in predicting Coefficient of elasticity of Rupture with 0.73 SWS. Based on the comparison of the single and the combined cultivar models it can be concluded that the combined variety models have a higher r^2 and lower ratio of RMSECV to RMSEC, which makes these models to be more robust and suggest the possibility that they can be applicable for DT parameter prediction.

Figure 91 and 92 represent the SVM model for predicting ascorbic acid content in the general model by combined cultivars and fused NDT methods. The figure 91 shows the data with marks according to the DAA, while figure 92 presents the data according to the cultivar information. Clearly visible on figure 92 that the higher vitamin C content is predicted in the 5-7th picks which means 60-74th DAA. In this maturity state the 'Ever Green' and No.117 cultivars has higher ascorbic acid content in harmony with the results shown in chapter 5.1.4.

Fig. 91 Scatter plot of AA, as predicted by SVM regression model and as measured in the laboratory. The SVM model was built with the fused NDT data and combination of cultivars. Data marked by the DAA.
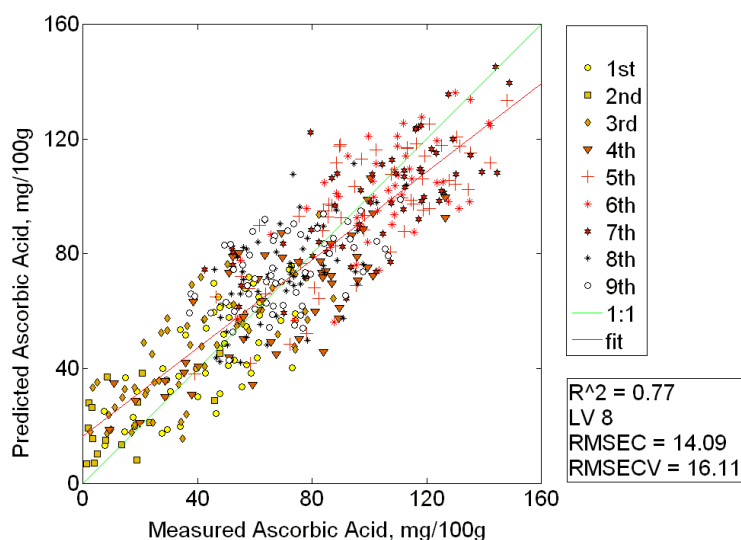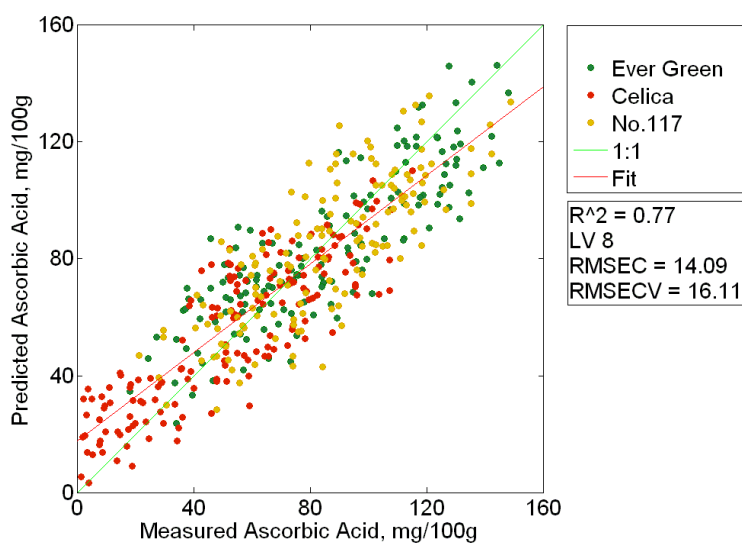

Fig. 92 Scatter plot of AA, as predicted by SVM regression model and as measured in the laboratory. The SVM model was built with the fused NDT data and combination of cultivars. Data marked by the cultivars.

5.6.3. 3rd level fusion: fused NDT parameters correlated with fused DT parameters on each cultivar separately and on combined cultivar dataset

Up until now in most of the cases the regression models were to predict single DT parameters. As well as in the literature the prediction is usually concerns on reference parameter. In the fused evaluation systems for classification of fruits and vegetables the estimation of quality is conducted by specialist, whose decision is subjective and its repeatability is poor (Steinmetz et al. 1995). Moreover, such a system is not flexible for change of cultivar; it is applicable only for the specific cultivar that the fusion process was developed. There is a need for flexible fusion system which is able to work with several cultivars as well as its reference parameters are objective in the estimation of quality of the product.

The 3rd level of fusion consist the step of fusing the DT quality parameters. In the fusion of DT parameters PCA was applied, and the 1st PC was taken as new combined quality index (NCQI). The advantage of PCA is that in the PC it can be eliminated the fact that some DT parameter might have correlation with each other, and in the same time PC gives the linear combination of the DT parameters with the highest variation. Scheme of the DT fusion is shown on Fig. 93. From the predicted NCQI values the DT values can be calculated with by the multiplication of the inverse matrix of the PCA coefficients. In this way the NCQI can be used in classification systems as well.

Table 37 shows the result of PLS, PCR, Kernel and SVM regression models for 'Ever Green', 'No, 117' and 'Celica' cultivars separately, as well as for the combination of the three cultivars. Efficient models were achieved with the fused DT and fused NDT models for all three cultivars with high correlation of determination. (SWS indices were calculated for each cultivar separately as well as separately for the combined varieties.) For 'Ever Green', 'No, 117' cultivars the PLS regression gave the best models based on the SWS index, whereas for 'Celica' cultivar the SVM learning machine resulted with the highest SWS. For the combined cultivar model the SVM resulted slightly higher SWS than PLS regression. Altogether it can be concluded that PLS and SVM methods were found to be most suitable to work with the combined dataset and build regression models for the fused DT and NDT parameters.
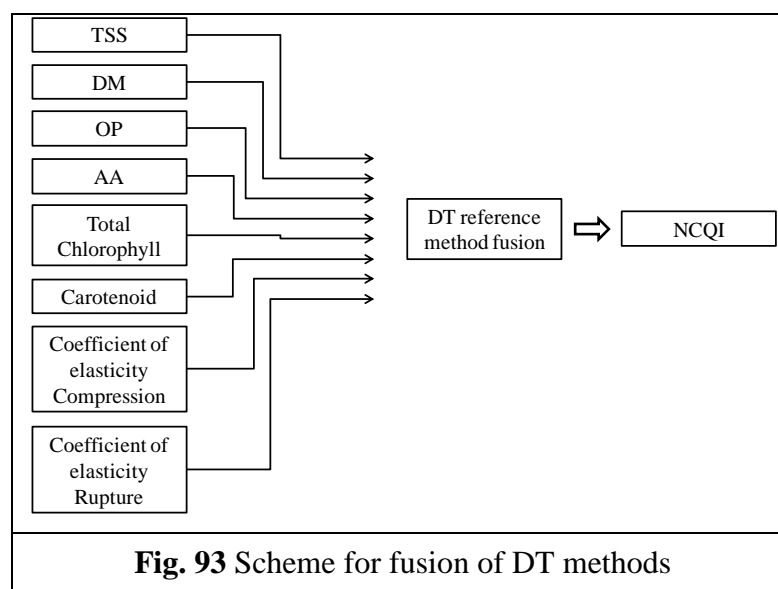
Fig. 93 Scheme for fusion of DT methods

Table 37 Performance measures of linear and non-linear regression models for NCQI, using fused dataset. Models for the three pepper varieties are presented: 'Ever Green', 'No, 117' and 'Celica' and combined cultivar's of data, respectively.

Cultivar	Regression analysis	LV	r^2	RMSEC	RMSECV	RPD	RMSECV /RMSEC	*SWS*
Ever Green	**PLS**	**5**	**0.95**	**0.37**	**0.50**	**2.9**	**1.34**	*0.80*
	PCR	8	0.92	0.61	0.64	2.3	1.05	*0.39*
	Kernel	5	0.91	0.52	0.68	2.2	1.30	*0.29*
	SVM	5	0.95	0.36	0.52	2.8	1.43	*0.71*
No.117	**PLS**	**8**	**0.97**	**0.30**	**0.43**	**3.4**	**1.45**	*0.82*
	PCR	12	0.94	0.51	0.57	2.6	1.11	*0.38*
	Kernel	8	0.94	0.41	0.60	2.5	1.44	*0.31*
	SVM	8	0.96	0.28	0.44	3.3	1.60	*0.73*
Celica	PLS	6	0.97	0.34	0.45	3.2	1.35	*0.53*
	PCR	11	0.95	0.49	0.53	2.8	1.08	*0.32*
	Kernel	6	0.95	0.47	0.51	2.9	1.09	*0.46*
	SVM	**6**	**0.97**	**0.27**	**0.37**	**3.9**	**1.39**	*0.77*
Ever Green & No.117 & Celica	PLS	8	0.95	0.47	0.55	2.7	1.15	*0.86*
	PCR	10	0.89	0.73	0.75	2.0	1.03	*0.28*
	Kernel	8	0.92	0.40	0.66	2.2	1.63	*0.48*
	SVM	**8**	**0.95**	**0.44**	**0.54**	**2.7**	**1.22**	*0.87*

The best models were depicted in figures 94-97 in scatter plots for 'Ever Green', 'No.117' and 'Celica' cultivars and for the combined varieties, respectively.

Based on the models built for the prediction of NCQI, it was found that the NCQI has negative values when the pepper fruit is still under reaching the physiological development stage (below 60th DAA). Below the 60th DAA the pepper fruit did not reach its maximum size and did not accumulate the optimal amount of internal components like: soluble solid, carotenoid or ascorbic acid. Therefore harvest time is not suggested when the NCQI is taking negative value.

Fig 94 Scatter plot of NCQI, as predicted by PLS regression model. The PLS model was built with the fused DT and NDT data and 'Ever Green' cultivar. Data marked by the harvest schedule.

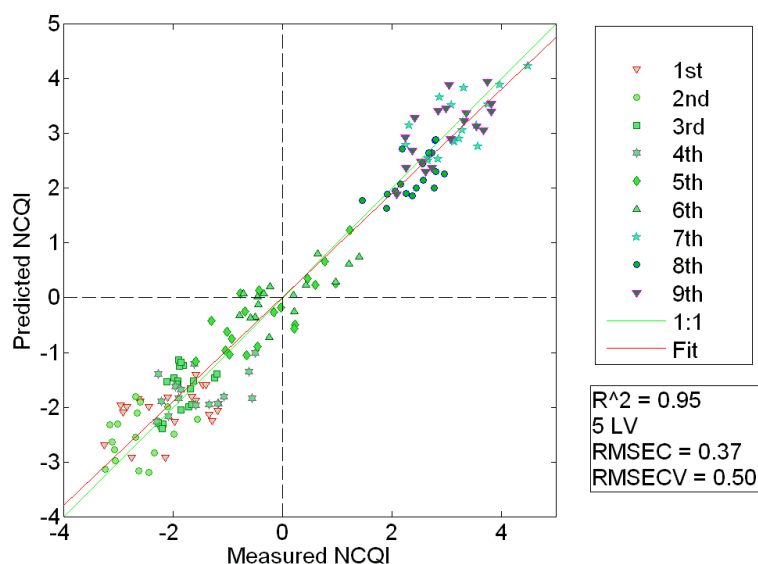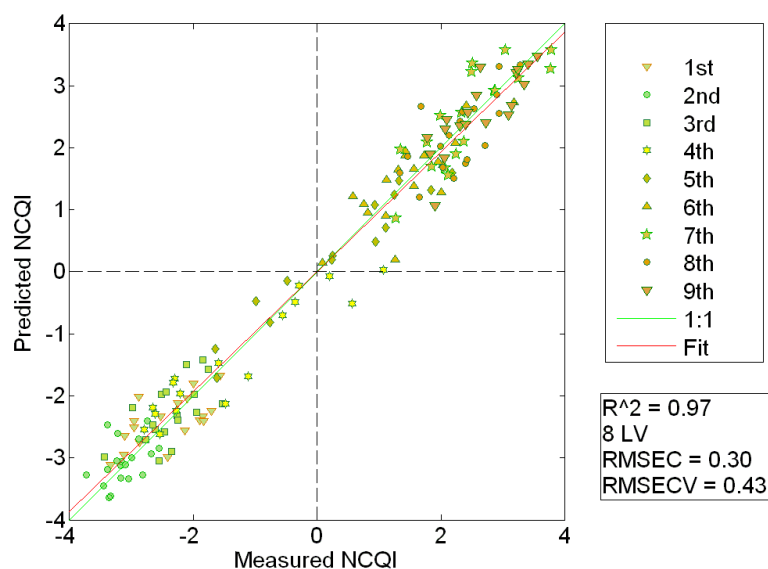
Fig 95 Scatter plot of NCQI, as predicted by PLS regression model. The PLS model was built with the fused DT and NDT data and 'No.117' cultivar. Data marked by the harvest schedule.
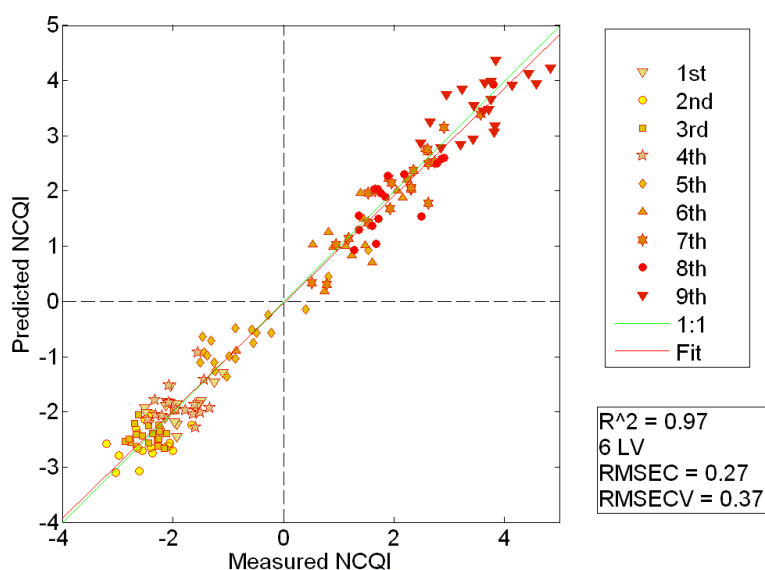

Fig 96 Scatter plot of NCQI, as predicted by SVM regression model. The SVM model was built with the fused DT and NDT data and 'Celica' cultivar. Data marked by the harvest schedule.
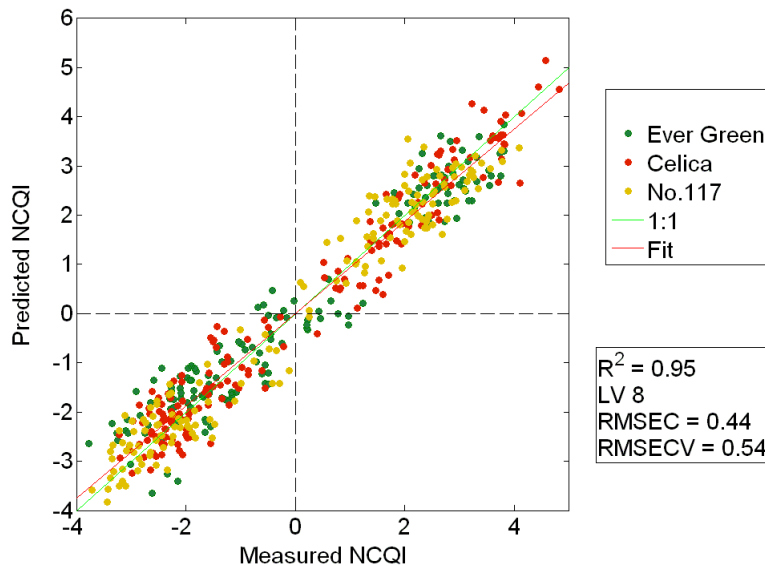
Fig 97 Scatter plot of NCQI, as predicted by SVM regression model. The SVM model was built with the fused DT and NDT data and combination of cultivars. Data marked by the cultivars.

Since the hyperspectral imaging is still considered to be quite expensive measurement method to consider its application for on-line sorting lines, therefore it was desirable to evaluate the fusion models with exclusion of this method. Table 38 presents comparison of the models with and without the hyperspectral imaging data. The models were built only with PLS and SVM regression since these two methods showed the best results for the prediction of NCQI. Based on the SWS scores PLS resulted with slightly better models. By excluding the hyperspectral data the SWS index decreases, but the PLS model is still predicting the NCQI index with a high r^2: 0.94, low RMSECV: 0.58 and low RMSECV/RMSEC: 1.15. PLS prediction and measured NCQI values is shown in the scatter plot on Figs. 98. VIP scores are shown on Fig. 99. The VIP score being above 1 indicates that the particular component significantly participating in the model. List of components can be found in the Appendix 9.2.3. The most significantly participating components are the first LV-s from the osmotic potential (SWIR), carotenoid (SWIR), rupture (SWIR) and compression (VIS-NIR) models, the h, SAM (USB) and quality point (USB) values, and the rate of relaxation.

Table 38 Performance measures of the PLS and SVM models for predicting NCQI, for the combined cultivars by fused NDT with and without the Hyperspectral imaging data.

NCQI	Data	Regression Method	LV	r^2	RMSEC	RMSECV	RPD	RMSECV/ RMSEC	SWS
Ever Green & No.117 & Celica	All NDT	PLS	8	0.94	0.475	0.545	2.7	1.15	0.53
		SVM	8	0.95	0.438	0.536	2.7	1.22	0.41
	NDT without Hyperspectral imaging	PLS	8	0.94	0.505	0.580	2.5	1.15	0.44
		SVM	8	0.94	0.504	0.580	2.5	1.15	0.43

Fig. 98 Scatter plot of NCQI, as predicted by PLS regression model. The PLS model was built with the fused DT and NDT data (without hyperspectral imaging) and combination of cultivars. Data marked by harvest schedule.
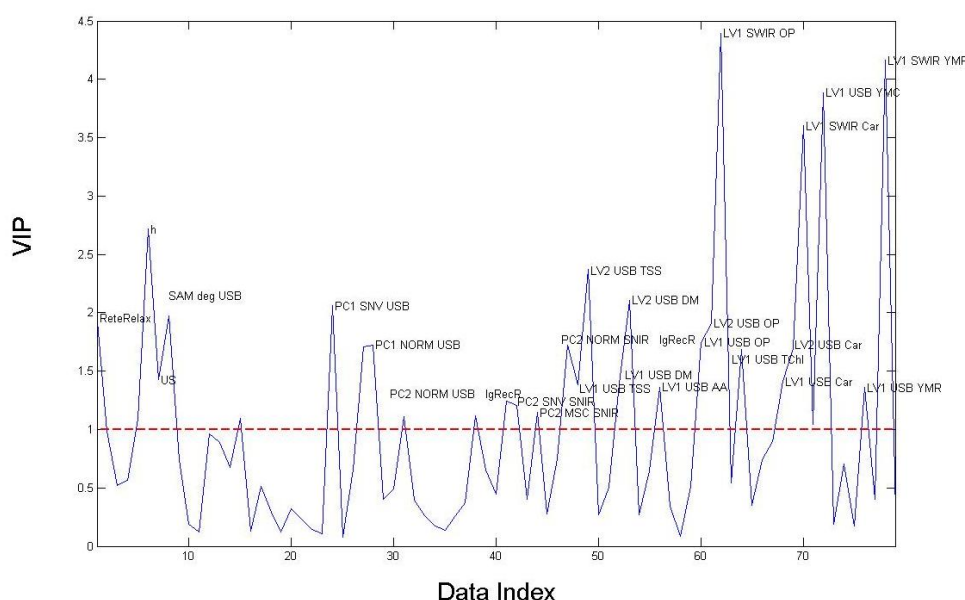
Fig. 98 VIP scores of the model depicted on Fig. 92.

It is generally desired to test the model applicability. Therefore the combined (three cultivars) dataset (540 samples) was divided randomly to a calibration set (300 samples) and a validation dataset (240 samples). PLS and SVM regression models were built and the models were applied on the validation set. The results are shown in Figures 100-101. Both PLS and SVM resulted with efficient models. Based on the calculated SWS indices the PLS model found to be slightly better than the SVM, with SWS values of 0.81 and 0.71, respectively.

Fig. 100 Scatter plot of NCQI, as predicted by PLS regression model. The PLS model was built with the fused DT and NDT data (without hyperspectral imaging) and combination of cultivars. Data marked by sample participation in calibration or validation (test) set.
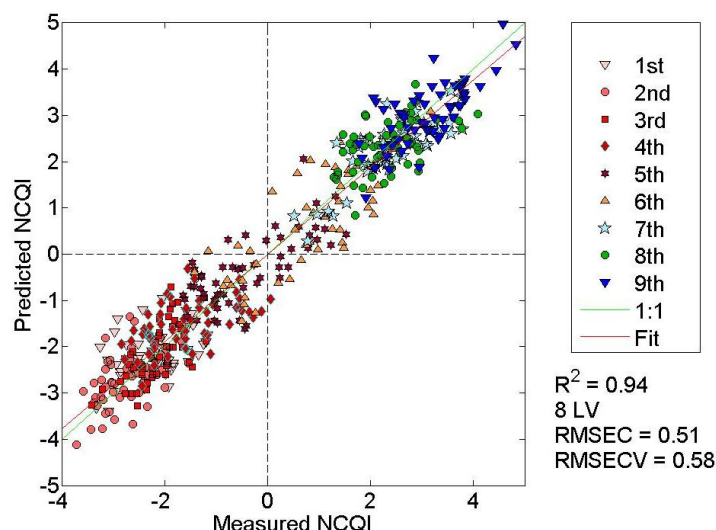

Fig. 101 Scatter plot of NCQI, as predicted by SVM regression model. The SVM model was built with the fused DT and NDT data (without hyperspectral imaging) and combination of cultivars. Data marked by sample participation in calibration or validation (test) set.
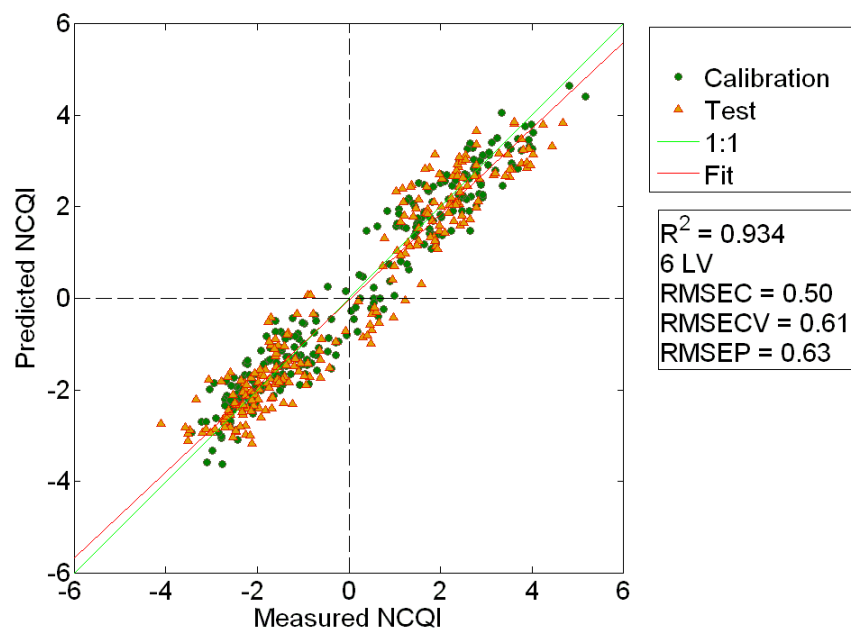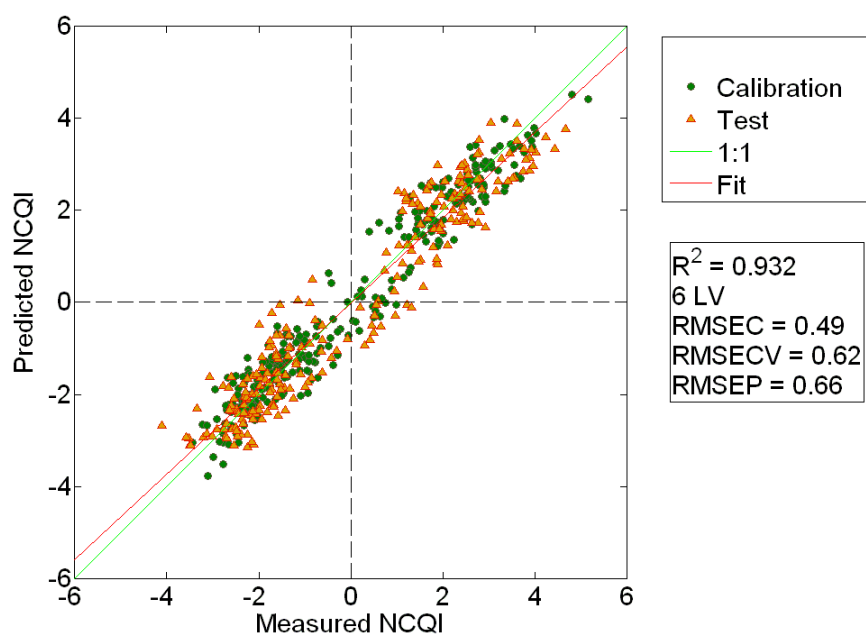
6. THESIS'S AND NEW SCIENTIFIC FINDINGS

During my doctorate research I followed and examined the growth and maturation of three cultivars of different final colour bell peppers: 'Ever Green' (green), 'No.117' (yellow) and 'Celica' (red). The bell pepper plants were grown on soil with drip irrigation in Ein Tamar, Israel in protected greenhouses. Plants were irrigated 3 times a day, with 5 m^3 solution contains 10 l fertilizer (7 % Nitrogen, 3% Phosphorus, and 7% Potassium). The changes occurring during maturation was followed by destructive and non-destructive methods and data were analysed by chemometric procedures.

1. I developed the standardized weighted sum index (SWS) for the evaluation and comparison of regression models. SWS index takes into account several parameters from the regression model, such as the latent variables, the correlation coefficient, the RMSEC, RMSECV, the ratio of RMSECV and RMSEC, and the RPD. Therefore it gives a more general and objective evaluation of the regression model about its goodness or robustness.

2. I established non-destructive measurement method of ascorbic acid, total chlorophyll and carotenoid content in the three measured bell pepper cultivars. I built efficient PLS prediction models by means of spectral measurements of VIS-NIR, SWIR spectral data and hyperspectral imaging for the estimation of ascorbic acid, total chlorophyll, carotenoid content for all three studied bell pepper cultivars. I found that VIS-NIR spectral measurement resulted with the best prediction models for ascorbic acid content, while hyperspectral imaging found to be the most efficient for total chlorophyll and carotenoid content estimation. The best model for vitamin C prediction had r^2: 0.78 and RMSECV: 15.1 mg/100g. The best model for prediction of total chlorophyll had r^2: 0.95 and RMSECV: 0.005 mg/g; for carotenoid content r^2 was 0.97 and RMSECV: 0.008 mg/g.

3. I found that fused non-destructive measurement data (NDT) with chemometric procedures are capable for the prediction of internal components (TSS, DM, OP, vitamin C, chlorophyll, carotenoid) and texture (coefficient of elasticity of compression and rupture) (DT).

   Comparing the single sensor PLS models to the multisensor PLS models the fused NDT data in each DT prediction resulted with higher SWS indices. I found that fused models are predicting the DT parameters with similar or lower number of latent variables; they have generally higher correlation of determination as well as lower RMSECV.

Therefore the fusion of the NDT parameters found to be efficient and beneficial for the prediction of DT quality parameters in the examined three bell pepper cultivars.

I developed linear and non-linear (PLS, PCR, Kernel, SVM) regression models using fused NDT dataset for the prediction of DT parameters. I found that comparing the different chemometric procedures - based on the SWS index - PLS and SVM models were the most suitable to predict DT quality parameters from the fused NDT measurements in the examined three bell pepper cultivars.

4. Prediction model was developed which combines the three bell pepper cultivars. The linear and non-linear (PLS, PCR, Kernel, SVM) prediction models were built with the fused NDT dataset. I found that Kernel and SVM models resulted with the most efficient models. In case of TSS, AA, OP, and coefficient of elasticity of compression SVM regression gave the highest SWS scores (0.67-0.77). Whereas for DM, total chlorophyll, and carotenoid Kernel method resulted with the highest SWS: 0.64-0.74.

5. I developed a new quality index NCQI in order to establish a way to evaluate the global quality of bell pepper. NCQI was created by the fusion of TSS, DM, OP, AA, total chlorophyll, carotenoid content, coefficient of elasticity of compression, and coefficient of elasticity of rupture variables. NCQI is the first principal component of the DT variables.

6. I developed PLS, PCR, Kernel and SVM regression models for the prediction of NCQI by the fused NDT parameter for 'Ever Green', 'No.117','Celica' and for the total data of the three cultivars. Efficient models were achieved with the fused DT and fused NDT models for all three cultivars with high correlation of determination (0.89-0.97). Based on the SWS scores I found PLS and SVM methods to be most suitable to work with the combined dataset and build regression models for the fused DT and NDT parameters.

7. Harvest time is not suggested when the NCQI is taking negative value. Based on the models built for the prediction of NCQI, it was found that the NCQI has negative values when the pepper fruit is still in the physiological development stage (below 60th DAA in the present study). Below the 60th DAA the pepper fruit did not reach its maximum size and did not accumulate the optimal amount of internal components like: soluble solid, carotenoid or ascorbic acid in case of the three examined bell pepper cultivar.

7. RECOMMENDATION FOR FURTHER RESEARCH

Further research work should be considered as a continuation of the present study.

- ❧ For better understanding and evaluation of the physiological changes in the whole pepper fruit during growth and maturation I suggest the in depth examination of the hyperspectral images in the VIS-NIR and SWIR spectral range.
- ❧ I suggest the examinations to be conducted in consecutive seasons with higher number of samples in order to validate the established models; make it applicable without depending on the seasons. Moreover, to examine several cultivars with differing shape, colour and growing condition in order to develop more robust regression models.
- ❧ I suggest examining the behaviour of the NCQI during storage and shelf life of the product. Moreover, to find the NCQI value which can indicate the critical condition of the fruit when it cannot be stored longer without quality degradation.
- ❧ I suggest including the shape and defect monitoring of the agricultural produce to be integrated to the non-destructive measurement methods and to the fusion.
- ❧ I suggest extending the fusion of the NDT and DT parameters for other agricultural products.
- ❧ I suggest to examine different combinations of sensors to be fused in order to find the most efficient and economical solution, which can be efficiently integrated into sorting and classification lines.
- ❧ For the purpose of proper harvest time estimation for farmers I suggest the development of a portable device for field application.

8. SUMMARY

Export and local market both demands high quality sorted fruits and vegetables, which long preserves its fresh condition on the market. Agricultural products' inner content and outer properties continues to change after harvesting, therefore it is crucial to determine the optimal harvest time properly. If the time of the harvest is not properly determined than it might negatively influences the quality of the product. It is important to find solution for growers and packers for rapid, objective and non-destructive evaluation methods for the determination of pepper quality change during growth, maturation and in the process of sorting and classification.

The main objective of the present study is to explore the relationship between several non-destructive testing methods and the state of maturity, inner composition, textural, and physiological parameters (DT parameters). Moreover, to develop a rapid reliable non-destructive cost effective system to measure quality index of bell pepper.

The present study examined the changes in the course of growth and maturation of intact bell pepper fruits. Three different cultivars were examined: 'Ever Green' (green cv.), 'No.117' (yellow cv.) and 'Celica' (red cv.).

During the growth and maturation the following destructive quality parameters were followed: total soluble solid, dry matter, ascorbic acid, osmotic potential, total chlorophyll and carotenoid content, coefficient of elasticity of compression and rupture tests. From the non-destructive methods the following were used to acquire information of the fruit: ultrasonic test, colour measurement, relaxation test, VIS-NIR (477-950 nm) and SWIR (850-1888 nm) spectral measurements and hyperspectral imaging (550-850 nm).

Sigmoid shape trend was found in case of TSS, DM and OP change with the advancement of DAA. The highest TSS, DM and OP contents were achieved by the 'No.117' yellow cultivar at the fully matured stage, whereas 'Ever Green' cultivar accumulated the least of these contents. Whether this observation is related to the final colour of the fruit or not, is a question requires further research.

The ascorbic acid content showed a different trend in the examined period of growth. The ascorbic acid content had increased and reached a maximum at the 67th-74th DAA, than decreased in case of all three cultivars. The highest AA content was reached by the 'Ever Green' variety (74th DAA) while the lowest vitamin C was accumulated by the 'Celica' cultivar at the 67th DAA.

Total chlorophyll content in the 'No.117' and 'Celica' cultivars has a sigmoid decreasing trend and the concentration of total chlorophyll significantly starts to decrease after the 47th DAA and

converges to zero. Meanwhile the total chlorophyll content in 'Ever Green' cultivar decreases to a certain extent but at the fully ripe stage its total chlorophyll content still higher than the 'No.117' and 'Celica' cultivars in their unripe green stage.

The carotenoid content of the 'No.117' and 'Celica' cultivars started to increase after the 60th DAA without stagnation. The same process occurs in case of the 'Ever Green' cultivar alike just with 7 days delay. I found a connection between the drop of total chlorophyll content and increase of carotenoid content in all three cultivars. The highest carotenoid concentration was found in the 'Celica' cv. followed by the 'Ever Green' and least carotenoid was accumulated by the 'No.117' cv..

Standardized weighted sum (SWS) index was developed for evaluation of the regression models. SWS index is complex number which includes the LV, r^2, RMSEC, RMSECV, RMSECV/RMSEC ratio and RPD. Therefore it provides a more complex description of the regression model robustness than the RPD index alone.

Efficient prediction models were built for the estimation of TSS, DM, OP, AA, total chlorophyll, carotenoid content, coefficient of elasticity of compression, and coefficient of elasticity of rupture destructive parameters by the VIS-NIR, SWIR and hyperspectral imaging.

PLS, PCR, Kernel and SVM regressions resulted with efficient prediction models for TSS, DM, OP, AA, total chlorophyll, carotenoid content, coefficient of elasticity of compression, and coefficient of elasticity of rupture by the fused NDT-s. The fused models were found more efficient than the single sensor models. Comparison of the PLS models of the single and multisensory models were based on the SWS index. PLS regression models by the fused NDT parameters achieved significantly lower RMSECV values than the single sensor models in case of each variety and each DT parameters. Based on the SWS index it was concluded that the PLS and the SVM regression models were most suitable to predict DT parameters from the fused NDT parameters.

PLS, PCR, Kernel and SVM regression models were built for the prediction of the DT parameters by the fused NDT parameters for each cultivar separately and as well as for the combination of cultivars. Based on the comparison of the single and the combined cultivar models that the combined variety models have a higher r^2 and lower ratio of RMSECV to RMSEC, which makes these models to be more robust and suggest the possibility that they can be applicable for DT parameter prediction.

PCR regression needed significantly more PC-s to build the models. Moreover, this method generally had higher RMSECV. Therefore based on the results of this study it is not suggested for analysis of combined varieties and fused NDT dataset for bell pepper evaluation. I found the

Kernel and SVM regressions resulted with the most efficient models for the combined cultivars and the fused NDT parameters.

New combined quality index (NCQI) was developed by the fusion of the reference parameters (DT): TSS, DM, OP, AA, total chlorophyll, carotenoid content, and coefficient of elasticity of compression and rupture. NCQI was created in order to establish a way to evaluate the global quality of bell pepper. NCQI is the first principal component of the DT variables.

Prediction models were built for the new combined quality index (NCQI) by the fused NDT parameter for 'Ever Green', 'No.117','Celica' and for the combination of the three cultivars.

Efficient models were achieved with the fused DT and fused NDT models for all three cultivars with high correlation of determination. PLS and SVM method found to be most suitable to work with the combined dataset and build regression models for the fused DT and NDT parameters.

Based on the models built for the prediction of NCQI, it was found that the NCQI has negative values when the pepper fruit is still in the physiological development stage (below 60th DAA in the present study). Below the 60th DAA the pepper fruit did not reach its maximum size and did not accumulate the optimal amount of internal components like: soluble solid, carotenoid or ascorbic acid in case of the three examined bell pepper cultivar. Therefore harvest time is not suggested when the NCQI is taking negative value.

For economical considerations fusion models were evaluated with the exclusion of the hyperspectral imaging on the combined cultivar dataset. By excluding the hyperspectral data SWS index decreased, but the PLS model still predicted the NCQI index with high correlation of determination and low RMSECV. For the evaluation of the applicability of this model the dataset was divided to calibration and validation sets. As a result efficient validation was achieved with high correlation of determination with low RMSEP.

9. Appendixes

9.1. References

1. ABBOTT, J.A. (1999): Quality measurement of fruits and vegetables. *Postharvest Biology and Technology*, (15) 207-225 p.

2. ABBOTT, J.A., LU, R., UPCHURCH, B.L., STROSHINE, R.L. (1997): Technologies for nondestructive quality evaluation of fruits and vegetables. *Hortic. Rev.,* 20, 1-120 p.

3. ALMÁSI, E., DOBRAYNÉ-VARGA, Á. (1977): Hűtőtechnológia II., KÉE-jegyzet, Budapest.

4. AOAC (2000): AOAC Official Method of Analysis, 967.21 Ascorbic Acid in Vitamin Preparations and Juices 2,6-Dichloroindophenol Titrimetric Method 45.1.14 Chapter 45, 16-17 p.

5. ARIANA, D.P., LU, R.F. (2010): Evaluation of internal defect and surface color of whole pickles using hyperspectral imaging. *Journal of Food Engineering*, 96 (4) 583-590 p.

6. BALTAZAR, A., ARANDA, J.I., GONZALEZ-AGUILAR, G. (2008): Bayesian classification of ripening stages of tomato fruit using acoustic impact and colorimeter sensor data. *Computers and electronics in agriculture*, 60, 113-121 p.

7. BARANSKI, R., BARANSKA, M., SCHULZ, H. (2005): Changes in carotenoid content and distribution in living plant tissue can be observed and mapped in situ using NIR-FT-Raman spectroscopy. *Planta,* 222, 448-457 p.

8. BARATA-SOARES, A.D., GOMEZ, M.L.P.A., MESQUITA, C.H. AND LAJOLO, F.M. (2004): Ascorbic acid biosynthesis: a precursor study on plants. *Braz. J. Plant Physiol.,* 16 (3), 147-154 p.

9. BARRY, C.S. (2009): The stay-green revolution: recent progress in deciphering the mechanisms of chlorophyll degradation in higher plants. *Plant Science,* 176 (3), 325–333 p.

10. BJORSVIK, H.R., MARTENS, H. (1992): Data Analysis: Calibration of NIR Instruments by PLS Regression. in: Burns, D.A., Cuirczak, E.W. (Eds.) Handbook of Near-Infrared Analysis (Chapter 7), Practical Spectroscopy Series, Volume 13. Marcel Dekker, New York. 159-180 p.

11. BLANCO, M., COELLOA, J., ITURRIAGAA, H., MASPOCHA S., PEZUELAA, C. (1993): Determination of Ascorbic Acid in Pharmaceutical Preparations by Near Infrared Reflectance Spectroscopy. *Talanta*. 40, 1671-1676 p.

12. BLASCO, J., ALEIXOS, N., MOLTO, E. (2007): Computer vision detection of peel defects in citrus by means of a region oriented segmentation algorithm. *Journal of Food Engineering,* 81(3) 535-543 p.

13. BEN-YEHOSHUA, S., SHAPIRO, B., CHEN, Z.E., LURIE, S. (1983): Mode of action of plastic film in extending life of lemon and bell pepper fruits by alleviation of water stress. *Plant Physiol.,* 73, 87-93 p.

14. BOURNE, M.C. (1982): Food Texture and Viscosity: Concept and Measurement. Academic Press, New York.

15. BREINHOLT, V., SCHIMERLIK, M., DASHWOOD, R., BAILEY, G. (1995): Mechanisms of Chlorophyllin Anticarcinogenesis against Aflatoxin B1: Complex Formation with the Carcinogen. *Chem. Res. Toxicol.,* 8 (4) 506-514 p.

16. BROOKS, R.R., IYENGAR S.S. (1998): Multi-sensor fusion. Prentice Hall. New York, NY.

17. BROWN, G.K., SARIG, Y. JR. (1994): Nondestructive Technologies for Quality Evaluation of Fruits and Vegetables. *Proceedings International Workshop, US-Israel BARD Fund, Spokane, WA, 15–19 June 1993. American Society for Agricultural Engineering, St. Joseph, MI.*

18. CARRINGTON, C.M.S AND PRESSEY, R. (1996): β-galactosidase II activity in relation to changes in cell wall galactosyl composition during tomato ripening, *J Am Hort Sci.* 121, 132-136 p.

19. CHEN, P. (1996): Quality evaluation technology for agricultural products. *Proceedings International Conference Agricultural Machinery Engineering, Seoul, Korea*, 1, 171-204 p.

20. CHENG, X., CHEN, Y.R., TAO, Y., WANG, C.Y., KIM, M.S., LEFCOURT, A.M. (2004): A novel integrated PCA and FLD method on hyperspectral image feature extraction for cucumber chllling damage inspection. *Transactions of the ASAE,* 47(4) 1313-1320 p.

21. CHENG, J., SHEN, H., YANG, X., YU, S., YUAN, L., SUN, Z. AND SUN, X. (2008): Changes in Biochemical Characteristics Related to Firmness During Fruit Development of Pepper (Capsicum annuum L.). *Europ.J.Hort.Sci.,* 73 (4) 155-161 p.

22. CHIVERS, R.C., RUSSELL, H., ANSON, L.W. (1995): Ultrasonic studies of preserved peaches. *Ultrasonics,* 33, 75-77 p.

23. CLARK, C.J., MCGLONE, V.A., JORDAN, R.B. (2003): Detection of Brownheart in ['']Braeburn' apple by transmission NIR spectroscopy. *Postharvest Biology and Technology,* 28 (1) 87-96 p.

24. CLAYTON, M., BIASI, B., MITCHAM, B. (1998): New devices for measuring firmness of cherries. *Perishables Handling Quarterly,* 92, 2-4 p.

25. CRISOSTO, C.H., VALERO, C., SLAUGHTER, D.C. (2007): Predicting pitting damage during processing in Californian clingstone peaches using color and firmness measurements. *Applied Engineering in Agriculture,* 23 (2) 189-194 p.

26. DAVIS, C.B., MARKEY, C.E., BUSCH, M.A., BUSCH, K.W. (2007): Determination of Capsaicinoids in Habanero Peppers by Chemometric Analysis of UV Spectral Data. *J. Agric. Food Chem.,* 55 (15) 5925-5933 p.

27. DEEPA, N., CHARANJIT K., BINOY G., BALRAJ S., KAPOOR, H.C. (2007): Antioxidant constituents in some sweet pepper (Capsicum annuum L.) genotypes during maturity. *LWT Swiss Society of Food Science and Technology*, 40, 121-129 p.

28. DEREJE, A. (2003): Screening Capsicum annuum Germaplasm for Variability in Ascorbic Acid, Total Soluble Solids and Dry Matter Content, Faculty of Agricultural, Food and Environmental Quality Sciences, The Hebrew University of Jerusalem, MSc Thesis

29. DIAZ-PEREZ, J.C., MUY-RANGEL, M.D., MASCORRO, A.G. (2007): Fruit size and stage of ripeness affect postharvest water loss in bell pepper fruit (Capsicum annuum L.). *Journal of the Science of Food and Agriculture,* 87, 68-73 p.

30. DULL, G.G. (1986): Nondestructive evaluation of quality of stored fruits and vegetable. *Food Technology*, 40(5) 106-110 p.

31. DURRANT-WHYTE H. F. (1988): Sensors models and multisensor integration. *The International Journal of Robotics Research,* 7(6) 97-112 p.

32. DUTHIE, G.; CROZIER, A. (2000): Plant-derived phenolic antioxidants. *Curr. Opin. Lipidol.,* 11, 43-47 p.

33. EDAN, Y., PASTERNAK, H., SHMULEVICH, I., RACHMANI, D., GUEDALIA, D., GRINBERG, S., FALLIK, E. (1997): Color and firmness classification of fresh market tomatoes. *Journal of Food Science,* 62 (4) 793-796 p.

34. ELMASRY, G., WANG, N., ELSAYED, A., NGADI, M. (2007): Hyperspectral imaging for non-destructive determination of some quality attributes for strawberry. *Journal of Food Engineering,* 81 (1) 98-107 p.

35. FACELI, K., DE CARVALHO, C.P.L.F., A., REZENDE, S.O. (2004): Combining intelligent techniques for sensor fusion. *Applied Intelligence*, 20, 199-213 p.

36. FAOSTAT (2012) United Nations, Food and Agriculture Organization. *FAOSTAT (05/02/2012)* http://faostat.fao.org

37. FEKETE, A., FELFÖLDI, J. (2000): System for fruit firmness evaluation. *Proc Intnl Conf Agricultural Engineering. Warwick, UK, July 2-7.,* Paper 00-PH-034.

38. FELFÖLDI, J. (1996): Firmness assessment of fruits and vegetables based on acoustic parameters. *J. of Food Physics,* 58, 39-47 p.

39. FELFÖLDI J., T. IGNÁT (1999): Dynamic method for quick and non-destructive measurement of the surface firmness of fruits and vegetables. *Hungarian Agricultural Engineering*, (12) 29-30. p.

40. FEARN, T. (2002): Assessing calibrations: SEP, RPD, RER and R^2. *NIR News,* 13, 12-14 p.

41. FEARN, T., PEREZ-MARIN, D., GARRIDO-VARO, A., & GUERRERO-GINEL, J. (2010): Inverse, classical, empirical and non-parametric calibrations in a Bayesian framework. *Journal of Near Infrared Spectroscopy*, *18*, 27-38 p.

42. FLITSANOV, U., MIZRACH, A., LIBERZON, A., AKERMAN, M., ZAUBERMAN, G. (2000): Measurement of avocado softening at various temperatures using ultrasound. *Postharvest Biol. Technol.*, 20, 279-286 p.

43. FRANK, C.A., NELSON, R.G., SIMONNE, E.H., BEHE, B.K., SIMONNE, A.H. (2001): Consumer Preferences for Color, Price, and Vitamin C Content of Bell Peppers. *HortScience,* 36 (4) 795-800 p.

44. FOX, J.A., DEL POZO-INSFRAN, D., HEE LEE, J., SARGENT, A.S. AND TALCOTT, T. (2005): Ripening Induced Chemical and Antioxidant Changes in Bell Peppers as Affected by Harvest, Maturity and Postharvest Ethylene Exposure. *Hort. Science*, 40(3) 732-736 p.

45. GAETE-GARRETON, L., VARGAS-HERNANDEZ, Y., LEON-VIDAL, C., PETTORINO-BESNIER, A. (2005): A novel noninvasive ultrasonic method to assess avocado ripening. *J. Food Sci.,* 70, E187-E191 p.

46. GARCÍA-RAMOS, F.J., VALERO, C., HOMER, I., ORTIZ-CA˜NAVATE, J., RUIZ-ALTISENT, M. (2005): Non-destructive fruit firmness sensors: a review. *Spanish Journal of Agricultural Research,* 3 (1) 61-73 p.

47. GATZEK, S., WHEELER, G.L., SMIRNOFF, N. (2002): Antisense suppression of L-galactose dehydrogenase in *Arabidopsis thaliana* provides evidence for its role in ascorbate synthesis and reveals light modulated L-galactose synthesis. *Plant J.,* 30, 541-553 p.

48. GELMAN, A., CARLIN, J.B., STERN, H.S., & RUBIN, D.B. (2004): Bayesian Data Analysis, (2nd ed.). Chapman and Hall/CRC, London, UK

49. GERBER, J.M., MOHD-KHIR, I., SPLITTSTOESSER, W.E. (1988): Row Tunnel Effects on Growth, Yield and Fruit Quality of Bell Pepper. *Scientia Horticulturae*, 36, 191-197 p.

50. GOMEZ-LADRON DE GUEVARA, R. AND PARDO-GONZALEZ, J.E. (1996): Evolution of Color during the Ripening of Selected Varieties of Paprika Pepper (Capsicum annuum L.). *J. Agric. Food Chem.*, 44, 2049-2052 p.

51. GOWEN, A.A., O'DONNELL, C.P., CULLEN, P.J., DOWNEY, G., FRIAS, J.M. (2007): Hyperspectral imaging—an emerging process analytical tool for food quality and safety control. *Trends in Food Science & Technology,* 18(12) 590-598 p.

52. GOWEN, A.A., O'DONNELL, C.P., TAGHIZADEH, M., CULLEN, P.J., FRIAS, J.M., DOWNEY, G. (2008): Hyperspectral imaging combined with principal component analysis for bruise damage detection on white mushrooms (Agaricus bisporus). *Journal of Chemometrics,* 22, 259-267 p.

53. GREENSILL, C.V., WOLFS, P.J., SPIEGELMAN, C.H., WALSH, K.B. (2001): Calibration transfer between PDA-based NIR spectrometers in the NIR assessment of melon soluble solids content. *Applied Spectroscopy,* 55 (5) 647-653 p.

54. HARKER, F.R., REDGWELL, R.J., HALLETT, I.C., MURRAY, S.H., CARTER, G. (1997): Texture of fresh fruit. *Hortic. Rev.*, 20, 121-224 p.

55. HALL D.L. (1992) Mathematical techniques in multisensor data fusion. Artech House Inc.

56. HORNERO-MENDEZ, D. AND MINGUEZ-MOSQUERA, M.I. (2000): Xanthophyll Esterification Accompanying Carotenoid Overaccumulation in Chromoplast of Capsicum annuum Ripening Fruits Is a Constitutive Process and Useful for Ripeness Index. *J. Agric. Food Chem.,* 48, 1617-1622 p.

57. HORNERO-MENDEZ, D. AND MINGUEZ-MOSQUERA, M.I. (2002): Chlorophyll disappearance and chlorophyllase activity during ripening of *Capsicum annuum* L fruits. *Journal of the Science of Food and Agriculture*, 82, 1564-1570 p.

58. HOWARD, L. R., TALCOTT, S. T., BRENES, C. H., AND VILLALON, B. (2000): Changes in phytochemical and antioxidant activity of selected pepper cultivars (Capsicum species) as influenced by maturity. *J. Agric. Food Chem.*, 48, 1713-1720 p.

59. HUNG, Y.C., PRUSSIA, S.E., EZEIKE, G.O.I. (1999): Nondestructive firmness sensing using a laser air-puff detector. *Postharvest Biology and Technology,* 16 (1) 15-25 p.

60. IGNÁT T., FELFÖLDI J., GILINGERNÉ P. M. (2003a): Fizikai és beltartalmi jellemzők alkalmazása paprika minőségi becslésére. *MTA Agrár Műszaki Bizottsága, XXVII. Kutatási és Fejlesztési Tanácskozás*, Gödöllő, 61-65 p.

61. IGNAT, T., MIZRACH, A., SCHMILOVITCH, Z., FEFOLDI, J., H. EGOZI, A. HOFFMAN (2010): Bell pepper maturity determination by ultrasonic technique. *Progress in Agricultural Engineering Sciences*, 6, 17-34 p.

62. IGNÁT T., MUHA V., GILINGERNÉ PANKOTAI M. (2003b): Étkezési paprika tárolási kísérletei. *Értékálló Aranykorona* 3(5) 17-18 p.

63. IGNAT T., SCHMILOVITCH, Z., FALIK, E., HOFFMANN, A., EGOZI, H., ALKALAY-TOVIA, S. (2011a): Measuring vitamin C content in pepper by VIS-NIR spectroscopy. *ISAE 2011 annual conference*, Beit Dagan, Israel, 14 . p.

64. IGNAT T., SCHMILOVITCH Z., FEFOLDI J., BERNSTEIN N., STEINER B., EGOZI H., HOFFMAN, A. (2011b): Chlorophyll content measurement in bell pepper by VIS-NIR spectrometry. *AGRI-SENSING International Symposium on Sensing in Agriculture*, Haifa, Israel, Feb. 2011 In: Book of abstract 23 p.

65. IMAHORI, Y., ZHOU, Y.F., UEDA, Y., CHACHIN, K. (1998): Ascorbate metabolism during maturation of sweet pepper (Capsicum annuum L.) fruit. *J. Jap. Soc. Hort. Sci*., 67, 798-804 p.

66. JANSSEN, H., NIEHSEN, W. (2004): Vehicle surround sensing based on information fusion of monocular video and digital map. *Intelligent Vehicles Symposium, 2004 IEEE*, 244-249 p.

67. JARRETT, R.L. (2007) Diversity of Fruit Quality Characteristics in Capsicum frutescens. *Hortscience,* 42(l) 16-19 p.

68. JOHNSTON, J.W., HEWETT, E.W., HERTOG, M. (2002): Postharvest softening of apple (Malus domestica) fruit: a review. *NZ J. Crop Hortic. Sci.,* 30, 145-160 p.

69. KADER, A.A. (1999): Fruit maturity, ripening, and quality relationships. *Acta Hort.,* 485, 203-208 p.

70. KAFFKA, K.J. AND GYARMATI, L.S. (1991): Qualitative (Comparative) analysis by near infrared spectroscopy. Biston, R. & Bartiaux-Thill, N. (Eds.) Proceedings of the Third International Conference on Near Infrared Spectroscopy, Agricultural Research Centre Publishing. Gembloux (Belgium) 135-139 p.

71. KAVDIR, I. AND GUYER, D.E. (2003): Apple Grading Using Fuzzy Logic. *Turk J Agric.,* 27, 375-382 p.

72. KIM, M.S., CHEN, Y.R., MEHL, P.M. (2001): Hyperspectral reflectance and fluorescence imaging system for food quality and safety. *Transactions of the ASAE,* 44 (3) 721-729 p.

73. KNEKT, P.; KUMPULAINEN, K.; JARVINEN, R.; RISSANEN, H.; HELIO-VAARA, M.; REUNANEN, A.; HAKULINEN, T.; AROMAA, A. (2002): Flavonoid intake and risk of chronic disease. *Am. J. Clin. Nutr.,* 76, 560-568 p.

74. KRAUTKRAMER, J., KRAUTKRAMER, H. (1990): Ultrasonic Testing of Materials. Springer-Verlag, Heidelberg, Germany

75. KUTTRUFF, H. (1991): Ultrasonics: Fundamentals and Applications. Elsevier, New York.

76. LAMMERTYN, J., NICOLAI, B., OOMS, K., DE SMEDT, V., DE BAERDEMAEKER, J. (1998): Nondestructive measurement of acidity, soluble solids, and firmness of Jonagold apples using NIR-spectroscopy. *Transactions of the ASAE,* 41(4) 1089-1094 p.

77. LÁNG Z. (1982): Terményvizsgálatok az étkezési paprika gépi betakarításához. *Kertgazdaság*, 14(5) 45-52 p.

78. LEE, K.S., KADER, A.A. (2000): Preharvest and postharvest factors influencing vitamin C content of horticultural crops. *Postharvest Biology and Technology*, 20, 207-220 p.

79. LEE, P.M. (2004) Bayesian Statistics an Introduction. 3rd Edn. Arnold, London, UK

80. LEJA, M., WYZGOLIK, G., KAMINSKA, I. (2008): Changes of some biochemical parameters during the development of sweet pepper fruits. *Scientific Works Of The Lithuanian Institute Of Horticulture And Lithuanian University Of Agriculture,* 27(2) 277-283 p.

81. LI, C., HEINEMANN, P., SHERRY, R. (2007): Neural network and Bayesian network fusion models to fuse electronic nose and surface acoustic wave sensor data for apple defect detection. *Sensors and Actuators B: Chemical*, 125, 301-310 p.

82. LICHTENTHALER, H.K. (1987): Chlorophylls and Carotenoids: Pigments of Photosynthetic Biomembranes. *Methods in Enzymology*, 148, 350-382 p.

83. LLEO, L., BARREIRO, P., RUIZ-ALTISENT, M., HERRERO, A. (2009): Multispectral images of peach related to firmness and maturity at harvest. *Journal of Food Engineering,* 93 (2) 229-235 p.

84. LOEWUS, F.A. (1961): Aspects of Ascorbic Acid Biosynthesis in Plants. *Annals of the New York Academy of Sciences*, 92, 57-78 p.

85. LU, R., CHEN, Y.R. (1999): Hyperspectral imaging for safety inspection of foods and agricultural products. Proc. SPIE 3544, 121, http://dx.doi.org/10.1117/12.335771

86. LU, R., PENG, Y. (2007): Development of a multispectral imaging prototype for real-time detection of apple fruit firmness. *Optical Engineering,* 46, 12 p.

87. LUNING P.A., VRIES R.V., YUKSEI D., EBBERHORST-SELLER T., WICHERS H.J, AND ROOZEN J.P. (1994): Combined instrumental and sensory evaluation of flavor of fresh bell peppers (Capsisum annuum) harvested at three maturation stages. *J. Agric. Food Chem.,* 42, 2885-2861 p.

88. LU, R., TIPPER, N.C. (2009): A portable device for the bioyield detection to measure apple firmness. *Applied Engineering in Agriculture,* 25 (4) 517-523 p.

89. LUO, R.C., CHIN-CHEN, Y., KUO, L.S. (2002): Multisensor fusion and integration: approaches, applications and future research directions. *IEEE Sensors Journal*, 2(2) 107-119 p.

90. MACNISH, A.J., JOYCE, D.C., SHORTER, A.J. (1997): A simple non-destructive method for laboratory evaluation for fruit firmness. *Australian Journal of Experimental Agriculture*, 37 p.

91. MAGNESS, J.R. AND TAYLOR, G.F. (1925): An improved type of pressure tester for the determination of fruit maturity. *USDA Circular,* 350 p.

92. MALCZEWSKI, J. (1999): GIS and Multicriteria decision analysis. ISBN 0-471-32944-4, 182-187 p.

93. MARCELIS, L.F.M, AND BAAN HOFMAN-EIJER, L.R. (1995): Growth analysis of sweet pepper fruits (Capsicum annuum L.). *Acta Horticulturae,* 412, 470-478 p.

94. MARIN, A., FERRERES, F., TOMAS-BARBERAN, F. A., AND GIL, M. I. (2004): Characterization and quantitation of antioxidant constituents of sweet pepper (Capsicum annuum L.). *J. Agric. Food Chem.*, 52:3861-3869 p.

95. MARKUS, F., DAOOD, H.G., KAPITANY, J., AND BIACS, P.A. (1999): Change in the carotenoid and antioxidant content of spice red pepper (paprika) as a function of ripening and some technological factors. *Journal of Agricultural and Food Chemistry*, 47, 100-107 p.

96. MARTÍNEZ S, CURROS A, BERMÚDEZ J, CARBALLO J, FRANCO I. (2007): The composition of Arnoia peppers (Capsicum annuum L.) at different stages of maturity. *Int J Food Sci Nutr.,* 58(2) 150-61 p.

97. MATELJAN, G. (2007): The World's Healthiest Foods: Essential Guide for the Healthiest Way of eating. GMF Publishing, http://www.whfoods.com

98. MEIR, S., ROSENBERGER, I., AHARON, Z., GRINBERG, S., FALLIK, E. (1995): Improvement of the postharvest keeping quality and colour development of bell pepper by packaging with polyethylene bags at a reduced temperature. *Postharvest Biology and Technology,* 5, 303-309 p.

99. MERZLYAK M.N., SOLOVCHENKO A.E., & GITELSON A.A. (2003): Reflectance spectral features and non-destructive estimation of chlorophyll, carotenoid and anthocyanin content in apple fruit. *Postharvest Biol. Technol., 27*, 197-211 p.

100. MINGUEZ-MOSQUERA, M.I. AND HORNERO-MENDEZ, D. (1994): Formation and transformation of pigments during the fruit ripening of Capsicum annuum cv Bola and Agridulce. *J Agric Food Chem.,* 42, 38-44 p.

101. MIZRACH, A., GALILI, N., ROSENHOUSE, G. (1989): Determination of fruit and vegetable properties by ultrasonic excitation. *Trans. ASAE,* 32, 2053-2058 p.

102. MIZRACH, A. (1999): Determination of avocado maturity by ultrasonic attenuation measurements. *Scientia Horticulturae,* 80, 173-180 p.

103. MIZRACH, A. (2000) Determination of avocado and mango fruit properties by ultrasonic technique. *Ultrasonics*, 38, 717-722 p.

104. MIZRACH, A. (2008): Ultrasonic technology for quality evaluation of fresh fruit and vegetables in pre- and postharvest processes. *Postharvest Biology and Technology,* 48, 315-330 p.

105. MIZRACH, A., FLITSANOV, U. (1999): Nondestructive ultrasonic determination of avocado softening process. *J. Food Eng*., 40, 139-144 p.

106. MIZRACH, A., FLITSANOV, U., EL-BATSRI, R., DEGANI, C. (1999a): Determination of avocado maturity by ultrasonic attenuation measurements. *Sci. Hortic*., 80, 173–180 p.

107. MIZRACH, A., FLITSANOV, U., SCHMILOVITCH, Z., FUCHS, Y. (1999b): Determination of mango physiological indices by mechanical wave analysis. *Postharvest Biol. Technol.,* 16, 179-186 p.

108. MIZRACH, A., FLITSANOV, U., AKERMAN, M., ZAUBERMAN, G. (2000): Monitoring avocado softening in low-temperature storage using ultrasonic measurements. *Comput. Electron. Agric.,* 26, 199-207 p.

109. MOHEBBI, M., AMIRYOUSEFI, M.R., HASANPOUR, N., ANSARIFAR, E. (2011): Employing an intelligence model and sensitivity analysis to investigate some physicochemical properties of coated bell pepper during storage. *International Journal of Food Science and Technology,* 47, 299-305 p.

110. NATALE, C.D., ZUDE-SASSE, M., MACAGNANO, A., PAOLESSE, R., HEROLD, B., D'AMICO, A. (2002): Outer product analysis of electronic nose and visible spectra: application to the measurement of peach fruit characteristics. *Analytica Chimica Acta,* 459, 107-117 p.

111. NAVARRO, J.M., FLORES, P., GARRIDO, C., MARTINEZ, V. (2006): Changes in the contents of antioxidant compounds in pepper fruits at different ripening stages, as affected by salinity. *Food Chemistry,* 96, 66-73 p.

112. NICOLAI, B.M., BEULLENS, K., BOBELYN, E., HERTOG, M.L., SCHENK, A., VERMEIR, S., LAMMERTYN, J. (2006): Systems to characterise internal quality of fruit and vegetables. *Acta Horticulturae,* 712, 59-66 p.

113. NICOLAI, B.M., BEULLENS, K., BOBELYN, E., PEIRS, A., SAEYS, W., THERON, K.I., LAMMERTYN, J. (2007): Nondestructive measurement of fruit and vegetable quality by means of NIR spectroscopy: a review. *Postharvest Biology and Technology,* 46, 99-118 p.

114. NIELSON, T.H., SKJAERBAEK H.C., AND KARLSEN P. (1991): Carbohydrate metabolism during fruit development in sweet pepper (Capsicum annuum) plants. *Physiologia Planetarium,* 82, 311-319 p.

115. NIKLISA, N.D., SIOMOSB, A.S., SFAKIOTAKISB, E.M. (2002): Ascorbic Acid, Soluble Solids and Dry Matter Content in Sweet Pepper Fruit: Change During Ripening'. *Journal of Vegetable Crop Production,* 8(1) 41-51 p.

116. NOH, H.K., PENG, Y., LU, R. (2007): Integration of hyperspectral reflectance and fluorescence imaging for assessing apple maturity. *Transactions of the ASAE,* 50 (3) 963-971 p.

117. ORBÁN, CS., FÜSTÖS, ZS., GILINGER PANKOTAI, M. (2011): Changes in the quality of sweet pepper types during the post-harvest ripening. *Journal on Processing and Energy in Agriculture*, 15(2) 109-112 p.

118. ORTIZ, C., BARREIRO, P., CORREA, E., RIQUELME, F., RUIZ-ALTISENT, M. (2001): Non-destructive Identi"cation of Woolly Peaches using Impact Response and Near-Infrared Spectroscopy. *J. Agric. Engng Res.,* 78 (3) 281-289 p.

119. OSUNA-GARCIA, J. A., WALL, M. M., AND WADDELL, C. A. (1998): Endogenous levels of tocopherols and ascorbic acid during fruit ripening of New Mexican-type chile (Capsicum annuum L.). *J. Agric. Food Chem.,* 46, 5093-5096 p.

120. OZER, N., ENGEL, B.A., SIMON, J.E. (1995): Fusion classification techniques for fruit quality. *Transactions of the ASAE*, 38, 1927-1934 p.

121. PARK, T.S., BAE, Y.M., SIM, M.J., KIM, D.E., CHO, S.I. (2008) Analysis of Capsaicinoids from Hot Red Pepper Powder by Near-Infrared Spectroscopy. *American Society of Agricultural and Biological Engineers*

122. PARK, B., WINDHAM, W.R., LAWRENCE, K.C., SMITH, D.P. (2007): Contaminant Classification of Poultry Hyperspectral Imagery using a Spectral Angle Mapper Algorithm. *Biosystems Engineering*, 96 (3) 323-333 p.

123. PENCHAIYA, P., BOBELYN, E., VERLINDEN, B. E., NICOLAI, B. M., SAEYS, W. (2009): Non-destructive measurement of firmness and soluble solids content in bell pepper using NIR spectroscopy. *Journal of Food Engineering,* 94, 267-273 p.

124. PEREZ-LOPEZ, A. J., MOISES DEL AMOR, F., SERRANO-MARTINEZ, A., FORTEA, M. I., AND NUN EZ-DELICADO, E. (2007): Influence of agricultural practices on the quality of sweet pepper fruits as affected by the maturity stage. *Journal of the Science of Food and Agriculture,* 87, 2075-2080 p.

125. PETRÓCZKI K. (2007): Az étkezési paprika sérülésvizsgálata. *MTA, AMB Kutatási és fejlesztési tanácskozás, Gödöllő,* 2, 94-98 p.

126. PIETTA, P. (2000) Flavonoids as antioxidants. *J. Nat. Prod.*, 63, 1035-1042 p.

127. PITRE, G., ETTENBERG, M.H., BRIDGES, A., DAHL, R., CRASE, B. (2010): Future outlook for the photonics industry 2010. Available from:

http://www.depsci.com/Documents/NewsRoom/PHOT-MarketOutlook-SMM.pdf

128. PORTEOUS, R.L., MUIR, A.Y.,WASTIE, R.L. (1981): The idenification of deeases and defect in potato tubers from measurements of spectral reflectance. *J. Agric. Eng. Res.,* 26, 151-160 p.

129. POVEY, M.J.W. (1998): Ultrasonics of food. *Contemp. Phys.*, 39, 467-478 p.

130. POVEY, M.J.W., WILKINSON, J.M. (1980): Application of ultrasonic pulse-echo techniques to egg-albumin quality testing—a preliminary report. *Br. Poult. Sci.,* 21, 489-495 p.

131. RAFFO, A., BAIAMONTE, I., NARDO, N., PAOLETTI, F. (2007): Internal quality and antioxidants content of cold-stored red sweet peppers as affected by polyethylene bag packaging and hot water treatment. *European Food Research and Technology,* 225, 395-405 p.

132. RITOTA, M., MARINI, F., SEQUI, P., VALENTINI, M. (2010): Metabolomic Characterization of Italian Sweet Pepper (Capsicum annum L.) by Means of HRMAS-NMR Spectroscopy and Multivariate Analysis. *J. Agric. Food Chem.,* 58 (17), 9675-9684 p.

133. ROGER, J.M., CHAUCHARD, F., BELLON-MAUREL, V. (2003): EPO-PLS external parameter orthogonalisation of PLS application to temperature-independent measurement of sugar content of intact fruits. *Chemometrics and Intelligent Laboratory Systems,* 66 (2) 191-204 p.

134. ROURA, S.I., MOREIRA, M.R., CRAPISTE, G.H., DEL VALLE, C.E. (2001): Biochemical characterization of two pepper varieties in the green and red ripening stages. *Italian Journal of Food Science*, 13, 391-397 p.

135. RUIZ-ALTISENT, M., RUIZ-GARCIAA, L., MOREDAA, G.P., LUB, R., HERNANDEZ-SANCHEZA, N., CORREAA, E.C., DIEZMAA, B., NICOLAIC, B., GARCÍA-RAMOS, J.

(2010): Sensors for product characterization and quality of specialty crops—A review. *Computers and Electronics in Agriculture,* 74, 176-194 p.

136. RUSSO, W.M., HOWARD, L.R. (2002): Carotenoids in pungent and non-pungent peppers at various developmental stages grown in the field and glasshouse. *Journal of the Science of Food and Agriculture,* 82, 615-624 p.

137. RUSSO V.M. AND BILES, C.L. (2003): Fertilizer rate and β-galactosidase and peroxidase activity in pepper fruit at different stages and years of harvest. *Plant Foods for Human Nutrition,* 58, 1-11 p.

138. SAATY, T.L. (1980): The analytic hierarchy process: Planning, priority setting, resource allocation. McGraw-Hill International Book Co. (New York and London), Book (ISBN 0070543712)

139. SAITO, Y., HATANAKA, T., UOSAKI, K., SHIGETO, K. (2003): Eggplant classification using artificial neural network, Neural Networks. *Proceedings of the International Joint Conference,* 2, 1013-1018 p.

140. SAKALDAS, M. AND KAYNAS, K. (2010): Biochemical and quality parameters changes of green sweet bell peppers as affected by different postharvest treatments. *African Journal of Biotechnology,* 9(48) 8174-8181 p.

141. SALUNKHE, D.K. (1976): Storage, processing, and nutritional quality of fruits and vegetables, Cleveland. Ohio, USA; CRC Press, Inc.

142. SCHMILOVITCH Z., HOFFMAN, A., EGOZI, H., EL-BATZRI, R., DEGANI, C. (2001): Determination of Avocado Maturity by Near-Infrared Spectrometry. *ISHS Acta Horticulturae,* 562, 175-180 p.

143. SCHMILOVITCH, Z., MIZRACH, A., HOFFMAN, A., EGOZI H., FUCHS, Y. (2000): Determination of Mango Physiological Indices by Near-Infrared Spectrometry. *J. Postharv. Biol. Technol.,* 19, 245-252 p.

144. SCHNITZLER, W.H., AND GRUDA, N. (2002): Hydroponics and product quality. In: Hydroponic Production of Vegetables and Ornamentals. 373–411 p. Savvas, D., and Passam, H. C., Eds., Embryo Publications-Athens.

145. SCHREINER, M., HUYSKENS-KEIL, S., KRUMBEIN, A., SCHONHOF, I., AND LINKE, M. (2000): Environmental effects on product quality. In: Fruit and Vegetable Quality. 85–95 p. Shewfelt, R. L., and Bruckner, B., Eds., Technomic Publishing Co., Inc., Lancester-Basel.

146. SCHULZ, H., BARANSKA, M., BARANSKI, R. (2005): Potential of NIR-FT-Raman spectroscopy in natural carotenoid analysis. *Biopolymers,* 77(4) 212-221 p.

147. SELF, G.K., ORDOZGOITI, E., POVEY, M.J.W., WAINWRIGHT, H. (1994): Ultrasonic evaluation of ripening avocado flesh. *Postharvest Biol. Technol*. 4, 111 p.

148. SERRANO, M., ZAPATA, P.J., CASTILLO, S., GUILLÉN, F., MARTÍNEZ-ROMERO, D., VALERO, D. (2010): Antioxidant and nutritive constituents during sweet pepper development and ripening are enhanced by nitrophenolate treatments. *Food Chemistry,* 118, 497-503 p.

149. SHENK, J.S., WORKMAN, J.J., WESTERHAUS, M.O. (1992): Application of NIR Spectroscopy to Agricultural Products. in: Burns, D.A., Cuirczak, E.W. (Eds.) Handbook of Near-Infrared Analysis (Chapter 15), Practical Spectroscopy Series, Volume 13. Marcel Dekker, New York. 333-431 p.

150. SHEPPARD, N., WILLIS, H.A., RIGG, J.C. (1987): Names, symbols, definitions and units of quantities in optical spectroscopy. *Spectrochimica Acta Part A: Molecular Spectroscopy,* 43(1) 1-9 p.

151. SIMONNE, A.H., SIMONNE, E.H., EITENMILLER, R.R., MILLS, H.A., GREEN, N. R. (1997): Ascorbic Acid and Provitamin A Contents in Unusually Colored Bell Peppers (Capsicum annuum L.). *Journal of Food Composition and Analysis,* 10, 299-311 p.

152. SIMONICHA, M.T., MCQUISTANA, T., JUBERTA, C., PEREIRAC, C., HENDRICKSB, J.D., SCHIMERLIKD, M., ZHUE, B., DASHWOODA, R.H., WILLIAMSA, D.E., BAILEY, G.S. (2008): Low-dose dietary chlorophyll inhibits multi-organ carcinogenesis in the rainbow trout. *Food and Chemical Toxicology,* 46(3) 1014-1024 p.

153. STEINMETZ, V., BIAVATI, E., MOLTO, E., PONS, R., FORNES, I. (1997): Predicting the maturity of oranges with non-destructive sensors. *Actae Horticulturae*, 421, 271-278 p.

154. STEINMETZ, V., CROCHON, M., TALOU, T., BOURROUNET, B. (1995): Sensor fusion for fruit quality assessment: application to melon. *Proceedings of the International Conference ASAE &Harvest and Post-harvest Technologies for Fresh fruits and Vegetables Mexico*, 488-496 p.

155. STEINMETZ, V., CROCHON, M., BELLON-MAUREL, V., GARCIA-FERNANDEZ, J.L., BARREIRO-ELORZA, P., VERSTREKEN, L. (1996): Sensors for fruit firmness assessment: Comparision and fusion. *Journal of Agricultural Engineering Research*, 64 (1) 15-27 p.

156. STEINMETZ, V., ROGER, J.M., MOLTO, E., BLASCO, J. (1999a): On-line Fusion of Colour Camera and Spectrophotometer for Sugar Content Prediction of Apples, *J. Agric. Engng Res.* 73, 207-216 p.

157. STEINMETZ, V., SEVILA, F., BELLON-MAUREL, V. (1999b): A Methodology for Sensor Fusion Design: Application to Fruit Quality Assessment, *J. agric. Engng Res*. 74, 21-31 p.

158. TADESSE, T., HEWETT, E.W., NOCHOLS, M.A., FISHER, K.J. (2002): Changes in physicochemical attributes of sweet pepper cv. Domino during fruit growth and development, *Scientia Horticulturae* (93) 91-103 p.

159. TAGHIZADEH, M., GOWEN, A., WARD, P., O'DONNELL, C.P. (2010): Use of hyperspectral imaging for evaluation of the shelf-life of fresh white button mushrooms (Agaricus bisporus) stored in different packaging films. *Innovative Food Science & Emerging Technologies* 11 (3), 423–431 p.

160. TERPSTRA, W., LAMBERS, J.W.J. (1983): Interactions between chlorophyllase, chlorophyll a, plant lipids and Mg^{2+}, *Biochim Biophys Acta*, 746, 23–31 p.

161. THIMANN, K.V. (1987): Plant senescence: A proposed integration of the constituent process. In: Thomson WW, Nothnagel EA, Huffaker RC (eds), Plant Senescence: Its Biochemistry and Physiology. Riverside Calif.: *Amer Soc Plant Physiologists*, 1-30 p.

162. TOMPOS, D., ISTELLA, S., IGNÁT, T. (2003): Assessment of fruit firmness of pepper using non-destructive physical measurements, in response to different growing and pruning technologies. *International Journal of Horticultural Science*, 9(1) 71-76 p.

163. TSOU, S.C.S., TUNG-LIANG HONG, BERKE, T. (1997): Use of near infra-red reflectance to measure capsaicinoids in pepper (Capsicum spp.), *Capsicum and Eggplant Newsletter* 16, 56–59 p.

164. VARSHNEY, P.K. (1997): Multisensor data fusion, *Electronics & Communication Engineering Journal,* 9(6), 245-253 p.

165. VERLINDEN, B.E., DE SMEDT, V., NICOLAI, B.M. (2004) Evaluation of ultrasonic wave propagation to measure chilling injury in tomatoes. *Postharvest Biol. Technol*. 32, 109–113 p.

166. VICENTINI, F., HORTENSTEINER, S., SCHELLENBERG, M., THOMAS, H., MATILE, P. (1995): Chlorophyll breakdown in senescent leaves: identification of the biochemical lesion on a stay-green genotype of Festuca pratensis Huds, *New Phytol*., 111, 3–8 p.

167. WANG, X., XUE, L., HE, X., LIU, M. (2011): Vitamin C content estimation of chilies using Vis/NIR spectroscopy, Electric Information and Control Engineering (ICEICE), 2011 International Conference, 1894-1897

168. WHEELER, G.L., JONES, M.A., SMIRNOFF, N. (1998): The biosynthetic pathway of vitamin C in higher plants, Nature 393, 365-369

169. WHITE, P.J. (2002): Recent advances in fruit development and ripening: an overview, J. Exp. Bot. 53, 1995–2000

170. WILLIAMS, P.C. (2001): Near-Infrared Technology in the Agricultural and Food Industries. in: P.C. Williams, K.H. Norris (Eds.), Implementation of Near-infrared Technology. American Association of Cereal Chemist, St.Paul, MN, USA, 145-169 p.

171. WILLIAMS, P.C., NORRIS, K.H. (2002): Near-Infrared Technology in the Agricultural and Food Industries, American Association of Cereal Chemists, St. Paul, MN, USA.

172. XUDONG, S., HAILIANG, Z., YANDE, L. (2009): Nondestructive Assessment of Quality of Nanfeng Mandarin Fruit by a Portable Near Infrared Spectroscopy, Int. J. Agric. Biol. Eng. 2, 65-71

173. ZUDE M. (2003): Comparison of indices and multivariate models to non-destructively predict the fruit chlorophyll by means of visible spectrometry in apples. *Anal. Chim. Acta, 481*, 119-126

174. ZUDE, M., HEROLD, B., ROGER, J.M., BELLON-MAUREL, V., LANDAHL, S. (2006): Non-destructive tests on the prediction of apple fruit flesh firmness and soluble solids content on tree and in shelf life, Journal of Food Engineering 77, 254–260

175. ZSOM-MUHA, V. (2008): Dinamikus módszerek kertészeti terménzek jellemzésére, Budapesti Corvinus Egyetem Élelmiszertudományi Kar Fizika-Automatika Tanszék, PhD Thesis

176. ZSOM, T., ZSOM-MUHA, V., BARANYAI, L., HERPPICH, W.B., FELFÖLDI, J., BALLA, CS. (2008): Non-Destructive Determination of Post-Harvest Ripening of Capsicum annuum 'Kárpia', Proc. IIIrd IC Postharvest Unlimited, Acta Hort. 858

9.2. Appendix

9.2.1. Preliminary experiment

The preliminary experiments were carried out during March-May 2009 on fruits taken from 2 greenhouses of 'Vergasa' (red) and 'Ever Green' (green) cultivars. Fruits were picked seven times in succession in the course of the growing period, from the sixth week after flowering until full ripening. Each picked batch contained 50 fruits. Shortly after picking, each fruit was weighed and its colour was measured by colorimeter. At this point, 25 fruits were subjected to NDT testing followed by the reference measurements. The remaining 25 fruits were stored at 7 ºC and 80% humidity for 14 days, and then moved to shelf-life conditions (20 ºC, 50-60% humidity) for 3 days. After that, the fruits were examined in the same manner as described above. On each fruit, one surface was chosen where the batteries of tests were carried out.
NDT tests:

- VIS-NIR spectrometry (same as chapter 4.2.2.)
- SWIR spectrometry (same as chapter 4.2.2.)
- Hyperspectral imaging (same as chapter 4.2.3. except that the hyperspectral images were taken from several fruits in the same time)
- ultrasound attenuation (same as chapter 4.2.4.)
- acoustic response (according to Felföldi, 1996)
- colorimetry (same as chapter 4.2.1.)
- relaxation test: based on the modeling of pressure gage (Ben-Yehoshua et al., 1983), same as chapter 4.2.5.

DT reference tests

- pressure gage on whole fruit: according to Ben-Yehoshua et al. (1983)
- puncture test on pepper disk (same as chapter 4.3.1.)
- compression of pepper disk (same as chapter 4.3.2.)
- total soluble solids (same as chapter 4.3.4.)
- dry weight (same as chapter 4.3.3.)
- ascorbic acid (same as chapter 4.3.5.).

Results from the NDT and DT tests were analyzed by chemometric procedures: partial least squares regression (PLSR), PCR software was used for model development. Evaluating the spectral data; comparisons were made among the PLS regression analysis of the reflectance spectra (R), and the pre-processed spectra's such as the first derivative of R (D_1R), log (1/R), D_1log(1/R) and D_2log(1/R). Correlation tests were carried out by SAS software using Spearman Correlation procedure.
Part of the results were presented at the International Conferences in Agricultural Engineering, Synergy and Technical Development 2009, Gödöllő (Ignat et al., 2009).

Results related to the relaxation tests:

Based on the strong relationship between the results of the pressure gage and the result of the relaxation test (r^2:0.92 for 'Ever Green' and r^2:0.91 for Vergasa' cultivars) in the second series of experiments in 2009 winter season only the relaxation test was performed.
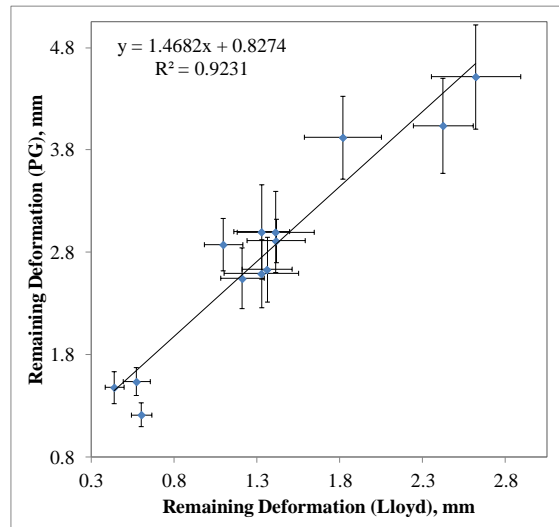
Fig. 92 Remaining deformation (Lloyd) from relaxation test vs. Remaining deformation (PG) from pressure gage test for 'Ever Green' cultivar
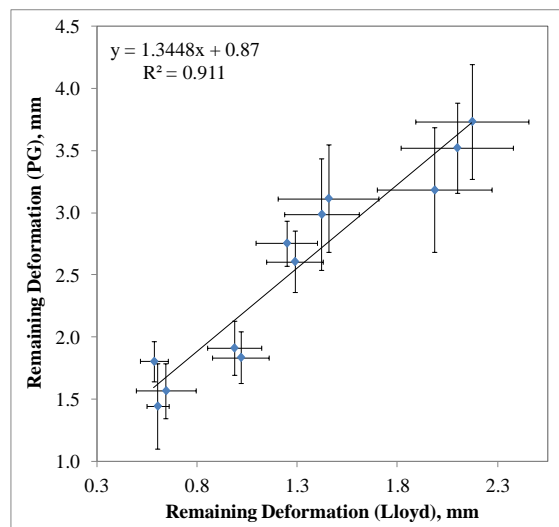
Fig. 93 Remaining deformation (Lloyd) from relaxation test vs. Remaining deformation (PG) from pressure gage test for 'Vergasa' cultivar

9.2.2. Pairwise Comaprison Method

The pairwise comparison method was developed by Saaty (1980). This method involves pairwise comparisons to create a ratio matrix. It takes as an input the pairwise comparisons and produces the relative weights as output. Specifically, the weights are determined by normalizing the eigenvector associated with the maximum eigenvalue of the (reciprocal) ratio matrix.

Comparison of models based on the r^2, LV, RMSEC, RMSECV, RMSECV/RMSEC and RPD. It requires assessing the relative importance of the six criteria. This can be done by the pairwise

comparison method. The procedure consists of three major steps: generation of the pairwise comparison matrix, the criterion weights computation, and the consistency ratio estimation.

a. *Development of the pairwise comparison matrix.* The method employs an underlying scale with values from 1 to 9 to rate the relative preferences for two criteria (Table 1).

Table 1 Scale of pairwise comparison

Intensity of importance	Definition
1	Equal importance
2	Equal to moderate importance
3	Moderate importance
4	Moderate to strong importance
5	Strong importance
6	Strong to very strong importance
7	Very strong importance
8	Very strong to extremely strong importance
9	Extreme importance

First step: the specialist (expert in chemometric procedures) sorts the criterions based on their importance by his/her opinion. Secondly as an example, suppose that the RMSECV is moderately to strongly preferred over the r^2 attribute. This is a numerical score of 4. Further, suppose that the RMSECV/RMSEC is strongly preferred to RPD. This is a numerical score of 5. All these scores are placed in the upper right corner of the pairwise comparison matrix (Table 2).

Table 2 Pairwise comparison of the evaluation criteria

Criterion	RMSECV	RMSECV/ RMSEC	LV	r^2	RPD	RMSEC
RMSECV	1	2	3	4	5	6
RMSECV/RMSEC	1/2	1	3	4	5	6
LV	1/3	1/3	1	3	4	5
r^2	1/4	1/4	1/3	1	4	5
RPD	1/5	1/5	1/4	1/4	1	4
RMSEC	1/6	1/6	1/5	1/5	1/4	1

From these information the remaining of the matrix can be determined. First we make the assumption that the comparison matrix is reciprocal; that is, if criterion *A* is twice as preferred to criterion *B*, we can conclude that criterion *B* is preferred only one-half as much as criterion *A*. Thus, if criterion *A* receives a score of 2 relative to criterion *B*, criterion *B* should receive a score of ½ when compared to criterion *A*. The same logic can be used to complete the lower left side of the matrix. Remains to enter shores to the diagonal from the left upper corner to the right lower corner. Observation is made that when comparing anything to itself, the evaluation scale must be 1, representing equally preferred criteria. Thus, 1s can be placed in the main diagonal of the matrix.

b. *Computation of the criterion weights.* Sum the values in each column of the pairwise comparison matrix. Then, divide each element in the matrix by its column total (the resulting matrix is referred to as the normalized pairwise comparison matrix). Finally compute the average of the elements in each row of the normalized matrix. These averages provide an estimate of the

relative weights of the criteria being compared (Table 3). Using this method, the weights are interpreted as the average of all possible ways of comparing the criteria.

Table 3 Determining the relative criteria weights

Criterion	RMSECV	RMSECV /RMSEC	LV	r^2	RPD	RMSEC
RMSECV	1	2	3	4	5	6
RMSECV/RMSEC	1/2	1	3	4	5	6
LV	1/3	1/3	1	3	4	5
r^2	1/4	1/4	1/3	1	4	5
RPD	1/5	1/5	1/4	1/4	1	4
RMSEC	1/6	1/6	1/5	1/5	1/4	1
SUM	**2.45**	**3.95**	**7.78**	**12.45**	**19.25**	**27**

Criterion	RMSECV	RMSECV/ RMSEC	LV	r^2	RPD	RMSEC	**Weight**
RMSECV	0.41	0.51	0.39	0.32	0.26	0.22	**0.35**
RMSECV/RMSEC	0.20	0.25	0.39	0.32	0.26	0.22	**0.27**
LV	0.14	0.08	0.13	0.24	0.21	0.19	**0.16**
r^2	0.10	0.06	0.04	0.08	0.21	0.19	**0.11**
RPD	0.08	0.05	0.03	0.02	0.05	0.15	**0.06**
RMSEC	0.07	0.04	0.03	0.02	0.01	0.04	**0.03**
SUM	1	1	1	1	1	1	**1**

c.   *Estimation of the consistency ratio.* It means to determine whether the comparisons are consistent or not. First determine the weighted sum vector by multiplying the weight for the first criterion times the first column of the original pairwise comparison matrix, then multiply the second weight times the second column of the original pairwise matrix, finally, sum these values over the rows. After that determine the consistency vector by dividing the weighted sum vector by the criterion weights determined previously (Table 4).

Table 4 Determining the consistency ratio.

Criterion	RMSECV	RMSECV/ RMSEC	LV	r^2	RPD	RMSEC	**Sum**	**Consistency vector: Row Sum/ Weight**
RMSECV	(0.35)(1)	(0.7)(2)	(1.05)(3)	(1.4)(4)	(1.75)(5)	(2.1)(6)	**7.36**	**7.36/0.35=6.75**
RMSECV/ RMSEC	(0.14)(0.5)	(0.27)(1)	(0.82)(3)	(1.1)(4)	(1.37)(5)	(1.65)(6)	**5.35**	**5.35/0.27=6.99**
LV	(0.05)(0.33)	(0.05)(0.33)	(0.16)(1)	(0.49)(3)	(0.66)(4)	(0.82)(5)	**2.24**	**2.24/0.16=6.94**
r^2	(0.03)(0.25)	(0.03)(0.25)	(0.04)(0.3)	(0.11)(1)	(0.45)(4)	(0.57)(5)	**1.23**	**1.23/0.11=6.6**
RPD	(0.01)(0.2)	(0.01)(0.2)	(0.02)(0.25)	(0.02)(0.25)	(0.06)(1)	(0.26)(4)	**0.38**	**0.38/0.06=6.13**
RMSEC	(0.01)(0.17)	(0.01)(0.17)	(0.01)(0.2)	(0.01)(0.2)	(0.01)(0.25)	(0.03)(1)	**0.067**	**0.067/0.03=6.22**

Determination of lambda (λ): The average value of the consistency vector.
$\lambda=(6.75+6.99+6.94+6.6+6.13+6.22)/6=6.61$

Determination of consistency index (CI): The calculation of CI is based on the observation that λ is always greater than or equal to the number of criteria under consideration (n) for positive, reciprocal matrixes, and $\lambda=n$ if the pairwise comparison matrix is a consistent matrix. Accordingly, λ-n can be considered as a measure of the degree of inconsistency. This measure can be normalized as follows:

$CI=(\lambda-n)/(n-1)$
$CI=(6.61-6)/(6-1)=0.121$

The CI term, referred to as the *consistency index,* provides a measure of departure from consistency. Further, the *consistency ratio* (CR) can be calculated, as follows:

$CR=CI/RI$
where, RI is the random index, the consistency index of the randomly generated pairwise comparison matrix. It can be shown that RI depends on the number of elements being compared. The CR is design in such a way that if CR<=0.1, the ratio indicates a reasonable level of consistency in the pairwise comparisons; if, however, CR>=0.1, the values of the ratio are indicative of inconsistent judgments. In such case one should reconsider and revise the original values in the pairwise comparison matrix.
$CR=0.121/1.24=0.098$
Since 0.098<0.1, the ratio indicates a reasonable level of consistency in the pairwise comparison.

9.2.3. List of fused NDT variables

Number	Parameter	Number	Parameter
1	Rate of Relaxation	58	PC2 MSC SNIR log(1/R)
2	Remaining Deformation	59	PC2 NORM SNIR R
3	Coefficient of elasticity of Relaxation	60	PC2 NORM SNIR log(1/R)
4	L	61	PC2 SNV Hyper R
5	C	62	PC2 SNV Hyper log(1/R)
6	h	63	PC2 MSC Hyper R
7	Ultrasonic attenuation	64	PC2 MSC Hyper log(1/R)
8	SAM degree Hyperspectral imaging	65	PC2 NORM Hyper R
9	SAM degree USB R	66	PC2 NORM Hyper log(1/R)
10	SAM degree USB log(1/R)	67	LV1 USB TSS
11	SAM degree SNIR R	68	LV2 USB TSS
12	SAM degree SNIR log(1/R)	69	LV1Hyper TSS
13	Dabs SNV USB R	70	LV2Hyper TS
14	Dabs SNV USB log(1/R)	71	LV1 SWIR TSS
15	Dabs MSC USB R	72	LV2 SWIR TSS
16	Dabs MSC USB log(1/R)	73	LV1 USBDM
17	Dabs NORM USB R	74	LV2 USBDM
18	Dabs NORM USB log(1/R)	75	LV1 Hyper DM
19	Dabs SNV SNIR R	76	LV2 Hyper DM
20	Dabs SNV SNIR log(1/R)	77	LV1 SWIR DM
21	Dabs MSC SNIR R	78	LV2 SWIR DM
22	Dabs MSC SNIR log(1/R)	79	LV1 USB AA
23	Dabs NORM SNIR R	80	LV2 USB AA
24	Dabs NORM SNIR log(1/R)	81	LV1 Hyper AA
25	Dabs SNV Hyper R	82	LV2 Hyper AA
26	Dabs SNV Hyper log(1/R)	83	LV1 SWIR AA
27	Dabs MSC Hyper R	84	LV2 SWIR AA
28	Dabs MSC Hyper log(1/R)	85	LV1 USB OP
29	Dabs NORM Hyper R	86	LV2 USB OP
30	Dabs NORM Hyper log(1/R)	87	LV1 Hyper OP
31	PC1 SNV USB R	88	LV2 Hyper OP
32	PC1 SNV USB log(1/R)	89	LV1 SWIR OP
33	PC1 MSC USB R	90	LV2 SWIR OP
34	PC1 MSC USB log(1/R)	91	LV1 USB Total Chlorophyll
35	PC1 NORM USB R	92	LV2 USB Total Chlorophyll
36	PC1 NORM USB log(1/R)	93	LV1 Hyper Total Chlorophyll
37	PC1 SNV SNIR R	94	LV2 Hyper Total Chlorophyll
38	PC1 SNV SNIR log(1/R)	95	LV1 SWIR Total Chlorophyll
39	PC1 MSC SNIR R	96	LV2 SWIR Total Chlorophyll
40	PC1 MSC SNIR log(1/R)	97	LV1 USB Carotenoid
41	PC1 NORM SNIR R	98	LV2 USB Carotenoid
42	PC1 NORM SNIR log(1/R)	99	LV1 Hyper Carotenoid
43	PC1 SNV Hyper R	100	LV2 Hyper Carotenoid
44	PC1 SNV Hyper log(1/R)	101	LV1 SWIR Carotenoid
45	PC1 MSC Hyper R	102	LV2 SWIR Carotenoid
46	PC1 MSC Hyper log(1/R)	103	LV1 USB Coefficient of elasticity of Compression
47	PC1 NORM Hyper R	104	LV2 USB Coefficient of elasticity of Compression
48	PC1 NORM Hyper log(1/R)	105	LV1 Hyper Coefficient of elasticity of Compression
49	PC2 SNV USB R	106	LV2 Hyper Coefficient of elasticity of Compression
50	PC2 SNV USB log(1/R)	107	LV1 SWIR Coefficient of elasticity of Compression
51	PC2 MSC USB R	108	LV2 SWIR Coefficient of elasticity of Compression
52	PC2 MSC USB log(1/R)	109	LV1 USB Coefficient of elasticity of Rupture
53	PC2 NORM USB R	110	LV2 USB Coefficient of elasticity of Rupture
54	PC2 NORM USB log(1/R)	111	LV1 Hyper Coefficient of elasticity of Rupture
55	PC2 SNV SNIR R	112	LV2 Hyper Coefficient of elasticity of Rupture
56	PC2 SNV SNIR log(1/R)	113	LV1 SWIR Coefficient of elasticity of Rupture
57	PC2 MSC SNIR R	114	LV2 SWIR Coefficient of elasticity of Rupture